Studies of Natural Product Derivatives:

Targeted Polymer Drug Conjugates

A thesis

submitted in partial fulfilment

of the requirements for the Degree

of

Doctor of Philosophy in Chemistry

at the

University of Canterbury

by

Sean Devenish

University of Canterbury, September 2004

Ah, but a man's reach should exceed his grasp,
Or what's a heaven for?

Robert Browning, *Andrea del Sarto*

Acknowledgements

My first thanks are to Professors John Blunt and Murray Munro for providing me with the opportunity to carry out the research outlined in this project. Beyond your academic and supervisory support, you have both always been friendly and accommodating, which is hugely appreciated.

I must also thank the entire technical and support staff of the Department of Chemistry, without whom the department would cease to function. In particular, I would like to thank Gill Ellis for carrying out bio-assays and Bruce Clark for training me to use the ESIMS and running samples that I couldn't or wouldn't do myself. Wayne MacKay deserves extra thanks for being the general 'fix-it guy' – somehow able to promptly fix any piece of equipment that might break down inconveniently. Thanks also to Rob McGregor for numerous, often urgent, glass repairs and also for allowing me to ruin all that perfectly good glass rod and tube.

I greatly appreciate the opportunity I had to work at the Centre for Polymer Therapeutics when it was still located in the University of London School of Pharmacy. The welcome provided to me by both staff and students there made my time in London a pleasure. Special thanks go to Professor Ruth Duncan and Dr Steve Brocchini for their supervisory roles during my stay.

For financial assistance I would like to acknowledge the University of Canterbury for a Doctoral Scholarship and the Foundation for Research in Science and Technology for a Bright Futures Scholarship. Thanks also to the New Zealand Vice Chancellors Committee's Claude McCarthy Fellowship for my funding in London and the Canterbury branch of the New Zealand Instititute of Chemistry for conference funding.

A huge thanks to the Marine Group members for putting up with my sometimes foul mood (sorry about that) and being a friendly and fun bunch of people. There are too many to mention by name, but Warren has been particularly close over the many years

and has somehow managed to drag me out of a bad mood more times than I care to remember. Other Marine Group members deserving of a special mention are Scott B, Marie, Sylvia, Jonno, Sonia, Timmy, Cherry and Christian.

Thanks also to the entire student population of the Chemistry Department for making the department one of the most social in the university and also for being generous with 'loans' of both chemicals and equipment.

Nearly last but still certainly not least, thanks to friends who accepted my desire to go back to the lab at ridiculous times and understood when I was late because I had been stuck in the lab. A special thanks goes to Sara for putting up with all of that and more in the 'early years' as well as to Russell and Andre for reminding that life does exist outside the lab – Steinlager jousting and Bristol Blue live on. I am also very grateful to Ashley for revving me up just when it was most needed.

More recently, Annabel's company and love has been a welcome relief from the 'excitement' of writing – I look forward to returning the favour.

To Mum, Dad, Lee, Charles, Margaret and Andre thanks for being so patient, interested and somehow managing to maintain enthusiasm for my work, even when I was down about things not working as I would have liked. Your support and encouragement was more important than you know. Without you all I doubt I would have finished this.

Abstract

Polymer drug conjugates are an emerging class of therapeutic agent that offer advantages in the treatment of cancer through long circulation times and passive targeting. A further benefit of using a polymeric framework is that it readily allows attachment of targeting motifs to enhance the drug specificity, as well as allowing variation of the drug component. In this work a series of targeted polymer drug conjugates were prepared that incorporated different drugs via peptide linkers designed to be stable in circulation but degradable at the target site.

In order to ensure stability in circulation, it was necessary to ensure the drugs were conjugated to the biodegradable linkers via amides, which required the introduction of amine functionalities to the natural product drugs. The required hemisyntheses were successfully carried out, although yields were sometimes disappointing.

An effort to allow an assessment of the pharmacokinetic effects of using a polymeric scaffold was made through the attempted synthesis of low molecular weight analogues of the polymer drug conjugates, with success in some cases.

A recently developed polymeric precursor was used in the preparation of the polymer drug conjugates but was found to undergo an unexpected side-reaction, which may prevent the long term development of this particular precursor. The desired conjugates were nonetheless successfully produced on a scale suitable for initial biological testing.

Both the high and low molecular weight constructs synthesised showed reduced cytotoxicities to P388 murine leukemia cells and are currently awaiting *in vitro* testing to truly evaluate their utility.

Table of Contents

Chapter 1: Introduction

Chapter 2: Peptide Synthesis

Chapter 3: Natural Product Modification

Chapter 4: Low Molecular Weight Conjugates

Chapter 5: Polymer Drug Conjugates

Chapter 6: Conclusion

Chapter 7: Experimental

Abbreviations

Acm	acetamidomethyl
ACN	acetonitrile
aFGF	acidic fibroblast growth factor
APN	Aminopeptidase N
ATR	attenuated total reflectance (in IR)
ATRP	atom transfer radical polymerisation
bFGF	basic fibroblast growth factor
br s	broad singlet (in NMR)
C	cysteine
CIGAR	constant time inverse-detection gradient accordion rescaled (heteronuclear multiple bond correlation spectroscopy) (in NMR)
COSY	correlation spectroscopy (in NMR)
d	doublet (in NMR)
DCC	dicyclohexylcarbodiimide
DCE	1,2-dichloroethane
DCM	dichloromethane
DEAD	diethyl azodicarboxylate
DEPT	distortionless enhancement by polarization transfer (in NMR)
DIPEA	diisopropylethylamine
DMAP	dimethylaminopyridine
DMF	dimethylformamide
DMSO	dimethylsulfoxide
DNA	deoxyribose nucleic acid
EPR	enhanced permeability and retention

equiv.	equivalent
ESIMS	electrospray ionisation mass spectrometry
Et_2O	diethyl ether
EtOAc	ethyl acetate
EtOH	ethanol
F	phenylalanine
Fmoc	9-Fluorenylmethoxycarbonyl
FT	fourier transform
G	glycine
HBTU	*O*-benzotriazol-1-yl-tetramethyluronium hexafluorophosphate
HOBt	1-hydroxybenzotriazole
HPLC	high pressure liquid chromatography
HPMA	*N*-(2-hydroxypropyl)-methacrylamide
HREIMS	high resolution electron ionisation mass spectrometry
HRESIMS	high resolution electrospray ionisation mass spectrometry
HSQC	heteronuclear single quantum coherence (NMR)
IMPRESS	improved resolution using symmetrically shifted pulses
IR	infra-red
L	leucine
LRESIMS	low resolution electrospray ionisation mass spectrometry
m	multiplet (in NMR)
MeOH	methanol
MPLC	medium pressure liquid chromatography
Mtr	4-methoxy-2,3,6-trimethylbenzenesulfonyl
N	asparagine
NHS	*N*-hydroxysuccinimide
NMR	nuclear magnetic resonance

NOESY	nuclear Overhauser enhancement spectroscopy (in NMR)
o	overlapping or obscured (in NMR)
PE	petroleum ether
PMA	phosphomolybdic acid
pMAOS	poly(methacryloxy succinimide)
ppm	parts per million (in NMR and errors in mass spectrometry)
q	quartet (in NMR)
R	arginine
RNA	ribose nucleic acid
ROESY	rotating frame nuclear Overhauser enhancement spectroscopy (in NMR)
s	singlet (in NMR)
SPPS	solid phase peptide synthesis
t	triplet (in NMR)
TES	triethylsilane
TFA	trifluoroacetic acid
THF	tetrahydrofuran
TLC	thin layer chromatography
TNF-α	tumour necrosis factor-α
UV	ultraviolet
VEGF	vascular endothelial cell growth facter
WHO	World Health Organisation
X	any amino acid

Chapter 1

Introduction

1.1 Cancer

Cancer, a disease caused by uncontrolled division of cells, is one of the leading causes of death and discomfort in the world today, particularly in developed nations. There are currently over 22 million cancer patients in the world; ten million people are diagnosed with cancer and six million die of cancer each year.[1] With an almost 20% increase in both cancer incidence and mortality from 1990 to 2000,[1] it is clear that cancer is a disease that is going to continue to be a great burden on society for many years to come. As developing nations improve their standards of living, the rates of cancer in those countries can be expected to rise dramatically, adding greatly to the worldwide cancer burden. Consequently, the number of new diagnoses is projected to rise to 20 million per year by the year 2020.[2]

In New Zealand a study carried out in 2002 looked at the cancer burden in the country in 1996/7 and forecast figures for 2011/12. The authors found that the number of people living with cancer in New Zealand was expected to increase by almost 50%, from 14 808 to 21 777, over the 15 year period, with annual deaths rising from 7 447 to 8 963, an increase of 20%.[3] The increase in the incidence of cancer in New Zealand will continue to place a heavy burden on both the health system and the patients and their families until such time as cancer becomes a curable disease.

The term cancer actually refers to a large family of disorders which can generally be broken into three broad classes based on the type of tissue involved.[4] Carcinomas are

cancers of the epithelial cells and are by far the most common type of cancer, representing around 90% of all cancers. This is thought to be due to the fact that epithelial cells are among the most rapidly dividing cells in the body, and also, being located on the suface of organs, are easily exposed to physical and chemical abuse. Leukemias are cancers of the haemopoietic cells and cells of the nervous system, while sarcomas originate in the connective tissue or muscle cells. There are cancers that do not fall into these categories, but they are relatively rare.

When a cancer develops, it begins as a benign tumour, which consists of a simple mass of cells undergoing uncontrolled cell division. A benign tumour is relatively easily treated as it is well contained. If a benign tumour goes unnoticed it will eventually develop into a malignant tumour, which is a cancer that has taken on the characteristics of invasion and colonisation of other areas of the body. This type of tumour is much more difficult to treat due to the presence of secondary tumours that are spread throughout the body.[5,6]

The progression of a healthy cell to a benign tumour and finally a malignant tumour is a result of accumulation of damage to the genetic material.[7] In a human lifetime, approximately 10^{16} cell divisions will be undertaken, with each replication of the genome presenting a 10^{-6} chance of making an error in any particular gene. This means that in the course of a lifetime, each gene will experience about 10^{10} mutations, so it is almost surprising that cancer does not occur more frequently or earlier in life.[8] The reason why cancer is not more common is that for a cell to become cancerous, it must accumulate independent mutations in between three and seven particular genes associated with control of cell division, which is highly unlikely in any particular cell.

Not all genes can cause cancer when mutated, and those that can are divided into two groups – oncogenes and tumour repressor genes. Oncogenes typically code for proteins whose action induces cell division. Typically, cancer-causing mutations in oncogenes will result in increased protein production or production of a constitutively active protein. Due to the dominant nature of a mutant oncogene, if just one of the two available copies of a particular oncogene is defective, it is sufficient to put a cell on the

pathway to cancer. Tumour repressor genes code for proteins that restrict or prevent cell division. Cells with only one operational copy of a tumour repressor gene will still produce some fully functional protein and therefore will not be transformed to a cancerous phenotype.

1.1.1 Current therapies

Traditional cancer treatment has relied on surgery, radiotherapy and chemotherapeutic agents. Surgery is typically the first form of treatment used in cancer therapy. Where possible, the bulk of the tumour mass is surgically excised.[5,9] However, this technique is generally unable to remove all of the cancerous cells, so surgery is followed by radiotherapy or chemotherapy or in some cases, both together. Surgery cannot be carried out when the tumour is so large that removal would result in unacceptable damage to the surrounding tissue and organs. In these cases, radiotherapy and chemotherapy can be utilised first in an effort to reduce the tumour to a resectable size. In some patients with a strong family history of cancer or a known genetic predisposition, cancer-prone organs may be removed as a preventative measure prior to the development of cancer.

Radiotherapy involves the targeted delivery of high intensity radiation to the area of a tumour.[9] Usually non-ionising radiation such as x-rays or gamma rays is used, with the ideal source being a linear accelerator which can provide a powerful and highly directed beam of radiation. The treatment regime is commonly carried out using moderate intensity irradiations daily to allow time for healthy tissue to heal between sessions. To further limit the damage to normal cells, the radiation is applied from a number of different directions during each session so that healthy tissue is exposed to the lowest possible dose while the tumour receives the maximum radiation. The effect of radiotherapy is to cause extensive DNA damage. Unfortunately, the damage is maximal in the presence of oxygen, which means that radiotherapy is less effective against hypoxic

areas of a tumour. The use of hyperbaric oxygen, hypoxic cell sensitizers and neutron radiation have all been proposed as methods of overcoming the intrinsic resistance of hypoxic cells to radiation, but have met with only limited success. Despite this limitation, radiotherapy remains an affordable and effective treatment for many cancer patients.

Chemotherapy is the last major weapon in the armamentarium of the oncologist, and has very varied utility. Some tumours are very responsive to chemotherapy; for example, 90% of patients with advanced germ cell tumours are cured by treatment with cisplatin, while others remain highly refractory. The World Health Organisation has assembled a list of 17 essential cancer drugs; all are generic, and thus affordable, drugs useful for treating the most responsive tumour types (**Table 1.1**).[10]

Table 1.1 The World Health Organisation essential cancer drug list

Drug	**Class/mechanism of action**
5-Fluorouracil	Anti-metabolite
6-Mercaptopurine	Anti-metabolite
Cytarabine	Anti-metabolite
Methotrexate	Anti-metabolite
Chlorambucil	DNA alkylator
Cisplatin	DNA alkylator
Cyclophosphamide	DNA alkylator
Procarbazine	DNA alkylator (presumed)
Daunorubicin	Topo II inhibitor
Doxorubicin	Topo II inhibitor
Etoposide	Topo II inhibitor
Vinblastine	Tubulin binder
Vincristine	Tubulin binder
Bleomycin	Nucleic acid oxidiser
Dactinomycin	RNA synthesis inhibitor
Prednisolone	Glucocorticoid
Tamoxifen	Anti-oestrogen

The chemotherapeutic agents used have typically been compounds which are toxic to mitotic, or dividing, cells and act by interfering with one or more of the processes involved in cell division. Most of the drugs on the WHO essential drug list can be placed in one of four groups based on their mechanism of action, as can most other cancer drugs, although currently a number of drugs are in development that have novel mechanisms of action.

1.1.1.1 Antimetabolites

The term antimetabolite refers to a compound that interferes with biosynthesis or utilisation of a normal cellular metabolite.[11] Due to their reliance on hindering a particular enzymatic reaction, or, in some cases, their requirement for enzymatic activation to produce the cytotoxic agent, resistance to antimetabolites is a common problem through simple up- or down-regulation of the relevant enzyme. In order to minimise the development of resistant cancer cells, antimetabolites are almost always used in combination with other chemotherapeutic drugs.

The majority of the drugs in the antimetabolite class are analogues of nucleic acid components that are selectively toxic to cells that are undergoing DNA replication. 5-fluorouracil[12] (**1**), 6-mercaptopurine[13] (**2**) and cytarabine[14] (**3**) are all nucleic acid analogues. All three of these drugs undergo metabolism within the target cell before being incorporated into the DNA, leading to formation of fatal protein adducts and single- and double-strand breaks.

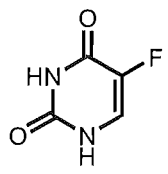

5-fluorouracil (**1**)

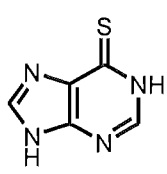

2-mercaptopurine (**2**)

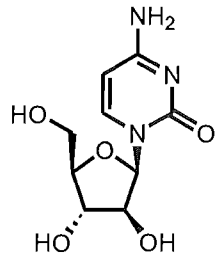

Cytarabine (**3**)

Methotrexate[15] (**4**) is not a nucleotide analogue; it acts as a potent inhibitor of dihydrofolate reductase, an enzyme involved in the biosynthetic pathway of nucleotides. Restricted biosynthesis of the nucleotides required for DNA replication leads to suspension of cell proliferation and induction of apoptosis.

1.1.1.2 DNA alkylators

The DNA alkylators are among the oldest anti-cancer drugs known;[16] the first drug ever used clinically for treatment of cancer was mechlorethamine (**5**), or nitrogen mustard, which is a strong alkylator of DNA. The primary cause of toxicity of mechlorethamine (**5**) is thought to be due to formation of DNA-DNA crosslinks, in which two bases of the DNA helix are alkylated by the two arms of the drug. This can result in either an inter- or intra-strand crosslink, both of which prevent any further DNA replication.

Chlorambucil[17] (**6**) is an analogue of mechlorethamine which is still commonly used today, primarily in the treatment of lymphocytic leukemia. The parent compound is active *in vitro*, but has been found to be rapidly converted to the slightly more toxic phenyl acetic acid mustard (**7**) in the body,[18] which may be the form responsible for the

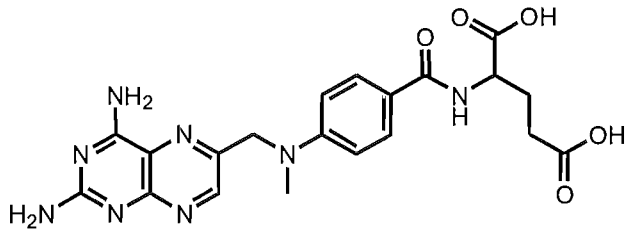

Methotrexate (**4**)

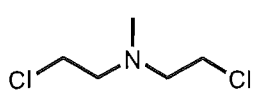

Mechlorethamine (**5**)

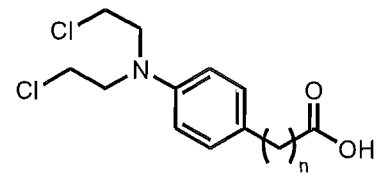

n = 3 Chlorambucil (**6**)

n = 1 Phenyl acetic acid mustard (**7**)

observed *in vivo* anticancer activity. Chlorambucil (**6**) can be administered orally as it has significantly lower alkylating ability than mechlorethamine (**5**) and thus is able to survive transition through the gut.

Cyclophosphamide[19] (**8**) is a widely used anti-cancer drug that relies on metabolic activation to produce an active alkylating species. Initially it was thought that the active derivative of cyclophosphamide (**8**) was norNH$_2$ (**9**), but more recently it has been found that phosphoramide mustard (**10**) is actually the species responsible for the majority of the DNA alkylation observed. Interestingly, researchers found that the metabolic derivatisation of cyclophosphamide (**8**) takes place primarily in the liver rather than the tumour, which explains the lack of cytotoxicity of cyclophosphamide (**8**) to tumour cells grown *in vivo*.

Another major class of DNA alkylating agents, the platinum complexes, contains the very well known drug cisplatin[20,21] (**11**). The discovery of the anti-cancer properties of cisplatin (**11**) was made serendipitously in 1965 when Rosenberg noted that *Escherichia coli* cells were unable to grow near a platinum electrode in an electrolysis bath containing ammonium chloride. Since that discovery, over 2 000 analogues of cisplatin (**11**) have

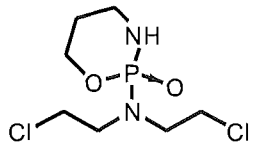

Cyclophosphamide (**8**)

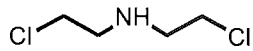

NorNH2 (**9**)

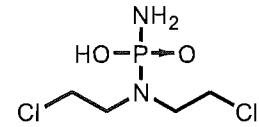

Phosphoramide mustard (**10**)

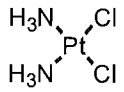

Cisplatin (**11**)

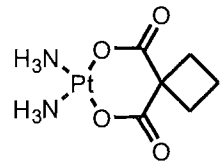

Carboplatin (**12**)

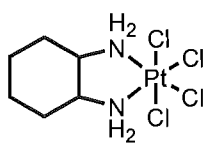

Iproplatin (**13**)

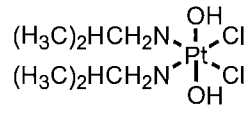

Tetraplatin (**14**)

been synthesised and examined for their ability to form cytotoxic intra-strand cross-links. A number of these analogues have progressed to clinical use, including carboplatin (**12**), iproplatin (**13**) and tetraplatin (**14**). The critical feature shared by all of these drugs is the presence of two labile ligands in a *cis* relationship. The remaining ligands can be relatively inert, and it is variation of these moeities that gives rise to distinct pharmacological properties by altering the physical and chemical properties of the drugs.

Procarbazine (**15**) is a synthetic antitumour compound which was developed in 1963 following discovery of cytotoxic activity in the members of a library of *N,N'*-dialkylhydrazines.[22] Structure-activity studies led to the discovery that one of the alkyl substituents on the hydrazine absolutely had to be a methyl group for any activity to be displayed, while alterating the other alkyl substituent changed the biological profile, including cytotoxicity, of the drug. Pure procarbazine (**15**) itself has no effect on isolated DNA, RNA or protein but in the body it is rapidly oxidised in the presence of oxygen and a redox active metal to the azo derivative **16** with production of hydrogen peroxide.[23] Further oxidation can lead to formation of a mixture of the azoxy derivatives **17** and **18**, which have been shown to cause extensive DNA damage and lead to single strand breaks.[24]

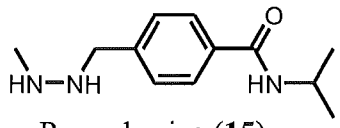

Procarbazine (**15**)

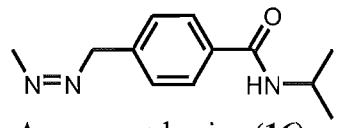

Azo-procarbazine (**16**)

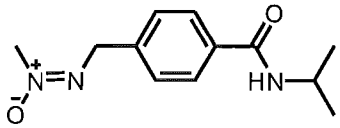

ONN-azoxy-procarbazine (**17**)

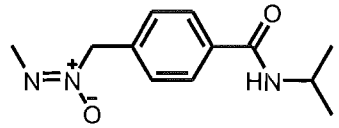

NNO-azoxy-procarbazine (**18**)

1.1.1.3 Topoisomerase inhibitors

Topoisomerases are enzymes that are able to cleave one or both strands of the DNA helix to release the supercoiling that is caused by localised unwinding during replication. After cleavage, the topoisomerase controls the motion of the cut end(s) to release the excess torsion before re-annealing the strands.[25] If this process does not occur, the DNA helix is put at risk of breaking during replication as the supercoiling becomes gradually tighter. Topoisomerase inhibitors are somewhat misnamed as they do not actually inhibit the activity of topoisomerases, but rather exert their toxicity by interacting with the DNA-enzyme complex and stabilising it in a 'cleavable' conformation. Action of cellular proteases on the complex leads to the release of cleaved DNA with residual protein material conjugated to the cut ends. The exact mechanism by which this DNA damage causes cell death is still not fully understood, but it is clear that extensive damage of this sort is beyond the repair capabilities of cells and leads eventually to cell death. Topoisomerase inhibitors can be broadly divided into two classes, depending on whether they interact initially with the DNA or the enzyme in the cleavable complex.

The structure of DNA, with a regular arrangement of stacked aromatic bases, is prone to disruption by other flat aromatic molecules which can intercalate (insert between adjacent base pairs). Intercalation of a drug molecule increases the base pair spacing from 3.4 Å to approximately 7 Å, leading to a change in the torsional angle of the helix.[26] This distortion is sufficient to trap the topoisomerase-DNA complex in its cleavable conformation. Interestingly, not all compounds that are able to intercalate into DNA are topoisomerase inhibitors; for example ethidium, which is a well known intercalator, does not cause any formation of cleavable complexes and does not show significant antitumour activity.[27] The specific features that lead to efficient stabilisation of the cleavable ternary complex are still not known.

The most well known family of intercalating topoisomerase inhibitors are the anthracyclines.[28] Members of this class of drug are widely used in modern cancer chemotherapy, in particular doxorubicin (**19**) and daunorubicin (**20**). The mechanism of

action of the anthracyclines is not restricted to intercalation, with both doxorubicin (**19**) and daunorubicin (**20**) showing the ability to undergo redox reactions resulting in the generation of toxic free radicals, and they are also known to be able to interfere with and alter plasma membranes. The primary limitation of all anthracyclines is their dose-limiting cardiotoxicity, which limits the recommended life-time dose to 550 mg/m^2, although reduction in cardiac efficiency has been noted with doses as low as 300 mg/m^2.[29] Efforts to ameliorate this side-effect have largely been unsuccessful, with the analogue epirubicin (**21**) reported to exhibit reduced cardiotoxicity, although not enough to warrant the replacement of doxorubicin (**19**) or daunorubicin (**20**) in clinical use.

The non-intercalating topoisomerase inhibitors are less well known and also rarer than those that interact directly with DNA. The epipodophyllotoxins are a family of semisynthetic compounds based on the naturally produced compound podophyllotoxin (**22**), which is a cytotoxin that exhibits no topoisomerase inhibitory activity and has not proven to be useful in cancer therapy.[30] Investigation of analogues of podophyllotoxin resulted in the discovery of etoposide[31] (**23**). This compound is a potent topoisomerase inhibitor, but shows no interaction with free DNA, indicating that it interacts with topoisomerase directly to stabilise the cleavable DNA-enzyme complex.

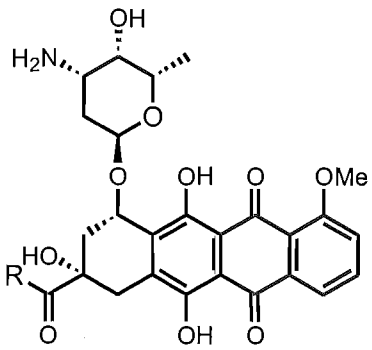

R = $-CH_2OH$ Doxorubicin (**19**)
$-CH_3$ Daunorubicin (**20**)

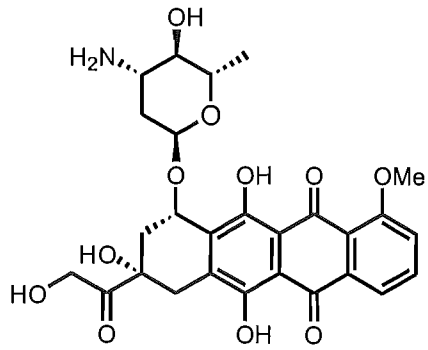

Epirubicin (**21**)

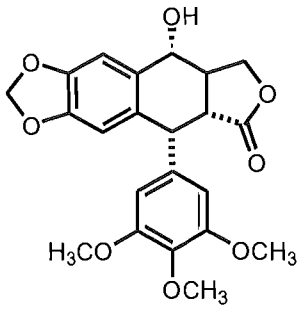

Podophyllotoxin (**22**)

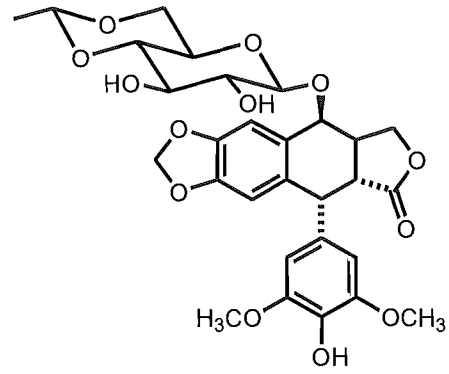

Etoposide (**23**)

1.1.1.4 Tubulin binders

Microtubules, which form an endoskeleton within cells, are essential to many cellular functions, not least of all separating the newly duplicated chromosomes during cellular replication through formation of the mitotic spindle. Due to their central role in both cell division and regular cellular maintenance, inhibition of their assembly or disassembly leads to cell death. The heterodimeric protein tubulin is the basic building block of microtubules, and a number of compounds are known to bind to tubulin and inhibit the proper activity of microtubules by inhibiting either polymerisation or depolymerisation of tubulin.[32]

The vinca alkaloids vinblastine (**24**) and vincristine (**25**) are efficient inhibitors of tubulin polymerisation.[32] At low concentrations (from 10 nM to 1 μM) they bind to the growing ends of the microtubules and prevent any further aggregation of tubulin heterodimers leading to an 'end-capping' effect. At higher concentrations (>10 μM) they can induce formation of crystals consisting of two intertwined microtubules. Despite their structural similarities, vinblastine (**24**) and vincristine (**25**) have distinct anti-cancer activity profiles and thus are both included in the World Health Organisation essential drugs list.

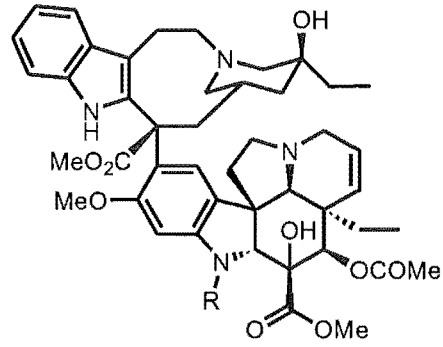

R = $-CH_3$ Vinblastine (**24**)
$-CHO$ Vincristine (**25**)

1.1.1.5 Others

The term 'bleomycin' actually refers to a mixture of related compounds, the predominant members of which are bleomycin A_2 (**26**) and bleomycin B_2 (**27**).[33] The members of the bleomycin family are thought to exert their cytotoxicity through oxidation of nucleic acids mediated by a redox active metal such as Fe^{2+} or Cu^{+} and requiring molecular oxygen. It is thought that the primary target of bleomycin is DNA, although there are some indications that damage to cytosolic RNA could be the main mechanism of cell death.

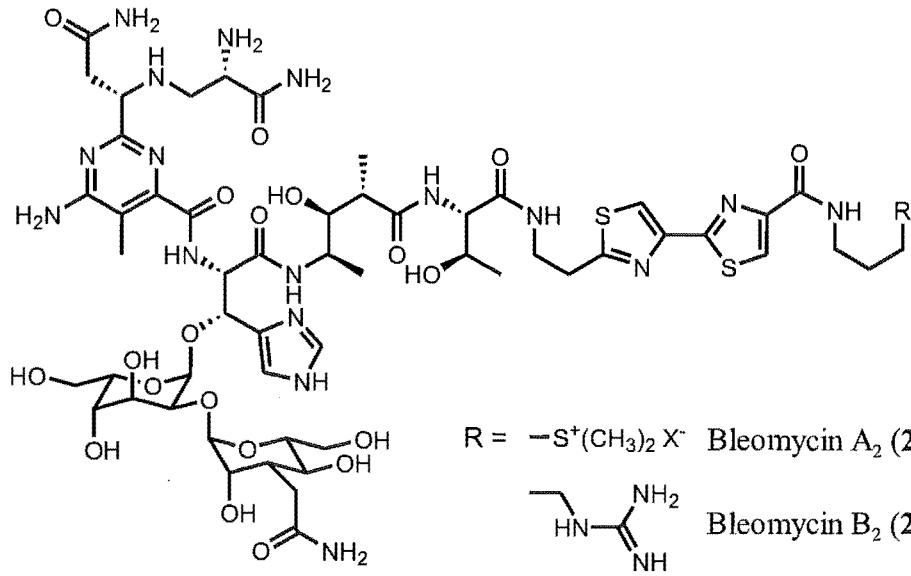

R = $-S^{+}(CH_3)_2\ X^{-}$ Bleomycin A_2 (**26**)

Bleomycin B_2 (**27**)

Dactinomycin,[34] (**28**) or actinomycin D, is an antitumour antibiotic that was isolated from an actinomycetes fungus in 1940. In mammalian cells it concentrates in the nucleus, where it is found to be bound to DNA. Despite its planar structure, which would suggest a mechanism of action involving intercalation and topoisomerase inhibition, it exerts its toxicity through inhibiting the synthesis of RNA from a DNA template.

Prednisolone[35] (**29**) is a glucocorticoid steroid that is used primarily in the treatment of lymphoma. The exact mechanism of action of prednisolone is not known; however, it is known that glucocorticoids bind to specific receptors on target cells and cause a reduction in the level of transcription of numerous genes. It also appears that some cells, in particular immature lymphocytes, are programmed to undergo apoptosis when exposed to high levels of glucocorticoids, which may well be the reason why prednisolone is effective against lymphoma.

Tamoxifen[36,37] (**30**), first synthesized in 1963, is an anti-oestrogen which has become the benchmark treatment for breast cancer. It works by competitively inhibiting the binding of oestrogen to the oestrogen receptor, leading to an attenuation of transcription of certain growth-related genes and a decrease in the rate of proliferation of cells. Interestingly, tamoxifen provided the first example of contrasting biological activity between isomeric forms in that the *trans*-isomer is an anti-oestrogen while the *cis*-isomer is a pure oestrogen.

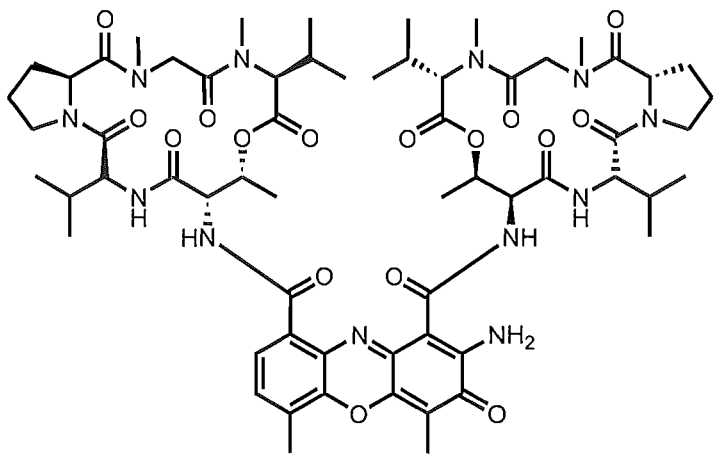

Dactinomycin (**28**)

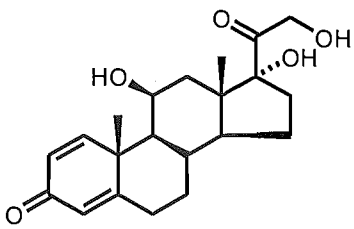

Prednisolone (**29**)

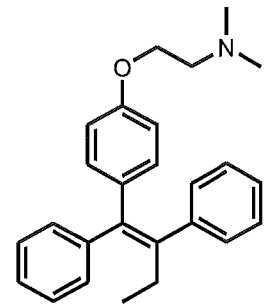

Tamoxifen (**30**)

1.1.1.6 Recent developments

While the toxins described thus far do show some ability to target the relatively rapidly dividing cells of a cancer, they also cause a number of unpleasant side effects due to toxicity to other, non-cancerous mitotic cells in the body such as those of the stomach lining, hair follicles and the blood cell progenitors in the bone marrow. Recently, research has focused on the development of anti-cancer drugs that are more specific. Tactics employed for improving the efficiency of drugs include causing cancer cells to revert to normal cells, targeting cytotoxins specifically to cancerous cells, or affecting the body's own response to the tumour rather than attacking the tumour directly.

Developments in the field of gene therapy have led some researchers to believe that it is possible to cause tumour cells to lose their cancerous characteristics and become normal tissue once again. One gene that has been seen as a potential target is the tumour suppressor gene p53, which is found to be mutated in over 50% of all tumours.[38] p53 codes for a protein that is able to detect genetic damage and either stop cell division to allow repair to take place, or induce cell death if the damage is extensive. If a fully functioning copy of the p53 gene could be delivered to cancer cells, it may be able to restore normal function, leading to a return of growth control and thus eliminating the cancer. Despite a number of clinical trials, no major successes have yet been reported.[39,40]

Cancer cells are known to express proteins on their cell surfaces that are not present on

normal cells. These proteins are known as tumour-associated antigens, and antibodies that bind to such antigens are currently being intensively researched to determine their ability to mediate anti-cancer activity. Some antibodies are able to directly cause the death of cells to which they bind through a process known as antibody-dependent cellular cytotoxicity.[41] More commonly, however, antibodies are being developed as targeting systems to deliver radioisotopes or cytotoxins directly and specifically to tumour cells.[42-45]

The antigens expressed by tumour cells are also able to be utilised by the body's own immune system. Some researchers have suggested that cancer cells occur spontaneously within the body relatively frequently, but are almost always eliminated by the immune system before they become a threat. Whether or not this is correct, the observation by Coley in the 1890s that a subcutaneous injection of a bacterial extract could lead to the elimination of some tumours has led researchers to investigate whether stimulation of the body's immune response could be used as a treatment for cancer.[46] To this end, current research is directed toward the development of a cancer vaccine, with more vaccines having been developed than can be tested in patients.[42] Unfortunately, it appears that tumours do not display unique antigens, although they do express many antigens at higher levels than healthy tissues. This means that vaccination may cause an autoimmune condition to arise in which the immune system attacks healthy tissue as well as cancer cells, although this may be a price worth paying.[42]

1.1.2 Angiogenesis

Angiogenesis is the process whereby existing blood vessels branch out to form new vasculature and takes place primarily during foetal development and to a lesser extent during certain tightly controlled processes in adults, such as wound healing and menstruation.[47,48] In 1971, Folkman first described the central role of angiogenesis in tumour development and outlined the concept of 'tumour dormancy' in the absence of

angiogenesis.[49] It is now known that angiogenesis is not only essential to the growth of a solid tumour, but, perhaps more importantly, is required to enable a tumour to metastasize and thereby spread through the body.[50] As angiogenesis must occur before a tumour can progress beyond about 2 mm^3,[50-52] inhibition of angiogenesis is seen as another valid target for anti-cancer therapy.[53]

Angiogenesis is controlled by a complex interplay of activators and inhibitors in a system that has been described as the 'angiogenic switch'.[48] There have been over forty regulators of angiogenesis identified to date, some of which are shown in **Table 1.2**.[54] It has been shown that the angiogenic activators aFGF, bFGF and VEGF are widely expressed in normal, healthy tissue without inducing angiogenesis, due to the concomitant expression of inhibitors of angiogenesis.[48] Within the tumour environment, it is thought that the induction of angiogenesis only begins with the onset of hypoxia,[55,56] which can, in turn, lead to either an increase in expression of activators of angiogenesis or a decrease in expression of inhibitors, with examples of both mechanisms known.[48] Interestingly, it is also known that primary tumours often release inhibitors of angiogenesis into the bloodstream, which has the effect of preventing the growth of any

Table 1.2 Selected regulators of angiogenesis

Activators	**Inhibitors**
Acidic Fibroblast Growth Factor (aFGF)	Angiostatin
Angiogenin	Canstatin
Basic Fibroblast Growth Factor (bFGF)	Endostatin
Follistatin	Interferons α/β
Interleukin-3	Interleukin-10
Interleukin-8	Interleukin-12
Leptin	Interleukin-18
Placental Growth Factor	Platelet factor-4
Platelet Derived Growth Factor	Restin
Pleiotrophin	Thrombospondin-1
Proliferin	Tumstatin
Vascular Endothelial Growth Factor (VEGF)	Vasostatin

metastasised tumour cells. This control is lost if the primary tumour is removed, leading to a rapid growth of numerous secondary tumours.

The process of angiogenesis, as shown in **Figure 1.1**, begins with initiation through release of activators of angiogenesis by the tumour. Following activation, the endothelial cells secrete proteases to dissolve the basal membrane. Initially cells migrate to form the budding neovasculature, but before long the cells just before the tip of the sprouting vessel undergo replication to supply sufficient cells to allow the vessel to grow. Eventually the vessel will meet another new sprouting vessel and form a loop, allowing blood to flow through. Further sprouts can develop from the initially formed loop if required, and, in the case of cancer, the rapidly developing tumour mass can cause persistent angiogenesis. Finally, the new capillary lays down a basal membrane and undergoes a number of physiological changes to become a properly developed blood vessel.[57]

Targeting angiogenesis as a way of preventing tumour growth has two intrinsic advantages over targeting the tumour itself.[57] First, the accessibility of endothelial cells to drugs administered via the blood means that much lower doses are required to ensure

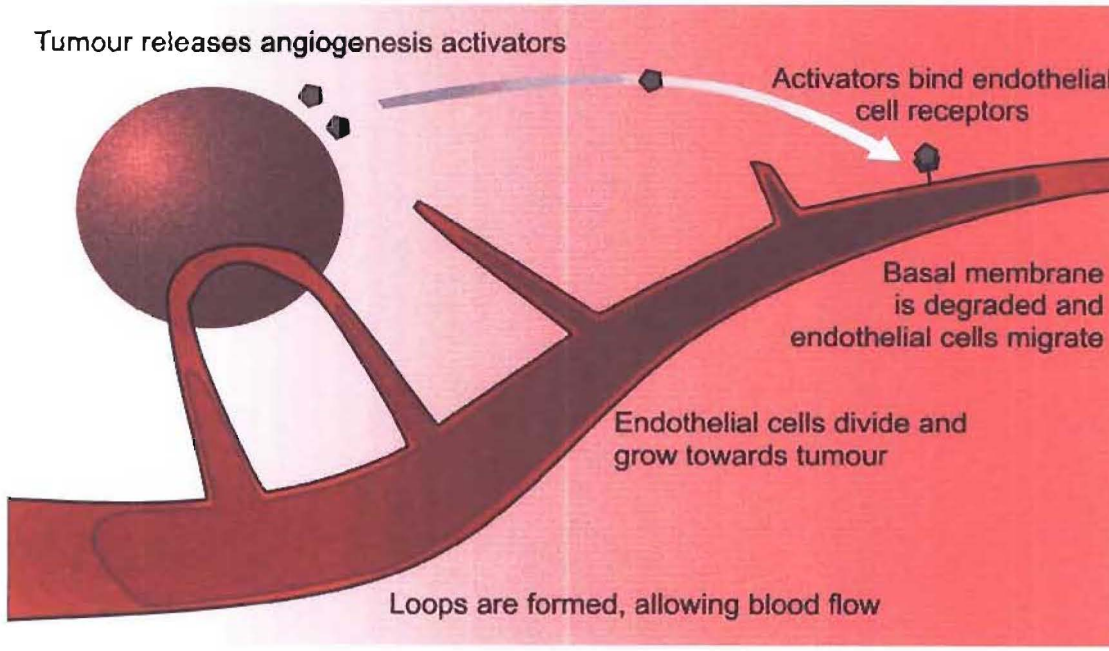

Figure 1.1 The process of angiogenesis

a therapeutic dose at the target tissue, which in turn reduces the severity of any side-effects of treatment. The second advantage is that the endothelial cells are genetically stable, unlike cancerous cells. This means that the cells targeted are phenotypically homogeneous, so the drug can be expected to have a uniform effect, even amongst different types of cancer. Perhaps more importantly, their genetic stability means that endothelial cells are not likely to develop resistance to drugs, which is a major problem with current cancer drugs that are targeted to the genetically plastic tumour cells themselves.

There are currently over 75 drugs in various stages of clinical trials aimed at developing an anti-angiogenic drug that is effective against cancer. In early 2004 the Federal Drug Administration in the United States approved Avastin (bevacizumab, a humanized recombinant anti-VEGF-antibody) for clinical use in combination chemotherapy with 5-fluorouracil (**1**) for treatment of patients with first line or previously untreated-metastatic cancer of the colon or rectum.[58] This is the first example of an anti-angiogenic drug being approved for clinical use, which is somewhat disappointing given their huge potential. There are, however, a number of conventional cancer chemotherapeutics that are thought to be anti-angiogenic, including compounds such as doxorubicin, cyclophosphamide and vincristine. These drugs are all able to exhibit anti-angiogenic activity at concentrations insufficient to kill tumour cells; however, their current clinical usage is not directed toward utilising their anti-angiogenic activities.

The fact that vascular development can be inhibited at sub-cytotoxic concentrations has led to suggestions that therapies aimed at preventing angiogenesis would be best administered using a schedule of low doses given frequently.[54,59] This so-called 'metronomic' dosing scheme is in strong contrast to that usually used in cancer chemotherapy i.e. administration of the maximum tolerated dose followed by an extended recovery period before re-administration.[60,61] Furthermore, it may be necessary to revise the endpoint targets when examining anti-angiogenic drugs as they have been found to lead to disease stabilisation rather than a reduction of the tumour mass.[62,63] Considering that improving patient survival and quality of life are the crucial goals in

disease treatment, these factors would be more appropriate markers of success than tumour regression, which will not necessarily be achieved through an anti-angiogenesis-based treatment regime.

1.1.2.1 Targeting angiogenesis

In 1998 a paper was published in *Science* that described the use of peptides to target doxorubicin to tumour vasculature.[64] The peptides that were used were isolated from phage display libraries, which are collections of bacteriophage, each of which display a single random peptide on their surface.[65,66] In order to isolate the desired peptides, a phage display library is injected into a subject, in this case nude mice bearing human breast carcinoma xenografts. Following distribution of the phage through the body of the subject, excision of the target tissue allows recovery and amplification of any bound phage. This process can be repeated to further purify the bound phage. Once a sufficiently enriched phage pool is obtained, the peptide ligands exposed on the phage surfaces are sequenced and quantified to determine relative affinity for the target tissue.

Three libraries were investigated for tumour vasculature targeting members.[64] The libraries contained cyclic peptides of the forms CX_5C, CX_7C and $CX_3CX_3CX_3C$, where C is cystine and X is any amino acid. Each library yielded one motif that stood out as targeting the implanted tumour. From the CX_5C library, the motif Gly-Ser-Leu was isolated, but no further study was carried out on that peptide. The CX_7C library yielded a peptide containing Arg-Gly-Asp, a sequence known to bind to $\alpha_v\beta_3$ and $\alpha_v\beta_5$ integrins.[67,68] The full sequence of the peptide was Cys-Asp-Cys-Arg-Gly-Asp-Cys-Phe-Cys, abbreviated as RGD-4C, which clearly has the potential to form a number of different disulfide bonds. Only in 2001 was the disulfide bond arrangement of the most active form of this peptide found to be 1-4 and 2-3, where the numbers represent the cysteine residues numbered from the *N*-terminus to the *C*-terminus.[69] A final motif, Asn-Gly-Arg, was isolated from the $CX_3CX_3CX_3C$ library. This sequence was already known

to bind the fibronectin receptor, integrin $\alpha_5\beta_1$.[68,70] Due to the size of the full peptide, the authors synthesised the minimal peptide, *cyclo*-Cys-Asn-Gly-Arg-Cys (CNGRC), and found that it was able to inhibit binding of the parent tridecapeptide.

More recent work on the CNGRC pentapeptide has revealed that, while it is able to bind to integrin $\alpha_5\beta_1$, its primary cellular target is aminopeptidase N.[71] Aminopeptidase N, also known as cluster differentiation antigen 13 (CD13), is a zinc-dependent transmembrane peptidase that is expressed in a variety of tissues throughout the body, with particularly high levels found in the lumen of the small intestine where it is involved in protein digestion.[72-74] The natural substrates of the enzyme are N-terminal hydrophobic amino acids;[74] thus the peptide CNGRC is not expected to be efficiently cleaved by aminopeptidase N. It has been found that CD13 exists in a number of isoforms throughout the body, with only the form found in the tumour vasculature being a strong binder of the CNGRC motif, thus providing the possibility of selective targeting despite the widespread distribution of the enzyme.[71]

The two targeting sequences RGD-4C and CNGRC were coupled directly to doxorubicin, although no precautions were taken to prevent the possibility of forming peptide oligomers.[64] Furthermore, no data were presented to show that the peptide-doxorubicin conjugates formed in a one-to-one ratio. The constructs were tested *in vivo* on mice bearing human breast carcinomas, and were found to greatly improve the survival of the mice and reduce the toxicity of doxorubicin. Examination of the tumours after extended treatment showed significant reduction in the tumour volume of mice treated with the doxorubicin conjugates and notable necroses. Finally, a substantial decrease in the number of metastases was reported for those mice treated with the targeted doxorubicin constructs.

More recently, the CNGRC motif has been studied further as a targeting residue to which doxorubicin was attached via a hydrolysable ester linker.[75] It was found that the intracellular distribution of the dox-CNGRC conjugate differed from that of free doxorubicin by being initially localised in the cytoplasm and moving slowly to the

nucleus, whereas free doxorubucin was seen only in the nucleus. Furthermore, addition of anti-APN antibodies did not change the intracellular distribution pattern of the conjugate, leading to the suggestion that the enzymatic activity of APN is not necessary for uptake of the conjugate. These results were reflected in the cytotoxicities determined for the conjugate and free doxorubicin which were not significantly different versus either APN positive or negative cells, suggesting that, in the studied systems, the CNGRC motif was playing little, if any, role in the behaviour of the conjugate.

While the observed results may cast doubt on the utility of the CNGRC motif as a targeting residue for anti-angiogenic directed cancer therapeutics, it is worth noting that the dox-CNGRC conjugate used in this research was notably more lipophilic than free doxorubicin, as determined by a 1-octanol/phosphate buffered saline (pH 7.2) distribution measurement (5.3 vs 1.2).[75] This would not necessarily be expected, and may in fact be a reason for the relatively poor activity of the conjugate, as it may have been entering the cells by passive diffusion rather than receptor-mediated endocytosis. If this was the case, the reduced hydrophilicity of the conjugate may have contributed to the observed slow diffusion into the nucleus or even led to the conjugate being trapped in the many lipid membranes of the cytoplasmic organelles with free doxorubicin diffusing to the nucleus following release by cytoplasmic esterases. In any case, more study of this conjugate is clearly required to fully understand the observed results.

Another research group has examined the use of the CNGRC motif to guide the delivery of TNF-α to the vascular endothelium.[76] TNF-α is an inflammatory cytokine that has been found to enhance the penetration into tumours, and hence the activity, of anticancer drugs (such as doxorubicin) when co-administered. Unfortunately, TNF-α is also highly toxic, with an effective dose being estimated at 10-50 times the maximum tolerated dose; therefore systemic administration is not viable. Conjugating the CNGRC targeting residue to TNF-α to was found to increase the effectivity of the drug by about five orders of magnitude, thus bringing the effective dose well below the maximum tolerated dose.

1.2 Natural Products

The term 'natural product' is commonly used to refer to any of the secondary metabolites produced by living organisms. These are compounds which play no part in the primary metabolism of an organism.[77] Because natural products are not required for the basic functioning of a producing organism, the enzymes involved in their synthesis are subject to relatively little evolutionary constraint; thus natural products represent a huge range of structural diversity compared to primary metabolites.

The structural diversity present in natural products has been exploited by humanity throughout the ages for a huge range of applications ranging from fragrances, flavours and dyes to medical remedies. The use of natural products in human medicine has received the most attention due to the necessity for ever-improved treatments for the array of ailments and diseases that afflict humans. The fact that over 60% of currently approved drugs are derived from natural products shows the value of investigating secondary metabolites for useful drug lead compounds.[78]

A number of theories have been suggested to explain why organisms produce secondary metabolites; however, the most convincing was presented in a strong argument by Williams et al.[77] They propose that organisms that biosynthesize natural products gain a competitive advantage over those that do not due to the specific interaction of the produced secondary metabolites with biological receptors in competing organisms. This theory has become the accepted dogma and provides strong support for the investigation of natural products in the search for medically relevant compounds.

1.2.1 Marine Natural Products

Investigation of the secondary metabolites of terrestrial organisms has obviously been

much more extensive due to convenience of both sample collection and familiarity with the organisms present. Over the last three decades there has, however, been a dramatic increase in the interest expressed in chemicals produced by aquatic, and in particular marine, organisms. This has largely been caused by the availability of Self Contained Underwater Breathing Apparatus (SCUBA), which allows divers to access the seabed at depths of up to 40 meters, and submersible vehicles that allow access to depths of 1 000 meters or more. Furthermore, the realisation that the oceans contain a biodiversity that surpasses that of the terrestrial environment and has been much less widely explored has provided motivation for researchers to begin investigating marine natural products.

The marine environment seems to encourage the production of novel structures due to the high levels of halogens and nitrogen present, as well as the need for soft, sessile animals to develop chemical defenses against predation. Indeed, it has been shown that many marine animals produce natural products while under stress, and furthermore that natural products are common in organisms without an immune system. An interesting feature of marine natural products research is the variability in the compounds produced by an organism depending on the location and season. It is possible that this variation may be due to the presence of natural product-producing symbiotic micro-organisms, although this is far from certain.[79]

Data from the National Cancer Institute (NCI) in the USA further illustrate the value of screening marine animals for potential pharmaceutical leads; the likelihood of discovering a novel anticancer lead compound has been found to be far greater when examining marine animals than other possible sources (**Figure 1.2**).[80] Results from the Australian Institute of Marine Sciences have further shown that marine sponges (Phylum: Porifera) provide a particularly rich source of cytotoxic natural products, with over 11% of specimens investigated displaying significant cytotoxicity.[80]

1.2.2 The Marine Chemistry Group

The Marine Chemistry Group at the University of Canterbury was formed in 1975 and in 1983 began a programme aimed at investigating biologically active natural products produced by marine organisms, with a particular focus on sponges, from the oceans around New Zealand.[81] Since 2000, the group has diversified somewhat with the development of a fungal programme to complement the well established sponge collection. The fungi obtained are largely marine in origin, although a significant number of terrestrial fungi have also been isolated.

The Group has an extensive collection of New Zealand marine organisms, all of which have had a subsample extracted and examined for biological activity in the Marine Chemistry Group's in-house antitumour, antiviral and antimicrobial assays. Those organisms that display promising bioactivity in the small-scale extract are then extracted on a larger scale. These extracts are subjected to bioactivity-guided fractionation to isolate the active component(s) which are then identified using spectrometric and spectroscopic techniques. Over the last 20 years, a number of potent cytotoxins have been discovered by members of the Marine Chemistry Group, some of which are shown in **Figure 1.3**.[82-87]

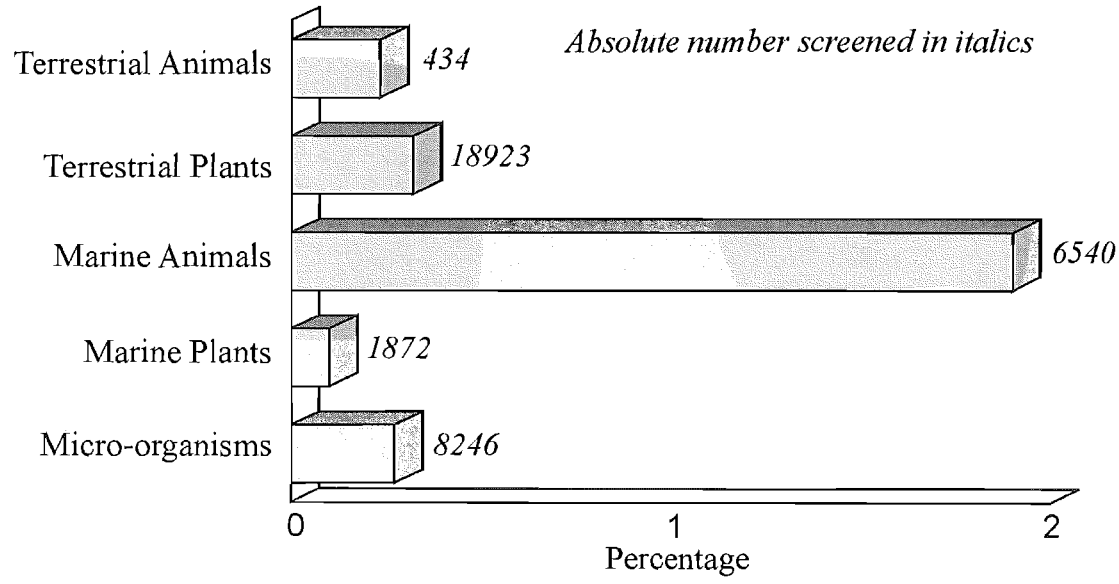

Figure 1.2 Anticancer leads with significant selective cytotoxicity in the NCI Preclinical Antitumor Drug Discovery Screen by source

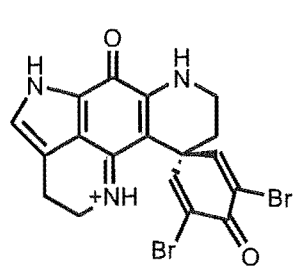

Discorhabdin C

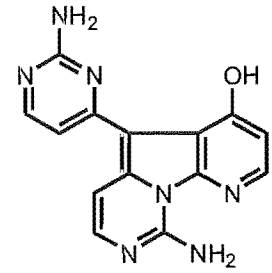

Variolin B

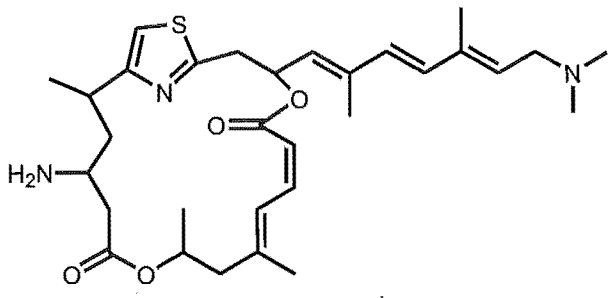

Pateamine

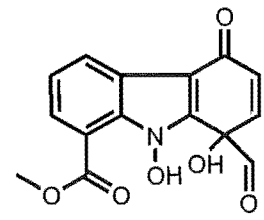

Coproverdine

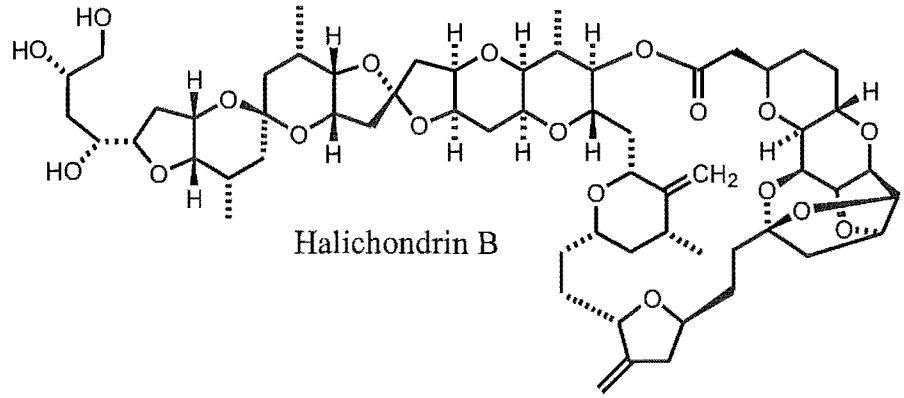

Halichondrin B

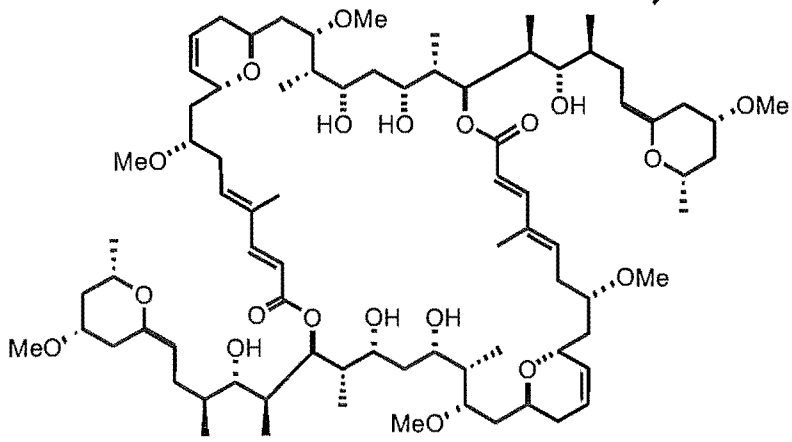

Swinholide H

Figure 1.3 Some cytotoxins discovered by members of the Marine Chemistry Group

Unfortunately, none of the compounds discovered by researchers in the Marine Chemistry Group have yet proceeded to development as pharmaceuticals. One reason for this is the extreme cytotoxicity displayed by many of these compounds, some of which are toxic at nanomolar concentrations. It has been suggested that future cancer chemotherapies will rely on the targeted delivery of highly toxic compounds to cancer cells,[88] and this is an area of research that is currently being investigated within the Marine Chemistry Group and indeed in the research described in this thesis which utilised the mycalamides (**31** and **32**), doxorubicin (**19**) and fumagillol (**35**).

1.2.3 Mycalamides A (31) and B (32)

Mycalamide A (**31**) was isolated and characterised from a highly active antiviral extract of a New Zealand sponge of the genus *Mycale*.[89] The sponge was of particular interest as a crude extract showed antiviral activity not just *in vitro*, but also *in vivo*, which was unusual for sponge extracts. When **31** was re-isolated to provide material for extensive biological testing, a closely related and also highly antiviral compound, mycalamide B (**32**), was isolated, although it was present in less than half the level of mycalamide A (**31**).[90]

Pure mycalamides A (**31**) and B (**32**) both showed good *in vitro* bioactivity against P388 murine leukemia and three human tumour cell lines, with nanomolar IC50s.[91] In all cases, **32** was between two- and six-fold more active than **31**. *In vivo*, both compounds possessed moderate to good activity against a range of murine and human tumours in a mouse model, with mycalamide B (**32**) again showing slightly better activity. An investigation into the mechanism of action of the mycalamides revealed that they inhibited protein synthesis, and it was suggested that this was the cause of their cytotoxicity.[91]

The total synthesis of enantiomerically pure **31** and **32** was first reported in 1990, and

served to confirm the stereochemistry which had previously been assigned on the basis of structural similarity to pederin (**33**).[92] A number of subsequent syntheses have been reported for both mycalamide A (**31**) and B (**32**).[93,94] While the syntheses remain lengthy, and therefore low yielding, synthesis would be a viable, albeit costly, source for material should either of the mycalamides or derivatives thereof show value as therapeutic agents.

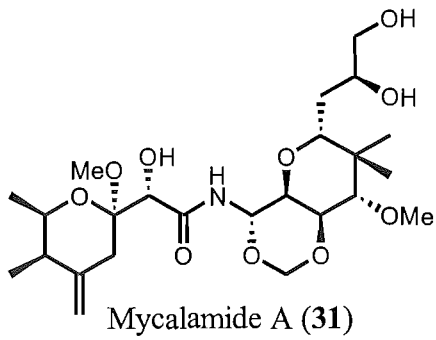

Mycalamide A (**31**)

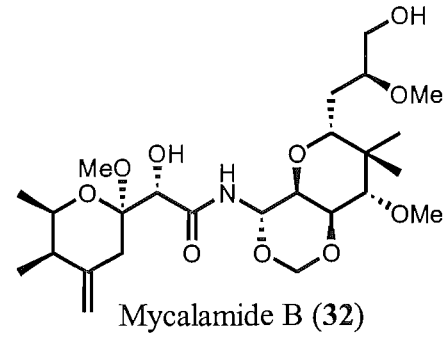

Mycalamide B (**32**)

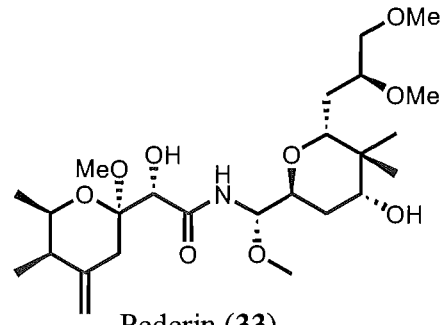

Pederin (**33**)

1.2.4 Fumagillol (35)

The natural product fumagillin (**34**) was isolated in 1949, although it was another eleven years before the structure was elucidated, and the stereochemistry was determined in1962.[95-97] It was initially investigated due to its activity against bacteriophage, but more recently, fumagillin (**34**) was rediscovered by workers in the laboratory of Judah Folkman in a serendipitous uncovering of its anti-angiogenic activity.[98]

Fumagillol (**35**), a hydrolysis product of fumagillin, is a convenient starting material for

producing derivatives of the core structure through reaction at the hydroxy group, and indeed a number of derivatives at this position have been prepared and investigated for anti-angiogenic activity.[99,100]

One fumagillol derivative, TNP-470 (**36**), is currently under investigation as a potential anti-angiogenic cancer therapeutic agent. The ability of **36** to inhibit endothelial cell proliferation *in vitro* is approximately 50 times higher than that of fumagillin (**34**).[98] Further *in vitro* examination of TNP-470 (**36**) has confirmed its ability to inhibit angiogenesis in a number of systems.[101,102] TNP-470 (**36**) has completed phase I trials and was found to cause only modest and reversible side effects, and led to disease stabilisation in some cases, although no objective responses were observed.[62]

The cellular target of fumagillin (**34**) and derivatives has been determined to be methionine aminopeptidase-2 (MetAP2).[103,104] MetAP2 is an intracellular peptidase that is able to catalyse the removal of N-terminal methionine residues from newly synthesised polypeptides. Fumagillin (**34**) binds in the active site of the enzyme where an histidine residue attacks the *spiro*-epoxide, leading to covalent modification and permanent inactivation of the enzyme.[105] The exact effect of MetAP2 inhibition is still not known, but it is known that fumagillin (**34**) does not cause a decrease in the bulk synthesis of

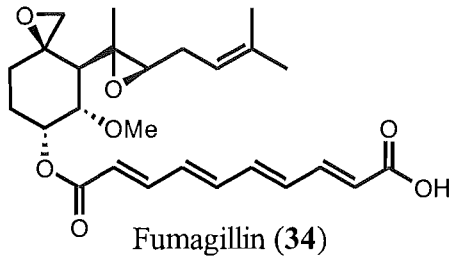

Fumagillin (**34**)

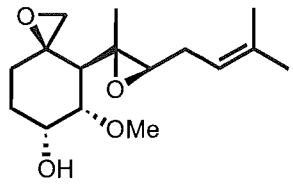

Fumagillol (**35**)

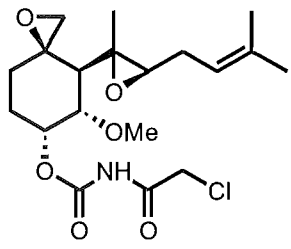

TNP-470 (**36**)

protein in affected cells, so some other downstream effect must be responsible for cessation of cell division.

The total synthesis of fumagillol has been reported, with an eleven step synthesis providing material indistinguishable from fumagillol prepared from natural fumagillin.[106] The synthesis is relatively efficient, and can be used to provide fumagillol on a medically relevant scale.

1.3 Polymer Drug Conjugates

The idea of using polymers as drug carriers was first put forward in 1975 by Ringsdorf and represents an entirely new way of transporting drugs to their target site.[107] The basic structure of a polymer drug conjugate (**Figure 1.4**) is based upon a biocompatible, water-soluble polymer to which a low molecular weight drug is attached. In order to enable the drug to be released at the target site, it is attached to the polymer by a biodegradable linker, or biolinker. The use of a polymeric scaffold presents the opportunity for attachment of other compounds, such as a second drug or a targeting residue. The conjugation of a second drug to a single polymeric backbone could be used to maximise the efficacy of a pair of drugs through synergistic effects, which are already well known in cancer chemotherapy. A targeting residue can be used to ensure selective drug delivery to the disease site.

In the absence of a targeting residue, passive targeting determines the biodistribution of a polymer drug conjugate. This is essentially the mechanism utilised by all of the low molecular weight pharmaceuticals currently used for treating cancer, in which the final distribution is determined by the body's circulatory system. With low molecular weight molecules, this results in an essentially even load through most of the body, with the liver rapidly processing the drug and the kidneys removing the drug and drug metabolites

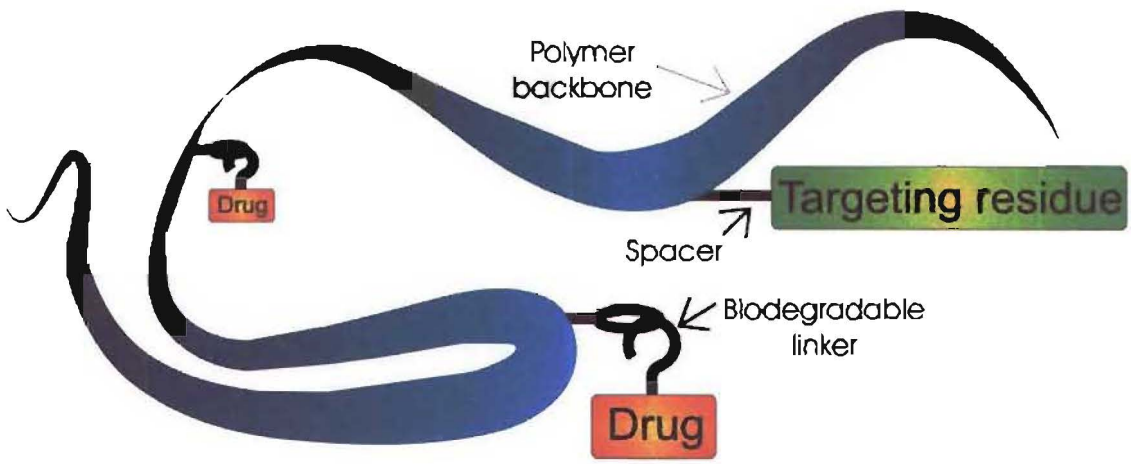

Figure 1.4 Schematic representation of a polymer drug conjugate

from the blood. This situation is far from ideal as the drug has to be administered in a high dose to achieve an effective concentration at the tumour site and also leads to extensive drug activity at non-cancerous sites.[108]

Polymer therapeutics are known to show a different biodistribution profile to low molecular weight drugs under passive targeting via a mechanism called the enhanced permeability and retention (EPR) effect (**Figure 1.5**).[109-111] The newly recruited vasculature of a tumour is incomplete, with gaps between endothelial cells which allow the extravasation of plasma and dissolved molecules. Hydrophilic polymers are not efficiently translocated across the endothelium present throughout healthy tissue, so only the 'leaky' vessels within a tumour allow a significant fraction of polymer therapeutic to escape the circulatory system. Beyond having a leaky vascular system, tumours also have poor lymphatic drainage. In ordinary tissue, plasma that escapes into the interstitial space is returned to the venous system via the lymphatic system. However, in a tumour the network of lymph vessels is not developed to the same extent as it is in non-cancerous tissue, leading to poor drainage of interstitial plasma. This reduction in interstitial drainage acts in concert with the increased rate of extravasation to cause an accumulation of solutes in a tumour. Polymers are known to be particularly susceptible to passive accumulation in tumours caused by the EPR effect, with between five and ten percent of a polymeric probe being accumulated per gram of tumour in a study using mouse models.[112] It has also been shown that the use of polymer-bound drugs leads to a

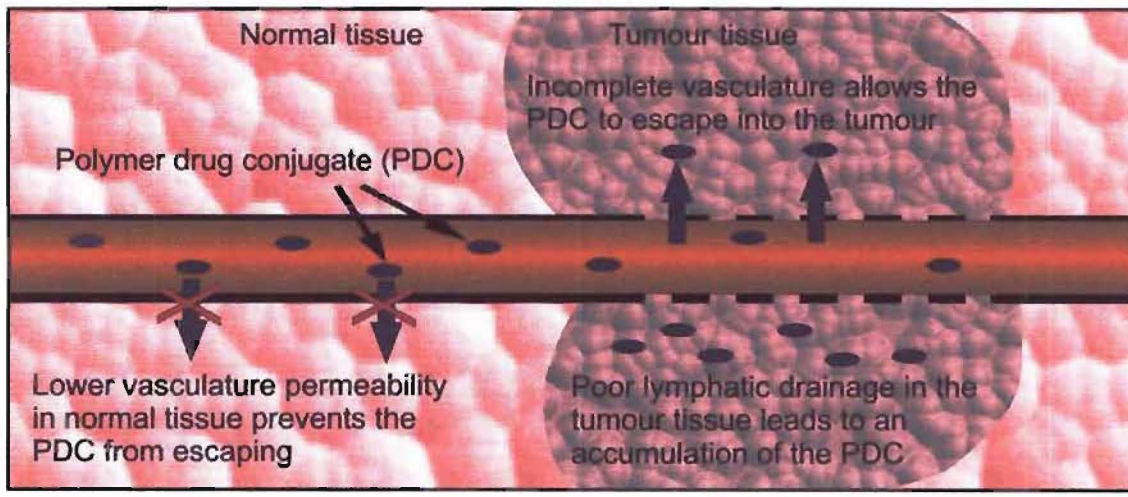

Figure 1.5 The enhanced permeation and retention (EPR) effect

more homogeneous drug distribution and thus more efficient antitumour activity within a tumour.[113]

Another advantage of polymer drug conjugates, quite unrelated to the EPR effect, is that the high molecular weights of the conjugates ensure a prolonged circulation time. One of the difficulties with using low molecular weight drugs is maintaining a therapeutic concentration of drug in the blood for any length of time without reaching a toxic concentration. The rapid elimination of low molecular weight compounds from the blood tends to lead to a treatment regime consisting of many dosings, which causes a saw-tooth like profile of drug concentration in the blood. Polymer therapeutics are only slowly eliminated from the blood compartment, thus acheiving a prolonged release type profile where a concentration within the therapeutic window can be maintained (**Figure 1.6**).[114,115] Increasing molecular weight has been shown to lead to longer circulation times and an increase in therapeutic efficiency of polymer doxorubicin conjugates.[116]

The conjugation of highly hydrophobic drugs to a hydrophilic polymer results in an overall increase in the solubility of the drug, which in some cases is an important consideration as it bypasses any requirement for drug administration via an oil or

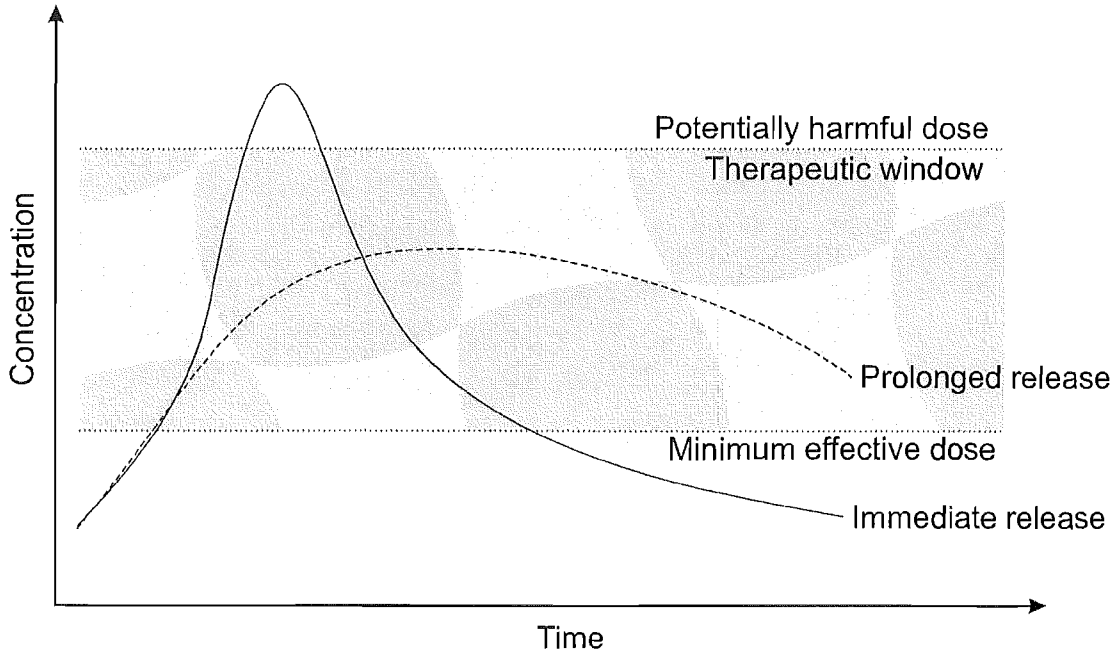

Figure 1.6 Comparison of prolonged and immediate release drug delivery

emulsion injection. The increased polarity and size of a polymer drug conjugate also lead to an alternative and more efficient mechanism of entry of the compound into cells (**Figure 1.7**).[114] Low molecular weight lipophilic drugs enter cells by simple diffusion across the plasma membrane into the cytosol, but this route is unavailable to polymer drug conjugates, which are instead taken into the cell by pinocytosis. Depending on the composition of a polymer-drug conjugate, it may be taken up by either fluid-phase, adsorptive or receptor-mediated pinocytosis.[117] Fluid-phase pinocytosis involves the capture of extracellular fluid and is the mechanism of uptake of soluble compounds which display no interactions with the cell membrane. Uptake is a slow process with a rate that is dependent solely on the concentration of the compound in the extracellular fluid. Adsorptive pinocytosis describes the uptake of compounds that interact non-specifically with the plasma membrane through either hydrophobic moeities that can insert into the membrane or cationic components that can interact with the charged phospholipid head groups on the surface of the membrane. The rate of adsorptive pinocytosis is greater than that of fluid-phase pinocytosis, due to an increase in the effective concentration of the polymer in the vicinity of the cell membrane, but the localisation remains random. Receptor-mediated pinocytosis is the uptake mode

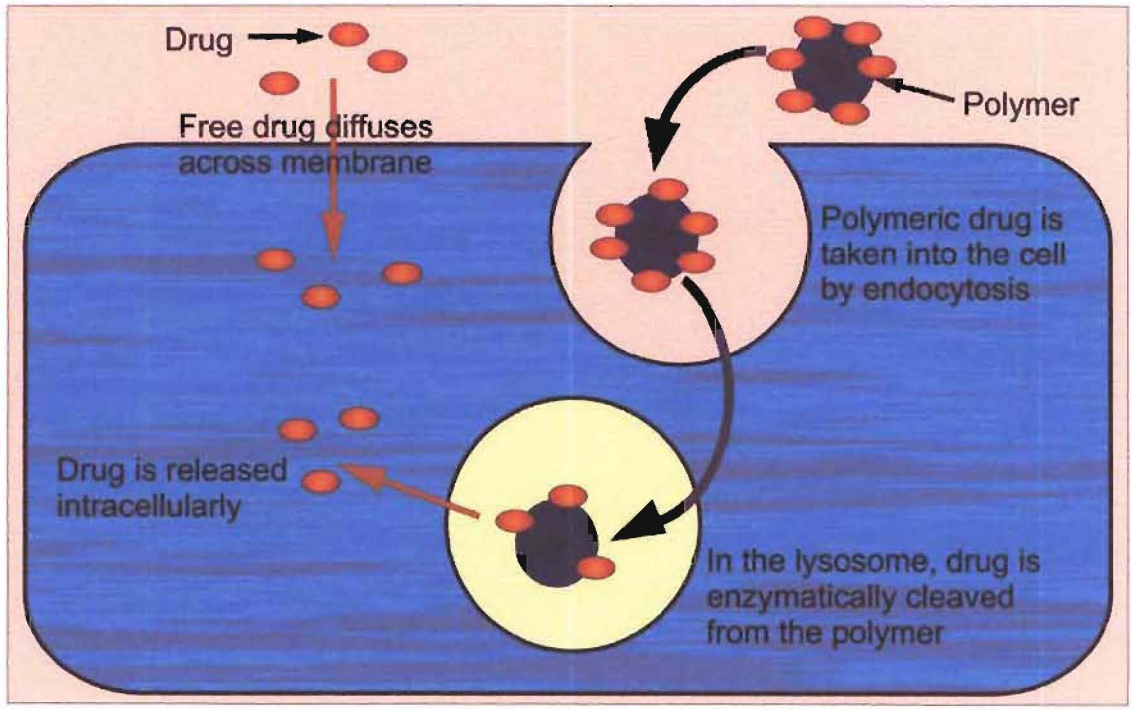

Figure 1.7 Comparison of cellular uptake of free and polymer bound drug

accessible to polymers conjugated to ligands for cell membrane receptors. These ligands can themselves be large or small molecules that bind to the receptors embedded in the cell membrane of ideally only target cells. This mode of uptake has the two advantages of targeting specific cells as well as increasing the rate of drug uptake beyond that of adsorptive pinocytosis.

Following pinocytosis, the newly formed intracellular vesicle fuses with transport vesicles from the *trans* Golgi network, leading to a progressive decrease in the pH of the vesicle as it becomes an endosome and finally a lysosome. As well as being acidic, lysosomes are rich in proteases and these two features can be harnessed to allow intracellular release of the drug from a polymer drug conjugate.[118] Just as they are unable to cross the cell membrane, polymers are unable to diffuse across the lysosomal membrane, so a release mechanism is required to free the drug which can then diffuse into the cytosol to exert its cytotoxicity.[119] The release mechanism is provided by the incorporation of a biodegradable linker between the polymer backbone and the drug moiety. Researchers have investigated the use of pH sensitive biolinkers,[120-122] but there is only a difference of about two pH units between the blood (pH 7.4), where the biolinker should be completely stable, and the lysosome (pH 5.5), where the biolinker should be rapidly degraded, so it has proven difficult to achieve the desired properties. Another possibility is to take advantage of the degradative enzymes that are found in the lysosome and not at significant levels elsewhere. To this end, peptide biolinkers have been developed that are totally stable in circulation, but are rapidly degraded by the peptidases of the lysosome.[123-125]

1.3.1 HPMA Copolymer Conjugates

Drug conjugates utilising *N*-(2-hydroxypropyl)methacrylamide (HPMA) copolymer as the backbone are amongst the earliest developed and most extensively studied.[126] HPMA is a hydrophilic, non-immunogenic and biocompatable polymer that was originally

developed as a plasma expander.[127]

PK1 (**37**) is a simple HPMA based drug conjugate containing doxorubicin conjugated to the polymer backbone by a Gly-Phe-Leu-Gly peptidyl biolinker. PK1 (**37**) has been found to be more effective than free doxorubicin in *in vivo* studies with mice,[128-130] with an apparent absence of any cardiotoxicity,[131,132] which is usually the dose-limiting toxicity in treatments with free doxorubicin. Phase I clinical trials have corroborated these results in humans, with the maximum tolerated dose being 4.5 times that of free doxorubicin.[133] PK1 (**37**) is currently undergoing Phase II clinical investigation to clarify the significance of its antitumour activity.

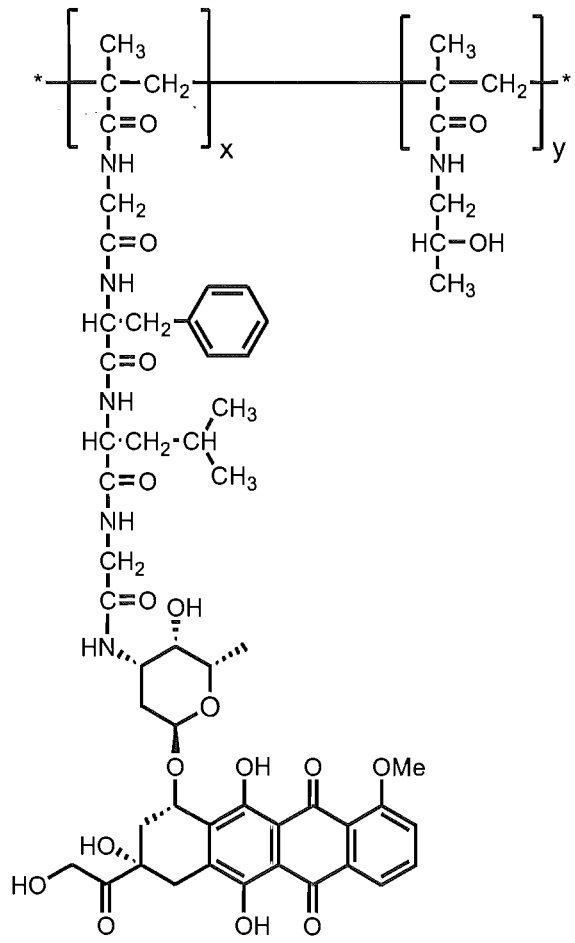

PK1 (**37**)

PK2 (**38**) is a second generation analogue of PK1 (**37**) in which a galactosamine targeting moiety has been incorporated to direct the conjugate to hepatocytes, which express the galactose-binding asialoglycoprotein receptor. Investigation of the biological distribution of PK2 (**38**) revealed that it did in fact selectively target the liver, with approximately 60% of the polymer being located in the liver after one hour, compared to 4% for the untargeted PK1 (**37**).[119] As with PK1 (**37**), PK2 (**38**) was found to possess greatly reduced cardiotoxicity compared to free doxorubicin.[134,135] PK2 (**38**) has entered phase I clinical trials and a recommended dose of 1.7 times that of free doxorubicin has been determined for future trials.[136]

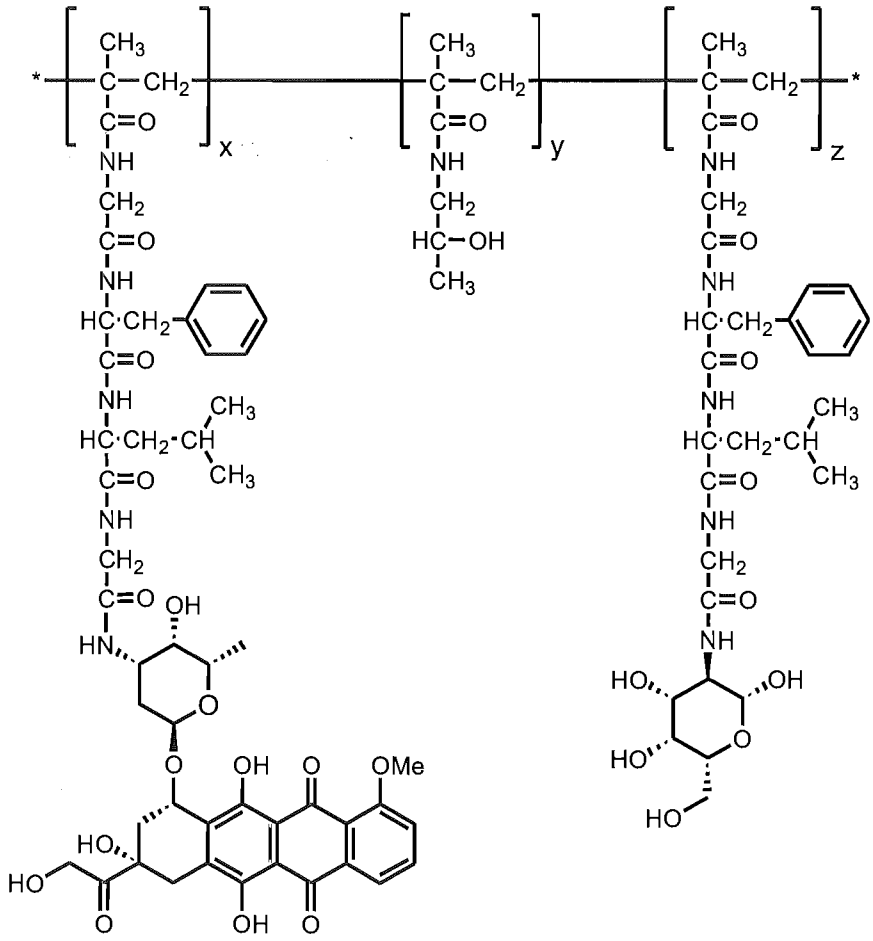

PK2 (**38**)

1.4 Aims of this work

The primary aim of the work presented in this thesis is to prepare polymer drug conjugates that are targeted to tumour neovasculature. This approach seeks to utilise the remarkable targeting properties of the small peptides discovered by Arap et al. (see Section **1.1.2.1**) in concert with the pharmacological advantages presented by a polymeric scaffold. In particular, the polymer was seen as providing a longer circulation time and reduced immunogenicity. The EPR effect was not a primary reason for moving to a polymeric structure as the active targeting was designed to ensure appropriate drug distribution.

The preparation and testing of polymers targeted to the developing tumour vasculature was undertaken as a proof of principle investigation to determine whether small targeting residues are able to direct the localisation of a much larger polymer to specific cells in the body. If this is found to be the case, it opens a number of possibilities for targeting not only the tumour vasculature, but any cellular address within the body. Researchers have previously demonstrated the ability of large molecules such as antibodies and proteins to target polymer drug conjugates.[137] Galactosamine has also been used to successfully target hepatocytes. The use of small peptidic targeting residues has the advantages of low molecular weight, high specificity, and provides the opportunity to develop novel sequences to target any desired tissue using the phage display libraries described previously (Section **1.1.2.1**).[65,66]

The pentapeptide *cyclo*-Cys-Asn-Gly-Arg-Cys was chosen to be used as the targeting moiety for four main reasons. First, it is a shorter peptide than the alternative RGD-4C motif, which simplifies the synthesis. Second, the RGD-4C peptide contains two aspartic acid residues, which require side chain protection whereas CNGRC contains asparagine, which can be used without any extra protection. Third, the optimal cystine bond arrangement was not defined until 2001, and there was concern prior to this that preparation of a homogeneous and active targeting component based on RGD-4C would

be difficult. Finally, the cellular target of CNGRC is the receptor aminopeptidase N, which is known to be internalised and recycled by cells.[73] This is important as it ensures that any polymer drug conjugate that binds to the receptor will be taken into the cell.

Beyond the preparation of polymer drug conjugates, a further aim of this work was to prepare monomeric conjugates which incorporated the targeting peptide, a biolinker and a drug. The testing of these low molecular weight conjugates beside their polymer-based analogues would enable some determination of the effect of the polymeric scaffold. The monomeric constructs would also allow an examination of the necessity of a biolinker, which is of interest as drug release was not addressed with the original targeted peptide-doxorubicin conjugates.[64]

Finally, the use of a number of different drug components was considered to be an important goal of this research. L-Tyrosinamide (**39**) was to be used as a drug substitute as it is a non-toxic amino acid derivative that can be radiolabelled with ^{123}I or ^{125}I for biodistribution studies.[138] The basic drug to be included was the well established and very well-researched drug doxorubicin (**19**). This would allow the effect of the targeting residue to be determined by comparison with PK1 (**37**). The anti-angiogenic compound fumagillol (**35**) was also to be used to determine whether targeting could enhance its toxicity to angiogenic cells. Finally, the marine natural products mycalamide A (**31**) and B (**32**), both discovered by researchers in the Marine Chemistry Group, were to be utilised in an attempt to control and take advantage of their extraordinary cytotoxicities.

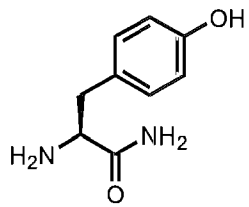

L-Tyrosinamide (**39**)

Chapter 2

Peptide Synthesis

2.1 Introduction

The chemical synthesis of peptides is a useful technique for the preparation of short oligopeptides or modified peptides which are either impractical or impossible to produce using recombinant expression systems. The central reaction sequence in peptide synthesis is the condensation of an *N*-protected amino acid with a carboxyl-protected amino acid followed by deprotection of one of the termini to allow another coupling reaction (**Figure 2.1**). This process is repeated, allowing the build-up of the full peptide sequence in an iterative manner.

There is a huge variety of protecting groups available for the termini as well as for the reactive functionalities found in the side-chains of some amino acids. The decision as to which protecting group should be used at any particular position is largely guided by both ease of use and orthogonality. For practical reasons, it is important to have relatively easily removed protecting groups on the termini of the peptide as these are the groups which must be removed most frequently. The protecting groups used on the

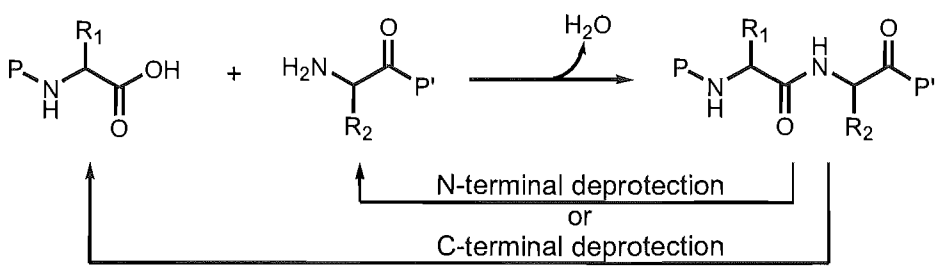

Figure 2.1 Representative peptide synthesis cycle

side-chains of amino acids are generally selected to be orthogonal, meaning they require different conditions for removal, to those on the termini. This allows the side-chains to remain protected during the peptide synthesis itself, with release of any potentially reactive groups only at the end of the synthesis.

The production of synthetic peptides was revolutionised in 1963 when Merrifield introduced the technique of Solid Phase Peptide Synthesis (SPPS).[139] This technique uses an insoluble resin in place of one the protecting groups. The preferred point of attachment of a peptide to the solid phase is at the carboxyl terminus. The primary advantage of using SPPS is that the growing peptide remains attached to the solid resin during the synthesis, allowing spent reagents to be removed from the reaction vessel by filtration. This greatly simplifies the synthetic process by obviating the need for purification after each reaction during the stepwise generation of a peptide; however, it does create a requirement for very high coupling efficiencies (ideally over 99%) because purifying the desired peptide away from a family of deletion peptides (where at least one amino acid residue is missing) can be a very difficult and time consuming task. The required reaction efficiencies can be achieved routinely using modern coupling reagents such as members of the phosphonium family (BOP, PyBOP, PyBroP) and the uronium family (HBTU, TNTU, TSTU) (**Figure 2.2**).[140]

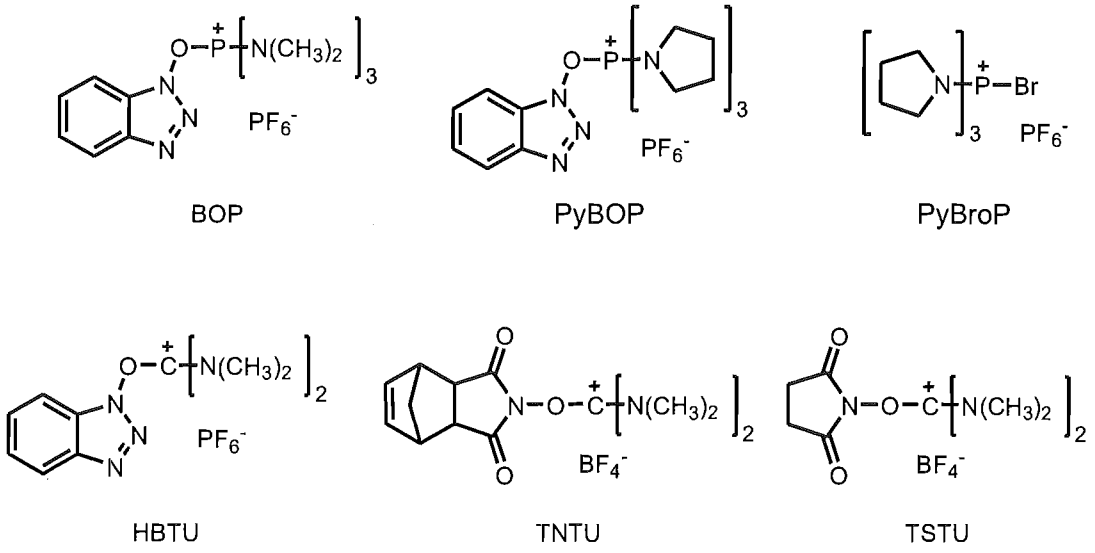

Figure 2.2 Some modern coupling reagents

There are currently two main systems commonly used for SPPS which rely on either acid-labile *t*-butyloxycarbonyl (tBoc) or base-labile fluorenylmethoxycarbonyl (Fmoc)[141,142] protection chemistry for the N-terminus of the growing peptide. The carboxyl terminus is protected by attachment to a base-labile or acid-labile solid phase respectively, thus ensuring total orthogonality between the two termini of the peptide.

The work in this project utilised only Fmoc *N*-terminal protection as the mild deprotection conditions were considered unlikely to cause degradation of chemically sensitive natural products. This provided the possibility for final deprotection of the peptides in the presence of the drug components at the end of the low molecular weight conjugate syntheses (see **Chapter 4**).

2.2 Tetrapeptide biolinker

Due to the overall strategy for the synthesis of the polymer drug conjugate, the tetrapeptide biolinker, Gly-Phe-Leu-Gly, was required in an *N*-protected form so that amine containing drugs could be coupled to the peptide without the potential for formation of polymers through coupling of unprotected tetrapeptide units. The Fmoc protecting group was chosen for *N*-protection as the gentle removal conditions were considered to be the most compatible with the natural product toxins that were to be used as the drug component.

There was no necessity for protection other than at the *N*-terminus during the synthesis of the tetrapeptide Fmoc-Gly-Phe-Leu-Gly-OH as all of the amino acid side-chains are unreactive.

2.2.1 Fmoc-Gly-Wang resin

Initially, loading of fresh Wang resin (*p*-alkoxybenzyl alcohol resin)[143] was carried out using the Sieber method recommended for high loading levels in which a high-capacity (2.07 mmol/g) resin is reacted with one equivalent of Fmoc-protected amino acid, 1.1 equivalents of 2,6-dichlorobenzoyl chloride and two equivalents of pyridine in DMF overnight.[144] During the course of this work it was found that superior results were obtained when reacting a low- to medium-capacity resin (0.83 mmol/g) with Fmoc-glycine (1.15 equiv.), 2,6-dichlorobenzoyl chloride (3.45 equiv.) and pyridine (6.9 equiv.) again in DMF overnight. On one occasion the reaction mixture was stirred at a moderate rate, and the following day all that could be recovered from the suspension by filtration was a fine white powder (where usually a granular tan solid could be expected). Examination of this powder under a light microscope revealed that the resin beads had been mechanically destroyed by the magnetic flea during the overnight stirring. After

this discovery the reaction mixture was always vigorously shaken instead of being stirred, which was found to be a suitable method for preventing damage to the resin while ensuring homogeneity of the reaction.

The determination of the level of substitution of Fmoc-protected amino acid onto the resin is a procedure which is prone some degree of error, so can only be considered to provide an approximate loading level which can be used to calculate required amounts of reagents later in the synthesis. In particular, the need to weigh very small amounts of resin (< 1 mg) accurately was the first problem. It was also found that the age of the 20% piperidine/DMF solution used in the analysis greatly affects the UV readings obtained, so it is imperative that only a freshly made solution is used, but the effect of the ages of the individual reagents remains unknown.

Once the level of Fmoc-glycine attached to the resin was determined and found to be sufficiently high (typically the loading level achieved was about 0.8 mmol/g), the remaining benzyl alcohol groups of the resin had to be end-capped. This was carried out using benzoyl chloride (4 equiv.) and pyridine (6 equiv.) in 1,2-dichloroethane. The equivalents are determined relative to the total number of potential sites of the unloaded resin, so in fact there was a huge excess of reagents as approximately 80% of the benzyl alcohol groups had already been reacted. The resin was washed and dried thoroughly prior to peptide synthesis.

2.2.2 Fmoc-Gly-Phe-Leu-Gly-Wang resin synthesis

The glassware used for all solid phase peptide syntheses allowed the resin to be agitated by bubbling N_2 through a frit and then subsequently switched to vacuum to allow drainage.

Fmoc-Gly-Wang resin was suspended in DMF and agitated for 15 minutes to preswell the resin beads, thus allowing easy access for reagents during the synthesis itself. The DMF was drained and a 20% piperidine/DMF solution was added, with bubbling, to deprotect the glycine residue. After ten minutes the reaction was drained and the resin was washed thoroughly with DMF and isopropanol. A small sample of the resin was removed and subjected to the Kaiser test (see Section **7.1**) to confirm the presence of a free amine. The resin was then rinsed again with DMF before changing the collection flask. It was found that if the collection flask was not replaced between deprotection and coupling stages, the nitrogen bubbling up through the resin could transfer piperidine vapour from the flask to the reaction suspension during coupling, which resulted in deprotection during this stage. This inevitably led to failure of the whole synthesis, so the importance of changing the collection flask cannot be overstated. The synthesis continued with the addition of a DMF solution containing Fmoc-Leucine (2 equiv.), HBTU (2 equiv.) and DIPEA (4 equiv.). After bubbling for 60 minutes, the resin was again drained, rinsed with DMF and subjected to the Kaiser test which indicated the absence of any free amine groups. The process was then repeated, with deprotection followed by coupling of Fmoc-glycine and finally Fmoc-phenylalanine. The synthesis cycle is represented in a general form in **Figure 2.3**. Following the final coupling step, the resin was washed thoroughly with DMF, MeOH and DCM before drying overnight under vacuum and in the presence of P_2O_5.

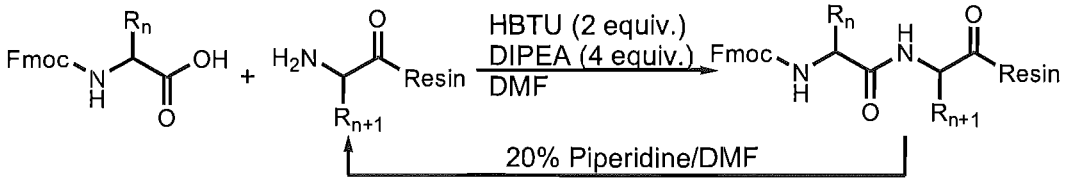

Figure 2.3 Synthetic cycle used throughout this research for peptide preparation

2.2.3 Fmoc-Gly-Phe-Leu-Gly-OH (40)

The peptide-bearing resin was cleaved twice with a strongly acidic mixture consisting of 95% TFA/2.5% H_2O/2.5% TES and rinsed with the same solution. The TES was included in the cleavage mixture as a cation scavenger, which was not entirely necessary in the case of this peptide as there are neither any sources of reactive cations from the cleavage process nor any residues which would be prone to attack; however, as the purification was easily achieved there was also no good reason to exclude TES from the reaction. The collected acidic solutions were diluted with water, which caused the formation of a soft, gel-like white precipitate and extracted with DCM. The combined organic fractions were taken to dryness and the solid residue was re-dissolved in THF, which was added to an excess of hexane to precipitate the pure peptide in a 36% yield. While this yield is lower than desired, the ease of synthesis and purification made the solid phase process a viable option.

2.2.4 Characterisation of Fmoc-Gly-Phe-Leu-Gly-OH (40)

The proton and carbon NMR spectra of Fmoc-Gly-Phe-Leu-Gly-OH (**40**) were readily assignable from COSY, HSQC and CIGAR 2D NMR experiments. The chemical shifts for the proton and carbon NMR spectra are shown in **Table 2.1** with the structure and important CIGAR correlations shown in **Figure 2.4**.

An obvious starting point for assigning the structure was the geminal methyl groups of leucine, H16 and H17 at 0.97 and 0.93 ppm respectively. COSY correlations enabled the stepwise identification of H15, H14, the α-proton H13 and amide NH12 in that order, with the HSQC spectrum providing the chemical shifts of all the corresponding carbon atoms. CIGAR correlations confirmed the structure of the leucine residue and provided the important inter-residue linkages from NH12 to the neighbouring carbonyl at C11 and also from H13 to the carbonyls at C11 and C18. C18 was also seen by the

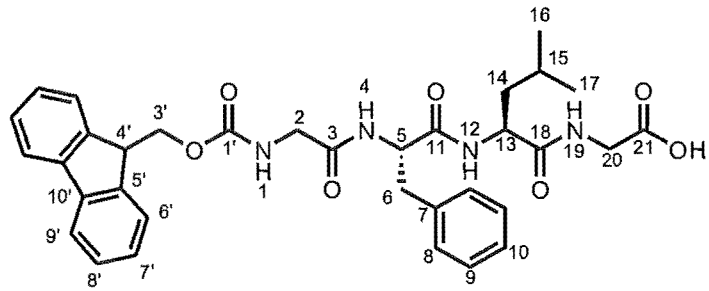

Fmoc-Gly-Phe-Leu-Gly-OH (**40**)

Table 2.1 Proton and carbon NMR data for **40** obtained in d_6-DMSO

Position	^{1}H	^{13}C	COSY	CIGAR
1	7.62		H2a, H2b	
2a	3.73	43.3	H1, H2b	C3, C1'
2b	3.61	43.3	H1, H2a	C3, C1'
3		169.6		
4	8.10		H5	C3
5	4.65	54.3	H4, H6a, H6b	C3, C6, C7, C11
6a	3.12	37.6	H5, H6b	C7, C8, C11
6b	2.88	37.6	H5, H6a	C7, C8, C11
7		138.3		
8	7.31	129.8		C6, C7, C8, C9, C10
9	7.31	128.5		C6, C7, C8, C9, C10
10	7.26	126.8		C6, C7, C8, C9, C10
11		171.7		
12	8.22		H13	C11
13	4.44	51.4	H12, H14	C11, C14, C15, C18
14	1.58	41.5	H13, H15	C13, C16, C17, C18
15	1.70	24.7	H14, H16, H17	
16	0.97	23.5	H15	C14, C15, C17
17	0.93	22.3	H15	C14, C15, C16
18		172.9		
19	8.19		H20a, H20b	C18, C20
20a	3.86	41.2	H19, H20b	C21
20b	3.81	41.2	H19, H20a	C21
21		172.0		
1'		157.2		
3'	4.35	66.3		C1', C4', C5'
4'	4.31	47.1		C3'
5'		144.0		
6'	7.80	125.9	H7'	C4', C8' C10'
7'	7.42	127.7	H6', H8'	C5', C9'
8'	7.51	128.3	H7', H9'	C6', C10'
9'	7.99	120.7	H8'	C5', C7', C10'
10'		141.5		

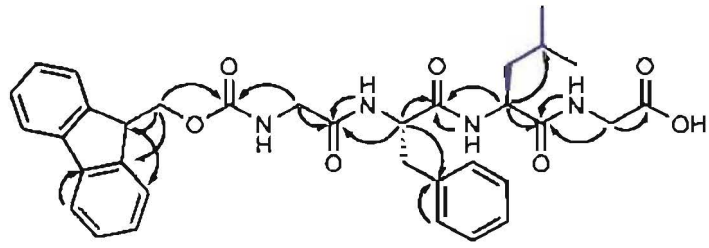

Figure 2.4 Important COSY (blue bonds) and CIGAR (black arrows) correlations observed for **40**

amide NH19, which showed a correlation to C20. The diastereotopic protons H20a and b were readily identified through HSQC correlations and in turn indicated the carbonyl C21, which was not correlated to any other protons, thus implying the presence of the expected C-terminal acid group. Referring back to the leucine residue, the carbonyl at C11 was observed to show a correlation from protons H5, H6a and H6b of the phenylalanine residue. These protons were all correlated to each other in the COSY spectrum, indicating the presence of an ABX system, and the HSQC spectral data confirmed the connectivity of H6a and H6b to C6 as well as providing the chemical shift of C5. H5 provided a CIGAR correlation to the relatively downfield, non-protonated aromatic carbon C7, and H6a,b provided correlations further into the aromatic ring to C8. The proton shifts of the phenylalanine aromatic ring were overlapping and not clearly identifiable in the proton spectrum; however, COSY, HSQC and CIGAR spectra clearly showed all of the expected correlations. The connection to the *N*-terminal glycine residue was provided by CIGAR correlations to the carbonyl C3 from both the α-proton H5 and the amide NH4 (which was in turn identified by a COSY correlation from H5). The glycine residue itself was identified by the diastereotopic protons H2a and H2b which showed CIGAR correlations to C3 and the distinctively upfield carbamate carbonyl C1'. HSQC spectroscopy gave the chemical shift of C2, and the COSY spectrum provided the chemical shift of NH1. Interestingly, NH1 did not show any correlations in the CIGAR spectrum which was unexpected given that all of the main chain amide protons had shown clear correlations to their neighbouring carbonyl carbon. The reason for this is not known, but carbamate protons in other peptides prepared also failed to show CIGAR correlations to neighbouring carbonyl groups so this would seem to be a general property of carbamates. H3' showed CIGAR correlations to C1', C4' and

C5', thus clearly indicating its position in the molecule. H4' shared a COSY correlation with H3', but did not provide any CIGAR correlations deeper into the aromatic ring(s) of the Fmoc group. The protons H6' to H9' were clearly identified by their relationships in the COSY spectrum, and their orientation was indicated by a CIGAR correlation from H6' to C4'. The last remaining chemical shift, that of C10', was provided by CIGAR correlations from H6', H8' and H9'.

The molecular formula for **40**, $C_{34}H_{38}N_4O_7$, was obtained by HRESIMS as the protonated adduct with a mass of 615.28 (1.95 ppm).

An analytical HPLC injection (C18, A: H_2O(A), B: ACN, gradient I) showed a single peak at a retention time of 15.37 min with a characteristic UV chromophore representing the Fmoc group of the tetrapeptide.

2.3 Targeting peptide

The targeting peptide, *cyclo*-Cys-Asn-Gly-Arg-Cys, was required in two forms – fully protected for coupling to the biolinker tetrapeptide to produce low molecular weight targeted drugs, and cyclised and fully deprotected for coupling directly to the polymer to produce the high molecular weight targeted drugs.

As with the biolinker synthesis, Fmoc was used for protection of the N-terminus. This was due to the need for deprotection in the presence of the drug components in the case of the low molecular weight conjugates.

The protecting group that was chosen for the cysteine residues was acetamidomethyl (Acm). There were a number of reasons for selecting this protecting group over other available options. Due to the need to prepare the targeting peptide in a fully protected form, it was not possible to use the most common cysteine derivative, *S*-trityl cysteine, as this protecting group is removed by TFA so would not survive cleavage of the peptide from the resin. Acm, along with a number of other groups, can be removed with concomitant oxidation to form a disulfide.[145] This process can be carried out while the peptide is still attached to the resin, providing a pseudo-dilution effect leading to the preferential formation of intramolecular disulfides. In the case of Acm, the deprotection-oxidation can be carried out using either I_2 or thallium (III) salts, which provides a degree of flexibility not offered by other groups which allow direct disulfide bond formation under only one set of reaction conditions each. The final advantage of the Acm group is its polarity which helps to prevent hydrophobic collapse of the resin-bound peptide by ensuring efficient solvation.

The nucleophilic guanidine of arginine was protected using the 4-methoxy-2,3,6-trimethylbenzenesulfonyl (Mtr) derivative. This was the most suitable protecting group as the nitro derivative, which is the only commercially available non-acid labile option, is prone to side reactions during acylation and cleavage as well as being incompatible with a disulfide due to its requirement for reductive cleavage. The remaining options are all

sulfonyl derivatives which display varying degrees of acid lability. Mtr was chosen as it is intermediate in lability, so could be removed without the need to resort to extreme conditions but could also be retained during removal of the peptide from the resin.

2.3.1 Fmoc-Cys(Acm)-Wang resin

Although this reaction was carried out in exactly the same manner as that described already for the loading of Fmoc-glycine onto Wang resin, the actual levels of substitution achieved were consistently lower than those achieved using the other amino acid. The reasons for this are unknown; however, a variation in the loading level achieved dependent on amino acid is well known, leading to the possibility of steric hindrance, electronic effects, or a combination of the two being likely cause(s).

2.3.2 Fmoc-Cys(Acm)-Asn-Gly-Arg(Mtr)-Cys(Acm)-Wang resin

The synthesis of this resin-bound peptide was initially carried out in exactly the same manner as described earlier for Fmoc-Gly-Phe-Leu-Gly-Wang. For the final two coupling reactions with Fmoc-asparagine and Fmoc-cysteine(Acm), HOBt (2 equiv.) was added to help prevent any dehydration of the asparagine amide side chain, which is a known side-reaction during peptide synthesis using unprotected asparagine (**Figure 2.5**).[141,146]

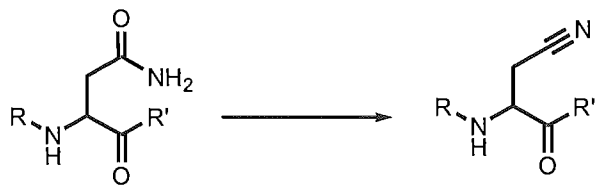

Figure 2.5 Conversion of asparagine to β-cyanoalanine under dehydrating conditions

Despite this precaution, the product of the synthesis when HOBt was included was still found to contain a sizable proportion (approximately one third of the total peptide present) of asparagine-dehydrated peptide.

While methods for the conversion of nitriles to amides have been reported,[147-149] it was felt that the most efficient technique would be to prevent the formation of the nitrile in the first place, so another synthesis of the peptide was carried out, with the HOBt additive replaced by *N*-hydroxysuccinimide. As *N*-hydroxysuccinimide esters are somewhat less 'activated' than HOBt esters, it was hoped that NHS might provide superior protection. This was found to be the case; in fact, with the addition of NHS, no dehydrated product could be detected by HPLC (C18, A: H_2O(A), B: ACN, gradient I) or ESIMS (**Figure 2.6**).

2.3.3 Fmoc-Cys(Acm)-Asn-Gly-Arg(Mtr)-Cys(Acm)-OH (41)

The protected targeting peptide was cleaved from the resin with a TFA solution containing phenol as a cation scavenger, and the acidic solution was diluted with water

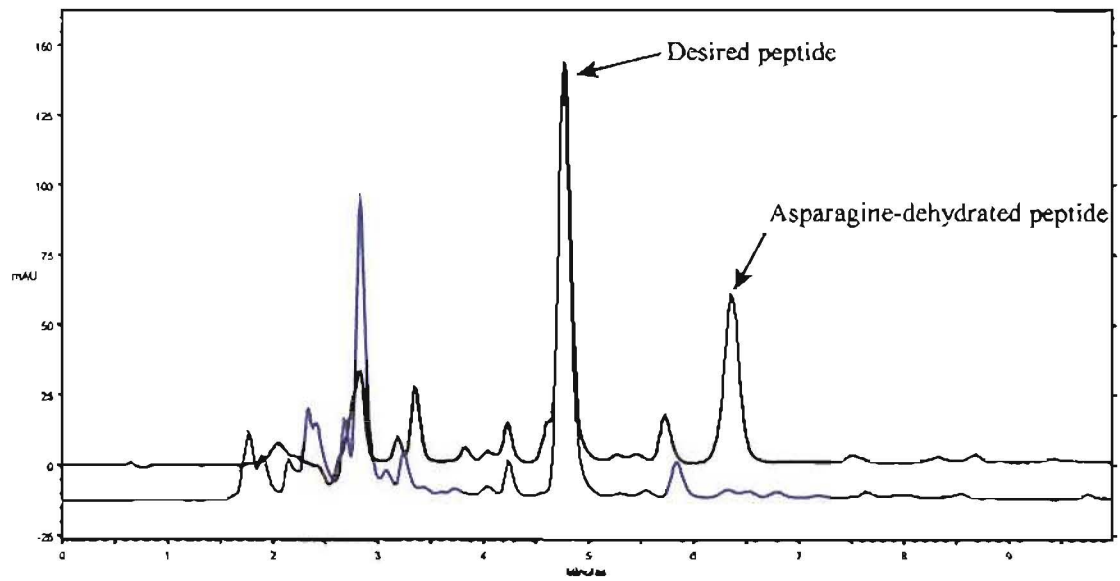

Figure 2.6 HPLC chromatogram of crude peptide from synthesis incorporating HOBt (black trace) and NHS (blue trace) to reduce asparagine dehydration

and dried immediately to prevent cleavage of the acid labile Mtr protecting group.

Initially, a small scale attempt at purification was carried out using normal phase chromatography on a bed of silica by diluting the combined acidic cleavage solutions with acetone, applying to the top of the dry silica bed then eluting with acetone, ACN and 20% H_2O/ACN. The desired peptide material eluted in the third fraction but was heavily contaminated with silica as well as retaining the initial contaminants. Other eluant systems attempted for silica chromatography on a small, trial scale, were a stepped gradient consisting of DCM, 1:1 DCM:acetone, acetone, 1:1 acetone:ACN, ACN, 1:1 ACN:MeOH and MeOH, in which the peptide eluted in the final, methanolic, fraction; and a gradient from 50% MeOH/ACN to 100% MeOH in 10% steps in which **41** eluted over the first three fractions. None of the silica chromatography carried out was successful in providing a significant purification of the peptide.

The combined peptide-containing fractions were dried and subjected to reverse phase chromatography using the MPLC system running an isocratic 80% MeOH/H_2O eluant with detection at 254 nm; however, the separation was poor, with both the desired peptide **41** and its asparagine dehydrated counterpart co-eluting.

Purification was then attempted using preparative HPLC (Dynamax C18) with a gradient running from 40% ACN/H_2O(A) to 60% ACN/H_2O(A) over 20 minutes with UV detection at 254 nm. Peaks eluting at 14 minutes and 18 minutes were collected and found by LRESIMS to be the desired peptide **41** and the dehydrated derivative respectively. While this did provide the pure peptides as desired, it was far too laborious and time-consuming to be carried out on as large a scale as required, thus work continued toward determining an appropriate preparative purification technique.

Purification was carried out using reverse phase MPLC run using an isocratic 50% ACN/H_2O(A) eluant, collecting three cuts – early, middle and late. The middle cut was pure except for the presence of a single contaminating *p*-substituted aromatic compound which co-eluted even under analytical HPLC conditions (C18, A: H_2O(A), B: ACN, gradient: 50% B (0 min), 50% B (4 min), 56% B (7 min), 100% B (8 min)) .

In order to remove this lower molecular weight contaminant, size exclusion chromatography was attempted using LH20 with MeOH as the eluting solvent but no separation was achieved – both high and low molecular weight compounds eluted together in one very broad peak. The chromatography was then repeated using 50% ACN/H_2O as the eluant, which was found to be a far superior solvent system. The first peak, eluting at a volume of approximately 270 mL consisted of primarily the desired peptide **41**.

It was found that by an iterative cycle of MPLC and size exclusion chromatography the fully protected peptide **41** could be isolated in a very pure state with a yield of 6.6%.

2.3.4 Characterisation of fully protected CNGRC (41)

Due to the poor solubility of **41** in nearly all solvent systems, a solvent mixture of 50% CD_3CN/D_2O had to be used for the NMR analysis. The presence of deuterated water resulted in the immediate exchange of all of the amide protons and hence they were not observed in any of the spectra. A full assignment of the proton and carbon chemical shifts was achieved using COSY, HSQC, CIGAR and IMPRESS 2D NMR experiments. The IMPRESS experiment is a variation of the CIGAR experiment which provides very high resolution over a short chemical shift range in the carbon dimension. It was necessary to use the IMPRESS experiment to resolve the different carbonyl chemical shifts because **41** contains eight amide carbonyls, which are spread over a range of only 3.2 ppm, and with a resolution of approximately 1 ppm, a regular CIGAR experiment is unable to differentiate most of these carbon atoms. The chemical shifts for the proton and carbon NMR spectra are shown in **Table 2.2** with the structure and important COSY, CIGAR and IMPRESS correlations shown in **Figure 2.7**.

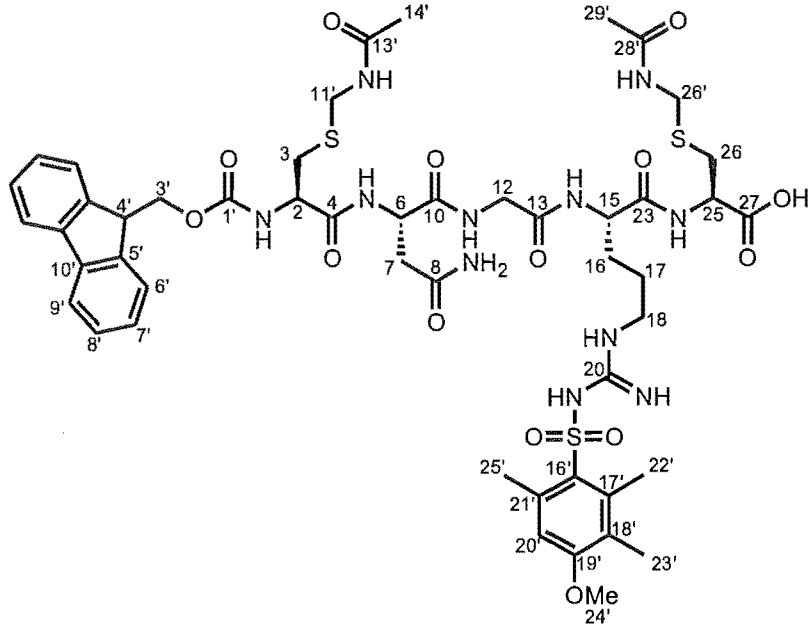

Fmoc-Cys(Acm)-Asn-Gly-Arg(Mtr)-Cys(Acm)-OH (**41**)

Table 2.2 Proton and carbon NMR data for **41** obtained in 50% CD_3CN/D_2O

Position	^1H	^{13}C	COSY	CIGAR	IMPRESS
2	4.38	54.2	H3a, H3b	C1'	C4
3a	3.03	31.8	H2	C2, C11'	C4
3b	2.82	31.8	H2	C2, C11'	C4
4		171.5			
6	4.65	50.7	H7	C7	C4, C8, C10
7	2.78	36.4	H6	C6	C8, C10
8		173.3			
10		171.8			
12a	3.91	42.9			C10, C13
12b	3.82	42.9			C10, C13
13		170.1			
15	4.32	52.6	H16a, H16b	C16	C13, C23
16a	1.79	27.9	H15, H17	C15	
16b	1.68	27.9	H15, H17	C15	
17	1.52	25.7	H16a, H16b, H18		
18	3.12	40	H17		
23		172.3			
25	4.57	52.2	H26a, H26b	C26	C23, C27
26a	3.08	31.3	H25	C25, C26'	C27
26b	2.93	31.3	H25	C25, C26'	C27
27		172			
1'		156.7			
3'a	4.39	66.5		C1', C4', C5'	

3'b	4.34	66.5		C1', C4', C5'	
4'	4.27	46.4		C3', C5', C6', C10'	
5'		143.4			
6'	7.71	124.9	H7'	C8', C10'	
7'	7.38	126.9	H6', H8'	C5', C6', C8', C9', C10'	
8'	7.46	127.4	H7', H9'	C5', C6', C9', C10'	
9'	7.85	119.6	H8'	C5', C6', C7', C10'	
10'		140.6			
11'a	4.2	40			C13'
11'b	4.34	40			
13'		172.3			
14'	1.95	21.64			C13'
16'		132.9			
17'		138.1			
18'		124.3			
19'		158.2			
20'	6.71	111.7		C18', C25'	
21'		131.4			
22'	2.55	17.3		C17', C16', C18'	
23'	2.1	10.8		C17', C18', C19'	
24'	3.82	55		C19'	
25'	2.63	22.8		C16', C20', C21'	
26'	4.27	40.6		C26	C28'
28'		172.1			
29'	1.94	21.6			C28'

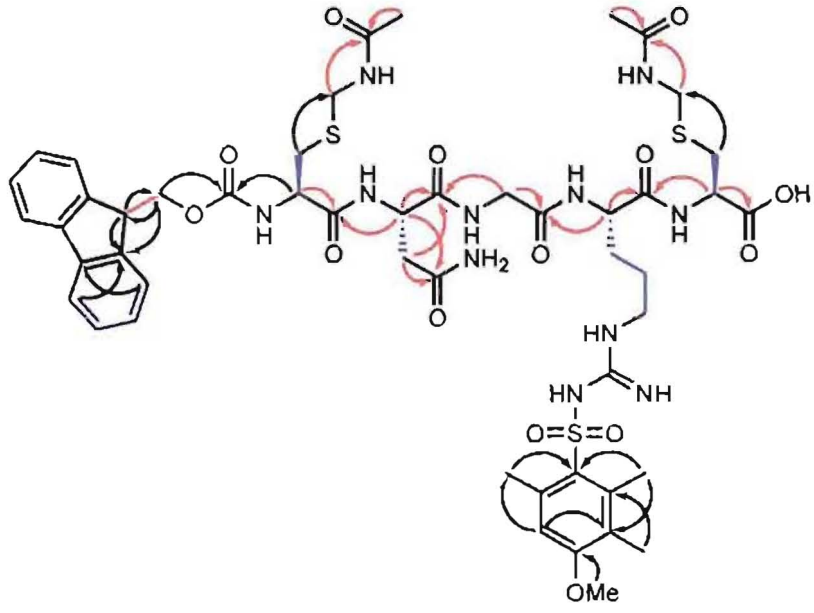

Figure 2.7 Important COSY (blue bonds), CIGAR (black arrows) and IMPRESS (red arrows) correlations observed for **41**

Individual residues were identified primarily using the COSY spectrum to elucidate the side chain proton resonances using the α-protons as starting points. With the proton chemical shifts in hand it was easy to determine the chemical shifts of the corresponding carbon atoms using the HSQC spectrum. The final step involved confirming that the peptide sequence was the desired one using CIGAR and IMPRESS correlations to observe inter-residue correlations from α-protons to amide carbonyls. In the case of this structure, the elucidation was started using the Fmoc group with its characteristic upfield carbonyl resonance as an entry point and proceeded along the peptide toward the C-terminus.

In general the assignment was straightforward; however, the β-protons and carbons of the two cysteine residues have very similar chemical shifts and it was necessary to examine the CIGAR correlations from both the α-protons and the methylenes of the acetamidomethyl protecting groups very carefully to clearly assign them. A final point of difficulty concerned the arginine protecting group. Due to the number of intervening bonds, it is not possible to directly confirm attachment of the protecting group; however, the full structure of the methoxytrimethylphenyl skeleton itself was elucidated. As there was no way to confirm the point of attachment, it was assumed that the protecting group had remained attached in the indicated position.

The molecular formula for **41**, $C_{49}H_{65}N_{11}O_{14}S_3$, was confirmed using HRESIMS in which the protonated adduct at 1128.39 (0.53 ppm) was observed.

An analytical HPLC injection (C18, A: H_2O(A), B: ACN, gradient: 50% B (0 min), 50% B (4 min), 56% B (7 min), 100% B (8 min)) showed a single peak at a retention time of 4.96 min which had a UV spectrum characteristic of the Fmoc protecting group.

2.3.5 *cyclo*-Cys-Asn-Gly-Arg-Cys-OH (42)

Following cysteine deprotection and oxidation, the N-terminus of the peptide was deprotected and *cyclo*-Cys-Asn-Gly-Arg-Cys-OH (**42**) was removed from the resin using a 95% TFA/5% H_2O solution which had been determined to be the optimal cleavage brew as described in Section **2.4.2.1**. The peptide was allowed to sit for 24 hours in the cleavage solution to allow the Mtr protecting group to be removed from the arginine residue then the TFA was removed to provide the crude peptide mixture.

The crude peptide mixture was dissolved in a minimal volume of water and applied to a C18 column that had been equilibrated to water. The column was then eluted with H_2O, 5% ACN/H_2O, 10% ACN/H_2O, 50% ACN/H_2O and finally 100% ACN with the peptide eluting in the first two fractions.

Due to the presence of the extremely basic arginine residue in this peptide, it was thought that ion-exchange chromatography may have been a suitable technique for purification. Initially, this was attempted on a small scale using strong cation exchange resin (Bond Elut SCX). The column was washed with ACN to prime it, then equilibrated to H_2O before addition of the peptide in distilled water. The column was eluted with a series of acidic washes consisting of 0.1% TFA/H_2O, 1% TFA/H_2O, 10% TFA/H_2O and 100% TFA; however, none of these fractions contained **42** so the column was finally washed with concentrated NH_4OH which did elute the peptide. Unfortunately the strongly basic eluant appeared to have damaged the column packing as a new contaminant co-eluted with the peptide, so the use of strong cation exchange was abandoned.

Weak cation exchange was attempted on a small scale (Bakerbond CBX) column which was primed with ACN then equilibrated to 0.1% concentrated NH_4OH/H_2O before application of the sample and initial elution in 0.1% concentrated NH_4OH/H_2O. The column was then run with water increasing in TFA concentration from 10^{-5}% to 0.1% by an order of magnitude each time. **42** eluted, along with all of the initial contaminants, in the first, ammoniacal, fraction and the last acidic fraction, which were combined and rerun with similar results.

An attempt was made to purify the material using normal phase chromatography on a 'flash' silica column with 0.1% TFA/H_2O as the eluant. As expected, **42** was late eluting; however, it came off as a very broad peak over three fractions and was still not pure so the use of normal phase chromatography was abandoned.

The combined silica fractions were evaporated to dryness and the material therein dissolved in water, filtered to remove silica that had leached from the column, and subjected to semi-preparative HPLC, which was successful in purifying **42**.

A second batch of peptide was taken directly from the first crude C18 purification to semi-preparative HPLC as described until enough mass was obtained for polymer synthesis at which point semi-preparative HPLC was halted and the remaining crude material stored.

2.3.6 Characterisation of *cyclo*-Cys-Asn-Gly-Arg-Cys-OH (42)

Due to the extreme polarity of **42**, no exchangable protons were observed in the NMR spectra as all experiments had to be run using D_2O. The proton and carbon spectra were fully assigned using COSY, HSQC and CIGAR 2D NMR experiments to confirm the assignments shown in **Table 2.3**. The important CIGAR correlations are shown in **Figure 2.8**.

The COSY spectrum allowed the rapid identification of the isolated spin systems corresponding to the five amino acids, with the HSQC spectrum providing the chemical shifts for all of the protonated carbon atoms. The connectivity of the amino acids was confirmed using the CIGAR correlations from the α-protons to neighbouring amide carbonyls. As in the case of **41**, the cystine residues have similar proton and carbon

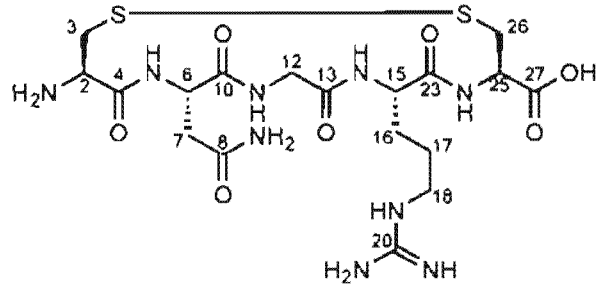

cyclo-Cys-Asn-Gly-Arg-Cys-OH (**42**)

Table 2.3 Proton and carbon NMR data for **42** obtained in D_2O

Position	^1H	^{13}C	COSY	CIGAR
2	4.07	52.9	H3a, H3b	C3, C4
3a	3.22	41.2	H2, H3b	C2, C4
3b	3.14	41.2	H2, H3a	C2, C4
4		167.3		
6	4.8	50.2	H7a, H7b	C4, C7, C8, C10
7a	2.73	36.2	H6, H7a	C6, C8, C10
7b	2.61	36.2	H6, H7b	C6, C8, C10
8		174.1		
10		171.7		
12a	4.04	42.4	H12b	C10, C13
12b	3.55	42.4	H12b	C10, C13
13		170.8		
15	4.18	53.6	H16a, H16b	C13, C16, C23
16a	1.74	27.3	H15, H16b, H17	C15
16b	1.66	27.3	H15, H16a, H17	
17	1.56	24.2	H16a, H16b, H18	
18	3.11	40.6	H17	C16, C17, C20
20		156.8		
23		173.9		
25	4.56	52.4	H26a, H26b	C23, C26, C27
26a	3.27	40.2	H25, H26a	C27
26b	3.01	40.2	H25, H26b	C25, C27
27		173.2		

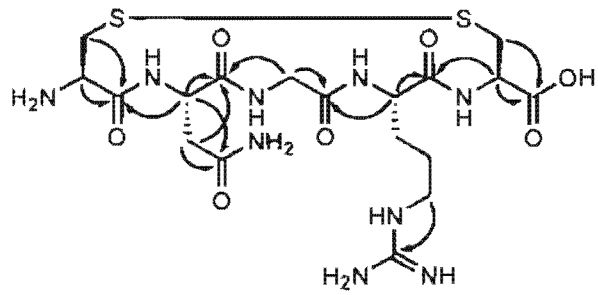

Figure 2.8 Important COSY (blue bonds) and CIGAR (black arrows) correlations observed for **42**

chemical shifts; however, these were easily distinguished through correlations from their quite distinct α-protons.

The molecular formula of **42**, $C_{18}H_{31}N_9O_7S_2$, was confirmed using HRESIMS in which the protonated adduct at 550.19 (0.73 ppm) was observed.

An analytical HPLC injection (C18, A: H_2O(A), B: ACN, gradient: 0% B (0 min), 0% B (4 min), 5% B (9 min), 100% B (10 min)) showed a single peak at a retention time of 7.95 min.

2.4 Targeted biolinker nonapeptide

The initial strategy for the synthesis of this peptide was to couple the already prepared fragment **41** to the resin bound biolinker. The use of fragment condensation strategies in the synthesis of oligopeptides is a well known and often successful approach that can help to improve the proportion of desired product in the crude material, thus simplifying purification.[141]

2.4.1 Fmoc-*cyclo*-Cys-Asn-Gly-Arg-Cys-Gly-Phe-Leu-Gly-OH (43)

Fmoc-Gly-Phe-Leu-Gly-Wang resin was deprotected and then coupling to the fully protected peptide **41** (0.9 equiv.) was attempted. The resin-bound peptide fragment was used in a slight excess as the protected peptide **41** was more valuable due to the laborious purification procedure carried out on it. After the standard one hour reaction time for coupling, the resin was drained and washed. The washings were collected and analysed by HPLC (C18, A: H_2O(A), B: ACN, gradient: 50% B (0 min), 50% B (4 min), 56% B (7 min), 100% B (8 min)) which revealed the presence of **41**. Due to the value of this peptide, these washings were dried down and stored to allow the later recovery of the peptide.

The peptide could have been cyclized and cleaved from the resin at this point; however, the free amine groups of the unreacted tetrapeptide had the potential to cause problems later on. The primary concern was that the amines could have catalysed the removal of the base-labile Fmoc protecting group which was required on the *N*-terminus of the nonapeptide. It is known that primary amines are generally able to cause only the very slow removal of Fmoc; however, the consequence of any slow deprotection would have been dire so all remaining free amine groups were acetylated with acetic anhydride.

Following cysteine deprotection and oxidation to form the cyclic peptide, the peptide was cleaved from the resin using an acidic mixture consisting of 87% TFA/8% phenol/5% H_2O. The peptide was left in this acidic mixture and the cleavage of the Mtr protecting group from the side chain of the arginine residue was monitored by HPLC (C18, A: H_2O(A), B: ACN, Gradient II). After 60 hours, the peptide was found to be fully deprotected so the cleavage mixture was removed to furnish the crude mixture containing Fmoc-*cyclo*-CNGRCGFLG-OH (**43**).

2.4.1.1 Purification of Fmoc-*cyclo*-CNGRCGFLG-OH (43)

The crude peptide material was dissolved in 50% ACN/H_2O and filtered to remove the insoluble material. A preliminary purification, aimed at removing all or most of the phenol which was included in the cleavage solution, was carried out using size exclusion chromatography. The soluble material was chromatographed on LH20, eluting with 50% ACN/H_2O. The material eluted from the column as one broad peak by UV detection at 254 nm, but fractions were taken across the peak despite the lack of clear separation. The peptide was found by mass spectrometry to be located in two of the early fractions along with a significant amount of contamination. The main contaminant, as determined by mass spectrometry, had a molecular mass of 464 Da, which does not correspond to any of the expected products of the synthesis. NMR spectroscopy clearly showed that the most abundant compound in the fraction contained an easily identified leucine residue, so it must have been a derivative of the tetrapeptide biolinker. Unfortunately, the NMR spectrum did not contain obvious peaks corresponding to an arginine residue, leading to the suspicion that the nonapeptide was only a minor component of the mixture. The insoluble material that was removed prior to size exclusion chromatography was analysed by HPLC (C18, A: H_2O(A), B: ACN, Gradient II) and found to have a similar make-up to the peptide-containing fractions from the LH20.

Because the major component of the contaminated peptide did not appear to contain an arginine residue, it was thought that cation-exchange chromatography could selectively retain **43**. A small sample of the contaminated peptide was subjected to weak cation-exchange chromatography on a Trisacryl M CM column which was equilibrated to 30% ACN/H_2O before application of the sample and elution with 30% ACN/H_2O followed by 30% ACN/H_2O + 0.1% TFA. The desired product eluted in the first two, non-acidified fractions, which was unexpected. Possible reasons for this failure could have been the high proportion of acetonitrile included in the eluant, which was necessary to prevent precipitation, or not using buffered solutions. Buffers were not used because this would have resulted in salt contamination of the product, which would have caused difficulties with removal as well as determination of the extent of contamination, as most salts used for buffer formation are spectroscopically silent.

The material was then chromatographed on a silica column running 50% ACN/H_2O + 0.1% TFA with UV detection at 254 nm; however, no peaks were detected so all fractions were combined and taken to dryness.

Semi-preparative HPLC (Phenomenex Luna C18 column) was then carried out on the combined silica fractions as well as the insoluble material isolated prior to size exclusion chromatography, running an isocratic solvent system of 35% ACN/H_2O + 0.1% TFA for 12 minutes followed by a one minute wash with 100% ACN before re-equilibration. Peaks eluting at 7:30, 8:00 and 12:00 minutes were collected and examined by NMR but were found to contain too little material to allow any structural determination to be carried out.

2.4.2 Resynthesis of Fmoc-*cyclo*-CNGRCGFLG-OH (43)

Following the failure of the attempted peptide-fragment coupling strategy, it was decided that the most efficient way of producing **43** was likely to be through stepwise SPPS. Some Fmoc-Gly-Phe-Leu-Gly-Wang resin which had been prepared earlier was extended

by standard SPPS techniques to produce the side-chain protected, resin-bound nonapeptide. *N*-hydroxysuccinimide was included in the final two coupling steps to protect the asparagine residue from side-chain dehydration. The acetamidomethyl-cysteine residues were deprotected and cyclised using thallium trifluoroacetate.

2.4.2.1 Cleavage of Fmoc-*cyclo*-CNGRCGFLG-OH (43)

Due to the difficulties experienced with the removal of the bisphenol derivative from **41** (Section **2.3.3**), an experiment was carried out to determine whether or not phenol was required in the cleavage mixture. Two small samples of resin-bound **43** were simultaneously cleaved using the standard mixture (87% TFA/8% phenol/5% H_2O) and a phenol-free mixture (95% TFA/H_2O). Monitoring of this reaction by HPLC (C18, A: H_2O(A), B: ACN, Gradient II) indicated that the arginine deprotection reaction proceeded more rapidly in the absence of phenol, with complete removal of the protecting group being achieved in 24 hours, whereas the same reaction took 60 hours in the presence of phenol (**Figure 2.9**). Importantly, it was also found that no extra side-products were formed when the cation-scavenging phenol was omitted.

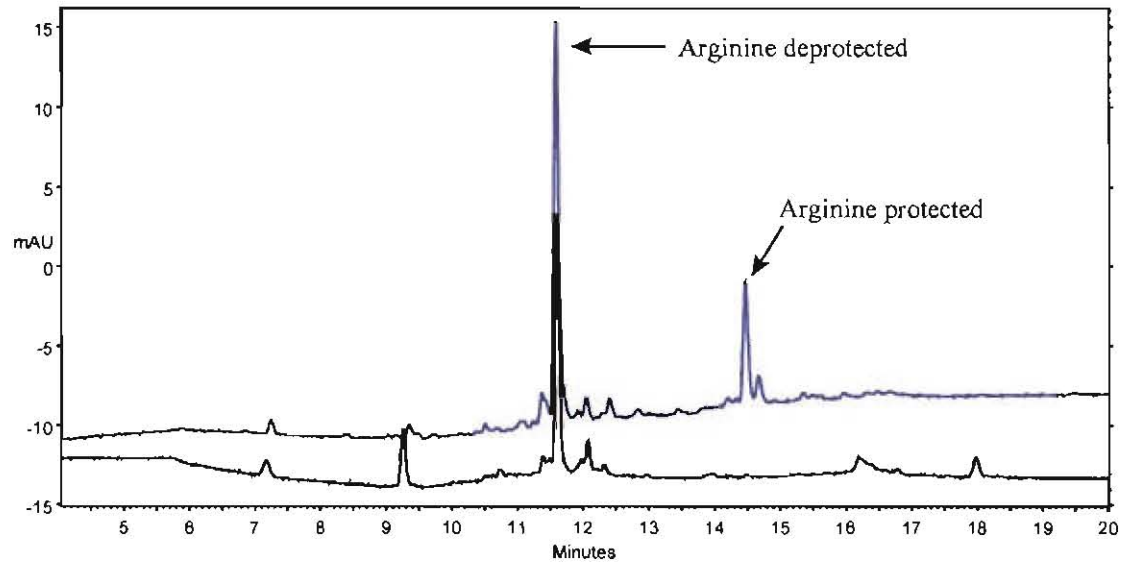

Figure 2.9 HPLC chromatogram showing state of arginine deprotection after cleavage for 24 hours with (blue trace) and without phenol (black trace)

The remaining resin was then cleaved and the arginine protecting group was removed over a 24 hour period after which the cleavage solvents were removed.

2.4.2.2 Purification of Fmoc-*cyclo*-CNGRCGFLG-OH (43)

The crude peptide preparation was dissolved with sonication and heating in 50% ACN/H_2O and then the peptide was precipitated by the addition of ACN. The precipitate was collected by filtration to provide an off-white solid which was washed with ACN and MeOH. The combined washings were analysed by HPLC (C18, A: H_2O(A), B: ACN, Gradient III) and found to contain some nonapeptide, but the peptide was heavily contaminated and present at only low levels, thus making it not worthwhile to try to extract the peptide. The solid, however, was predominantly peptide so was purified immediately by preparative HPLC (C18, A: H_2O(A), B: ACN, gradient: 50% B (0 min), 50% B (4 min), 56% B (7 min), 100% B (8 min), 100% B (9 min, 50% B (10 min), 50% B (13 min)). This was a very slow process due to the low solubility of the nonapeptide in just about all solvent systems suitable for HPLC. This low solubility presented problems both in loading the peptide onto the HPLC, which was done from a 50% ACN/H_2O solution that often contained a small amount of gelatinous precipitate, and in the peak shape, with the peptide eluting as a very broad peak which was prone to tailing at higher loadings.

2.4.3 Characterisation of Fmoc-*cyclo*-CNGRCGFLG-OH (43)

The proton and carbon NMR spectra of **43** were fully assigned through the use of COSY, HSQC-DEPT, CIGAR and IMPRESS 2D NMR experiments. The chemical shifts determined are shown in **Table 2.4**, while **Figure 2.10** shows the important CIGAR and IMPRESS correlations.

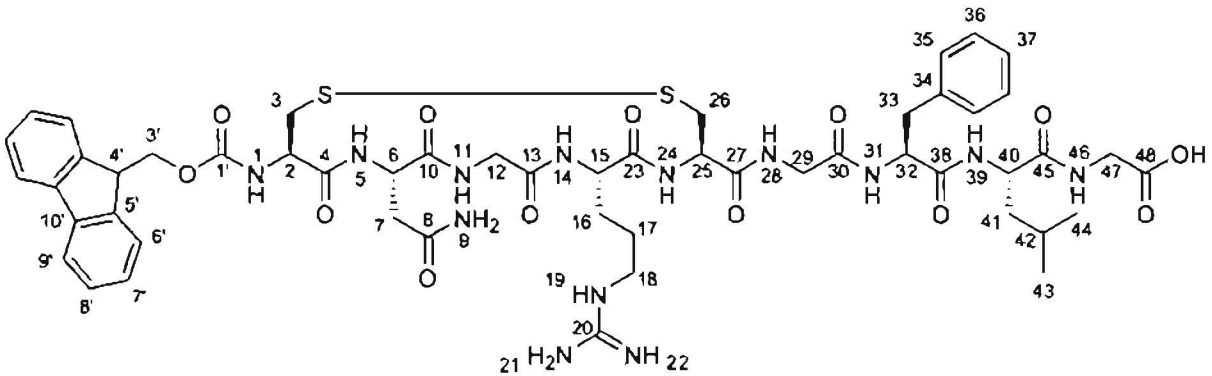

Fmoc-cyclo-Cys-Asn-Gly-Arg-Cys-Gly-Phe-Leu-Gly-OH (**43**)

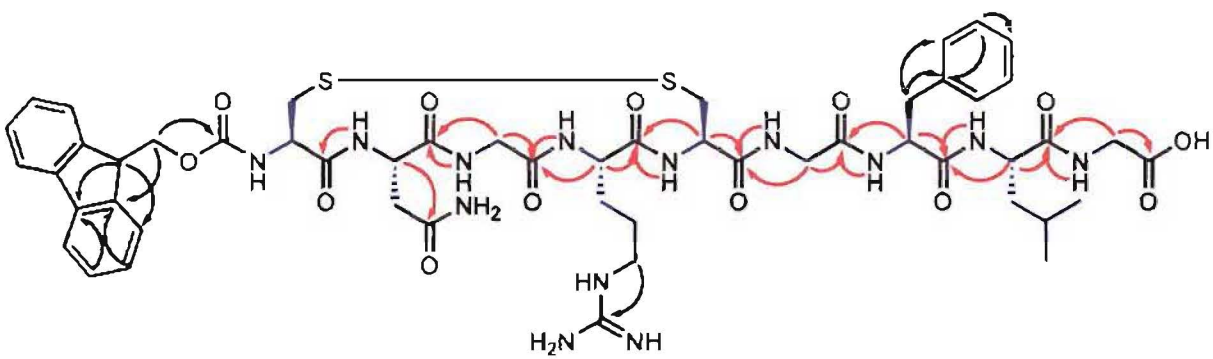

Figure 2.10 Important COSY (blue bonds), CIGAR (black arrows) and IMPRESS (red arrows) correlations observed for **43**

Table 2.4 Proton and carbon NMR data for **43** obtained in d_6-DMSO

Position	^{1}H	^{13}C	COSY	CIGAR	IMPRESS
1	7.86		H2		
2	4.27	55.0	H1, H3a, H3b		
3a	3.27	41.3	H2, H3b		
3b	3.01	41.3	H2, H3a		
4		171.0			
5	8.77		H6	C10	C4
6	4.62	49.8	H5, H7a, H7b	C7, C8, C10	C8, C10
7a	2.81	36.3	H6, H7b	C6, C8	C8, C10
7b	2.40	36.3	H6, H7a	C6, C8	C8, C10
8		172.0			
10		170.9			
11	7.94		H12a, H12b		C10
12a	4.28	42.9	H11, H12b	C13	C10, C13
12b	3.51	42.9	H11, H12a	C13	C10, C13
13		169.9			
14	7.79		H15	C13	C13
15	4.43	52.0	H14, H16a, H16b		C13, C23
16a	2.00	28.5	H15, H16b, H17		
16b	1.63	28.5	H15, H16a, H17		
17	1.55	25.3	H16, H18		
18	3.17	40.6	H17, H19	C16, C17, C20	
19	7.62		H18		
20		156.9			
23		171.9			
24	8.11		H25		C23
25	4.57	52.0	H24, H26a, H26b		C23, C27
26a	3.31	41.1	H25, H26a		
26b	3.05	41.1	H25, H26b		
27		170.2			
28	8.34		H29	C27	C27
29	3.75	42.1	H28	C27, C30	C27, C30
30		168.5			
31	8.09		H32		C30
32	4.63	54.0	H31, H33a, H33b	C30, C33, C34, C38	C30, C38
33a	3.13	37.8	H32, H33b	C32, C34, C35	C38
33b	2.84	37.8	H32, H33a	C32, C34, C35, C38	C38
34		137.8			
35	7.31	129.5		C35	
36	7.33	128.3		C34, C36, C37	
37	7.26	126.5			
38		171.0			

39	8.25		H40	C38	C38
40	4.41	51.2	H39, H41	C41, C42	C38, C45
41	1.58	41.4	H40, H42	C40, C43, C44	C45
42	1.69	24.3	H41, H43, H44	C40	
43	0.97	23.3	H42	C40, C42, C44	
44	0.93	21.9	H42	C40, C42, C43	
45		172.6			
46	8.20		H47	C45, C47	C45
47	3.83	40.9	H46		C45, C48
48		171.3			
1'		156.4			
3'	4.46	66.0	H4'	C1', C4', C5'	
4'	4.32	46.9	H3'	C3', C5', C6', C10'	
5'		144.0			
6'	7.80	125.5	H7'	C4', C8', C10'	
7'	7.42	127.4	H6', H8'	C5', C9', C10'	
8'	7.51	128.0	H7', H9'	C5', C6', C10'	
9'	7.97	120.4	H8'	C7', C10'	
10'		141			

Again, the COSY and HSQC-DEPT spectra were used to identify the proton shifts and then the carbon shifts of each amino acid residue, with the CIGAR spectrum being used to confirm the assignments by providing intra-residue correlations. The connectivity between individual residues was confirmed using the correlations provided by the IMPRESS spectrum, which had to be used to allow the ten amide carbonyls, which are spread over just 4.1 ppm, to be individually identified.

The molecular formula for **43**, $C_{52}H_{67}N_{13}O_{13}S_2$, was confirmed by HRESIMS which allowed the identification of the protonated parent ion at 1146.45 Da (0.87 ppm).

An analytical HPLC injection (C18, A: H_2O(A), B: ACN, Gradient III) showed a single peak at a retention time of 9.0 min which had strong UV absorbance in a spectrum characteristic of the Fmoc group.

2.5 Conclusions from peptide synthesis

The synthesis of the required peptides was successfully carried out, albeit with low yields in some cases and also often requiring tedious semi-preparative HPLC purification. All the peptides prepared were characterised fully by NMR spectroscopy and HRESIMS.

A modified method for loading the initial amino acid onto the resin was found to improve the loading level over that achieved when following the literature method exactly. Resins thus prepared had similar or higher levels of amino acid loading than those available commercially, with the cost of preparation being significantly lower than the commercial purchase price.

The successful preparation of the fully protected targeting peptide was followed by an unsuccessful attempt at coupling said peptide to resin-bound tetrapeptide biolinker. Synthesis of the nonapeptide by stepwise addition of single amino acids was found to be a much more suitable approach than fragment coupling.

The complete prevention of dehydration of the asparagine side-chain in the presence of *N*-hydroxysuccinimide is an interesting phenomenon that has not been reported in the literature thus far. Further work to determine whether this is a general property of NHS or simply a fortunate occurrence in this case would be worthwhile.

Chapter 3

Natural Product Modification

3.1 Introduction

In order to ensure that the drug conjugate would be stable in circulation, it was deemed necessary to use amide bonds rather than esters for attachment of the drug to the biolinker. A number of other functionalities could be utilised that would provide bonds that are stable in circulation, but the advantage of an amide linkage is that it can be selectively hydrolysed by enzymatic action following endocytosis, thus releasing the free drug intracellularly. The intracellular release of drug is central to the mechanism of action of polymer drug conjugates, as discussed in Section **1.3**.

In the case of doxorubicin, there is an amine group present so no derivatisation was required; however, in the case of the other natural products, mycalamides A and B and fumagillol, modification was necessary to provide the primary amine functionality. In all cases it was important to ensure that no alterations were made to any part of the molecule other than the desired site of reaction in order to guarantee that the modified drug would have maximal bioactivity.

3.2 Mycalamide A (31)

The modification of mycalamide A (**31**) has been extensively investigated through the formation of acyl, alkyl and silyl derivatives, reaction with a variety of basic nucleophiles and examination of acid-catalysed reactions and redox behaviour.[150-152] Despite this, the synthesis of an amine derivative has not yet been reported. It is, however, known that the mycalamide A (**31**) skeleton is very sensitive to acid, with catastrophic degradation caused by even trace quantities of strong acids such as the HCl present in commercial $CDCl_3$.

Work previously carried out by Marie Squire on derivatisation of mycalamide A (**31**) had investigated the possibility of following a modification scheme established by Rachel Lill for the conversion of homohalichondrin B to an amine derivative (**Figure 3.1**).[153] The synthesis proceeded successfully through to the azide, albeit in a low overall yield due to compounding losses at each step, at which point the reduction over Lindlar's catalyst gave a product with a mass two Daltons higher than expected.[154] It was thought that this was most likely due to reduction of the exocyclic methylene at C4, but this was never confirmed. Due to the formation of this undesired product, an alternative route was investigated in this work. This alternative route required the direct conversion of the easily formed aldehyde to an amine through reductive amination.

3.2.1 Mycalamide A oxidative cleavage

Initial attempts at the oxidative cleavage of mycalamide A (**31**) were carried out in methanol using an aqueous solution of sodium periodate and reacting overnight. These reaction conditions did produce the desired aldehyde; however, mass spectrometry clearly showed that the product was actually a mixture of the aldehyde, the methyl hemi-acetal and the hydrate. Whether or not these aldehyde derivatives would have interfered with the following reaction is not known, but it is likely that they could have provided a

competing equilibrium which would have resulted in a lower yield or at the very least a slower reaction during reductive amination.

The method of Daumas et al. of carrying out the oxidative cleavage using sodium periodate adsorbed to silica suspended in DCM (**Figure 3.2**) was a vast improvement over the methanolic method.[155] The reaction required only one hour instead of 18 hours,

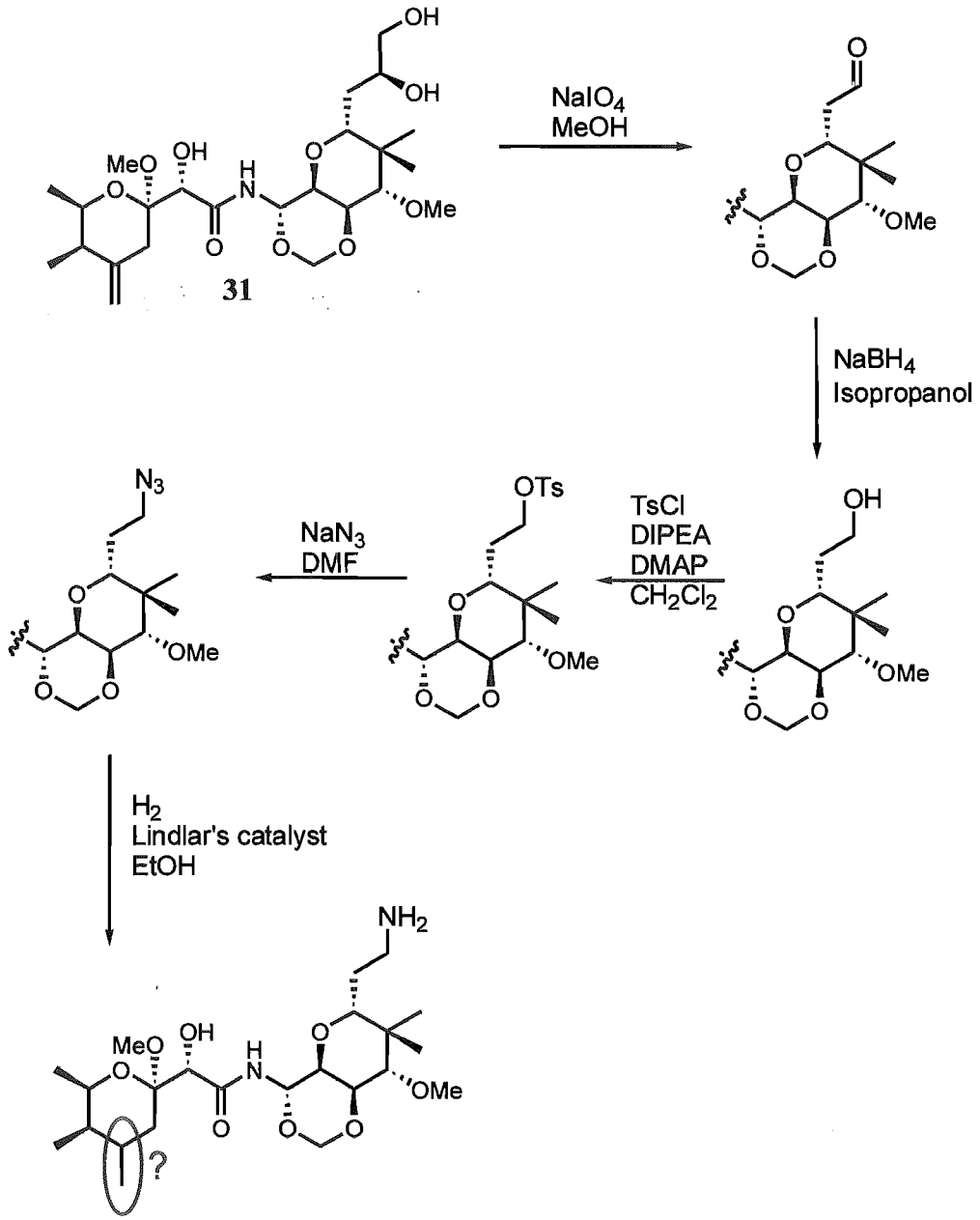

Figure 3.1 Unsuccessful route attempted for conversion of mycalamide A (**31**) to an amine derivative.

the product of the reaction was easily worked up by filtration to provide pure aldehyde free of hydrate and hemi-acetal contaminants, and the yield was quantitative as opposed to around 90%. The reaction was carried out many times and was always found to be very reliable.

The proton and carbon chemical shifts of **44** were fully assigned using the 2D NMR experiments COSY, HSQC-DEPT and CIGAR and are shown in **Table 3.1** with important CIGAR correlations being shown in **Figure 3.3**.

Elucidation of the structure of **44** began at the distinctive downfield triplet of H10 which showed a COSY correlation to the amide NH9 and also provided a convenient entry point to the spin system that extends through to H13. This spin system was readily identified from the COSY spectrum. The CIGAR correlation from H10 to the carbonyl C8 was important to link the two hemispheres of the mycalamide structure as the amide NH9 did not provide any correlations in the CIGAR spectrum. The carbonyl C8 also displayed a CIGAR correlation from the downfield singlet proton H7, which showed further correlations to the quaternary C6 and the methylene C5. A CIGAR correlation from a the singlet at 3.29 ppm in the proton spectrum identified the C6-methoxy. The diastereotopic protons of C5 were easily identified in the HSQC-DEPT spectrum, and in turn provided CIGAR correlations to both carbons of the olefin. One of the protons of the exocyclic methylene displayed a CIGAR correlation to C3. Starting from H3 the complete spin system indicated in **Figure 3.3** was readily identified using the COSY spectrum, with carbon chemical shifts being provided by an HSQC-DEPT experiment. Referring back to the right-hand hemisphere of the molecule, the cyclic acetal carbon

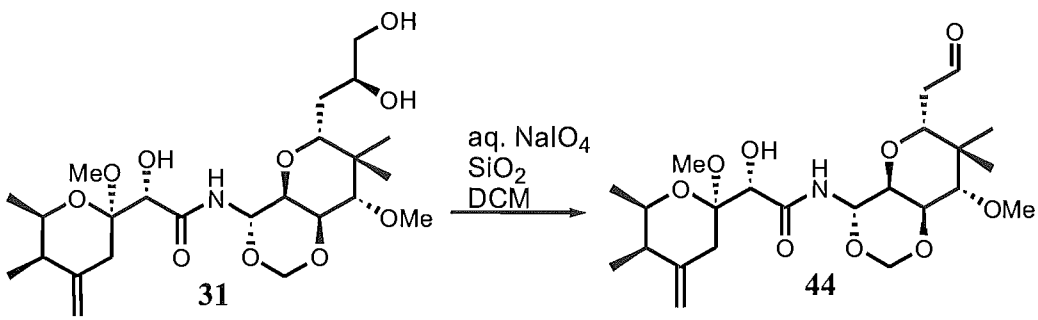

Figure 3.2 Oxidative cleavage of mycalamide A (**31**)

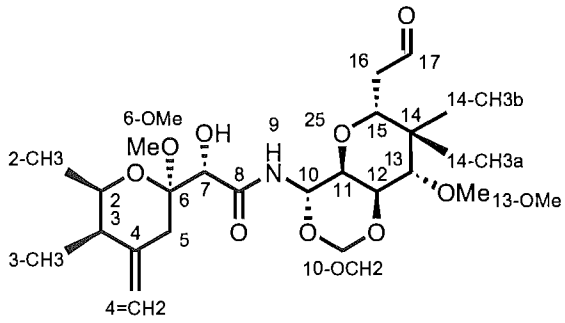

17-oxy-18-nor-mycalamide A (**44**)

Table 3.1 Proton and carbon NMR data for **44** obtained in $CDCl_3$

Position	1H	13C	COSY	CIGAR
2	4.02	69.5	H2-CH3, H3 (w)	C3-CH3
2-CH3	1.17	17.9	H2	C2, C3
3	2.23	40.9	H2, H3-CH3	C5
3-CH3	0.92	12.1	H3	C2, C3, C4
4		145		
4=CH2a	4.84	111	H4=CH2b	C3
4=CH2b	4.75	111	H4=CH2a	C5
5a	2.36	33.2	H5b	C4, C4=CH2, C6
5b	2.08	33.2	H5a	C4, C4=CH2, C6
6		100		
6-OCH3	3.29	48.5		C6
7	4.27	71.2		C5, C6, C8
8		171.9		
9	7.48		H10	
10	5.88	74	NH9, H11	C8
10-OCH2a	5.13	86.5	H10-OCH2b	C12
10-OCH2b	4.87	86.5	H10-OCH2a	C12
11	3.76	70.6	H10, H12	C12, C13
12	4.2	74.1	H11, H13	C10-OCH2, C10
13	3.51	79.1	H12	C12, C13-OCH3, C14, C14-CH3a
13-OCH3	3.56	61.8		C13
14		41.2		
14-CH3a	1.02	23.3		C13, C14, C14-CH3b, C15
14-CH3b	0.86	13.6		C13, C14, C14-CH3a, C15
15	4.09	74.2	H16	C17, C16
16	2.37	43.3	H15, H17	C17, C14
17	9.54	200.7	H16	

10-OCH_2 was identified by a CIGAR correlation from H12. H13 provided useful correlations in the CIGAR spectrum to both the methoxy attached to C13 and the

quaternary carbon C14. The two methyl groups attached to C14 were easily identified as they both showed clear CIGAR correlations to C14 itself as well as to C13 and C15. The final spin system of the molecule, that consisting of H15, H16 and H17 was identified in the COSY spectrum with the carbon chemical shifts being derived from an HSQC-DEPT experiment. The expected modification of the mycalamide A side chain was confirmed by the lack of any NMR correlations beyond position 17, indicating the loss of C18 as well as the characteristically downfield chemical shifts of both H17 and C17 at 9.54 and 200.7 ppm respectively.

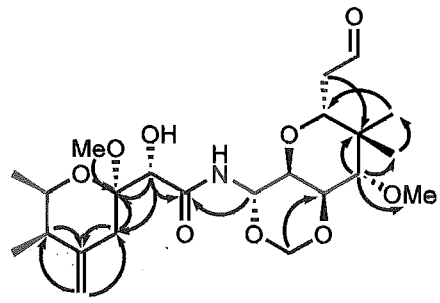

Figure 3.3 Important COSY (blue bonds) and CIGAR (black arrows) correlations observed for **44**

The molecular formula of **44**, $C_{23}H_{37}NO_9$, was confirmed by HRESIMS which identified the sodiated parent ion at 494.24 Da (1.42 ppm).

Analytical HPLC (C18, A: H_2O, B: ACN, Gradient I) of **44** showed a single peak eluting at 14.4 minutes which had no UV chromophore.

3.2.2 Reductive amination of aldehyde

The reductive amination of 17-formyl-normycalamide A was carried out using a variety of conditions in an attempt to improve the yield of the reaction but a reliable, high-yielding method was not found.

Initially, the reaction was carried out using the standard reductive amination method of Borch et al., using ammonium acetate (10 equiv.) and sodium cyanoborohydride (0.7 equiv.) in dry MeOH.[156] Analysis of the product by low resolution ESIMS indicated that a dimer had formed at a level of about one fifth that of the monomer (**Figure 3.4**). While ESIMS is not quantitative without prior calibration due to the different levels of ionisation of different molecules, both of the molecules of interest were structurally related and could be expected to have similar ability to ionise. In any case, it was clear that an unacceptably high proportion of dimer was being formed.

The reaction was then carried out using extra ammonium acetate (100 equiv.) in order to try to reduce the amount of dimer forming. This was successful to some extent, with the level of dimer formed dropping to around one eighth of the total product (as determined by mass spectrometry). Other attempts were made with the inclusion of dehydrating agents (silica and powdered, activated 4Å molecular seives) but in both cases the reaction product consisted only of completely degraded material.

By NMR spectroscopy it was observed that the crude reaction products seemed to be getting less pure as time went on. Simultaneously, the ammonium acetate that was used was beginning to smell more like acetic acid and less like ammonia. It was thought that as the hygroscopic ammonium acetate absorbed water, ammonia was being released due

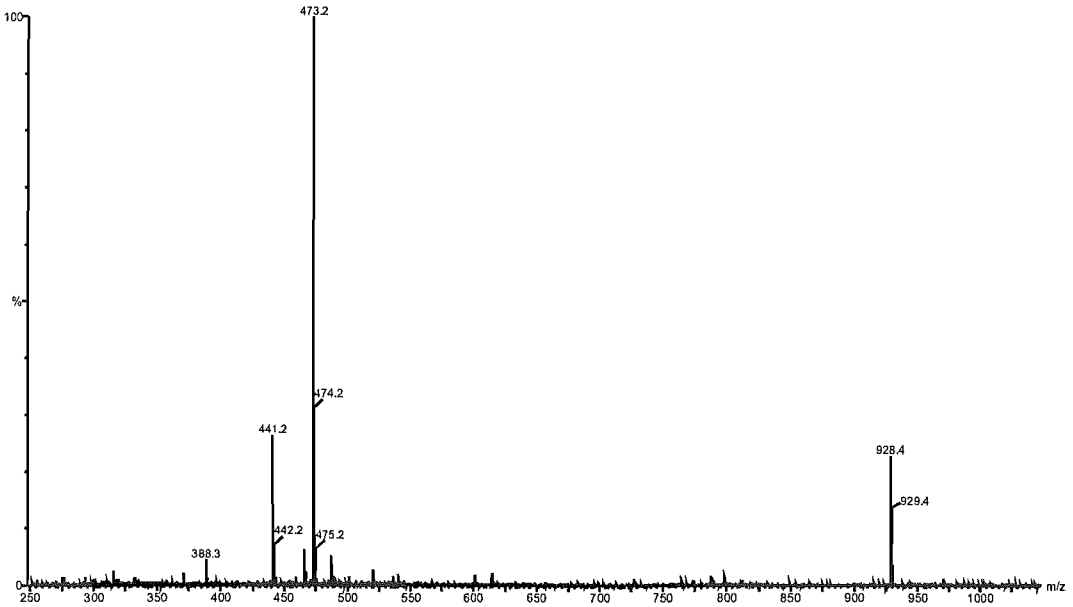

Figure 3.4 ESIMS of crude product of reductive amination of **44**

to its low boiling point (-33°C) while the higher boiling acetic acid (118°C) was remaining behind. Over time this was leading to an overall acidification of the ammonium acetate, which was apparently sufficient to cause the catastrophic degradation of the mycalamide A skeleton.

To remedy the problem of acidic ammonium acetate, two measures were taken. Firstly, the methanol that was used for the reaction was saturated with ammonium carbonate prior to use. This is a relatively basic salt (pH 9-10 at 100 gL^{-1} H_2O) with the added advantage that it can remove acid by losing carbon dioxide. Secondly, the ammonium acetate was treated prior to use by grinding to a fine powder and drying under vacuum to remove both excess acetic acid and any water that may have been absorbed by the salt.

The purification of the amine derivative of mycalamide A (**45**) was attempted a number of times using a variety of different techniques. Column chromatography was carried out using C18, silica and diol; and HPLC was performed on C18. None of these solid phases were successful in allowing the purification of the product. Ion-exchange chromatography was also attempted using weak-cation exchange resin but the mycalamide skeleton would dissolve in water only if methanol was present at high concentrations (about 50%), which was enough to strip the column immediately. The best that could be achieved was a de-salting step using C18 to remove the bulk of the mass from the crude reaction product.

The method that was finally used for the reductive amination of 17-formyl-normycalamide A (**44**) used the best combination of the techniques attempted, and the

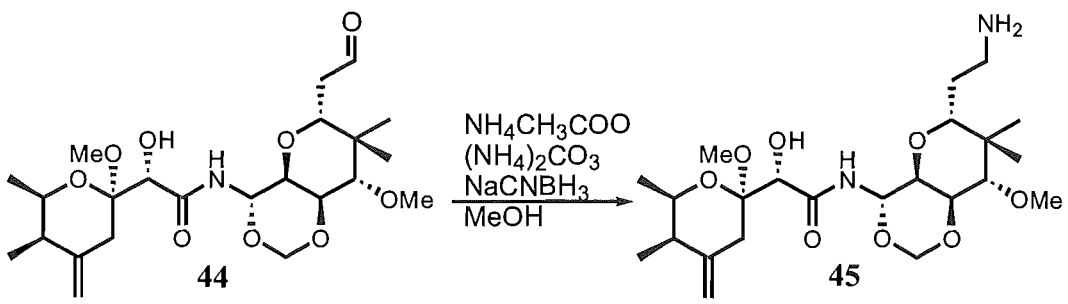

44 **45**

Figure 3.5 Reductive amination of **44** to form amine **45**

crude reaction product was carried through to the next step before being purified: **44** and ammonium acetate (100 equiv.) were stirred together in ammonium carbonate saturated dry MeOH for 30 minutes to allow imine formation to proceed. Sodium cyanoborohydride (5 equiv.) was added, again as a solution in ammonium carbonate saturated dry MeOH (**Figure 3.5**). The reaction was monitored by TLC and when the aldehyde had been consumed the reaction was worked up by passage through a C18 cartridge. The crude amine was examined by LRESIMS and the level of dimer was found to be below 5%; however, NMR spectroscopy showed that the product was not pure **45**. The non-polar material eluted from the cartridge was acylated (Section **4.4.1** and Section **5.5.1**) without further purification.

45 was never characterised due to the lack of a pure sample; however, HRESIMS was carried out on an impure sample and confirmed the molecular formula as $C_{23}H_{40}N_2O_8$ by detection of the protonated parent ion at 473.29 Da (1.7 ppm).

3.3 Mycalamide B (32)

While the derivatisation of mycalamide B (**32**) has not been studied to the same extent as mycalamide A (**31**), it is known that mycalamide B (**32**) is prone to the same degradative behaviour in the presence of acid as is mycalamide A (**31**).

The modification of mycalamide B (**32**) could not be carried out using the same oxidation-reductive amination technique that had been used for mycalamide A (**31**) due to the lack of the vicinal diol functionality, thus preventing oxidative cleavage to provide an aldehyde. While it is possible to selectively oxidise a primary alcohol to an aldehyde, the reaction can easily over-oxidise to form a carboxylic acid, which would potentially be sufficient to catalyse the destruction of the mycalamide B (**32**) skeleton. Furthermore, the disappointing yields of the reductive amination procedure along with the difficulties experienced with dimer formation also discouraged any consideration of that strategy. Instead, it was decided to attempt to 'activate' the primary alcohol directly.

3.3.1 Mycalamide B tosylate (46)

It was hoped that the primary alcohol of mycalamide B (**32**) could be tosylated preferentially in the presence of the unprotected, but hindered, secondary alcohol. The first attempt was carried out using tosic anhydride in pyridine, and while the primary alcohol did show a higher reactivity, sulphonylation of the secondary alcohol was observed before position 18 had reacted fully. The identity of the derivatives was determined by LRESIMS of individually collected peaks from the analytical HPLC chromatograph (C18, A: H2O, B: ACN, Gradient II) which showed the sodiated ions for mono- and di-tosylated mycalamide B (**46** and **47**) at 694.1 and 848.1 Daltons respectively (**Figure 3.6**). The points of attachment of the tosylate moeities were not determined, but were assumed to be as indicated (**Figure 3.7**). This showed that the

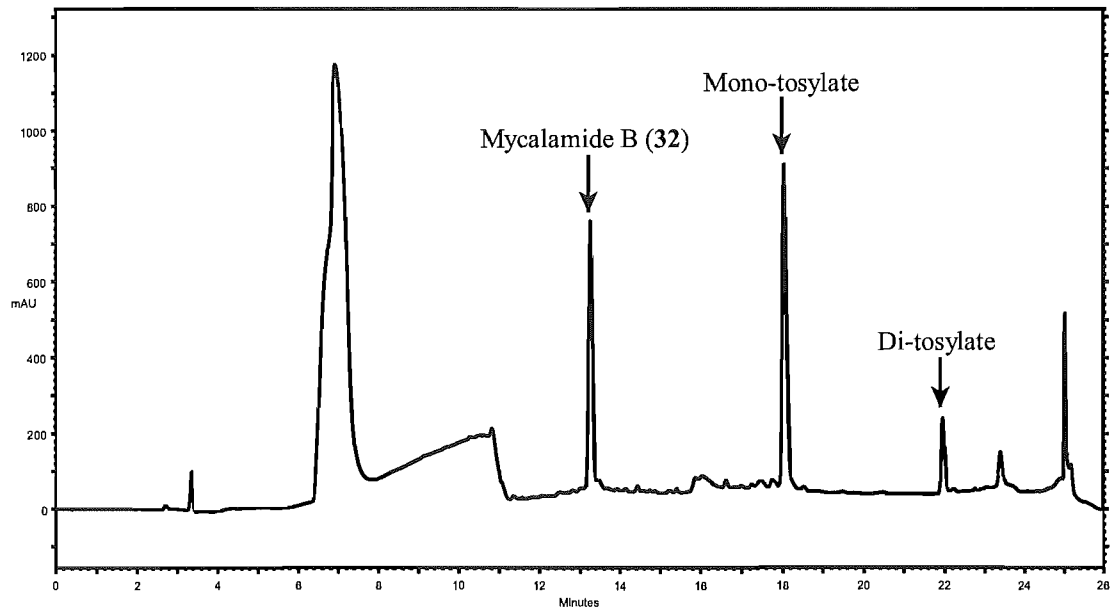

Figure 3.6 HPLC trace showing mycalamide B (**32**) tosylation reaction progress

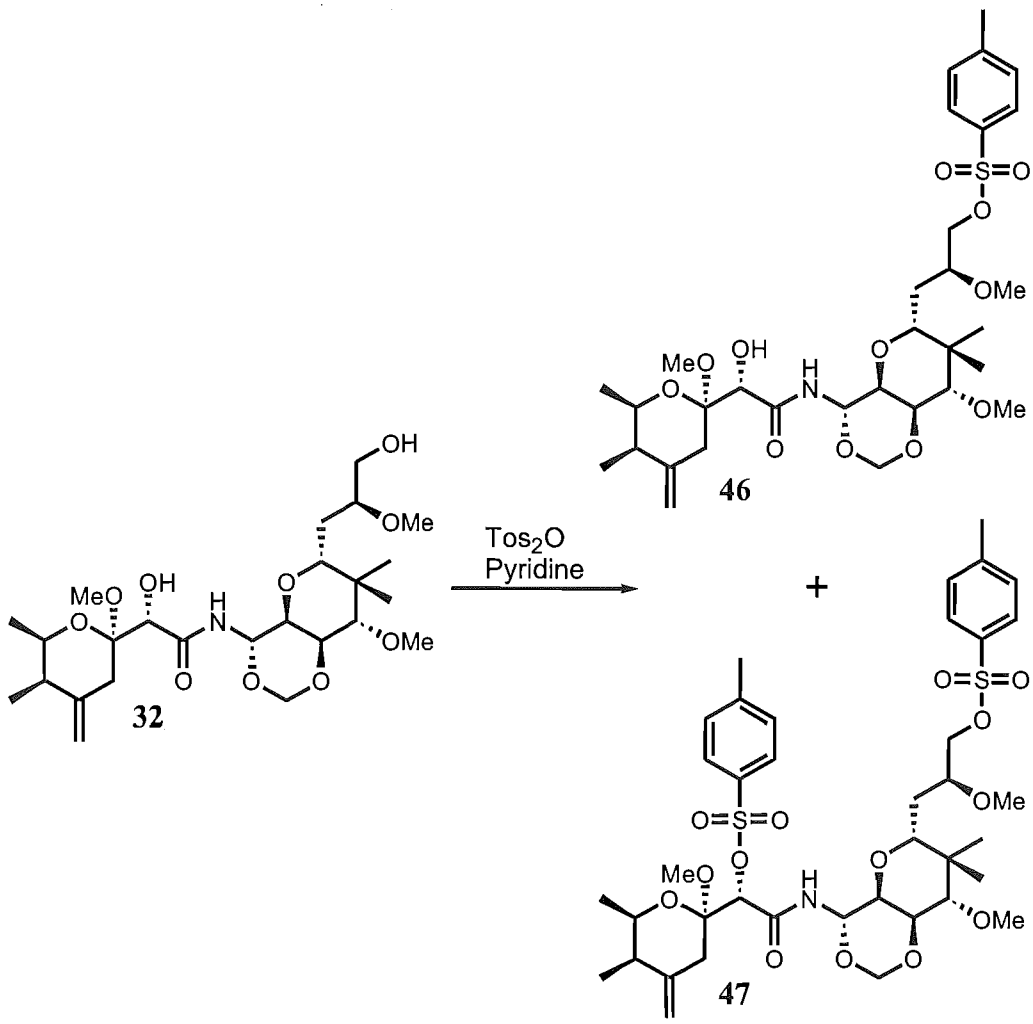

Figure 3.7 Attempted mycalamide B (**32**) tosylation

chemospecificity of the reaction was insufficient, so an attempt was made using tosic acid with DCC as a dehydrating agent in the hope that the bulk of the activated isourea adduct would prevent reaction at the secondary alcohol. However, this was found not to be the case. Analysis of this reaction by HPLC (C18, A: H2O, B: ACN, Gradient II) did show transformation of the starting mycalamide B (**32**), but the product was not the desired tosylate **46** and was therefore not further examined. Finally, a number of experiments were carried out using 2,4,6-collidine as a base instead of pyridine, as evidence has suggested that the use of a highly hindered base can enhance the selectivity of tosylation reactions.[157] To this end, reactions were carried out using both tosyl chloride and tosic anhydride at low temperature with 2,4,6-collidine used as the base, but in all cases ditosylate **47** product formation was also observed.

3.3.2 Mycalamide B phthalimide (48)

A number of attempts were made to synthesise the mono-phthalimide derivative of mycalamide B (**48**) as an intermediate to the desired amine form (**Figure 3.8**). Mitsunobu chemistry[158] was used to activate the alcohol to nucleophilic displacement, and it was hoped that the large size of the triphenylphosphine, which forms an adduct with the reacting alcohol in the proposed mechanism, would direct reaction exclusively to the primary alcohol. Unfortunately, despite the use of a number of solvents as well as varied reaction temperatures, the phthalamide **48** was not successfully produced.

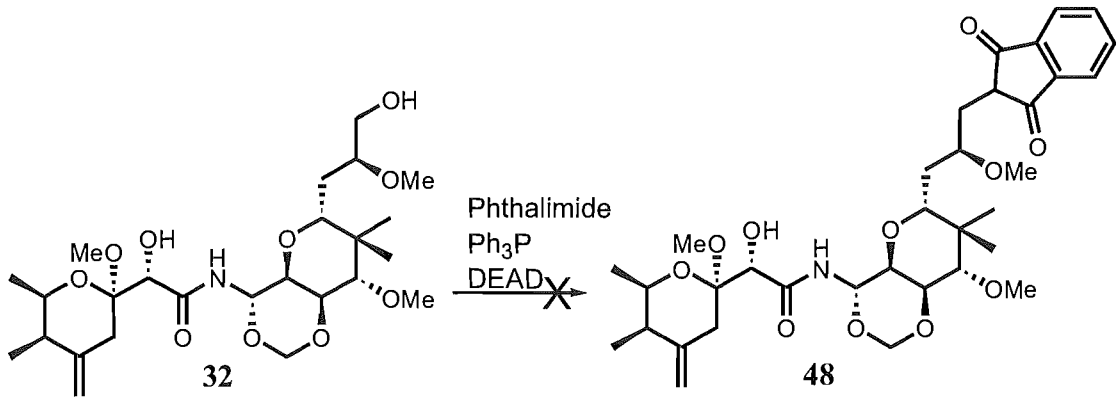

Figure 3.8 Attempted formation of phthalimide derivative **48** of mycalamide B (**32**)

3.3.3 Mycalamide B azide (49)

Work that was being carried out simultaneously toward the derivatisation of fumagillol (**35**) into an amine had indicated that the use of zinc azide as the nucleophile under Mitsunobu conditions[159] could be useful for conversion of mycalamide B (**32**) to an amine derivative. It was hoped that in the case of mycalamide B (**32**), the use of the Mitsunobu reaction would prevent the derivatisation of the secondary alcohol seen in the tosylation reactions. The reasoning was that the bulky triphenylphosphine reagent forms an adduct with the reacting alcohol in the first step of the Mitsunobu reaction; this adduct could be expected to be very sensitive to the steric environment and thus direct reaction to the primary alcohol. This was found to be the case, but on one occasion a small amount of the di-azide product was isolated when a total of four equivalents of triphenylphosphine and diethyl azodicarboxylate were used.

The final reaction, shown in **Figure 3.9**, used for the production of the mono-azide derivative of mycalamide B (**49**), relied on the monitoring of reaction progress with the reaction being refreshed until the starting material had been completely consumed. Thus, mycalamide B (**32**) and PPh_3 (2.5 equiv.) were added to a suspension of zinc azide (1 equiv.) in dry toluene. DEAD (2.5 equiv.) was added. After four hours, HPLC (C18, A: H_2O, B: ACN, Gradient II) showed the reaction was still not complete so a solution containing a further 0.75 equivalents of PPh_3 and DEAD in toluene was added. Further HPLC analysis (C18, A: H_2O, B: ACN, Gradient II) after another four hours showed some starting material remaining, so the reaction was again refreshed with additional PPh_3 (0.5 equiv.) and DEAD (0.5 equiv.) in toluene. After another two hours of

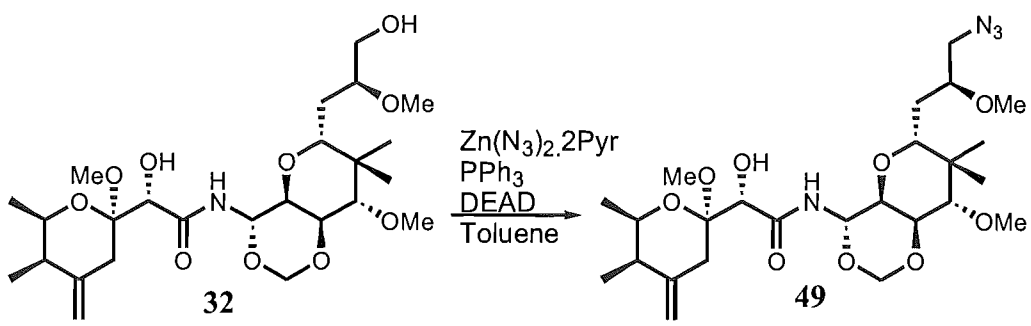

Figure 3.9 Formation of azide derivative **49** of mycalamide B (**32**)

reaction, HPLC (C18, A: H_2O, B: ACN, Gradient II) indicated that the starting material had been completely consumed, so the reaction solvent was removed under vacuum and the gummy residue purified by chromatography on a C18 cartridge to furnish the desired azide **49** in an 84% yield.

The proton and carbon NMR chemical shifts of **49** were fully assigned through the use of COSY, HSQC-DEPT and CIGAR experiments. The important CIGAR correlations are shown in **Figure 3.10,** while **Table 3.2** provides the carbon and proton NMR data.

The main core of the mycalamide structure through to the side chain attached to C15 was identified in much the same fashion as already described for the mycalamide A derivative **45** (Section **3.2.1**). From H15, a COSY correlation could be seen to H16; however, no further correlations were observed in the COSY spectrum, most likely due to the splitting of H16 and H17 causing too low a signal-to-noise ratio. A CIGAR correlation was observed from H15 to both C16 and C17 as well as back in to the ring at C13. H16 in turn provided CIGAR correlations back to C15 as well as the important correlation to the terminal carbon, C18, at 52.2 ppm. The diastereotopic protons H18a,b were identified from the HSQC-DEPT spectrum and showed CIGAR correlations to C16 and C17. The methoxy attached to C17 was identified using a CIGAR correlation from a singlet at 3.25 ppm to C17 itself. The HSQC-DEPT spectrum allowed identification of the proton H17 from which no correlations could be observed in any of the other 2D NMR spectroscopy experiments run.

The transformation of the terminal alcohol to an azide was confirmed by changes in NMR characteristics at position 18 with no significant changes being observed elsewhere in the molecule. The chemical shifts of the terminal protons H18a,b (3.41, 3.22 ppm) were similar to those reported for mycalamide B (**32**) (3.47 ppm), although diastereotopic splitting has not been observed in the parent compound. More importantly, C18 had shifted significantly upfield from 63.5 ppm to 52.2 ppm, which would be expected upon replacement of an hydroxyl with an azide.

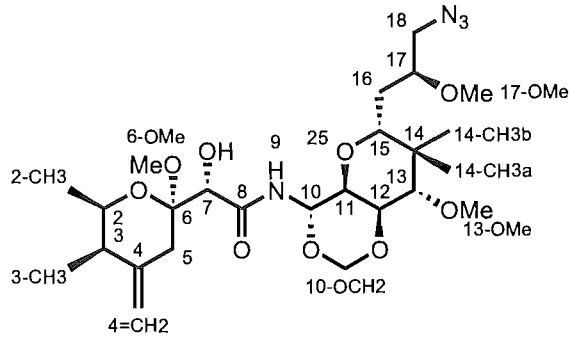

18-azido-18-deoxy-mycalamide B (**49**)

Table 3.2 Proton and carbon NMR data for **49** obtained in $CDCl_3$

Position	^1H	^{13}C	COSY	CIGAR
2	4.07	69.6	H2-CH3	C2-CH3, C3-CH3, C4, C6
2-CH3	1.22	18	H2	C2, C3
3	2.28	41.2	H3-CH3	C3-CH3, C4, C5
3-CH3	1.03	12.2	H3	C2, C3, C4
4		144.8		
4=CH2a	4.88	111.4	H4=CH2b	C3, C5
4=CH2b	4.76	111.4	H4=CH2a, H5b (w)	C3, C5
5a	2.41	33.6	H5b	C3, C4, C4=CH2, C6
5b	2.23	33.6	H5a, H4=CH2b (w)	C3, C4, C4=CH2, C6
6		100		
6-OCH3	3.32	48.6		C6
7	4.3	71.2		C5, C6, C8
8		171.7		
9	7.53		H10	
10	5.78	74	H9, H11	C8, C10-OCH2
10-OCH2a	5.12	86.5	H10-OCH2b	C10
10-OCH2b	4.87	86.5	H10-OCH2a	C10
11	3.78	70.9	H10, H12	C12, C13, C15
12	4.21	74.3	H11, H13	C10, C10-OCH2
13	3.44	79.1	H12	C12, C13-OCH3, C14, C14-CH3a, C14-CH3b
13-OCH3	3.56	61.8		C13
14		41.6		
14-CH3a	1	23.3		C13, C14, C14-CH3b, C15
14-CH3b	0.87	13.6		C13, C14, C14-CH3a, C15
15	3.31	75.5	H16	C13, C16, C17
16	1.6	30.8	H15	C17, C18
17	3.3	77.6		
17-OCH3	3.25	56.7		C17
18a	3.41	52.2	H18b	C16
18b	3.22	52.2	H18a	C17

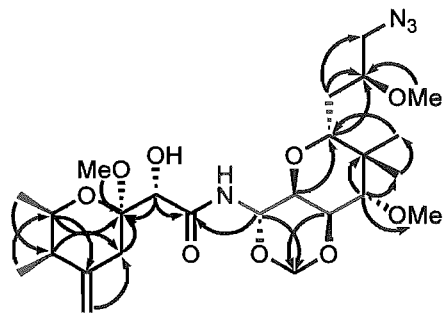

Figure 3.10 Important COSY (blue bonds) and CIGAR (black arrows) correlations observed for **49**.

The molecular formula of **49**, $C_{25}H_{42}N_4O_9$, was confirmed by HRESIMS in which a peak at 565.28 Daltons (0.35 ppm), corresponding to the sodiated ion, was observed.

Analytical HPLC (C18, A: H_2O, B: ACN, Gradient II) of **49** showed a single peak eluting at 16.3 minutes which had only end absorption.

3.3.4 Mycalamide B amine (50)

The reduction of mycalamide B azide (**49**) was carried out using modified Staudinger conditions (**Figure 3.11**).[160,161] **49** and PPh_3 (1.5 equiv.) were reacted together in dry THF at 40°C. After three hours, TLC showed the replacement of **49** with a more polar, UV-absorbing compound which was presumed to be the phosphine-imine. Water was

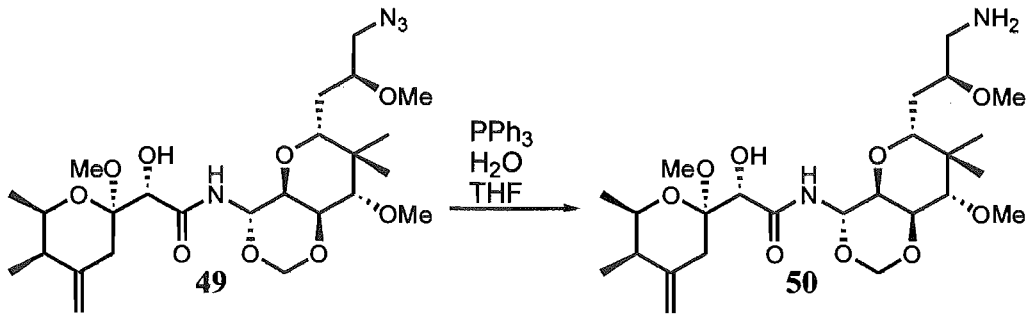

Figure 3.11 Formation of 18-deoxyamino-mycalamide B (**50**)

added and the reaction was continued for a further three hours at 40°C, at which point TLC indicated that the reaction was complete by the loss of UV activity of the baseline spot and appearance of the non-polar UV-active spot of triphenylphosphine oxide. Due to the difficulties already experienced with attempted chromatography of other natural product amine derivatives, the product **50** was acylated without further purification.

3.4 Fumagillol (35)

The derivatisation of fumagillol (**35**) has been studied to some extent, with the development of 6-*O*-acyl, 6-*O*-sulfonyl, 6-*O*-alkyl and 6-*O*-(*N*-substituted carbamoyl) derivatives having been reported.[99] 6-Amino-6-deoxyfumagillol and derivatives thereof (6-*N*-alkyl, 6-*N*-acyl, 6-*N*-sulfonyl, 6-*N*-ureido and 6-*N*-thioureido forms) are also already present in the literature.[100] All of the work reported thus far has been focussed on development of a more potent small molecule anti-angiogenic drug than the natural product parent fumagillin (**34**), and has resulted in the discovery of TNP-470 (**36**).

During the course of this work, which was focussed on the development of the two enantiomeric 6-amino fumagillol derivatives, a number of novel intermediates were prepared. Unfortunately, due to a lack of readily available biological testing resources these were not examined for anti-angiogenic activity. While it may have been possible to arrange testing, the aim of the work was to prepare polymer drug conjugates containing the two 6-amino fumagillol derivatives, so testing of the intermediates was not pursued.

3.4.1 Fumagillol oxidation

The secondary alcohol group of fumagillol was oxidised to a ketone by chromate oxidation (**Figure 3.12**). Initially, the method used was the same as that presented by Marui and Kishimoto,[100] but it was found that superior results were achieved when the amounts of chromate and pyridine used were doubled. Thus, fumagillol (**35**) was added to a solution of chromate (15 equiv.) and pyridine (30 equiv.) in dichloromethane and allowed to react for 90 minutes, after which TLC indicated that the reaction was complete. The purification method used was also simpler than that of Marui and Kishimoto,[100] consisting simply of passage through a dry silica bed to provide the pure ketone **51** in a 97% yield. The reported yield is 82%.

The proton NMR data for **51** have been reported.[100] However, carbon chemical shifts and assignments have not been given, thus a full assignment of the chemical shifts of **51** was undertaken. The proton and carbon chemical shifts are presented in **Table 3.3**, with **Figure 3.13** showing the important CIGAR correlations observed.

The assignment of the chemical shifts of **51** began at the most downfield proton, H4', which was clearly olefinic as it was attached to a carbon with a chemical shift of 118.2 ppm. H4' showed CIGAR correlations to both of the vinyl methyl groups C6' and C7' and also exhibited long range COSY correlations to H6' and H7' as well as a regular COSY correlation to H3'a and b. Both H3'a and b were correlated to H2 in the COSY spectrum, which in turn showed CIGAR correlations to both the quaternary centre C1' as well as C4 of the cyclohexyl core. The methyl group H8' was easily assigned due to both its low chemical shift and the fact that it was the only position other than H4 and H3'a, b which showed CIGAR correlations to both of the side chain epoxide carbons C1' and C2'. The assignments of the core ring structure began with a COSY correlation from H4 which allowed the identification of H5, which in turn provided access to the methoxy group C8 through a CIGAR correlation. The spiro-epoxide protons H7a and b both showed CIGAR correlations to C4, confirming the presence of this group at the expected ring position. The remaining spin system of H1a,b and H2a,b was easily identified in the COSY spectrum and the orientation was confirmed by CIGAR correlations from H1b to C5 and H2b to C4. All of the protons of the cyclohexyl ring displayed CIGAR correlations to C6, which was distinctive for its downfield shift of 207.1 which, along with an absence of attached protons, confirmed the successful oxidation of fumagillol to the ketone derivative **51**.

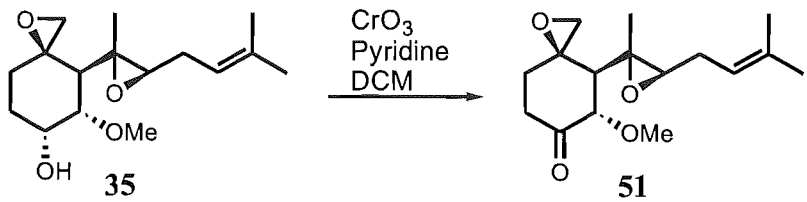

35 **51**

Figure 3.12 Oxidation of fumagillol (**35**)

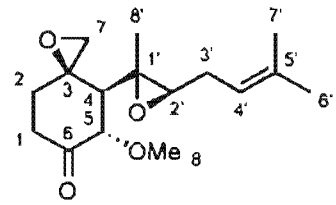

6-dehydro-fumagillol (**51**)

Table 3.3 Proton and carbon NMR data for **51** obtained in $CDCl_3$

Position	^1H	^{13}C	COSY	CIGAR
1a	2.66	36.8	H1b, H2a, H2b	C2, C3, C5, C6
1b	2.48	36.8	H1a, H2a, H2b	C2, C3, C5, C6
2a	2.04	33.2	H1a, H1b, H2b	C1, C3, C4, C6, C7
2b	1.69	33.2	H1a, H1b, H2a	C1, C3, C4, C6, C7
3		58.4		
4	1.86	53.6	H5	C2, C5, C6, C1', C8'
5	4.07	83.2	H4	C3, C4, C6
6		207.1		
7a	3.04	51.8	H7b	C2, C3, C4
7b	2.71	51.8	H7a	C2, C3, C4
8	3.48	58.5		C5
1'		58.6		
2'	2.58	60.4	H3'a, H3'b	C4, C1', C3', C4'
3'a	2.37	27.3	H2', H3'b, H4'	C1', C2', C4', C5'
3'b	2.13	27.3	H2', H3'a, H4'	C1', C2', C4', C5'
4'	5.16	118.2	H3'a, H3'b, H6', H7'	C6', C7'
5'		135		
6'	1.72	25.7	H4'	C4', C5', C7'
7'	1.63	18	H4'	C4', C5', C6'
8'	1.27	13.8		C4, C1'

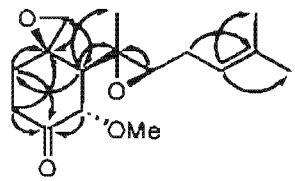

Figure 3.13 Important COSY (blue bonds) and CIGAR (black arrows) correlations observed for **51**.

Interestingly, the proton H5 can be seen as a doublet of doublets in the proton spectrum. The larger coupling constant, 10.6 Hz, is due to the coupling with H4, but there is a

much smaller coupling constant of 0.7 Hz that can be identified for a long range coupling across the ketone to proton H1a.

The molecular formula for **51**, $C_{16}H_{24}O_4$, was confirmed using HREIMS in which the positive ion at 280.17 (0.49 ppm) was observed.

3.4.2 Fumagillone reductive amination

The reductive amination of dehydrofumagillol **51** has been previously reported.[100] When the reaction was performed according to the reported technique, the desired amine was formed but all attempts to purify the amine **52** were either completely unsuccessful or gave a very low return of slightly impure **52**. Among the phases used for chromatography were reverse phase (C18), normal phase (silica, florisil) and ion exchange (CBX). The best results for the reaction were achieved using the modified technique that had been developed during the investigation of the reductive amination of the mycalamide A derivative **45** (Section **3.2.2**) (**Figure 3.14**). Briefly, **51** was dissolved along with ammonium acetate (100 equiv.) in ammonium carbonate saturated MeOH. After 15 minutes, sodium cyanoborohydride was added and the reaction was allowed to stir for two hours before being dried down and passed through a C18 cartridge to remove the extremely polar salt contaminants to provide the crude amine **52**.

The amine **52** was reacted further without delay, as an investigation into the stability of **52** revealed that it was prone to degradation. The proton NMR spectrum of a sample of crude **52** was collected, then the sample was dried and stored in the refrigerator for

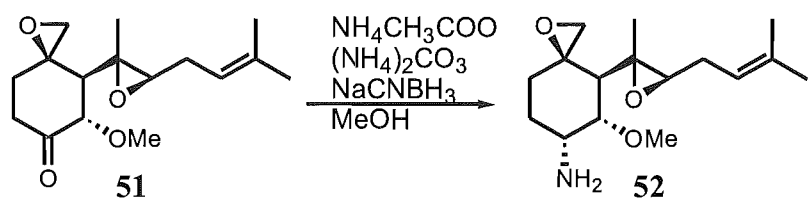

51 **52**

Figure 3.14 Reductive amination of 6-dehydro-fumagillol (**51**)

eleven days before having its spectrum taken again. The spectra obtained are shown in **Figure 3.15**, and clearly show the complete degradation of the molecule. Previous work has shown that the *N*-methyl derivative of **52** rapidly degrades through attack of the amine nitrogen on the spiro-epoxide and it was proposed that this reaction occurred due

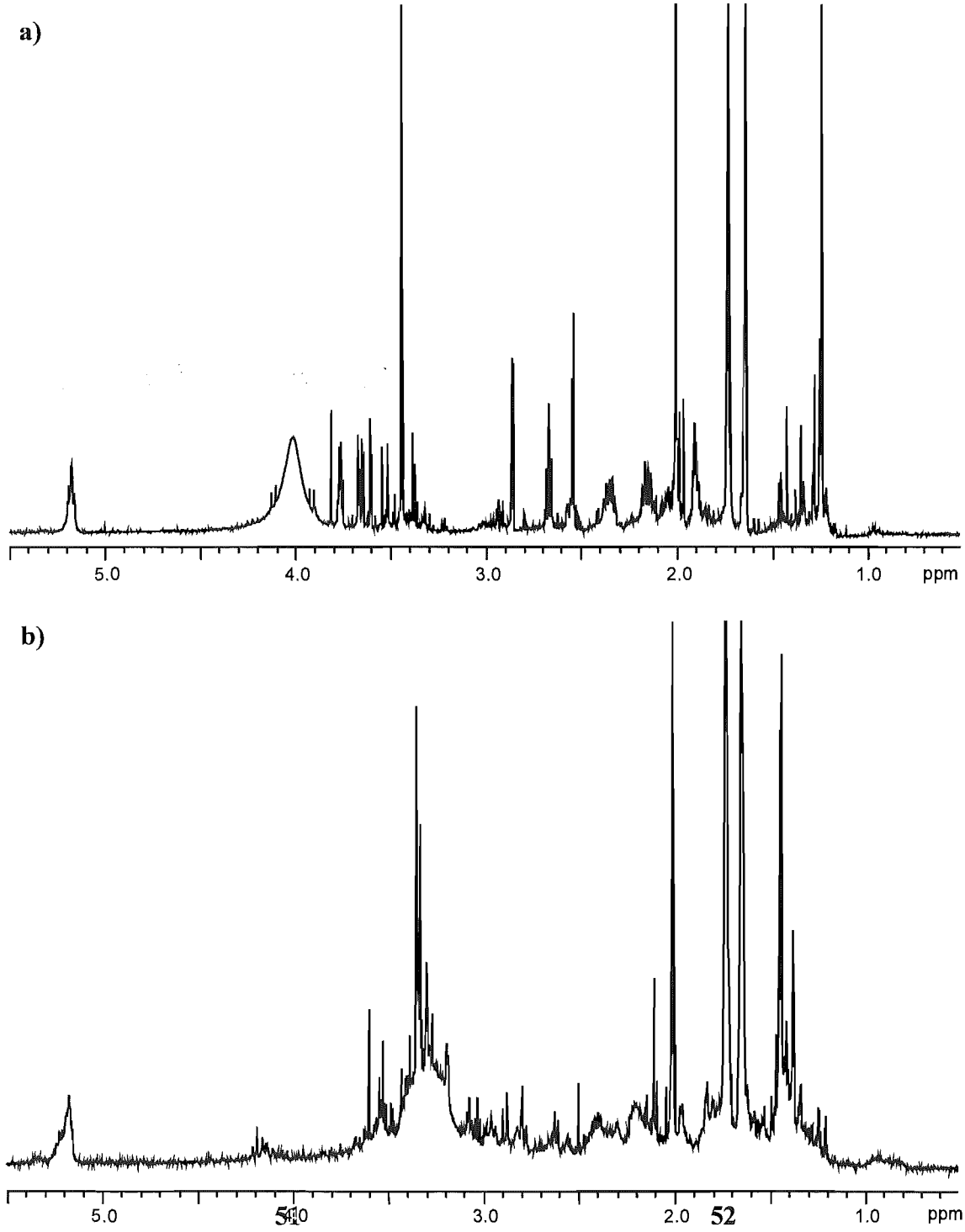

Figure 3.15 Proton NMR spectra of crude **52** after a) six hours; b) eleven days

to the higher nucleophilicity of a secondary amine over a primary.[100] It was found, however, that it is possible to trap the amine by acylating the crude reaction product, thus preventing the amine acting as an intramolecular nucleophile. In order to prevent any similar intramolecular reaction occurring with **52**, it was decided that **52** would be acylated immediately and without purification beyond desalting.

3.4.3 Fumagillol *S*-tosylate (53)

It was thought that an alternative route to the 6*R* amine derivative of fumagillol that could provide the desired product in a higher yield than the somewhat disappointing reductive amination pathway would be to produce the tosylate by Mitsunobu chemistry and then displace the tosylate in an S_N2 manner with ammonia. To this end, fumagillol was reacted with zinc tosylate (1 equiv.),[162] triphenylphosphine (10 equiv.) and diethyl azodicarboxylate (10 equiv.) (**Figure 3.16**). After ten hours, the reaction mixture was filtered and chromatographed on silica; however, none of the desired tosylate **53** could be isolated and instead the only reaction product that was observed was the elimination product **54**.

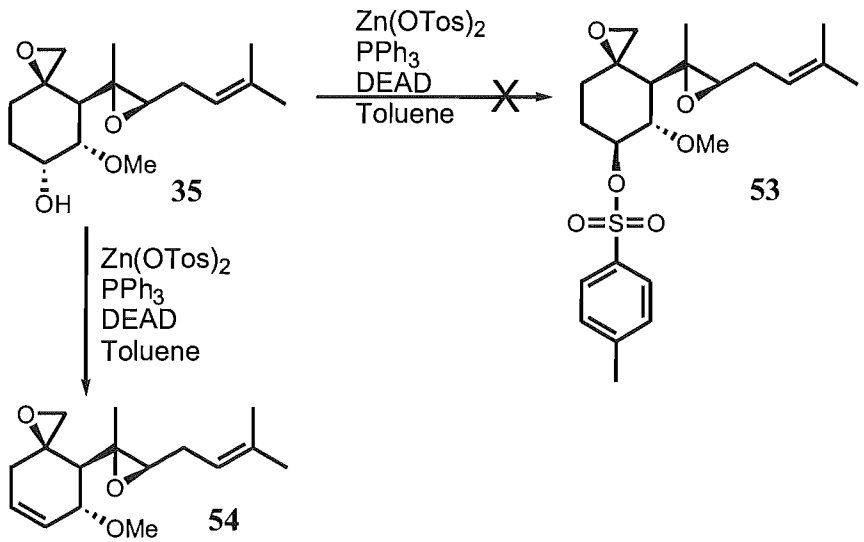

Figure 3.16 Attempted tosylation of fumagillol (**35**) using Mitsunobu conditions

The exact mechanism of the elimination is not known; however, evidence indicates that it is probably a direct elimination of the triphenylphosphine adduct. This could be caused by the reactive triphenylphosphine adduct being present for an extended period due to the poor nucleophilicity, and perhaps to some degree the steric bulk, of the tosylate anion. The fact that the tosylate was successfully produced by sulfonylation of the alcohol at C6 (Section **3.4.6**) and did not spontaneously eliminate to form **54** indicates that it was probably not the tosylate itself that was leaving. However, this is not definitive proof, as the differing stereochemistry at C6 may prevent access to the E2 elimination mode by preferring a confirmation in which there is no proton in an anti-position to the tosylate. Further evidence that it was the triphenylphosphine adduct that was eliminating, and not the tosylate, was the formation of **54**, albeit at low levels, when sodium azide was used as a nucleophile (Section **3.4.8**). The azide anion is a strong nucleophile and as such is a poor leaving group, indicating that **54** was most likely to have been formed directly from the triphenylphosphine adduct.

The proton and carbon NMR chemical shifts of **54** were fully assigned through the use of COSY, HSQC-DEPT and CIGAR experiments. The important CIGAR correlations are shown in **Figure 3.17** while **Table 3.4** provides the carbon and proton NMR data.

The side chain of the structure was essentially identical to that already described for the ketone derivative **51**, but the shifts of atoms in the ring differed significantly. C5 was identified by a CIGAR correlation from the clearly identifiable singlet methoxy protons at 3.39 ppm. From H5, COSY correlations could be observed successively around the ring to H2 via the extremely downfield protons H6 and H1. The chemical shifts of C6 and C1, at 127.8 and 127.3 respectively, were also consistent with formation of an olefin group. CIGAR correlations from the olefinic protons further confirmed the position of the double bond to be as indicated. The spiro-epoxide was clearly intact as indicated by the characteristic diastereotopic pair of doublets at 2.84 and 2.60 ppm as well as the chemical shift of C7 at 52.6 ppm.

The molecular formula for **54**, $C_{16}H_{24}O_3$, was confirmed using HREIMS in which a peak at 264.17 (1.75 ppm) was observed.

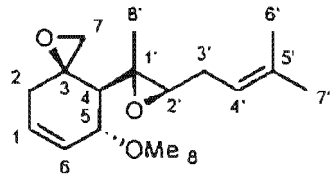

6-deoxy-fumagillol (**54**)

Table 3.4 Proton and carbon NMR data for **54** obtained in $CDCl_3$

Position	^1H	^{13}C	COSY	CIGAR
1	5.84	127.3	H2a, H2b, H6	C2, C3, C5, C6
2a	2.38	34.1	H1, H2b, H6 (w)	C1, C3, C4, C6, C7
2b	2.05	34.1	H1, H2a, H6 (w)	C1, C3, C4, C6, C7
3		57.2		
4	1.6	50.5	H5	C2, C3, C5, C6, C7, C1', C2', C8'
5	4.22	76	H4, H5	C6, C8,
6	5.97	127.8	H1, H2a (w), H2b (w), H5	C1, C2, C4, C5
7a	2.84	52.6	H7b	C2, C3, C4
7b	2.6	52.6	H7a	C2, C3, C4
8	3.39	55.4		C5
1'		59.2		
2'	2.72	62	H3'a, H3'b	C4, C1', C3', C4'
3'a	2.37	27.4	H2', H3'b, H5', H6' (w), H7' (w)	C1', C2', C4', C5'
3'b	2.2	27.4	H2', H3'a, H5', H6' (w), H7' (w)	C1', C2', C4', C5'
4'	5.21	118.6	H3'a, H3'b, H6', H7'	C3', C6', C7'
5'		134.7		
6'	1.74	25.8	H3'a (w), H3'b (w), H4'	C2', C4', C5', C7'
7'	1.66	18	H3'a (w), H3'b (w), H4'	C2', C4', C5', C6'
8'	1.28	14.4		C4, C1', C2'

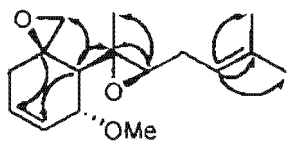

Figure 3.17 Important COSY (blue bonds) and CIGAR (black arrows) correlations observed for **54**.

3.4.4 Fumagillol phthalimide (55)

The synthesis of the fumagillol phthalimide derivative **55** was carried out with inversion of stereochemistry at C6 using Mitsunobu chemistry. Triphenylphosphine (2 equiv.) and

diethyl azodicarboxylate (2 equiv.) were added to a solution of fumagillol (**35**) and phthalimide (1.5 equiv.) in THF and the reaction stirred overnight (**Figure 3.18**). The following day TLC indicated that the starting material had been consumed, so the reaction solvent was removed under a stream of nitrogen, and the residue chromatographed on silica. Some of the desired phthalamide **55** was obtained pure from this column, but most was contaminated with 1,2-carbethoxyhydrazine, which was removed by passage through a second silica column. The pure fractions from both columns were combined to provide **55** in a 68% yield.

The proton and carbon chemical shifts of **55** were fully assigned through the use of the 2D NMR experiments COSY, HSQC-DEPT and CIGAR. The only significant differences in chemical shifts from other derivatives were observed in the ring positions. In particular, H6, which was found to have a very similar chemical shift to that of the alcohol parent compound (4.34 ppm vs 4.36 ppm), was found to be attached to a carbon at 52.9 ppm, which is notably upfield from the corresponding shift of the alcohol at 64.1 ppm. Furthermore, H6 showed a CIGAR correlation to a carbon at 168.3 ppm which was assigned as the two identical carbonyl carbons of the phthalimide group, and thus confirmed the attachment of the phthalimide directly to C6.

The stereochemistry of **55** at C6 was identified as *S* using the coupling constant between H6 and H5, which is dependent on the dihedral angle between the two protons. The Karplus equation describes this relationship and is represented graphically in **Figure 3.19**.[163] The shape of the graph is constant, but the exact magnitude of the coupling constant varies depending on nearby substituents, as indicated by the three curves

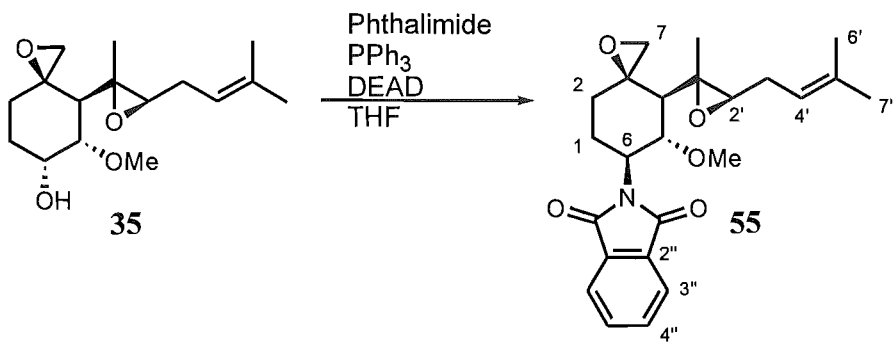

Figure 3.18 Formation of 6*R*-phthalimidoyl-6-deoxy-fumagillol (**55**)

shown. For six-membered rings in the chair conformation, the coupling between two neighbouring axial protons is typically 8-13 Hz, while the coupling between an axial and an equatorial proton is usually 2-6 Hz, which is also the expected range for a di-equatorial coupling.

Unfortunately, the splitting pattern of H6 itself could not be fully characterised due to the complexity caused by coupling to the diastereotopic pair of protons of H1. However, H5 was observed as a triplet with a coupling constant of 10.6 Hz, with the splitting pattern being formed by coupling to both H6 and H4. H4 could be clearly seen and was a doublet with a 11.2 Hz coupling indicating that the coupling between H5 and H6 must have been of the order of 11 Hz to cause the doublet of doublets splitting pattern of H5 to appear as a triplet. A coupling of around 11 Hz is consistent with the *anti* stereochemistry as shown in **Figure 3.20**.

The molecular formula for **55**, $C_{24}H_{29}NO_5$, was confirmed using HRESIMS in which the potassiated adduct at 450.17 (0.22 ppm) was observed.

Analytical HPLC (C18, A: H_2O(A), B: ACN, gradient: 70% B (0 min), 80% B (10

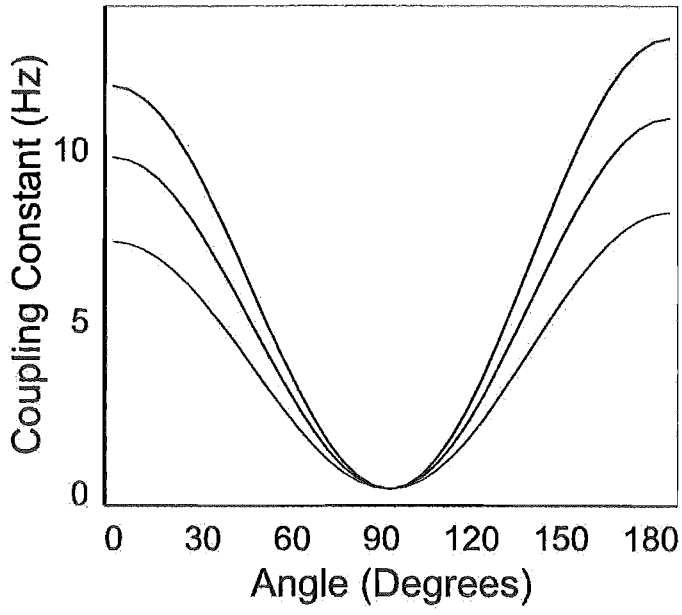

Figure 3.19 Graph of the Karplus equation

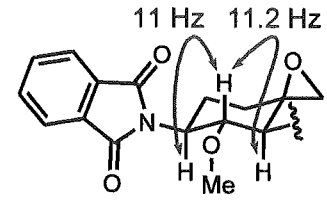

Figure 3.20 Stereochemical relationships of H4, H5 and H6 in **55**

min), 100% B (11 min)) of **55** showed a single peak eluting at 6.5 minutes which had a distinctive UV chromophore that extended as far as 340 nm and had a strong maximum at 220 nm.

3.4.5 Phthalimide cleavage

The most commonly used technique for cleavage of a phthalimide group to afford a primary amine is refluxing the phthalimide-containing compound with hydrazine in EtOH.[164,165] Fumagillol (**35**) was refluxed in EtOH with hydrazine hydrate (10 equiv.) for three hours then dried down. A proton NMR spectrum obtained on the crude reaction product confirmed that fumagillol was stable to the reaction conditions. In particular neither of the epoxides had been attacked by the strongly nucleophilic hydrazine. **55** was then refluxed for five hours in EtOH with hydrazine hydrate (5 equiv.) and dried down. The solid residue was extracted with DCM and the organic-soluble material examined by proton NMR spectroscopy and found to consist of almost pure starting material (**55**). Due to the failure of hydrazine hydrate to remove the phthalimide moiety under the conditions used, further attempts were made using methylamine, which has also been reported as a useful reagent for phthalimide removal,[166] but this was found to rapidly attack the spiro-epoxide. Following unsuccessful attempts to aminolyse the phthalimide group using a large excess of aqueous ammonia, the reaction was abandoned as it appeared that any nucleophile that would attack the phthalimide carbonyl groups would also ring-open the epoxide. An alternative strategy to produce the desired amine was required.

3.4.6 Fumagillol *R*-tosylate (56)

Initially, tosylation of the alcohol of fumagillol (**35**) was carried out following the published method.[99] Fumagillol (**35**) was reacted with tosyl chloride (1.25 equiv.) with dimethylaminopyridine (1.5 equiv.) present as both a nucleophilic catalyst and the general base for the reaction. The product of the reaction was found to contain a mixture of two compounds – the desired tosylate **56** and a compound lacking any epoxide resonances in the proton NMR spectrum. Further analysis of this side product was not carried out as the production of chlorinated adducts from nucleophilic attack of chlorine on the epoxides was already known.[99] The desired product **56** was obtained in a relatively low yield of 37% (reported yield of 61%), so further work was carried out in an attempt to improve this.

It was found that tosic anhydride is a superior sulphonylating reagent to tosyl chloride (**Figure 3.21**). It appears to be more reactive, requiring shorter reaction times than the chloride, and also does not produce any epoxide-opened products. Fumagillol (**35**) and tosic anhydride (1.5 equiv.) were dissolved in dry pyridine, with reaction progress monitored by HPLC (C18, A: H_2O, B: ACN, Gradient II) and TLC after ten minutes showing the complete consumption of the fumagillol starting material. The product **56** was isolated by a single passage through a C18 cartridge to provide pure tosylate **56** in a 95% yield.

The proton and carbon NMR spectra of **56** were fully assigned through the use of

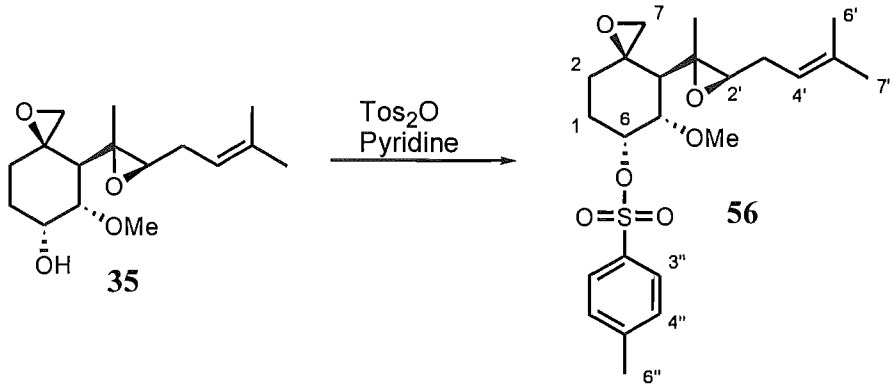

Figure 3.21 Tosylation of fumagillol (**35**) with retention of stereochemistry

COSY, HSQC-DEPT and CIGAR 2D experiments. Both C6 and H6 were significantly further downfield than seen for any other derivative of fumagillol, including the parent alcohol, at 75.5 ppm and 5.04 ppm respectively. These chemical shifts are consistent with the attachment of a strong nucleofuge which has a strong electron withdrawing effect leading to activation of nucleophilic attack at the point of attachment. The stereochemistry of C6 was determined as earlier explained (Section **3.4.4**) using the coupling constant between H6 and H5. This was found to be 2.5 Hz, which clearly indicates that the protons have a *gauche* relationship thus confirming the stereochemistry as 6*R*.

The molecular formula for **56**, $C_{23}H_{32}O_6S$, was confirmed using HREIMS in which the positive ion at 436.19 (1.17 ppm) was observed.

Analytical HPLC (C18, A: H_2O, B: ACN, Gradient II) of **56** showed a single peak eluting at 18.5 minutes which had a UV absorbance that extended as far as 280 nm and had maxima at 196 nm and 226 nm.

3.4.7 Tosylate displacement

Following the successful production of the tosylate **56**, a number of reactions were set up to displace the tosylate group with a variety of nucleophiles, namely ammonia gas, ammonium carbonate, sodium azide and potassium phthalimide. All of the reactions were performed in DMF and were carried out at 40°C. Despite allowing the reactions to proceed for a week, no displacement of the theoretically labile tosylate group was seen.

Examination of the accessibility of rear-side attack on the tosylate **56** suggests that the reaction should proceed. Analysis of the coupling constants in the proton NMR spectrum showed that in solution, the tosylate group is axially disposed. This can be seen by the coupling between H4 and H5 being 10.5 Hz, which has to be due to a di-axial relationship. With a 2.5 Hz coupling between H5 and H6, H6 must be equatorial,

leaving the tosylate group to be axial. This initially seems unlikely as a tosylate is a bulky group and as such would be expected to favour an equatorial position, but the side-chain and methoxy groups are both able to take equatorial positions when the tosylate is axial, leading to an overall minimum in steric energy. In a boat conformation it is possible to have both the tosylate and the fumagillol side-chain in equatorial positions. This causes the dihedral angle between H4 and H5 to be approximately 60°, which would lead to a coupling constant of 2-6 Hz, not the observed 10.5 Hz and thus this conformation is not dominant in solution.

3.4.8 Fumagillol azide (57)

Following the failure of the phthalimide and tosylate routes to provide the 6*R* amine derivative of fumagillol, a route using an azide intermediate was attempted (**Figure 3.22**). Fumagillol (**35**) was reacted with zinc azide (1 equiv.), triphenylphosphine (2.5 equiv.) and diethyl azodicarboxylate (2.5 equiv.) for 12 hours. Analytical HPLC (C18, A: H_2O, B: ACN, Gradient II) at this point indicated that about half of the starting material had been consumed, so the reaction was refreshed with a solution of 2.5 equivalents each of triphenylphosphine and diethyl azodicarboxylate in toluene. Following a further 12 hours of reaction, the mixture was chromatographed on silica to provide the desired azide **57** in a somewhat disappointing yield of 43%. Evidence of formation of the elimination product **54** was seen in proton NMR spectra which may help to account for the reduced yield as it would appear that S_N2 displacement of the triphenylphosphine oxide moiety formed during the Mitsunobu reaction may be impeded by steric hindrance as already discussed (Section **3.4.3**).

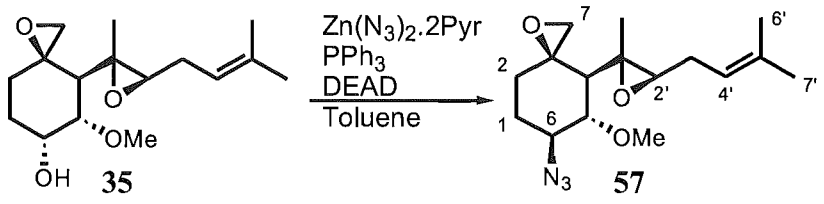

Figure 3.22 Formation of an azide derivative of fumagillol (**35**)

The proton and carbon NMR chemical shifts of **57** were fully assigned by reference to COSY, HSQC-DEPT and CIGAR spectra. The most significant change in chemical shift relative to the parent alcohol was H6, which had moved by 0.9 ppm upfield; however, the chemical shift of C6 was almost identical to that of the alchohol at just 0.8 ppm downfield. The stereochemistry of the azide at C6 was again confirmed to be *S* by analysis of the coupling constant between H5 and H6. H5 was a heavily split multiplet, but H6 was clearly seen as a doublet of doublets with coupling constants of 9.2 and 10.7 Hz. The latter coupling was derived from H4, which was observed as a doublet, which implied a 9.2 Hz coupling between H5 and H6 which is consistent with an *anti* relationship as shown.

The molecular formula for **57**, $C_{16}H_{25}N_3O_3$, was confirmed by HRESIMS, which allowed observation of the potassiated adduct having a mass of 346.15 (1.73 ppm).

Analytical HPLC (C18, A: H_2O, B: ACN, Gradient II) of **57** showed a single peak eluting at 17.3 minutes which had a UV chromophore that gradually decreased from a maximum at 192 nm to show no absorbance by 240 nm

3.4.9 Fumagillol azide reduction

Reduction of the azide **57** to an amine was carried out using triphenylphosphine (1.1 equiv.) and excess water (**Figure 3.22**). The reaction was seen to be complete by TLC after 18 hours, so the product was isolated by chromatography on a small silica column. Unlike other attempts to purify the natural product amine derivatives produced, in the case of **58**, the amine could be purified without difficulty in a 53% yield.

In order to ensure the success of the reaction, it was found that it was necessary to include water from the beginning of the reaction, which differs from the usual method for

Staudinger reduction of azides where water is only added after the phosphine-imine has had time to form.[160]

The proton and carbon NMR chemical shifts of **58** were fully assigned through the use of COSY, HSQC-DEPT and CIGAR 2D experiments. The NMR characteristics of **58** were found to be very similar to those observed for the azide **57** with only position 6 exhibiting significantly different chemical shifts. H6 had moved upfield by approximately 0.5 ppm relative to the azide **57**, while C6 was observed at 53.8 ppm where the corresponding atom in **57** had a chemical shift of 64.9 ppm. These upfield shifts are consistent with the transformation from an azide to an amine. The stereochemistry of C6 was again confirmed using the coupling constant between H5 and H6, which was found to be about 9.5 Hz, indicating an *anti* relationship and hence the *S* stereochemistry shown.

The molecular formula for **58**, $C_{16}H_{27}NO_3$, was confirmed using HRESIMS in which the protonated adduct at 282.21 (3.90 ppm) was observed.

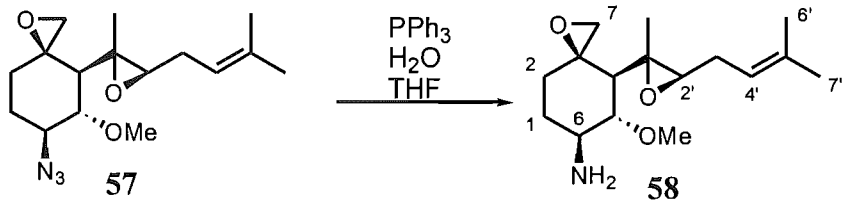

Figure 3.22 Reduction of azide **57** to afford amine **58**

3.5 Biological Activity

The purified natural product derivatives were submitted for bioactivity testing against the P388 murine leukemia cell line. The toxicities determined are shown below in **Table 3.5**.

The bioactivity of the crude amine derivative of mycalamide A (**45**) was an order of magnitude lower than that of the parent compound and the intermediate aldehyde derivative **45**; however, this is not unexpected and is most likely due to a combination of being both impure and significantly more polar. While the crude material did contain a high proportion of the desired amine, any contaminants would have reduced the apparent bioactivity by contributing inactive or less active mass. Increasing the polarity of a drug can often lead to a decrease in activity due to a reduction in the drug's ability to diffuse across the cytoplasmic membrane, so the introduction of an amine functionality would be expected to lead to a decrease in activity. In light of these two factors, the observed ten-fold decrease in activity is of no concern.

Mycalamide B (**32**) was not submitted for bioactivity testing in an amine form as this material was acylated immediately after synthesis. However, based on the results obtained for the crude mycalamide A amine (**45**) and the mycalamide B azide **49**, the IC_{50} of the mycalamide B amine could be expected to be approximately 20 nmol/L.

Table 3.5 Cytotoxicities of natural product derivatives

Compound	IC_{50} (g/mL)	IC_{50} (mol/L)
Mycalamide A (**31**)	1.5×10^{-9}	3.0×10^{-9}
Crude 17-amino-18-nor-mycalamide A (**45**)	14.0×10^{-9}	29.6×10^{-9}
Mycalamide B (**32**)	1.0×10^{-9}	1.9×10^{-9}
18-azido-18-deoxy-mycalamide B (**49**)	1.0×10^{-9}	1.8×10^{-9}
Fumagillol (**35**)	248.3×10^{-6}	876.5×10^{-6}
6-dehydro-fumagillol (**51**)	38.0×10^{-6}	135.6×10^{-6}
6-deoxy-fumagillol (**54**)	23.6×10^{-6}	89.3×10^{-6}
6*R*-phalimidyl-6-deoxy-fumagillol (**55**)	7.2×10^{-6}	17.5×10^{-6}
6*R*-tosyl-6-deoxy-fumagillol (**56**)	17.5×10^{-6}	40.2×10^{-6}
6*S*-azido-6-deoxy-fumagillol (**57**)	41.6×10^{-6}	135.3×10^{-6}

The fumagillol derivatives, like their parent compound, all showed low activity in the P388 bioassay used. This is because the fumagillol family of compounds is known to possess selective activity against endothelial cells, with nanomolar concentrations preventing proliferation and micromolar concentrations being cytotoxic. It would be useful to assay the fumagillol derivatives prepared here against an endothelial cell line. However, this is not currently available at the University of Canterbury. Samples of all compounds have been stored for assay at a future date should the opportunity arise.

Given the variety of derivatives at position 6 already reported that have shown no significant decreases in bioactivity,[99,100,167] it is not anticipated that the derivatives prepared in this work will have notably decreased bioactivity against endothelial cells compared to the parent fumagillol (**35**).

3.6 Conclusions from natural product modification

The required derivatisation of natural products to amine forms was successfully carried out, although the yields attained were often less than would be desired. This problem was compounded by the fact that most reactions were carried out on a small scale (less than 10 mg, often as little as 1 mg) due to the value of the starting materials. Working on this scale lends greater significance to losses accrued during transfer or purification.

The chemical sensitivity of the natural products investigated was a hindrance to their derivatisation as it limited the possible reagents and conditions that could be used as well as reducing the yields obtained. The scale-up of reactions that would be required should these compounds prove pharmaceutically useful could well present insurmountable problems, and in all likelihood the drug components would have to be replaced with other, more chemically stable, drugs. Nevertheless, the use of the highly toxic compounds described in this work remains a useful proof-of-principle for the utilisation of highly cytotoxic compounds in targeted constructs.

The instability of the compounds is also a cause for concern in terms of their pharmaceutical application as it is possible that they may be degraded in the lysosome following cleavage from the rest of the drug conjugate. However, until biological testing is carried out this concern cannot be addressed.

The reductive amination reaction to form primary amines used in this work was somewhat disappointing. The tendency for dimerisation was reduced by using a large excess of ammonium salt, but the yields were never as high as was believed might be achieved from an examination of the literature.

The poor behaviour of amines in reverse phase chromatography, and in particular HPLC, meant that purification of nearly all the amines was not achievable. Many attempts were made using silica but degradation was often observed despite the inclusion of bases in the eluting solvent. Ion chromatography would be an obvious choice for purification of

amines; however, the use of acidic solvents was precluded by the chemical sensitivity of the compounds.

The derivatisation of the mycalamides had a negligible effect on the bioactivity of the compounds, while the fumagillol derivatives were all more cytotoxic to P388 murine leukemia cells than the parent compound was.

Chapter 4

Low Molecular Weight Conjugates

4.1 Introduction

The synthesis of low molecular weight conjugates was carried out in order to allow determination of the effects of both the biodegradable linker and the polymer. The original work describing the targeting of doxorubicin using the *cyclo*-CNGRC motif did not provide any release mechanism for the doxorubicin, so the activity observed was presumably caused by the intact conjugate. Incorporating a biodegradable linker could be expected to improve the activity of the conjugate by allowing doxorubicin to be released upon entry to the cell and thus freeing the drug from potential hindrance in reaching and binding to the DNA. It was hoped that the low molecular weight conjugate utilising doxorubicin described in this chapter could be used to determine whether the above supposition is correct or not by comparing its activity with that reported for the original, non-biodegradable conjugate.

The preparation of low molecular weight conjugates of the other drugs was desirable to allow a comparison of their bioactivities to those of their polymer based analogues. This would allow some initial conclusions to be drawn concerning the effect of a polymeric structure on the efficacy of a targeted anti-angiogenic drug conjugate.

4.2 L-Tyrosinamide (39)

4.2.1 Fmoc-*cyclo*-CNGRCGFLG-L-Tyrosinamide (59)

L-Tyrosinamide (**39**, 2 equiv.) was condensed with **43** (1 equiv.) by reaction with DCC (1.9 equiv.) and NHS (2 equiv.) in DMF. NHS was included in the reaction to help prevent any dehydration of the asparagine side chain, as discussed in Section **2.3.2.** HPLC analysis (C18, A: H_2O(A), B: ACN, Gradient III) after overnight reaction indicated that no product had been formed so the reaction was recharged with another 5.4 equivalents of DCC. Analysis of the reaction after another 24 hours indicated that some product had been formed but that most of the material was still unreacted so the reaction was again recharged, but this time with HBTU (2 equiv.) instead of DCC in the hope that it would be a more efficient coupling reagent in DMF (**Figure 4.1**). One hour after the addition of HBTU, HPLC (C18, A: H_2O(A), B: ACN, Gradient III) indicated that the reaction was complete so water was added to destroy any unreacted HBTU. The product, **59**, was isolated in a 57% yield by direct semi-preparative HPLC (C18, isocratic 40% ACN/H_2O(A)) purification of the reaction mixture.

Due to the small quantity and complexity of the product, it was not fully characterised. A proton NMR spectrum which was collected showed a number of characteristic signals such as the leucine geminal methyl groups and the L-tyrosinamide aromatic signals. 2D NMR experiments were carried out on the compound, with COSY and ROESY spectra providing useful information, but the HSQC-DEPT, CIGAR and IMPRESS experiments provided little in the way of usable data. The fragments identified using the COSY spectrum are shown in **Figure 4.2**, as are some of the important ROESY correlations which were observed. The proton chemical shift data for **59** are provided in **Table 4.1**.

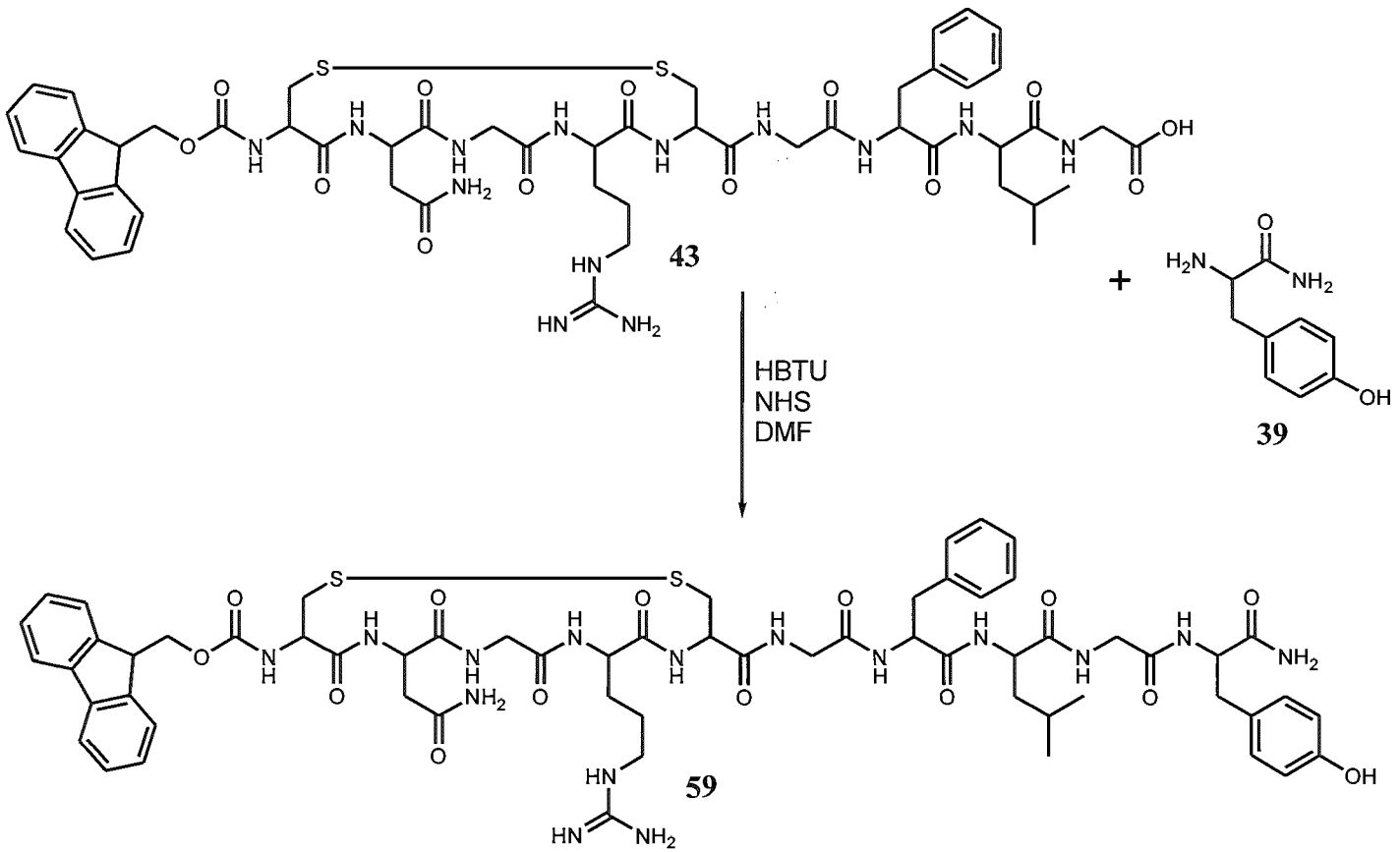

Figure 4.1 Reaction to form the protected nonapeptide-L-tyrosinamide conjugate (**59**)

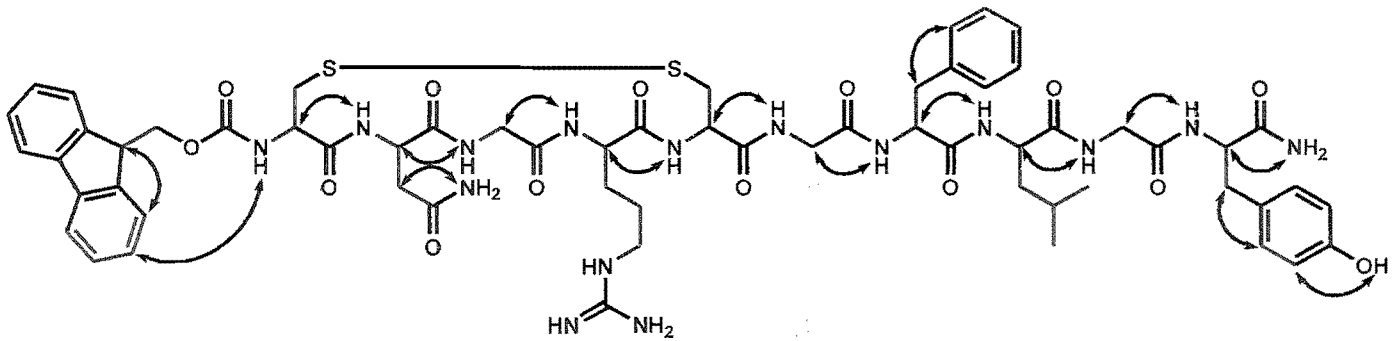

Figure 4.2 Important COSY (blue bonds) and ROESY (black arrows) correlations observed for **59**

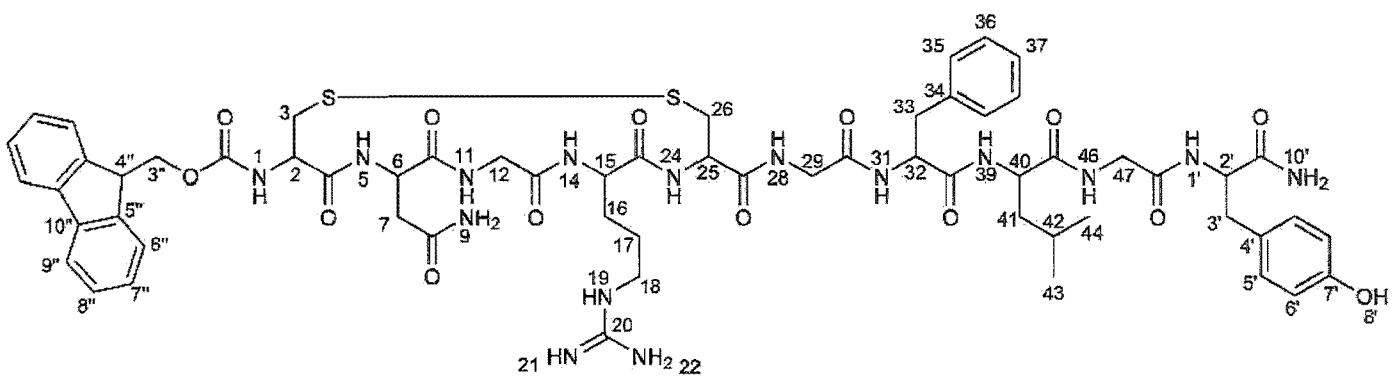

Fmoc-*cyclo*-Cys-Asn-Gly-Arg-Cys-Gly-Phe-Leu-Gly-L-Tyrosinamide (**59**)

Table 4.1 Proton NMR data for **59** obtained in d_6-DMSO

Position	^{1}H	COSY	ROESY
1	7.88	H2	H2, H3a, H7"
2	4.28	H1, H3a, H3b	H1, H3a, H3b, H5
3a	3.02	H2, H3b	H1, H2, H3b
3b	3.28	H2, H3a	H2, H3a
5	8.77	H6	H2, H6
6	4.64	H5, H7a, H7b	H5, H7a, H7b, H11
7a	2.38	H6, H7b	H6, H7b, H9
7b	2.79	H6, H7a	H6, H7a, H9
9	7.43		H7a, H7b
11	7.92	H12a, H12b	H6, H12a
12a	3.51	H11, H12b	H11, H12b
12b	4.29	H11, H12a	H12a, H14
14	7.78	H15	H12b, H15, H16a
15	4.44	H14, H16a, H16b	H14, H16a, H16b, H17, H24
16a	1.62	H15, H16b, H17	H14, H15, H17
16b	2.02	H15, H16a, H17	H15, H17
17	1.54	H16a, H16b, H18	H16a, H16b, H18
18	3.17	H17, H19	H17, H19
19	7.61	H18	H18
24	8.09	H25	H15, H26a
25	4.57	H24, H26a, H26b	H26b
26a	3.07	H25, H26b	H24
26b	3.31	H25, H26a	H25
28	8.34	H29	H25, H29
29	3.75	H28	H28, H31
31	8.13	H32	H29, H32, H33a, H35
32	4.63	H31, H33a, H33b	H31, H33a, H33b, H35, H39
33a	2.84	H32, H33b	H31, H32, H33b, H35
33b	3.11	H32, H33a	H32, H33a, H35
35	7.31		H31, H32, H33a, H33b
36	7.3		
37	7.24		
39	8.29	H40	H32, H40, H41, H46
40	4.35	H39, H41	H39, H41, H42, H43, H44, H46
41	1.56	H40, H42	H39, H40, H43, H44, H46
42	1.67	H41, H43, H44	H40, H43, H44
43	0.97	H42	H40, H41, H42
44	0.92	H42	H40, H42
46	8.06	H47a, H47b	H39, H40, H41, H47a, H47b
47a	3.67	H46, H47b	H46, H47b, H1'
47b	3.82	H46, H47a	H46, H47a, H1'
1'	7.99	H2'	H47a, H47b, H2', H3'a, H5', H10'
2'	4.41	H1', H3'a, H3'b	H1', H3'a, H3'b, HH5', H10'

3'a	2.77	H2', H3'b	H2', H3'b, H5'
3'b	2.98	H2', H3'a	H2', H3'a, H5'
5'	7.09	H6'	H1', H2', H3'a, H3'b, H6'
6'	6.73	H5'	H5', H8'
8'	9.26		H6'
10'	7.48		H1', H2'
3"	4.42	H4"	H6"
4"	4.33	H3"	H6"
6"	7.82	H7"	H3", H4", H7"
7"	7.41	H6", H8"	H1, H6", H8"
8"	7.5	H7", H9"	H7", H9"
9"	7.99	H8"	H9"

Every amino acid could be discerned in the COSY spectrum by begining with the characteristic correlations between the amide protons and the α-protons. From these starting points it was possible to step through the side chains, where applicable, and identify the proton chemical shifts for all ten amino acids. The proton chemical shifts of **59** were very similar for those determined for the nonapeptide **43** with even the amide chemical shifts showing near coincidence. The only positions which deviated by more than 0.04 ppm were the α-proton of the leucine residue, H39, which had moved 0.06 ppm upfield compared to **43**, and the amide, H45, and α-protons, H46, of the *C*-terminal glycine residue. H45 had moved upfield by 0.14 ppm relative to **43**, while H46 had developed diastereotopic splitting, with one proton appearing at an almost unchanged (0.01 ppm upfield) position at 3.82 ppm while the other had moved significantly to 3.67 ppm. These changes in chemical shift are consistent with conversion of the *C*-terminal glycine acid functionality to an amide.

The ROESY spectrum provided a useful series of correlations along the 'backbone' of the peptide between neighbouring amides and α-protons. It must be remembered that since the ROESY experiment relies on through space nOe correlations, caution must be taken when interpreting the data and particular when looking to determine connectivity. With that restriction in mind, the correlation between the L-tyrosinamide amide H1' and the α-protons of the C-terminal glycine H46a,b did indicate that these protons were

spatially near each other. This evidence, combined with the observation of changes in chemical shifts elucidated from the COSY spectrum indicates that the desired compound **59** was successfully formed.

The molecular formula for **59** of $C_{61}H_{77}N_{15}O_{14}S_2$ was confirmed by HRESIMS which observed the protonated ion at 1308.53 (0.69 ppm).

Analytical HPLC (C18, A: H_2O(A), B: ACN, Gradient III) of **59** showed a single peak eluting at 9.3 minutes with a strong UV chromophore characteristic of the Fmoc group.

4.2.2 H_2N-*cyclo*-CNGRCGFLG-L-Tyrosinamide (60)

The Fmoc protecting group of **59** was removed by dissolving **59** in 20% piperidine/MeOH (Figure **4.3**). Following cleavage of the protecting group, the reaction residue was purified by passage through a C18 cartridge which was eluted with a stepped gradient from H_2O to MeOH. **60** was not found to have eluted in any of the fractions from the aqueous-methanol gradient so the column was stripped with 100% DMSO, which also failed to elute **60**. Finally, an acidified solution consisting of 90% MeOH/H_2O with 0.1% TFA was passed through the column and was successful in removing **60** which was isolated in a near quantitative yield of 98%.

Due to the paucity of material, no attempts were made to characterise **60** using 2D NMR spectroscopy; however, a proton spectrum was obtained and showed peaks characteristic of the phenyl group of phenylalanine, the geminal methyls of leucine and the para substituted phenyl ring of L-tyrosinamide. The characteristic Fmoc peaks were absent from the spectrum, indicating the deprotection of **59** had been successful.

HRESIMS confirmed the molecular formula of **60** to be $C_{46}H_{67}N_{15}O_{12}S_2$ through detection of the protonated parent ion at 1086.46 Daltons (0.28 ppm).

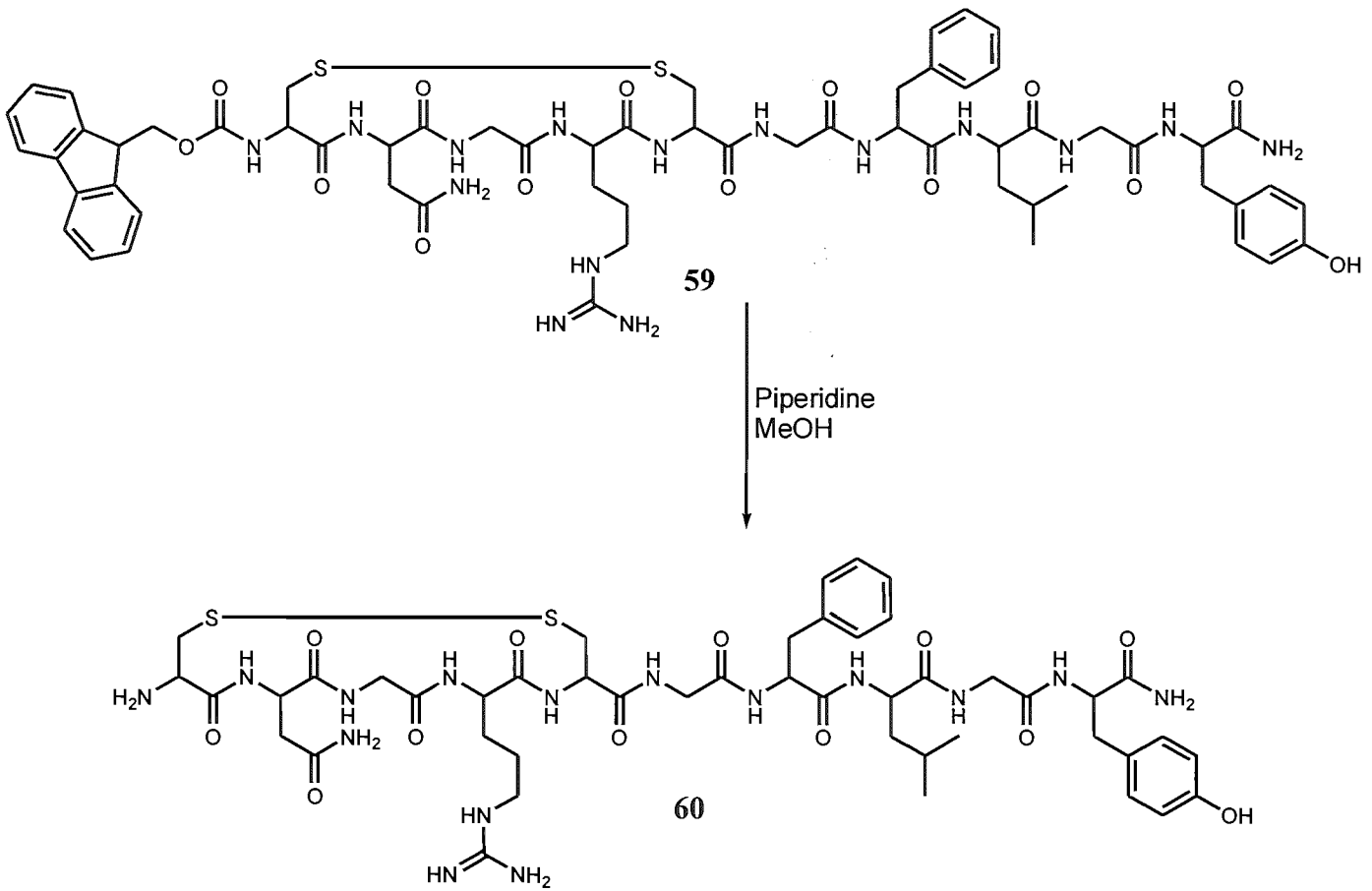

Figure 4.3 Fmoc removal to form low molecular weight drug conjugate **60**

4.3 Doxorubicin (19)

4.3.1 Fmoc-*cyclo*-CNGRCGFLG-Doxorubicin

Doxorubicin (**19**, 1.1 equiv.) was acylated with **43** using HBTU (1.9 equiv.) and NHS (2 equiv.) in DMF. An analytical HPLC chromatograph (C18, A: H_2O(A), B: ACN, Gradient III) of the reaction taken after 16 hours of reaction indicated that the reaction was complete due to the absence of the starting peptide **43**. Water was added to the reaction to quench any unreacted HBTU and the reaction solution was purified directly by semi-preparative HPLC (C18, isocratic 45% ACN/H_2O(A)) to afford the desired doxorubicin conjugate in a 29% yield.

An examination of the conjugate was carried out using NMR, but due to the structural complexity of the compound and the small amount isolated, it was not possible to fully characterise the compound. A proton spectrum was obtained and showed characteristic signals of the peptide and doxorubicin components such as the leucine geminal methyl groups, the aromatic signals of the Fmoc moiety and the downfield benzyl methoxy group of doxorubicin. A COSY spectrum was used to identify the proton chemical shifts of the amino acid residues and, more importantly, the glycone moiety of doxorubicin. From the characteristic downfield anomeric proton of doxorubicin at 5.32 ppm, the proton chemical shifts of the sugar could be traced to an amide proton at 7.60 ppm, thus confirming that doxorubicin had been successfully conjugated to the protected nonapeptide. An HSQC-DEPT and a ROESY experiment were run but unfortunately provided almost no data due to a poor signal to noise ratio.

The molecular formula of the conjugate, $C_{79}H_{94}N_{14}O_{23}S_2$, was confirmed using HRESIMS which showed a peak corresponding to the protonated parent ion at 1671.61 Daltons (0.00 ppm).

Analytical HPLC (C18, A: H_2O(A), B: ACN, Gradient III) of the conjugate showed a single peak eluting at 17.8 minutes which had a strong UV chromophore that included many local maxima and extended to the limit of the detector (600 nm). The chromophore was characteristic of doxorubicin.

4.3.2 H_2N-*cyclo*-CNGRCGFLG-Doxorubicin

The deprotection of the protected nonapeptide-doxorubicin conjugate was not carried out due to the degradation observed in the same reaction of the corresponding tetrapeptide derivative during the synthesis of the analogous polymer drug conjugates. In that reaction, described in detail in Section **5.4.2**, it was found that doxorubicin was completely degraded during the brief exposure to piperidine required to remove the Fmoc protecting group. The sensitivity of doxorubicin to basic conditions is known, but it was hoped that the short reaction time would prevent complete decomposition but this was not found to be the case.

Due to the likelihood of damaging the conjugate during any attempts to deprotect the *N*-terminus, the decision was made to assay the biological activity of the conjugate with the Fmoc group in place.

4.4 Mycalamide A (31)

4.4.1 Fmoc-*cyclo*-CNGRCGFLG-Mycalamide A

Crude **45** was acylated with the peptide **43** (1.3 equiv.) using HBTU (1.9 equiv.) and NHS (2.0 equiv.) in DMF. After overnight reaction at room temperature, a sample was examined using analytical HPLC (C18, A: H_2O(A), B: ACN, Gradient III) which showed two major peaks and a number of minor peaks with spectra corresponding to the Fmoc chromophore (**Figure 4.4**). None of these peaks eluted at the established retention time of the peptide **43** (9.0 min). HPLC was then repeated, but without acidified water, as the acid in the water would have catalysed degradation of conjugated mycalamide A. Under these conditions, only one major peak with the Fmoc chromophore was observed (**Figure 4.4**). Semi-preparative HPLC (C18, isocratic 40% ACN/H_2O) was used to collect this peak. Re-injection of the collected material on the analytical HPLC (C18, A: H_2O(A), B: ACN, Gradient III) showed a single peak eluting at 6.7 min, 0.8 min earlier than the previously determined retention time. LRESIMS analysis of the material provided a molecular mass of 1 145, which is the mass of the starting peptide **43**. There was no observable peak in the LRESIMS spectrum that corresponded to the molecular

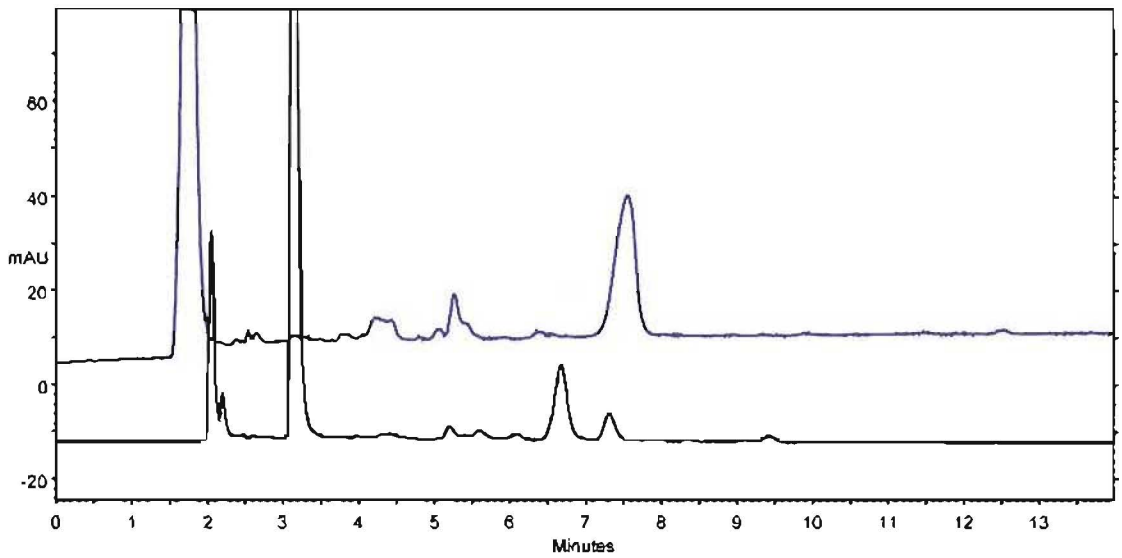

Figure 4.4 HPLC chromatogram of product of acylation of **45** run with (black) and without (blue) TFA

mass of the desired conjugate. LRESIMS investigation of the waste from the attempted semi-preparative purification similarly showed no sign of the desired product.

Due to the limited supply of both mycalamide A (**31**) and the nonapeptide **43**, it was not possible to attempt this reaction a second time. The reason for the failure of the coupling reaction remains unknown.

4.5 Mycalamide B (32)

4.5.1 Fmoc-*cyclo*-CNGRCGFLG-Mycalamide B

Crude **50** was acylated with the peptide **43** (1.3 equiv.) using HBTU (1.9 equiv.) and NHS (2.0 equiv.) in DMF. After overnight reaction at room temperature, a sample was examined using analytical HPLC (C18, A: H_2O(A), B: ACN, Gradient III) which showed two major peaks, eluting at 9.2 min and 12.7 min, and one minor peak at 21.6 min, all possessing the Fmoc chromophore. The sample was also run in the absence of TFA (C18, A: H_2O, B: ACN, Gradient III) and gave a similar chromatogram in which the two major peaks eluted slightly earlier (**Figure 4.5**). Semi-preparative HPLC (C18, isocratic 40% ACN/H_2O) was used to collect the major compound, which had an unreliable retention time but eluted at around 5.5 minutes. This collected material was examined by LRESIMS. The mass spectrum obtained showed a very small amount of the desired product (molecular mass 1 643), but a much larger proportion (approximately 35 times as much) of the starting peptide **43**. Re-examination of the collected material by analytical HPLC (C18, A: H_2O, B: ACN, Gradient III) showed a single peak eluting at

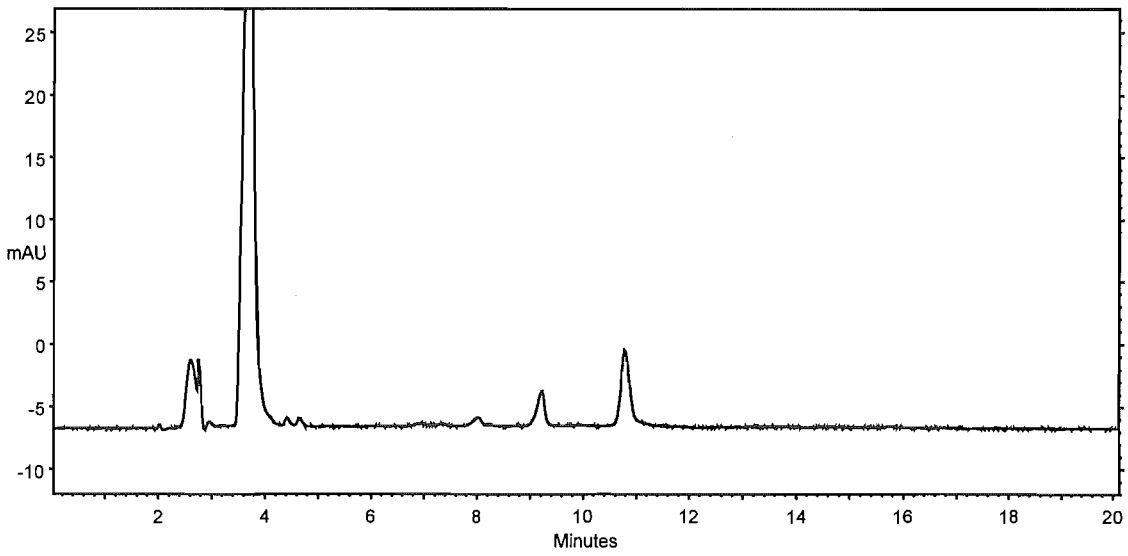

Figure 4.5 HPLC chromatogram of the crude reaction product of **32** acylation run without TFA

6.5 min. This elution time was significantly earlier than the 10.8 minutes established prior to semi-preparative HPLC purification, and may indicate that the reaction product was unstable and had hydrolysed. This would not occur if an amide had been formed with the mycalamide B derivative **50** thus it is likely that the acylation reaction failed. It is possible that the compound that was collected was an HOBt or NHS ester (**Figure 4.6**), which are active esters and as such are liable to hydrolyse and can be formed during acylations with HBTU and NHS.

Due to the limited supply of both mycalamide B (**50**) and the nonapeptide **43**, it was not possible to attempt this reaction a second time.

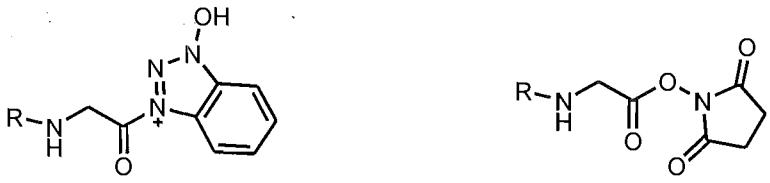

Figure 4.6 Possible reaction products of attempted acylations with HBTU and NHS

4.6 *R*-Fumagillol

4.6.1 Fmoc-*cyclo*-CNGRCGFLG-*R*-Fumagillol

Crude **52** was acylated with the peptide **43** (1.3 equiv.) using HBTU (1.9 equiv.) and NHS (2.0 equiv.) in DMF. After overnight reaction at room temperature, a sample was examined using analytical HPLC (C18, A: H_2O(A), B: ACN, Gradient III) which showed two major peaks eluting at 9.3 and 12.8 min, with the earlier eluting peak being slightly larger. As this peak was presumed to be the starting peptide **43**, the reaction was recharged with extra **52** (1.3 equiv.) and HBTU (1.0 equiv.) and allowed to react for a further 24 hours. Analytical HPLC of the further reacted material showed a single major peak at 11.0 min, which was collected by semi-preparative HPLC (C18, isocratic 40% ACN/H_2O(A)) in which it eluted at about 4.7 minutes. A LRESIMS spectrum obtained for the collected material showed a parent ion with a molecular mass of 1173.7, which neither corresponds to the desired product, nor any likely side-product, being just 28 daltons heavier than the starting peptide **43**. This mass difference could be caused by formation of an ethyl ester at the carboxyl terminus of the peptide, although there was no ethanol present in the reaction and this mass increase was not observed in any of the other coupling reactions, which were all carried out under the same conditions.

4.7 *S*-Fumagillol

4.7.1 Fmoc-*cyclo*-CNGRCGFLG-*S*-Fumagillol

Crude **58** (contaminated with triphenylphosphine oxide) was acylated with the peptide **43** (1.3 equiv.) using HBTU (1.9 equiv.) and NHS (2.0 equiv.) in DMF. After overnight reaction at room temperature, a sample was examined using analytical HPLC (C18, A: H_2O(A), B: ACN, Gradient III) which showed a single major peak with a chromophore corresponding to that of Fmoc eluting at 21.7 min and a series of four minor peaks at 21.1, 21.4, 24.5 and 24.8 minutes, all of which possessed the Fmoc chromophore. While waiting for semi-preparative HPLC, the sample was stored at 4°C for 36 hours. Re-examination by analytical HPLC (C18, A: H_2O(A), B: ACN, Gradient III) at this point showed that the sample had degraded to a set of six peaks displaying the Fmoc chromophore, eluting at 18.6, 18.9, 19.5, 19.7, 22.6 and 23.1 minutes (**Figure 4.7**). As this decomposition was not observed in the preparation of the tetrapeptide biolinker adduct (Section **5.8.1**), in which pure **58** was used, the reaction was repeated, but using **58** that had been purified to remove the contaminating triphenylphosphine oxide. HPLC

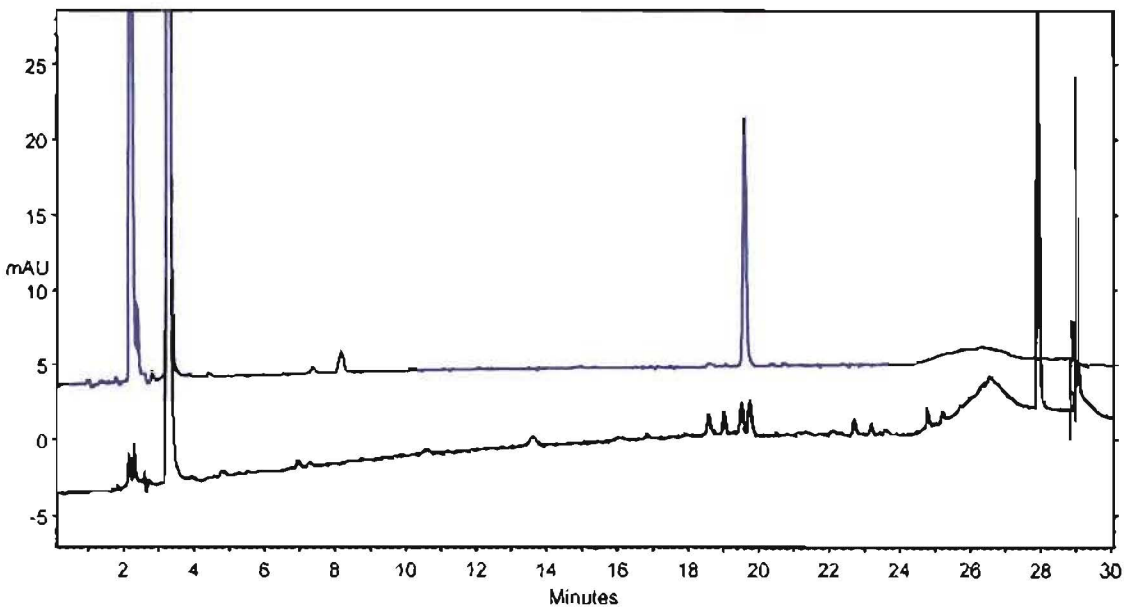

Figure 4.7 Chromatogram of crude reaction product after overnight reaction (blue trace) and 36 hours storage (black trace)

analysis (C18, A: H_2O(A), B: ACN, Gradient III) after overnight reaction showed a single peak eluting at 19.6 minutes, but following storage overnight at 4°C prior to purification again led to complete degradation. An analytical HPLC chromatogram (C18, A: H_2O(A), B: ACN, Gradient III) showed a series of peaks similar to those seen in the first instance. LRESIMS was carried out on the sample, but no ions corresponding the the desired product could be seen in the spectrum. At this point, the apparent instability of this compound led to a decision to abandon any further work toward formation of the nonapeptide adduct.

4.8 Biological activity

The purified natural low molecular weight conjugates were submitted for bioassay against the P388 murine leukemia cell line. The toxicities determined, with concentrations referring to the drug component, are shown below in **Table 4.2**.

As was hoped, the peptide conjugates prepared were not significantly cytotoxic. Unfortunately it was not possible to determine their exact toxicity as it was desirable to retain as much mass as possible for *in vivo* testing so the conjugates were tested at only one concentration. The primary purpose of this assay was to show that the peptide components themselves were not cytotoxic.

The doxorubicin conjugate showed a toxicity at least five-fold lower than that of free doxorubicin as would be expected following conjugation to the large and relatively polar peptide construct. In the absence of receptor-mediated uptake, the conjugate should not release free doxorubicin and so will remain inactive, as doxorubicin must translocate to the cell nucleus to exert its toxicityThe . APN receptor targeted by this construct is not displayed at a significant level on non-endothelial cells so P388 murine leukemia cells will not endocytose these constructs efficiently.

Table 4.2 *In vivo* toxicities of low molecular weight conjugates

Compound	IC_{50} (g/mL)	IC_{50} (mol/L)
Doxorubicin (**19**)	700×10^{-9}	1.3×10^{-6}
H_2N-*cyclo*-CNGRCGFLG-L-tyrosinamide (**60**)	$> 2.1 \times 10^{-6}$	$> 11.5 \times 10^{-6}$
Fmoc-*cyclo*-CNGRCGLFG-doxorubicin	$> 4.0 \times 10^{-6}$	$> 7.5 \times 10^{-6}$

4.9 Conclusions About Low Molecular Weight Conjugates

Two low molecular weight conjugates were successfully prepared. The first incorporated L-tyrosinamide for use in biodistribution studies, while the second utilised the proven anti-cancer drug doxorubicin. The doxorubicin conjugate was prepared to allow an assessment of the effect of inclusion of an established biodegradable linker by comparison of the biological activity of the construct with that of Arap et al.[64] Initial testing against P388 murine leukemia cells indicated that the conjugates could be suitable for *in vivo* studies as they did not display significant cytotoxicity against this generic cell line.

The preparation of the two mycalamide conjugates was unsuccessful, with the most likely cause being failure of the acylation reaction. The reason for this failure is not known, and is particularly puzzling given the success of the analagous reactions during polymer drug conjugate synthesis (**Chapter 5**).

The preparation of two enantiomeric fumagillol conjugates was also unsuccessful, although in these cases it would appear that degradation was the cause of the failure. These problems were not noted during the preparation of biolinker toxins (**Chapter 5**), which indicates that the pentapeptide targeting motif may be somehow responsible for the observed decomposition. This is somewhat surprising, given that the pentapeptide does not contain any highly reactive functionalities. The only functional groups which it does not share with the tetrapeptide biolinker are the arginine guanidine, the asparagine terminal amide and the cystine disulfide. Of these, only the disulfide or the strongly basic guanidine (pKa 12.5) could be reasonably expected to present any possibility of undesired reaction. An unprotonated guanidine group is strongly nucleophilic so could lead to degradation via nucleophilic attack, although it should have remained protonated throughout the work as no strong bases were used at any point. The cystine disulfide should not have presented any problems as disulfide bonds are relatively stable. If this work is pursued further, it would be necessary to examine the stability of the natural

products in the presence of isolated guanidine and disulfide functionalities to determine the cause of the observed degradation.

The analysis of reaction progress was complicated by the tendency of the nonapeptide to show non-reproducible retention times on all HPLC systems used. This is likely due to the presence of the free guanidinium group in the arginine side-chain. Non-reproducible behaviour of compounds containing free amine groups has been observed in other samples investigated during the course of this research, and is thought to be due to slight variations in the level of ionisation of the amine group. It appears that the guanidine functionality is also prone to this behaviour despite being significantly more basic than all amines.

Finally, due to the small quantities of starting materials available, in particular the nonapeptide, it was not possible to re-attempt the unsuccessful syntheses to try to circumvent the acylation and degradation difficulties. While it would have been possible to resynthesise the peptide, this would have required a very significant investment of time, which was not justifiable given the indeterminate nature of the difficulties experienced.

Chapter 5

Polymer Drug Conjugates

5.1 Introduction

The synthesis of polymer drug conjugates has typically been carried out through the aminolysis of a co-polymer of HPMA with a *p*-nitrophenol activated ester of the biolinker, the so called polymeranalagous reaction (**Figure 5.1**).[123] The reaction progress is monitored by quantitation of the amount of released *p*-nitrophenol using UV to detect the highly coloured *p*-nitrophenoxide ion in basic conditions. The co-polymer itself is produced by free radical polymerisation of the component monomers in appropriate proportions, but this results in a polymer with high polydispersity. This distribution leads to a decrease in the efficacy of the polymer drug conjugate as some of the polymer will have a very low molecular weight, and so be rapidly eliminated, while some will be very

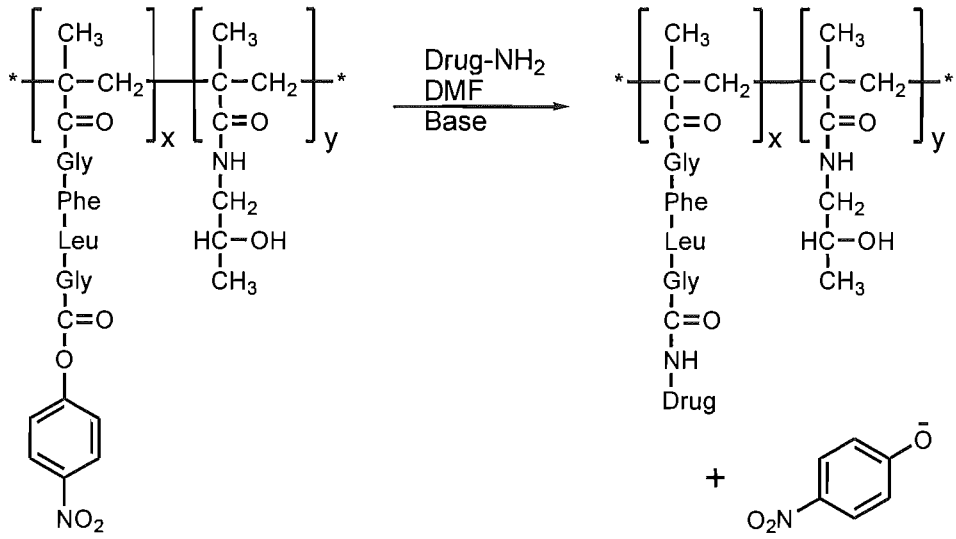

Figure 5.1 Synthesis of a polymer drug conjugate from HPMA copolymer

high molecular weight and thus may be permanently retained if it exceeds the renal threshold (~ 50 kDa). Furthermore, achieving regulatory approval may be difficult in the case of a highly polydisperse and thus poorly characterised drug.

To circumvent these problems, the use of polymer precursors synthesised using atom transfer radical polymerisation (ATRP) to ensure a low polydispersity has been proposed.[168, 169] ATRP is a form of controlled radical polymerisation in which the radical of a growing polymer can exchange with a more stable metal atom, thus ensuring that the polymer radical is maintained at a low concentration, which in turn leads to a greatly reduced rate of premature termination of polymerisation.[170] The polymer precursor proposed is poly(methacryloxy succinimide) (pMAOS, **61**). This is a homopolymer of an activated ester of methacrylic acid which can be aminolysed to produce the final polymer drug conjugate (**Figure 5.2**).

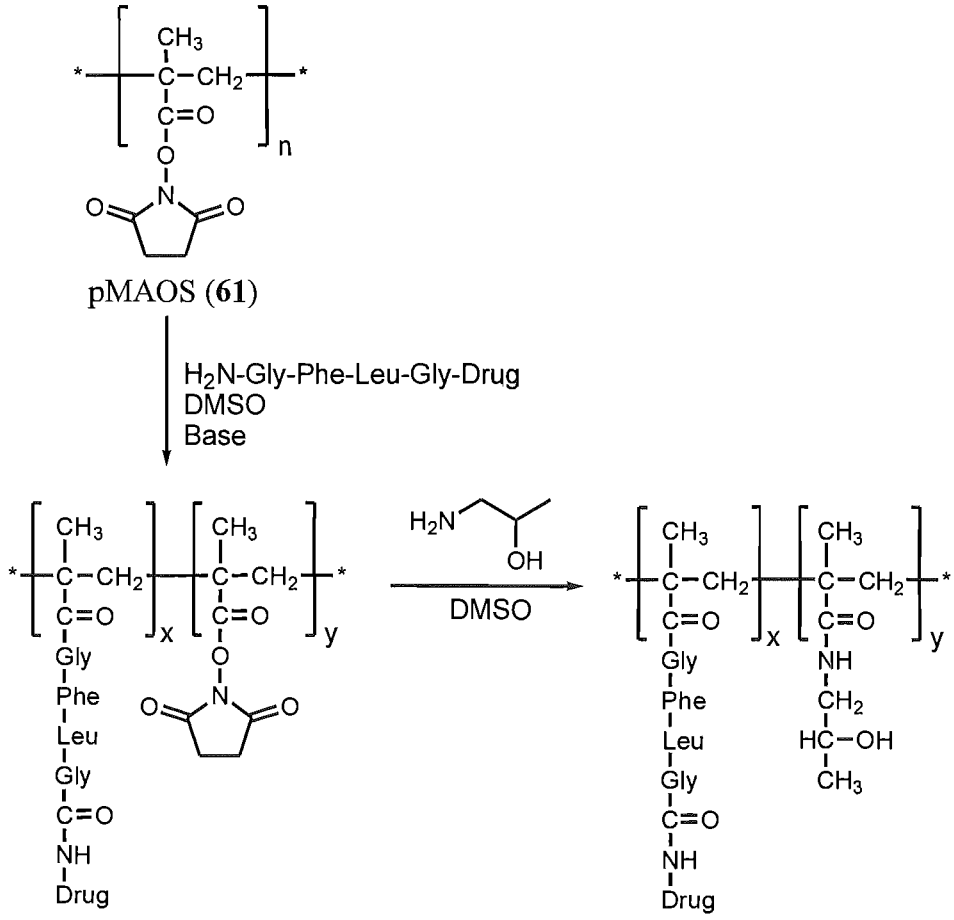

Figure 5.2 Synthesis of a polymer drug conjugate from pMAOS

The use of this type of activated polymer precursor has a further advantage that the components to be incorporated, such as the biolinker, can be changed easily without requiring new polymerisation reactions to be carried out. Furthermore, it has the advantage that targeting residues no longer have to be attached via the biodegradable linker as in PK2 (**38**), but rather can be attached directly to the polymer backbone, *via* a spacer if desired.

A sample of pMAOS was supplied for this work by Miss Hsin-I Chang and had a weight average molecular weight of 16 100 and a polydispersity of 1.18.[171]

5.2 Optimisation of Polymer Aminolysis

The mildest conditions reported to date for the aminolysis of pMAOS (**61**) are an initial treatment with a peptide-drug substitute (0.1 equiv.) for 2.5 hours at 50°C followed by complete aminolysis with 1-amino-2-propanol (2 equiv.) for 1.25 hours at 50°C. The characterisation of the polymer was carried out using FT-IR in attenuated total reflectance mode to observe the loss of the characteristic IR absorbance of the oxysuccinimide ester at 1735 cm^{-1}.[169]

Due to the tendency for degradation, we try to avoid subjecting natural products to elevated temperatures, in particular conditions significantly higher than body temperature (37°C) are considered to present an undesirable risk to the integrity of the natural products. For this reason, it was necessary to investigate the aminolysis of pMAOS (**61**) at a reduced temperature.

Initially, a reaction was carried out aminolysing pMAOS (**61**) with L-tyrosinamide (**39**, 0.25 equiv.) at 40°C in the presence of Et_3N (0.5 equiv.) with DMSO as the solvent. The reaction progress was monitored by ATR-IR at 1735 cm^{-1} but the peak height fluctuated, with some measurements providing a reading greater than the initial reading. Examination of the region surrounding the peak of interest in the IR spectrum revealed that there were broad peaks nearby which were influencing the baseline selection, and thus the measured height of the peak at 1735 cm^{-1}. Due to these difficulties, it was decided that a different analytical technique should be investigated.

A time course investigation was carried out using proton NMR spectroscopy. pMAOS (**61**) was reacted with phenylglycine methyl ester (0.25 equiv.) at 50°C in d_6-DMSO in the presence of Et_3N (0.75 equiv.). It was hoped that the downfield movement of the α-proton from its initial position of 5.37 ppm could be observed upon conjugation to the polymer backbone. Unfortunately the phenylglycine appeared to have a very low reaction rate with the polymer, presumably due to steric hindrance, as the reaction

remained largely incomplete after 13 hours. This low reactivity precluded the use of phenylglycine as a valid model.

An alternative method of examining the progression of the aminolysis reaction was attempted in which reaction samples were purified prior to analysis by NMR spectroscopy. This series of experiments also provided an opportunity to investigate the purification of the polymer product. Initially, pMAOS (**61**) was reacted with 1-amino-2-propanol (2 equiv.) at 40°C in dry DMSO for four hours. The first attempt at polymer purification was made using a CentriPrep ultrafiltration system with a molecular weight cut-off of 5 000 Da; however, the purification was unsuccessful as the polymer passed through the membrane. The failure of the ultrafiltration membrane to retain the polymer drug conjugate could well have been because the membrane is designed to retain globular molecules such as proteins. The polymer is linear and would not be expected to form a globular structure as it contains no extended hydrophobic domains to drive hydrophobic collapse, which is believed to be crucial to the formation of protein tertiary structure.[172]

The contaminated polymer was then passed through an LH20 column, eluting with MeOH, which did remove most of the contaminants as determined by proton NMR spectroscopy; however, some contamination remained. The polymer was then passed through LH20 a second time, again eluting with MeOH, to remove the remaining low molecular weight contaminants.

The proton NMR spectrum of the purified polymer (**Figure 5.3**) showed an unexpected broad peak at 2.56 ppm so 2D NMR experiments were carried out. The HSQC-DEPT spectrum showed that the protons at 2.56 ppm were correlated to two carbons at 28.2 and 30.8 ppm and that these were both methylenes. A CIGAR experiment revealed that the same protons were also correlated to two carbonyl carbons at 170.3 and 173.5 ppm as well as carbons at 28.2 and 30.8. The evidence thus collected strongly suggested that the succinimide moiety had undergone a ring opening reaction by attack of the nitrogen nucleophile on an imide carbonyls rather than the desired ester carbonyl (**Figure 5.4**).

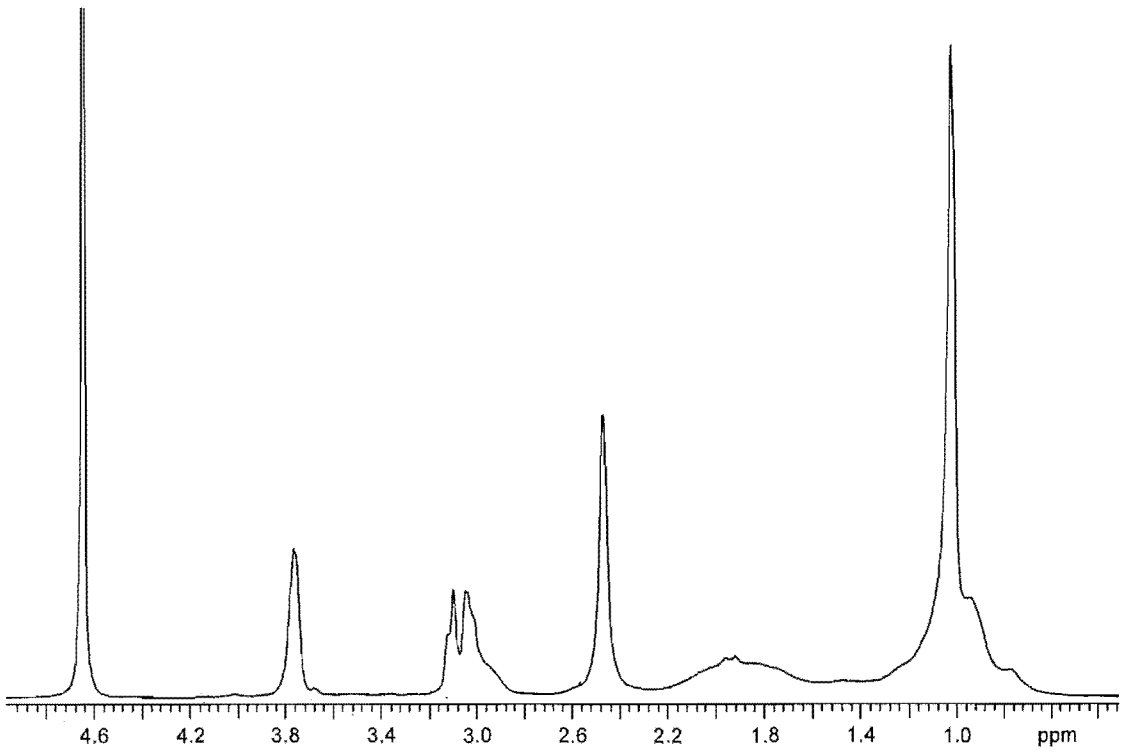

Figure 5.3 Proton NMR spectrum of polymer showing unexpected peak at 2.56 ppm

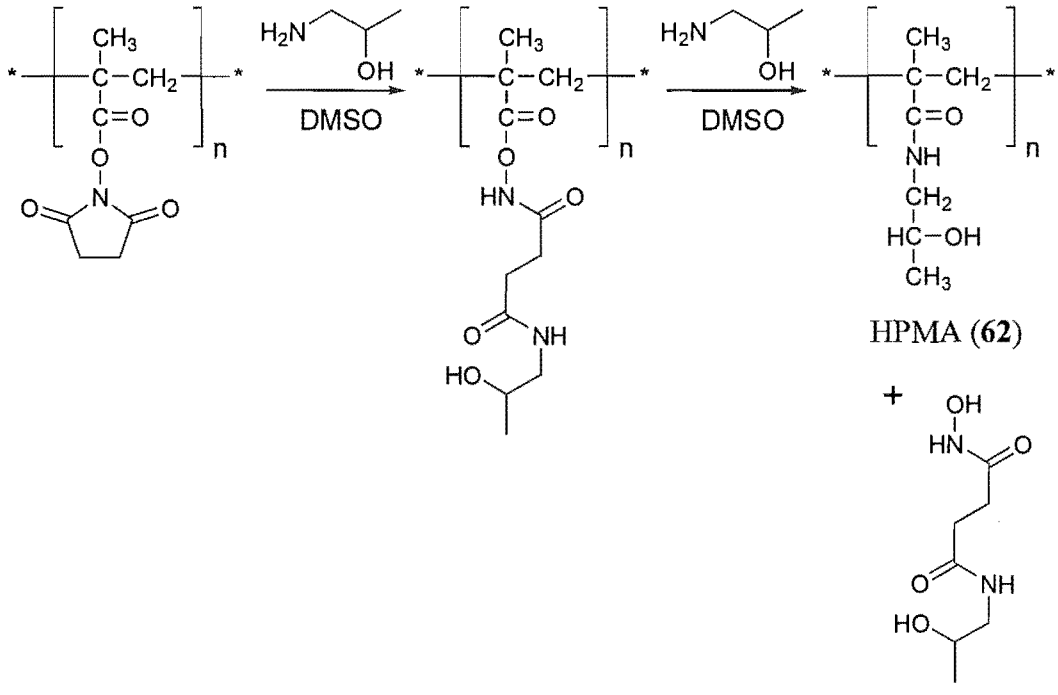

Figure 5.4 Proposed side reaction of pMAOS polymer precursor

This is a known reaction that has been previously reported for reactions of succinimidyl esters with amino acids in which one of the reagents is sterically hindered.[173-175]

The polymer was reacted a second time with 1-amino-2-propanol (2 equiv.) in dry DMSO for 16 hours at 40°C in an effort to displace the putative oxysuccinamide groups. After purification by passage twice through LH20 eluted with MeOH, proton NMR spectroscopy revealed that the peak at 2.56 ppm was greatly reduced in size. The later eluting, low molecular weight fractions from the LH20 column were examined, with one containing a mixture of compounds which seemed to include the unexpected side product from the polymer aminolysis. This fraction was passed through a silica column (0.6 g, 60 x 5 mm) and then finally purified by semi-preparative HPLC (C18, isocratic 2% ACN/H_2O(A)) to provide two pure isomers (**63** and **64**).

The proton and carbon NMR spectra of **63** and **64** were fully assigned using COSY, HSQC and CIGAR 2D NMR experiments. The chemical shift assignments are shown in **Tables 5.1** and **5.2** with the important COSY and CIGAR correlations shown in **Figures 5.5** and **5.6**.

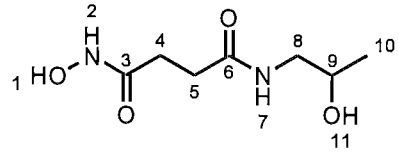

N-*Z*-Hydroxy-*N'*-(2-hydroxypropyl)-succinamide (**63**)

Table 5.1 Proton and carbon NMR data for **63** obtained in d_6-DMSO

Position	^{1}H	^{13}C	COSY	CIGAR
1	8.7		H2	
2	10.39		H1	C3
3		168.6		
4	2.18	28	H5	C3, C5, C6
5	2.33	30.7	H4	C3, C4, C6
6		171.3		
7	7.82		H8	C6, C8
8	2.98	46.5	H7, H9	C6, C9, C10
9	3.62	65.3	H8, H10, H11	C8
10	1.01	21.2	H9	C8, C9
11	4.65		H9	C8, C9, C10

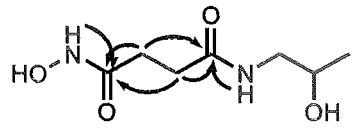

Figure 5.5 Important COSY (blue bonds) and CIGAR (black arrows) correlations observed for **63**

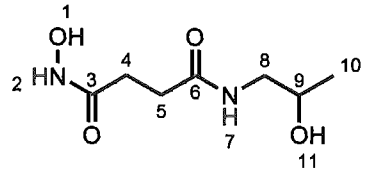

N-E-Hydroxy-*N'*-(2-hydroxypropyl)-succinamide (**64**)

Table 5.2 Proton and carbon NMR data for **64** obtained in d_6-DMSO

Position	^{1}H	^{13}C	COSY	CIGAR
1	7.37		6.82	
2	6.82		7.37	
3		173.7		
4	2.38	30.74*		C3, C5, C6
5	2.38	30.66*		C3, C4, C6
6		171.7		
7	7.86		H8	C6, C8
8	3.06	46.5	H7, H9	C6, C9, C10
9	3.7	65.3	H8, H10, H11	C8, C10
10	1.09	21.2	H9	C8, C9
11	4.73		H9	

* These values may be interchanged

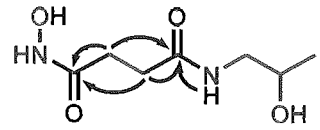

Figure 5.6 Important COSY (blue bonds) and CIGAR (black arrows) correlations observed for **64**

Initially NMR spectra were obtained in D_2O, but in order to visualise the exchangable protons spectra were re-collected in *d*6-DMSO. The spectra of the *Z*-isomer in D_2O were pure, but when obtained in *d*6-DMSO, the material had partially (about 25%) isomerised to the *E*-isomer. This is likely to have occurred during removal of the D_2O solvent which was carried out at approximately 45°C.

The assignments of the proton and carbon chemical shifts of the two isomers was straightforward but required the use of 1D NOESY experiments to complete the characterisation of the two isomers. In **63**, correlations were observed between the amide proton H7 and the methylene protons H5 as well as between the hydroxyamide H2 and the methylene H4. This unambiguously established the orientation of the succinamide moiety. With **64**, the protons of the succinamide moiety were coincident, although the chemical shifts of C4 and C5 did differ, albeit by only 0.1 ppm, which is less than the default resolution of the CIGAR experiment. In the CIGAR experiment that was run, the amide H7 did not show a correlation beyond the carbonyl group, so even if this experiment had been reacquired at a higher resolution it would not have been possible to establish the orientation of the carbon chemical shifts of the succinamide moiety. NOESY experiments run on **64** did, however, show correlations between H4/H5 and both H1 and H2, thus allowing the assignment of the stereochemistry as *E*, whereas in **63**, only H2 showed a correlation in to the succinamide protons. Neither H1 nor H2 showed CIGAR correlations to the carbonyl C3, so the orientation of these two chemical shifts was determined by the relative strengths of their correlations to H4/H5 as observed in the NOESY experiments run. The proton at 7.37 showed a stronger correlation and was thus assigned as H1, as this proton is closer to H4/H5, at a distance of approximately 2.3 Å, than H2, at approximately 3.6 Å.

The molecular formula of **63**, was confirmed by HRESIMS in which the expected parent ion was not observed, but rather the protonoted, deoxygenated ion, $C_7H_{15}N_2O_3$ at 175.11 Daltons (1.18 ppm) was identified. The loss of oxygen from hydroxamic acids under mass spectrometric conditions has been previously reported for electron ionisation mass spectrometry.[176] Strangely, the isomeric **64** did not exhibit deoxygenation to any notable extent, thus the formula $C_7H_{15}N_2O_4$ was obtained by observation of a peak at 191.10

Daltons (1.50 ppm) . The loss of oxygen from **63** is confirmed to be occurring only in the mass spectrometer by the observation of conversion of **63** to **64** during removal of d_6-DMSO as previously discussed.

A further aminolysis reaction was carried out, this time at 60°C with 1-amino-2-propanol (3 equiv.) in dry DMSO. Samples were removed periodically and purified by LH20 chromatography eluting with MeOH, then analysed by proton NMR. The sample taken after the reaction had been underway for two hours showed complete aminolysis of the polymer precursor and no peak at 2.56 ppm, thus indicating that poly(*N*-2-hydroxypropyl-methacrylamide) (HPMA, **62**) had been successfully formed. An identical reaction was then carried out but at the reduced temperature of 40°C. A sample removed from the reaction after eight hours did contain a peak at 2.56 ppm in the proton NMR spectrum, but the next sample, after 14 hours, had a proton NMR spectrum consistent with HPMA.

With the determination of suitable reaction conditions for aminolysis of the polymer precursor in the presence of natural product derivatives, it was possible to continue with formation of the desired polymer drug conjugates.

5.3 L-Tyrosinamide (39)

5.3.1 Fmoc-Gly-Phe-Leu-Gly-L-Tyrosinamide (65)

The coupling reaction between L-tyrosinamide (**39**, 1 equiv.) and **40** was carried out using DCC (1.9 equiv.) and NHS (2 equiv.) (**Figure 5.7**). Following overnight reaction, the reaction was found to be complete by analytical HPLC (C18, A: H_2O(A), B: ACN, Gradient II) so the THF solvent was removed and the crude reaction mixture was purified by preparative HPLC (C18, isocratic 90% MeOH/H_2O(A)) to furnish the desired conjugate **65** in a 45% yield.

The proton and carbon NMR chemical shifts for **65** were fully assigned through reference to 2D COSY, HSQC-DEPT and CIGAR spectra. Because the spectra were obtained in CD_3OD, none of the exchangable amide protons were observed, and more importantly, the chemical shifts could not be be compared directly to those already established for the tetrapeptide **40**, for which NMR spectra were obtained in d_6-DMSO. The crucial correlation which confirmed the successful formation of **65** was a CIGAR correlation from the α-proton of the L-tyrosinamide residue to the carbonyl of the C-terminal glycine.

Interestingly, in CD_3OD, all of the carbon chemical shifts of the Fmoc-Gly-Phe-Leu-Gly portion of **65** were slightly downfield (by between 0.1 and 3.4 ppm) from the corresponding shifts of **40** in d_6-DMSO with the exception of the β-methylene of the leucine residue and the carbonyl of the C-terminal glycine. Both of these positions were slightly upfield compared to the parent compound. The main chain carbons (α-carbons and carbonyls) exhibited the greatest changes in chemical shift, with the carbonyls in particular showing relatively large increases in chemical shift (between 2.5 and 3.4 ppm) with the exception of the carbonyl of the C-terminal glycine which was upfield by 0.1 ppm. These changes are likely to be due to the fact that methanol is a hydrogen bond donating solvent, and so can cause a slight increase in the polarity of a carbonyl bond,

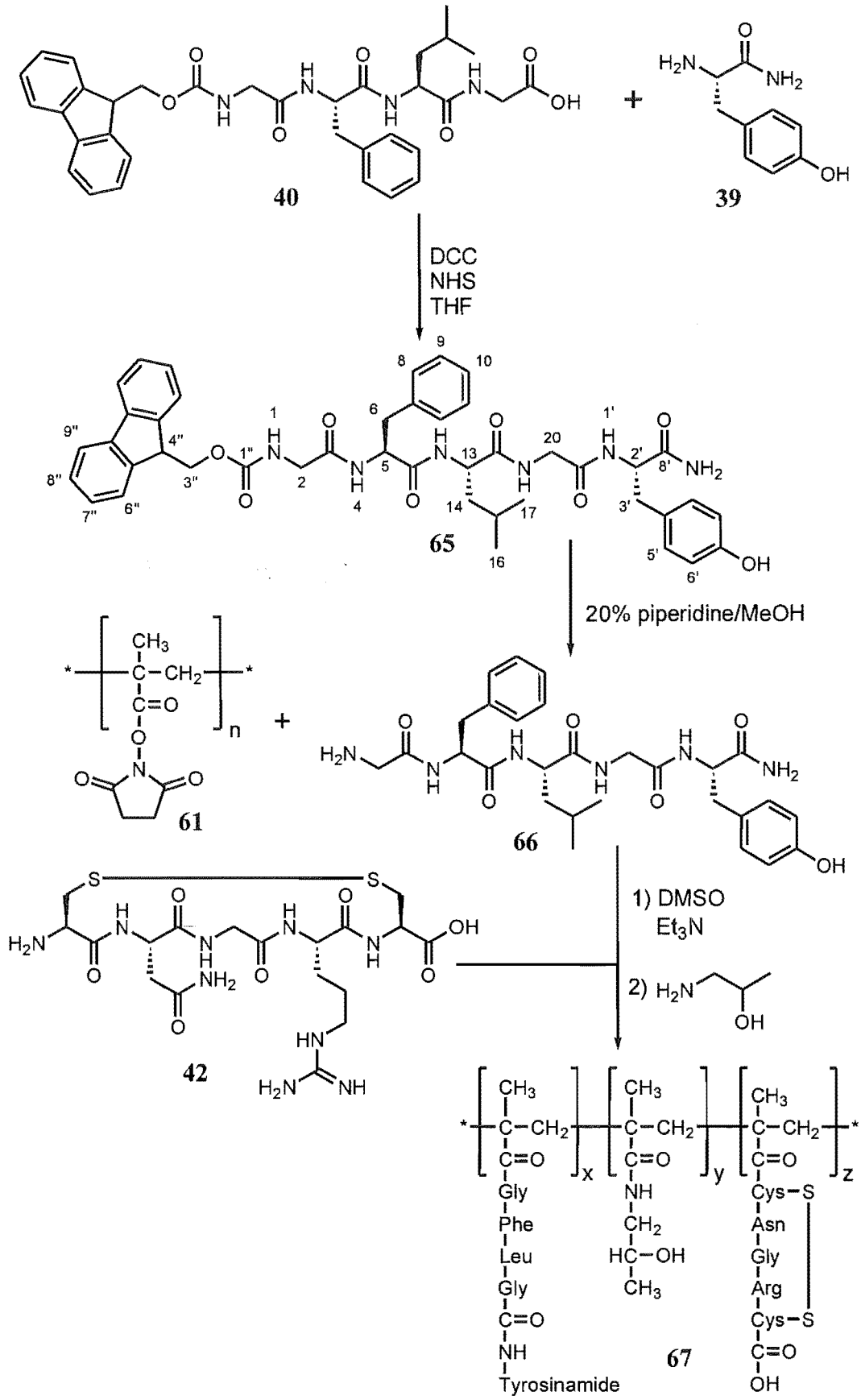

Figure 5.7 Reaction scheme leading to formation of a polymer drug conjugate

with a reduction in electron density around the carbon atom and hence a higher chemical shift. The fact that the C-terminal carbonyl was shifted in the opposite direction to the others strongly suggests a change in chemical environment expected for the successful formation of the conjugate **65**.

The formula for **65**, $C_{43}H_{48}N_6O_8$, was confirmed by HRESIMS in which the protonated ion at 777.36 Da (0.38 ppm) was identified.

5.3.2 H_2N-Gly-Phe-Leu-Gly-Tyrosinamide (66)

The Fmoc protecting group of **65** was removed by dissolving the compound in a solution of 20% piperidine/MeOH for 20 minutes, after which **66** was isolated in a 55% yield by passage through a C18 cartridge.

A proton NMR spectrum was obtained of **66** (**Figure 5.8**), and showed the expected

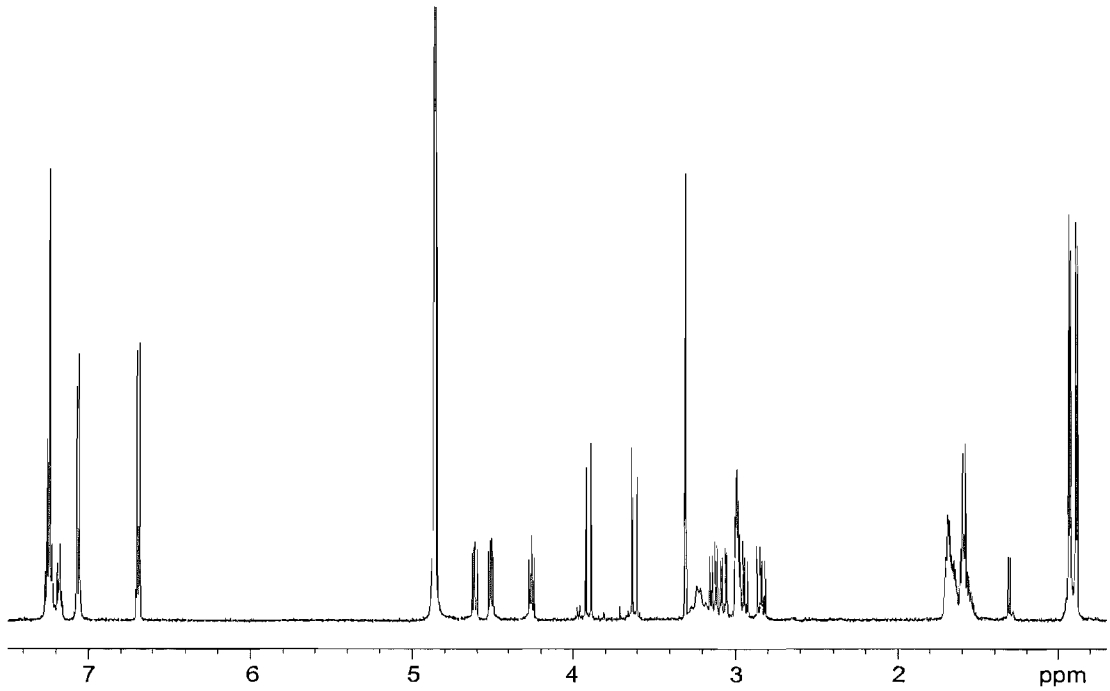

Figure 5.8 Proton NMR spectrum of **66**

peaks and an absence of peaks corresponding to an Fmoc group; however, a full characterisation was not carried out as the material was carried through to form the polymer conjugate as soon as possible to avoid any potential for degradation at this late stage.

Analysis of **66** by HRESIMS allowed identification of the protonated parent ion at 555.29 Da (1.26 ppm), which confirmed the formula of $C_{28}H_{38}N_6O_6$.

5.3.3 Synthesis and purification of targeted polymer drug conjugate (67)

The polymer drug conjugate **67** was formed by reaction of the polymer precursor **61** (50 equiv.) with **66** and the targeting peptide **42** (1 equiv.) in the presence of triethylamine (3 equiv.) followed by quenching of the active ester groups of the polymer with 1-amino-2-propanol (150 equiv.). The crude polymer was passed twice through an LH20 column, eluting with MeOH, to provide the product **67** in a 57% yield.

Due to the fact that **67** is a heterogeneous polymer, characterisation of the material could not be carried out to the usual standard. The formation of the co-polymer was confirmed by NMR and LRESIMS analysis of all of the fractions obtained from the LH20 fractionation.

The proton NMR spectrum of the purified polymer **67** was free of low molecular weight contaminants. There was a single peak that could be identified as being due to one of the aromatic protons of the L-tyrosinamide moiety (**Figure 5.9**). Integration of this peak gave a relative integral of 4.3 relative to the methine of the 1-amino-2-propanol at 96. While there is certain to be some inaccuracy in this ratio due to the peak broadness and differing relaxation times, it does indicate that the biolinker tetrapeptide construct was incorporated into the polymer at an approximately quantitative level. There were no peaks corresponding to the targeting moiety that could be identified as these all fall in the region of the spectrum that is dominated by the polymer itself. There was a small peak at

2.5 ppm due to ring-opened succinamide that integrated for approximately 20 protons, corresponding to about 5% incorporation. It was decided that it would not be worthwhile to react the polymer again in an attempt to aminolyse this material as it may have needed a prolonged reaction time, would have led to a reduced yield and was present at a relatively low level. LRESIMS of the polymeric fraction had a very low ion current and showed no recognisable ions as the polymer itself is not ionisable under ESIMS conditions.

None of the late eluting, and thus low-molecular weight compound containing, fractions showed any signs of either the biolinker-tetrapeptide, **66**, or the targeting peptide **42**, which indicated that they must have been entirely consumed by reaction with the polymer precursor.

The combined evidence from the examination of all the fractions led to the belief that the desired polymer conjugate **67** had been successfully formed and purified to a sufficient level for bioactivity studies.

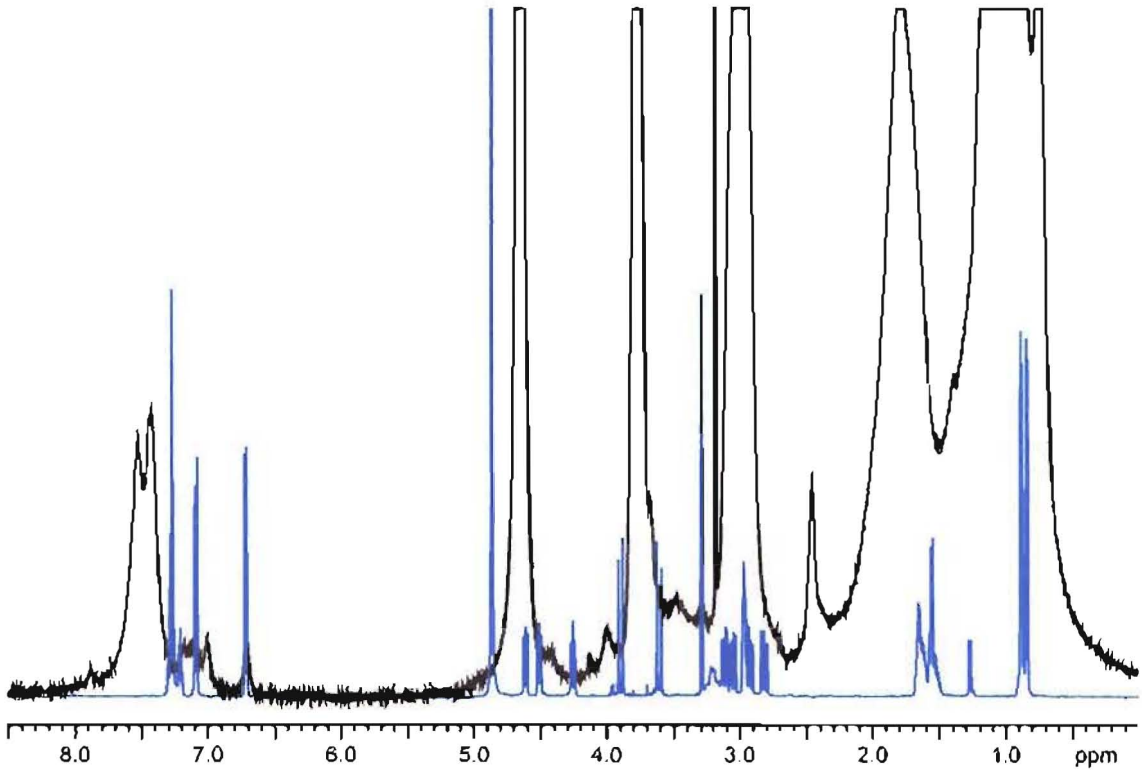

Figure 5.9 Overlaid proton NMR spectra of polymer conjugate **67** (black) and precursor **66** (blue)

5.4 Doxorubicin (19)

5.4.1 Fmoc-Gly-Phe-Leu-Gly-Doxorubicin (68)

Prior to using doxorubicin (**19**), it was necessary to desalt the commercially obtained doxorubicin hydrochloride to ensure solubility in organic solvents. Doxorubicin (**19**) is known to be sensitive to alkali conditions so the neutralisation was carried out by adding dilute aqueous ammonia, to an aqueous solution of doxorubicin hydrochloride. Upon addition of the base, the solution immediately changed colour from a deep red-orange to violet. The basic solution of doxorubicin (**19**) was then passed through a C18 cartridge without delay, trapping the doxorubicin (**19**) as a red layer on the solid phase. The cartridge was rinsed with more of the dilute aqueous ammonia followed by water and the doxorubicin (**19**) was eluted with acetone. It was never possible to remove all of the red colour from the cartridge, regardless of the solvents used; however the doxorubicin (**19**) was recovered in a 92% yield, so the residual colour on the cartridge accounted for only a small proportion of the mass.

Doxorubicin was (**19**) conjugated to the biolinker **40** (1.1 equiv.) with DCC (1.9 equiv.) in the presence of NHS (2 equiv.) and then purified by preparative HPLC (C18, isocratic 90% MeOH/H_2O(A)) to afford the desired conjugate **68** in a 52% yield.

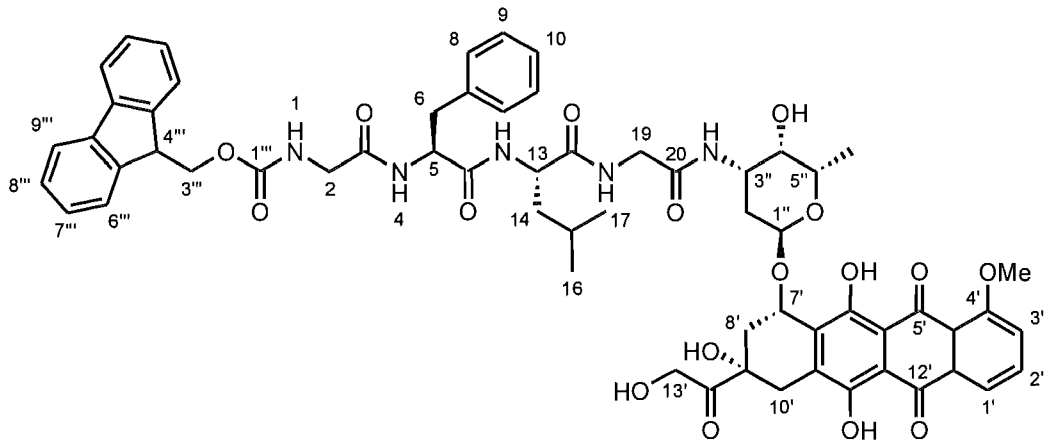

Fmoc-Gly-Phe-Leu-Gly-Doxorubicin (**68**)

The proton and carbon NMR chemical shifts of **68** were fully assigned using COSY, HSQC-DEPT and CIGAR experiments with the exception of the amide proton H1, which was not apparent in the COSY spectrum, and four quaternary carbon shifts in the anthraquinone moiety of doxorubucin (C5a', C6', C11' and C11a') which could not be seen in the CIGAR spectrum. Too little material was collected to allow the collection of a carbon spectrum to detect those four resonances so a full characterisation could not be carried out.

Unfortunately no CIGAR correlations were observed from doxorubicin to the carbonyl of the *N*-terminal glycine of the tetrapeptide biolinker; however, H3" showed a correlation in the COSY spectrum to a proton at 7.04 ppm, which was clearly an amide proton due to its downfield chemical shift and absence from the HSQC-DEPT spectrum. Further evidence for the structure indicated was that the proton chemical shift of position 3" had moved approximately 1 ppm downfield from those reported for the free base in $CDCl_3$ and CD_3OD.[177] The chemical shifts of all of the positions, except the amide proton, of the sugar moiety agreed closely with those determined for PK1 (**37**), although these data were obtained in a different solvent.[178] Finally, the chemical shift of the terminal carbonyl of the peptide, C21, had moved upfield by 2.8 ppm, which could be expected upon conversion from a free acid to an amide.

The formula of **68**, $C_{61}H_{65}N_5O_{17}$, was confirmed by HRESIMS which showed a peak for the sodiated parent ion at 1162.43 Da (0.69 ppm).

5.4.2 H_2N-Gly-Phe-Leu-Gly-Doxorubicin

In order to remove the Fmoc protecting group of **68**, it was dissolved in a solution of 20% piperidine/MeOH for 20 minutes and then passed through a C18 cartridge. A number of red coloured fractions, indicative of the presence of doxorubicin, were collected from the cartridge; however, none of them showed any sign of the desired product by NMR or LRESIMS. In fact, none of the red fractions showed any peaks in

the NMR spectra corresponding to doxorubicin thus suggesting that the red compound was only present at a very low level. HPLC (C18, A: H_2O(A), B: ACN, Gradient I) analysis of all the fractions from the cartridge showed the presence of a large number of compounds with just one major peak, eluting at 16.8 minutes, with a doxorubicin-like chromophore (**Figure 5.10**). This major peak was collected and analysed by LRESIMS but the peaks in the mass spectrum corresponded to neither the desired product nor any other likely products of the reaction.

It is known that doxorubicin is unstable to basic conditions, so it may be that the conditions for removal of the Fmoc protecting group were too harsh and caused the degradation of the doxorubicin component of **68**. The main pathway for alkaline degradation of doxorubicin involves loss of the glycoside followed by aromatisation of the A-ring.[179, 180] It was hoped that the doxorubicin conjugate would be able to survive the relatively mild deprotection conditions; however, it appears that complete degradation occurred.

The deprotection of a protected peptide *N*-terminus in the presence of doxorubicin may not be achievable. Doxorubicin is known to be sensitive to acidic conditions with cleavage of the sugar moiety occuring at low pH (<2) thus precluding the use of the other most commonly used *N*-terminal protecting group, tBoc (t-butoxycarbonyl).[181]

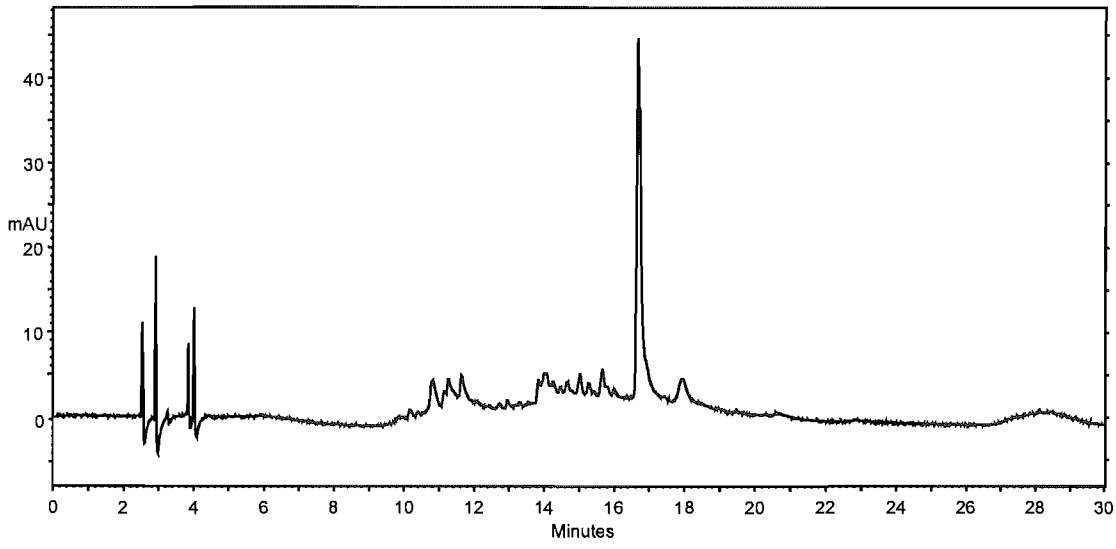

Figure 5.10 HPLC chromatogram of product of attempted deprotection of **68**

The reductive conditions required for removal of the Cbz (benzyloxycarbonyl) group are not compatible with doxorubicin and can lead to deoxygenation of the quinone moiety and also cleavage of the glycoside residue.[182] The only protecting group which seems to present a strong possibility of success is the trityl group or derivatives thereof. This is rapidly cleaved under acidic conditions, which may be mild enough to allow the reaction to be carried out in the presence of doxorubicin, although this is not certain. The preparation of an *N*-trityl protected biolinker would require the use of a different solid phase, most likely using tBoc chemistry to build up the peptide before incorporation of the final *N*-trityl glycine because the trityl group is not compatible with the acid-cleaved resins used for Fmoc SPPS.

Due to the complications experienced with the deprotection of **68**, the preparation of a polymer drug conjugate incorporating doxorubicin as the drug component was abandoned.

5.5 Mycalamide A (31)

5.5.1 Fmoc-Gly-Phe-Leu-Gly-Mycalamide A (69)

The crude reductive amination product **45** was acylated with the biolinker **40** (1.1 equiv.) using DCC (1.9 equiv.) and NHS (2 equiv.) until analytical HPLC (C18, A: H_2O, B: ACN , Gradient II) indicated consumption of the majority of the starting material. The crude reaction product was purified directly by preparative HPLC (C18, A: H_2O, B: ACN, Gradient II) to provide **69** in a 23% yield, calculated over two steps from formyl-normycalamide A (**45**).

The proton and carbon NMR chemical shifts of **69** were fully assigned through the use of 2D COSY, HSQC-DEPT and CIGAR experiments. The chemical shifts of the peptide component of **69**, determined using $CDCl_3$ + 0.05% d_5-pyridine, were similar to those determined for the tetrapeptide **40** in d_6-DMSO with the exception of the amide protons which were all shifted significantly upfield. This could be due to the fact that d_6-DMSO is a hydrogen bond acceptor, so can form hydrogen bonds with the protons of the amides leading to an electron withdrawing effect and thus a downfield shift whereas $CDCl_3$ is unable to accept hydrogen bonds so the amide protons appear upfield by comparison.

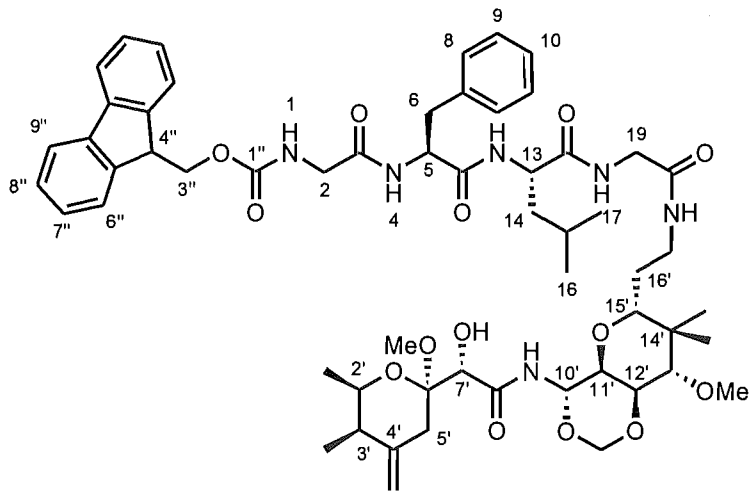

Fmoc-Gly-Phe-Leu-Gly-Mycalamide A (**69**)

Evidence of the success of the reductive amination reaction to produce **45** was provided indirectly by the identification of the amide linkage between mycalamide A and the biolinker. The chemical shift of C17', 36.2 ppm, is consistent with direct attachment of an amide. Furthermore, H17', a diastereotopic pair of protons at 3.38 and 2.78 ppm, showed a COSY correlation to a proton at 7.04 ppm which was an amide proton as evidenced by the lack of a correlation for this proton in the HSQC-DEPT spectrum. The connectivity of the tetrapeptide and drug components were easily established and a crucial CIGAR correlation from 17'-NH to the carbonyl C21 was evidence that the conjugate had been formed as desired.

The molecular formula of $C_{57}H_{76}N_6O_{14}$ for **69** was confirmed by HRESIMS which provided a peak corresponding to the sodiated parent ion at 1091.53 (1.65 ppm).

5.5.2 H_2N-Gly-Phe-Leu-Gly-Mycalamide A (70)

Compound **69** was deprotected by dissolving the compound in 20% piperidine/MeOH and standing at room temperature for 20 minutes before drying. The crude reaction product was purified by chromatography on a C18 cartridge, using a stepped MeOH/H_2O gradient to provide **70** in a quantitative yield.

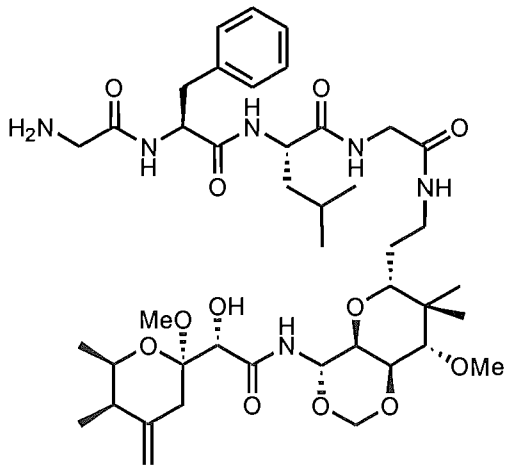

H_2N-Gly-Phe-Leu-Gly-Mycalamide A (**70**)

The proton NMR spectrum of **70** showed all of the expected resonances were present, while at the same time confirming the absence of any peaks corresponding to the Fmoc protecting group (**Figure 5.11**). The material was carried directly through to form a polymer conjugate without any further characterisation to eliminate any possibility of degradation.

The formula of **70**, $C_{42}H_{65}N_6O_{12}$, was confirmed by HRESIMS which showed a peak at 847.48 Daltons (0.94 ppm) that corresponded to the protonated parent ion.

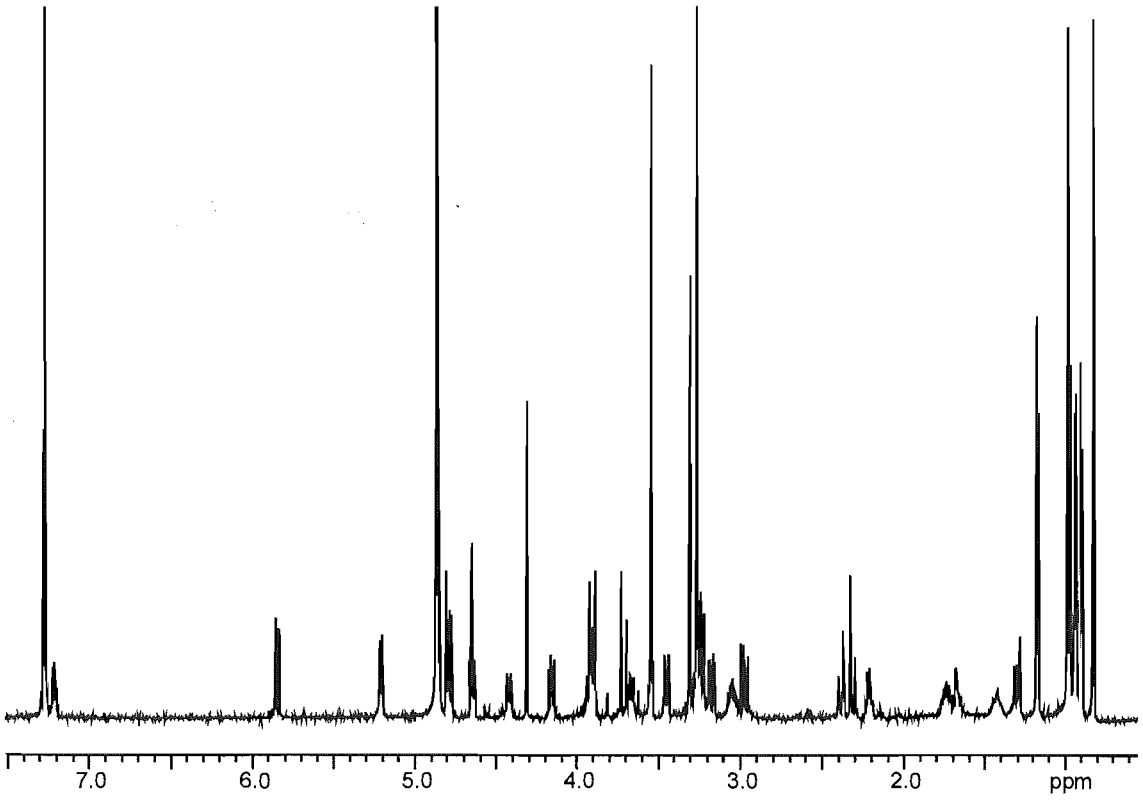

Figure 5.11 Proton NMR spectrum of **70**

5.5.3 Synthesis and purification of targeted polymer drug conjugate

The biolinker-drug moiety **70** and the targeting peptide **42** (1 equiv.) were coupled with the polymer (**61,** 50 equiv.) in the presence of triethylamine (3 equiv.). After overnight reaction, the remaining activated esters of the polymer were aminolysed with 1-amino-2-

propanol (150 equiv.). The purified polymer drug conjugate was obtained in a 53% yield by subjecting the total reaction solution to size separation chromatography twice on an LH20 column run with MeOH.

Proton NMR spectroscopy and LRESIMS of all of the fractions collected from the size exclusion chromatography showed that the polymer had been satisfactorily purified away from low molecular weight contaminants. Furthermore, it showed a lack of any signs of either free biolinker-drug or free targeting components, thus indicating that the conjugation of these to the polymer backbone had proceeded successfully.

Close examination of the proton NMR spectrum of the polymer revealed a small peak at 5.70 ppm which is the same position as the H10 of mycalamide A (**31**) appears. Relative to the methine of the hydroxypropylamide set to 96 protons, the peak at 5.70 ppm integrated for 2.6 protons which is slightly higher than expected. This is not surprising given that there are a number of peptidic protons obscured by the methine and the low level of the peak as well as the peak broadness will lead to inaccuracies. The presence of this peak provides positive confirmation that the biolinker drug construct has been successfully conjugated to the polymer backbone. It is not possible to identify any resonances from the targeting peptide in the spectrum, but on the basis of the successful conjugation of the biolinker drug moiety and the lack of any apparent free peptide, it is assumed that the targeting peptide has also successfully reacted.

5.6 Mycalamide B (32)

5.6.1 Fmoc-Gly-Phe-Leu-Gly-Mycalamide B (71)

Crude **50** was acylated with **40** (1.1 equiv.) using DCC (1.9 equiv.) in the presence of NHS (2 equiv.) in an overnight reaction. The solvent was removed and the crude product purified directly by preparative HPLC to provide the product **71** in a 79% yield, calculated over two steps from the azide **49**.

The proton and carbon NMR chemical shifts for **71** were fully assigned through reference to 2D COSY, HSQC-DEPT and CIGAR spectra with the exception of the carbonyl carbons C17 and C21 which were not observed in the CIGAR spectrum due to a paucity of material.

The NMR chemical shifts determined for the mycalamide B portion of **71** confirmed that the azide **49** had been successfully reduced and the amine so formed had been acylated with the peptide **40**. The chemical shift of C18' was the only carbon chemical shift that differed by more than 1 ppm from those of **49**, being shifted upfield by 10.5 ppm to 41.7 ppm. This lower chemical shift is consistent with a directly attached amide. The only proton chemical shifts that differed significantly from those of corresponding positions in

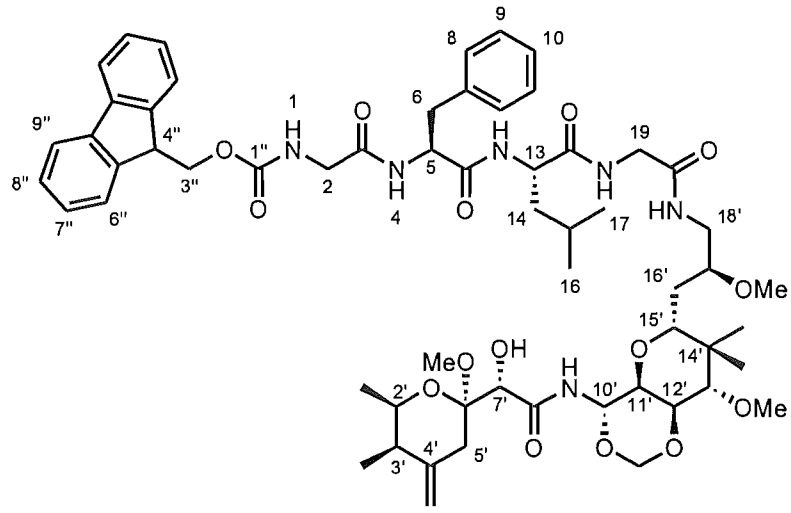

Fmoc-Gly-Phe-Leu-Gly-Mycalamide B (**71**)

49 were in the side chain. Interestingly, H16'a and b were seen as a separate pair of diastereotopic protons in **71** where they were coincident in **49**, while the opposite was observed for the protons of H18'. A correlation could be clearly seen in the COSY spectrum from H18' to an amide proton at 6.73 ppm. This single correlation confirmed both the success of the reduction of the azide **49** to an amine, and the following acylation of that amine. Unfortunately no correlations from the amide proton 18'-NH were seen in the CIGAR spectrum so the connectivity of **71** could not be unequivocally proven but the fact that there was only one carboxylic acid group capable of acylating the amine mitigates the need for direct proof somewhat. In the peptide component of **71**, the chemical shifts of the C-terminal glycine residue were very similar to those determined for the other tetrapeptide-drug conjugates, which strongly indicated that the amide had been formed as desired.

The formula of $C_{59}H_{80}N_6O_{15}$ for **71** was confirmed using HRESIMS which allowed identification of the sodiated parent ion at 1135.56 Daltons (0.26 ppm).

5.6.2 H_2N-Gly-Phe-Leu-Gly-Mycalamide B (72)

The Fmoc protecting group of **71** was removed by dissolving it in a 20% piperidine/MeOH solution and standing for 20 minutes before removing the solvents. The reaction product was purified by chromatography on a C18 cartridge to provide **72** in a 96% yield.

A proton NMR spectrum was taken of **72** and showed the absence of all the Fmoc resonances of the parent compound but all of the expected peaks were present. No further NMR spectroscopy experiments were carried out on **72** as it was reacted to form a polymer drug conjugate as soon as possible.

The molecular formula for **72** of $C_{44}H_{69}N_6O_{13}$ was confirmed by HRESIMS which showed a peak for the protonated parent ion at 891.51 Daltons (4.49 ppm).

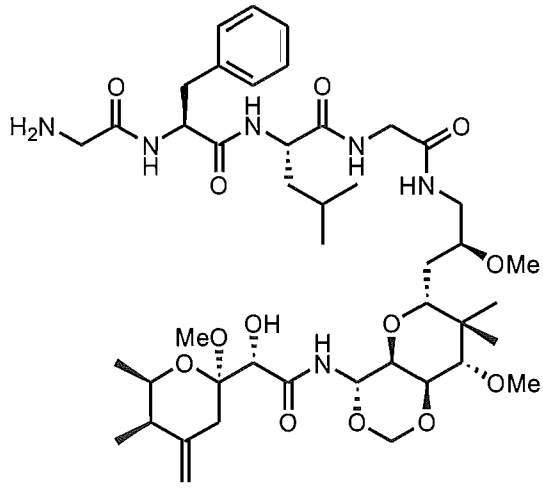

H_2N-Gly-Phe-Leu-Gly-Mycalamide B (**72**)

5.6.3 Synthesis and purification of polymer drug conjugate

The polymer precursor **61** (50 equiv.) was stirred with **72**, **42** (1 equiv.) and triethylamine (3 equiv.) in dry DMSO overnight before quenching the remaining active sites of the polymer precursor with 1-amino-2-propanol (150 equiv.). The product polymer was isolated in a 66% yield by passage twice through LH20, eluting both times with MeOH.

All fractions from the purification of the polymer conjugate were analysed using both proton NMR spectroscopy and LRESIMS. Neither the free biolinker-drug **72** nor the targeting peptide **42** were detected in the low molecular weight compound containing fractions, while the late eluting, high molecular material was found to be free of contamination to a level suitable for biological testing.

Upon close examination of the proton NMR spectrum of the polymer, a small hump at 5.70 ppm could be observed. This peak was too small to allow integration, which could

suggest that the coupling of the biolinker drug moiety to the polymer backbone had occurred at less than quantitative yield; however, it did show that some coupling had occurred. It is possible to identify a low shoulder on the amide proton peak at around 7.2 ppm that was not present in a sample of pure HPMA. This peak is thought to be primarily due to the aromatic protons of phenylalanine as it has been observed in proton NMR spectra of other polymer drug conjugates, an example of which is provided in **Figure 5.9**. Unfortunately, the peak cannot be accurately integrated as it lies over the edge of the amide proton peak; however, it does indicate that the tetrapeptide residue has been incorporated, and thus, by inference, that the drug itself has been conjugated to the polymer backbone.

5.7 *R*-Fumagillol

5.7.1 Fmoc-Gly-Phe-Leu-Gly-*R*-Fumagillol (73)

The crude product of the reductive amination to form **52** was acylated with the tetrapeptide biolinker **40** (1.1 equiv.) using DCC (1.9 equiv.) in the presence of NHS (2 equiv.). After overnight reaction, the product was examined by analytical HPLC and was found to contain six peaks which had UV spectra corresponding to the Fmoc chromophore (**Figure 5.12**). These six peaks were individually collected (C18, A: H_2O, B: ACN, gradient: 68% B (0 min), 68% B (2 min), 71% B (14 min)) and were all found to contain compounds similar to the desired product **72** as their proton NMR spectra showed resonances corresponding to both the peptide and fumagillol components. The largest peak in the HPLC chromatogram, eluting at 11.8 min, corresponded to the product **72**, which was isolated in a disappointing 13% yield, calculated over two steps from the ketone **51**.

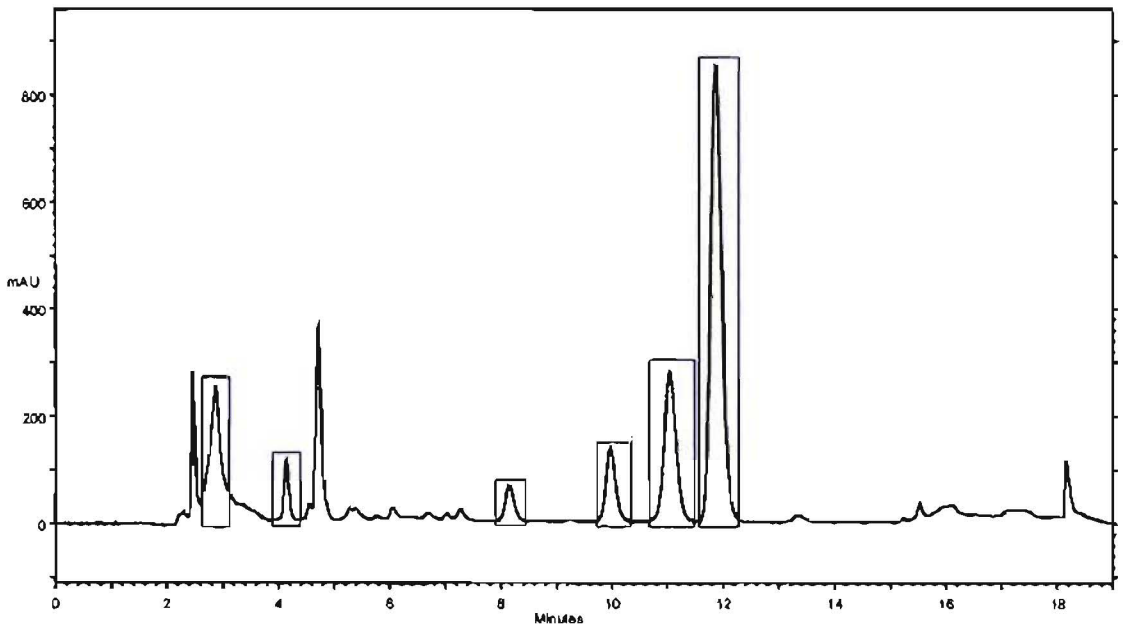

Figure 5.12 HPLC trace of reaction product from acylation of crude **52** with the tetrapeptide biolinker. Collected peaks are boxed in blue.

The proton and carbon NMR chemical shifts of **72** were full assigned using the 2D NMR experiments COSY, HSQC-DEPT and CIGAR. Assignment of the majority of the structure was straightforward and was carried out as already described for the smaller components (Sections **2.2.4** and **3.4**).

The carbon chemical shift of the modified position of fumagillol, C6', was 44.5 ppm which is consistent with the attachment of an amide to that carbon atom. Further, the proton H6' showed a correlation in the COSY spectrum to a proton at 6.65 ppm, which was clearly an amide proton as the HSQC-DEPT spectrum showed that it was not attached to a carbon atom. These factors indicated, albeit indirectly, that the reductive amination of the ketone **51** had proceeded as expected.

The formation of the desired peptide drug construct was confirmed through the observation of a CIGAR correlation from H6' to the amide carbonyl C21.

Observation of the coupling constants of H5' in the proton spectrum allowed determination of the stereochemistry of H6'. The measured coupling constants for H5' were 4.4 and 10.7 Hz, with the larger of the two constants being due to coupling to H4'. Thus, the coupling between H5' and H6' is 4.4 Hz, which, although slightly larger than the reported value for the free amine of 3 Hz, is consistent with a *gauche* relationship as discussed in Section **3.4.4**.

The molecular formula of **72**, $C_{50}H_{63}N_5O_9$, was confirmed by HRESIMS which allowed identification of the protonated parent ion at 878.47 Daltons (0.57 ppm).

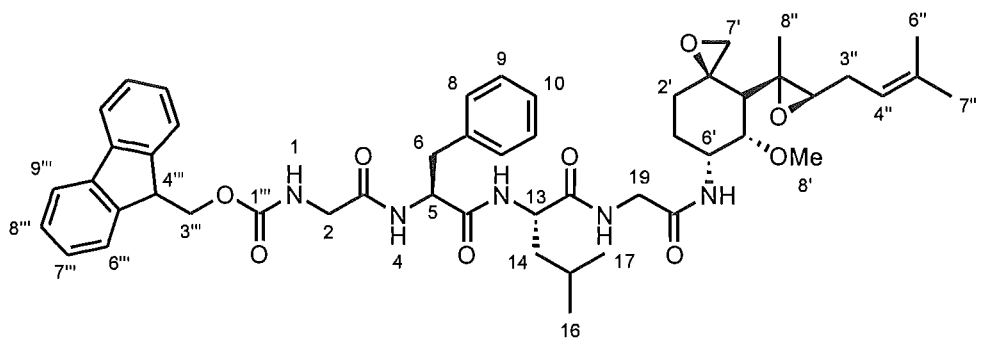

Fmoc-Gly-Phe-Leu-Gly-*R*-Fumagillol (**73**)

The side products, which were also isolated, were obtained in insufficient quantities to allow their structural characterisation.

5.7.2 H_2N-Gly-Phe-Leu-Gly-*R*-Fumagillol (74)

Compound **72** was dissolved in a solution consisting of 20% piperidine/MeOH and allowed to stand for 20 minutes before removing the solvents under a stream of nitrogen. The deprotected product **74** was isolated in an 81% yield by passing the crude reaction material through a C18 cartridge.

A proton NMR spectrum of **74** which was obtained showed the expected peaks and an absence of peaks corresponding to an Fmoc group; however, a full characterisation was not carried out as the material was carried through to form the polymer conjugate immediately to avoid any potential for degradation.

Confirmation of the molecular formula of **74**, $C_{35}H_{52}N_5O_7$, was provided by HRESIMS which showed a peak corresponding to the protonated adduct ion at 656.40 Daltons (2.89 ppm).

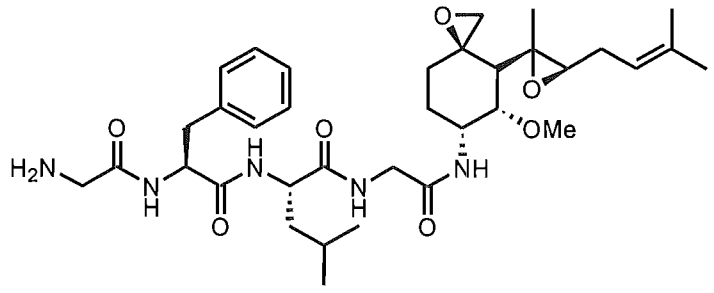

H_2N-Gly-Phe-Leu-Gly-*R*-Fumagillol (**74**)

5.7.3 Synthesis and purification of targeted polymer drug conjugate

The polymer precursor **61** (50 equiv.) was reacted overnight in dry DMSO with **74** and **42** (1 equiv.) in the presence of triethylamine (3 equiv.). The remaining active ester groups of the polymer were then reacted with 1-amino-2-propanol (150 equiv.) after which the polymer was purified by chromatography by gel filtration on LH20. After two columns the low molecular weight contaminants were removed and the polymer was isolated in a 53% yield.

Proton NMR spectroscopy and LRESIMS of all of the fractions collected from the size exclusion chromatography showed that the polymer conjugate had been satisfactorily purified away from low molecular weight contaminants. Furthermore, they showed that neither the biolinker-drug or targeting components were present as unconjugated contaminants, thus indicating that the coupling of these to the polymer backbone had proceeded successfully.

There are no proton NMR shifts in **74** that are suitable for providing positive confirmation of drug conjugation to the polymer as all resonances fall in the same region as protons of the polymer backbone itself. The olefinic proton at 5.15 ppm is the most likely candidate, but in the proton spectrum of the polymer that was obtained this region is obscured by the HOD solvent peak. As described in Section **5.6.3**, a shoulder on the amide peak at 7.2 ppm which can be ascribed to the aromatic protons of the phenylalanine residue could be clearly seen. This could not be used for quantification, but did provide positive evidence of successful conjugate, which, when taken in concert with the lack of evidence of a failed reaction, suggests that the desired polymer has been formed.

5.8 *S*-Fumagillol

5.8.1 Fmoc-Gly-Phe-Leu-Gly-*S*-Fumagillol (75)

Compound **75** was produced by acylating **58** with **40** (1.1 equiv.) using DCC (1.9 equiv.) and NHS (2 equiv.) in THF overnight. After removing the reaction solvent, the biolinker-drug conjugate **75** was isolated by preparative HPLC (C18, isocratic 69% ACN/H_2O) in a 56% yield.

The proton and carbon NMR chemical shifts of **75** were fully assigned through reference to COSY, HSQC-DEPT and CIGAR spectra. The assignment of the peptide and drug elements of the compound were made in a similar manner to that used for the characterisation of the separate components (Sections **2.2.4** and **3.4**).

CIGAR correlations from both the amide proton and H6' of the fumagillol moiety to the C-terminal carbonyl of the peptide confirmed that **75** had formed as expected. The chemical shift of position 6' was also consistent with the formation of the amide bond with the proton shifting downfield by 1.16 ppm and the carbon moving upfield by 4.0 ppm relative to the amine **58**.

The spectra were taken in d_6-DMSO so a useful comparison of the data for the peptide portion of **75** with the parent peptide **40** could be made. Almost all of the chemical shifts

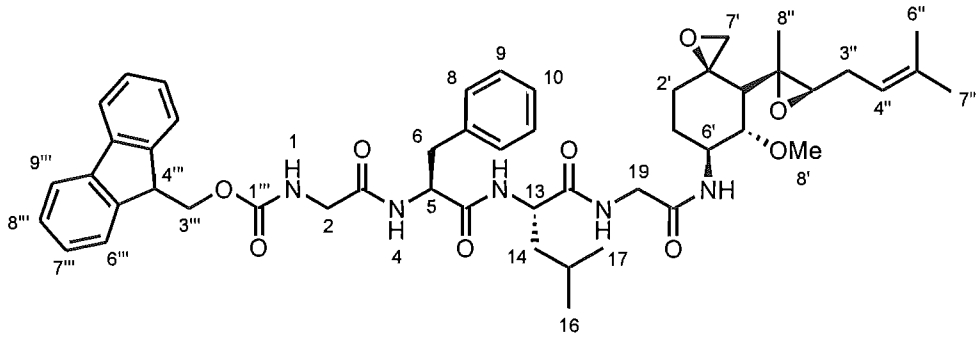

Fmoc-Gly-Phe-Leu-Gly-*S*-Fumagillol (**75**)

were in close agreement, falling within 0.6 ppm (^{13}C) and 0.03 ppm (^{1}H) of each other. The only shifts of **75** which fell outside these ranges were the α-proton of leucine, which was 0.09 ppm downfield, the α-carbon of the C-terminal glycine, which was 1.5 ppm downfield and the carbonyl of the carboxy terminal glycine, which was 3.3 ppm upfield. The α-protons of the C-terminal glycine had not only shifted notably upfield (by 0.1 and 0.05 ppm), but the two protons had become coincident where they were observed as two separate diastereotopic protons in the parent peptide.

The coupling patterns of H5' could not be determined due to an overlap with the two α-protons of the C-terminal glycine residue so the stereochemistry at position 6' could not be confirmed as *S*. The chemical shifts of **75** could, however, be compared with those of the enantiomeric structure **73**. Despite having their spectra taken in different solvents, the chemical shifts of these two structures were similar, with the most significant differences being observed near 6'. In particular, the chemical shifts of C6' and H6' were shifted 5.3 ppm and 0.78 ppm upfield respectively compared to **73**. This difference is too great to be purely due to a solvent change, so it can be fairly concluded that the stereochemistry of 6' was different in **75** and **73**, and thus **75** must have had *S* stereochemistry as proposed.

The molecular formula for **75** of $C_{50}H_{63}N_5O_9$ was confirmed by HRESIMS which showed a peak for the protonated parent ion at 878.47 Daltons (0.57 ppm).

5.8.2 H_2N-Gly-Phe-Leu-Gly-*S*-Fumagillol (76)

Compound **75** was deprotected using 20% piperidine/MeOH, and after removing the solvents, the reaction material was purified by passage through a C18 column to afford **76** in a 25% yield.

A proton NMR spectrum was taken of **76** and showed the absence of all the Fmoc resonances of the parent compound and the presence of all of the expected peaks. Due to the degradation observed during the attempted preparation of a low molecular weight analogue as described in Section **4.7.1**, **76** was reacted to form a polymer drug conjugate as soon as possible and so no further NMR spectroscopy experiments were carried out.

The molecular formula of $C_{35}H_{52}N_5O_7$ for **76** was confirmed by HRESIMS which provided a peak corresponding to the sodiated parent ion at 656.40 (1.98 ppm).

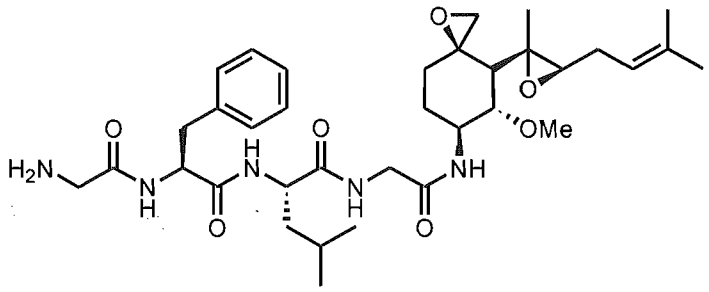

H_2N-Gly-Phe-Leu-Gly-*S*-Fumagillol (**76**)

5.8.3 Synthesis and purification of targeted polymer drug conjugate

Compounds **76** and **42** (1 equiv.) were reacted with the polymer precursor **61** (50 equiv.) in the presence of triethylamine (3 equiv.). After overnight reaction, 1-amino-2-propanol (150 equiv.) was added to the reaction to aminolyse the remaining active ester sites of the polymer precursor. Following a further 12 hours of reaction, the reaction solution was applied directly to an LH20 column and eluted with MeOH. After a second passage through LH20, the pure polymer conjugate was isolated in a 70% yield.

Proton NMR spectroscopy and LRESIMS of all of the fractions collected from the size exclusion chromatography showed that the polymer had been satisfactorily purified away from low molecular weight contaminants. Furthermore, it showed a lack of any signs of either the biolinker-drug or targeting components being free, thus indicating that the conjugation of these to the polymer backbone had proceeded successfully.

As outlined in Section **5.7.3** for the enantiomeric fumagillol derivative, no protons could be clearly discerned that were due to the drug itself. Again the aromatic protons of the phenylalanine residue could be identified on the edge of the polymer backbone amide resonance. This was a non-quantitative indicator of successful conjugation of **76** to the polymer backbone.

5.9 Biological activity

The purified polymer drug conjugates were submitted for bioactivity testing against the P388 murine leukemia cell line. The toxicities determined, relative to the drug component, are shown below in **Table 5.3**.

All of the polymer drug conjugates were not cytotoxic to P388 murine leukemia cells at the concentrations tested. No attempt was made to retest the compounds at a higher concentration in order to determine an actual toxicity level as it was felt that this would be a waste of compound. The results below do establish that, in the case of the mycalamides, the polymer bound drugs are significantly less cytotoxic than the free drugs, which is expected. With the L-tyrosinamide and fumagillol derivative polymer drug conjugates, the low molecular weight compounds showed negligible cytotoxicity and these results simply show that their polymeric derivatives have not gained notable cytotoxicity.

Due to the nature of polymer drug conjugates, and even more so targeted polymer drug conjugates, *in vitro* testing is of limited utility as they are only able to show their full potential, through the EPR effect, reduced immunogenicity and enhanced circulation times, in *in vivo* studies.

Table 5.3 Results of cytotoxicity testing of polymer drug conjugates expressed relative to the drug component

Compound	IC_{50} (g/mL)	IC_{50} (mol/L)
L-tyrosinamide polymer drug conjugate (**67**)	$> 280 \times 10^{-9}$	$> 1.5 \times 10^{-6}$
Mycalamide A polymer drug conjugate	$> 700 \times 10^{-9}$	$> 1.5 \times 10^{-6}$
Mycalamide B polymer drug conjugate	$> 760 \times 10^{-9}$	$> 1.5 \times 10^{-6}$
R-Fumagillol polymer drug conjugate	$> 430 \times 10^{-9}$	$> 1.5 \times 10^{-6}$
S-Fumagillol polymer drug conjugate	$> 430 \times 10^{-9}$	$> 1.5 \times 10^{-6}$

5.9 Conclusions from Polymer Drug Conjugate Preparation

With the exception of doxorubicin, all of the desired polymer drug conjugates are believed to have been successfully prepared. In the case of doxorubicin, the base-catalysed deprotection of the amino terminus of the tetrapeptide led to total decomposition of the doxorubicin moiety. While this could be possibly circumvented through the use of alternative protecting group chemistry, it was not considered to be important enough to warrant the time and effort of resynthesis.

Quantitation of the levels of drug and targeting motif was difficult in some cases and impossible in most. The targeting peptide has no proton NMR resonances that fall outside the range dominated by the polymer backbone and no UV absorbance at all. Detection of the level of attachment of this structure to the polymer is thus not possible. Use of IR to detect the targeting peptide would also not be possible as the peptide contains no functionalities with strong and distinctive absorbtion bands. The biolinker-drug components could be detected in some cases through olefinic resonances of the drug component and in all cases peaks could be seen that corresponded to aromatic protons. In the case of both L-tyrosinamide (**39**) and mycalamide A derivative **45**, it was possible to use integration of a peak in the proton NMR spectrum to obtain an estimate of the amount of drug present. In all other cases quantification using proton NMR spectroscopy was not possible. The problem of quantification and characterisation of the polymer drug conjugates is concerning, although the use of poorly characterised drugs in research is not without precedent.

The strategy of acylating the crude amines produced by derivatisation of the natural products prior to purification was found to be far superior to purification of the free amine. The free amines had poor chromatographic properties and could not be usefully analysed by HPLC; however, acylation with the Fmoc-protected biolinker greatly improved their chromatographic behaviour as well as providing the characteristic Fmoc chromophore which was useful in analytical examinations.

The observed ring opening reaction of the succinimide of the polymer precursor is a cause for concern for the long term development of the NHS-activated ester precursor. It appears that this side-reaction is driven by the high steric hindrance of the carbonyl of the polymerised methacrylic acid causing reaction to occur at the slightly less hindered succinimide carbonyl. Although no adducts of peptide-drug with the succinimide moiety were detected by ESIMS or proton NMR spectroscopy, it would be advantageous to subsititute the NHS with a different activating group which is unable to undergo side-reactions such as *p*-nitrophenol.

Chapter 6

Conclusion

6.1 Summary and Conclusions

The aim of this project was to produce a family of targeted polymer drug constructs incorporating both a peptidic targeting motif to direct the drug to angiogenic endothelial cells and a natural product drug attached *via* a biodegradable linker. A secondary target of this work was the production of a series of low molecular weight analogues of the polymeric constructs that could be used to assess the benefit of using a polymer backbone.

The biolinker and targeting motif and the targeted biolinker construct were all successfully prepared by stepwise solid phase peptide synthesis. The yields obtained were, with the exception of the biolinker, lower than desired but no optimisation of the synthesis was carried out. If the targeting motif or the targeted biolinker construct are to be prepared on a larger scale, it will be necessary to carry out studies varying the protecting groups and strategies used in order to maximise the yield and minimise the amount purification required. Due to the limited amounts required for initial biological testing, it would not have been worthwhile to carry out such an investigation for this project.

The natural products used, mycalamides A (**31**) and B (**32**) and fumagillol (**35**), required modification to provide amine functionalities suitable for conjugation to the biolinker. This was successfully carried out, although the yields obtained were often disappointing and purification of the amine derivatives was found to be problematic. In all cases the

amines could be purified and characterised following acylation. The difficulties experienced throughout this work with degradation indicate that it would be wise to focus future work on drugs that are chemically stable. This would not only simplify any synthetic or hemi-synthetic procedures, but would also remove the possibility of drug degradation following administration, for example in lysosomes.

The preparation of low molecular weight drug conjugates was plagued with failure of the acylation reaction. In the case of L-tyrosinamide and doxorubicin the reaction was successful; however, in all other instances the desired product could not be prepared. The cause of the failed reaction remains unknown but is likely to be due to the presence of the targeting peptide, as the analagous reactions in the polymer drug syntheses were all successful. An alternative preparation of the low molecular weight conjugates could be carried out in which the targeting motif is coupled to the biolinker after the drug, although this has the disadvantage of exposing the valuable drug to more reactions and thus risking degradation.

With the exception of doxorubicin, all of the desired polymer drug conjugates were successfully prepared. The level of characterisation of the conjugates was not ideal, and this is an area that will require much work if polymer drug conjugates are to come into clinical use. The use of very low polydispersity polymers is a useful starting point, but techniques are required that will enable the accurate quantification of all components of the conjugate. To this end, it may be worthwhile to incorporate specific labels such as ^{2}H or ^{13}C for NMR analysis or use highly UV active components so their level of incorporation can be accurately determined.

The compounds produced have been tested *in vitro* against the P388 murine leukemia cell line, with results being largely unsurprising. The free mycalamide derivatives tested all showed strong cytotoxicity, while the fumagillol derivatives all displayed low toxicity to the P388 cells. The conjugates were all non-toxic at the concentrations tested. The conjugates have not yet been tested *in vivo*, but a proposed dosing regime can be outlined. For the doxorubicin conjugate, a dose of 5 μg/week/mouse is planned. This is a relatively small dose, but is in line with the putative anti-angiogenic action of the drugs.

At this dose level there is sufficient drug conjugate for 136 doses, thus allowing for the possibility of alternative dosing schemes or extended duration trials. The L-tyrosinamide conjugates will be radiolabelled with ^{123}I or ^{125}I prior to administration to allow a determination of biodistribution and pharmacokinetics to be made. This will highlight the difference between the low and high molecular weight conjugates. The remaining conjugates, all polymeric, have been prepared in quantities that are more than adequate for *in vivo* testing, even if a dose as high as 10 μg/week/mouse was used, which is unlikely given the cytotoxicity of the mycalamides and the anti-angiogenic activity of fumagillol.

In the absence of *in vivo* testing it is difficult to comment on the likely future of the compounds produced in this work; however, the independent promise of both polymeric and anti-angiogenic drugs suggests that a combination of these two approaches may well lead to a useful treatment for cancer.

Chapter 7

Experimental

7.1 General Methods

Nuclear Magnetic Resonance Spectroscopy

All proton detected NMR spectra were obtained on a Varian Inova 500 spectrometer at 23°C, operating at 500 MHz. Carbon detected NMR spectra were recorded on a Varian Unity 300 spectrometer at 23°C, operating at 75 MHz. Other NMR experiments described in this thesis *viz* COSY, ROESY, NOESY, and the reverse detected HSQC, CIGAR and IMPRESS experiments were obtained on the Inova 500 spectrometer at 500 MHz. Chemical shifts in this thesis are described in parts per million (ppm), on the δ scale, and were referenced to the appropriate solvent peaks: $CDCl_3$ referenced to $\mathbf{C}HCl_3$ at δ_H 7.26 ppm (^1H) and $\mathbf{C}HCl_3$ at δ_C 77.0 ppm (^{13}C); CD_3OD referenced to $\mathbf{C}HD_2OD$ at δ_H 3.30 ppm (^1H) and $\mathbf{C}D_3OD$ at δ_C 49.3 ppm (^{13}C); D2O referenced to **H**OD at δ_H 4.7 ppm (1H) and $(\mathbf{C}_2H_4O)_2$ (added dioxan) at δ_C 67.4 ppm; d_6-DMSO referenced to $CD_3(\mathbf{C}HD_2)SO$ at δ_H 2.6ppm and $(\mathbf{C}D_3)_2SO$ at δ_C 39.6 ppm; d_3-acetonitrile referenced to $\mathbf{C}HD_2CN$ at δ_H 2.0 ppm and $\mathbf{C}D_3CN$ at δ_C 1.3 ppm or $CD_3\mathbf{C}N$ at δ_C 117.7 ppm. ^1H NMR spectra were recorded using an acquisition time (AT) of 2.0 s; ^{13}C NMR spectra were recorded using an AT of 0.878 s and a delay (D1) of 1 s. COSY experiments were typically recorded using an AT of 0.137 s and a relaxation delay (D1) of 1.0 s. ROESY experiments were carried out with an AT of 1.89 s, a relaxation delay (D1) of 1.0 s and a mixing time of 0.3 s. NOESY experiments were recorded with an AT of 1.0 s, a delay (D1) of 1.0 s and a mixing time of 0.5 s. HSQC-DEPT experiments with the Pulsed Field Gradient system were generally run with an AT of 0.133 s, a relaxation delay (D1)

of 1.0 s and $J_{C\text{-}H}$ of 130-165 Hz. CIGAR experiments with the Pulsed Field Gradient system were run with an AT of 0.303 s, a delay (D1) of 1.0 s, J = 140 Hz and a $^{n}J_{CH}$ of 8.0 Hz. IMPRESS experiments were acquired using the Pulsed Field Gradient system with an AT of 0.128 s, a D1 of 1.0s, J = 140 Hz and a $^{n}J_{CH}$ of 8.0 Hz.

Mass Spectrometry

Mass spectrometry of some samples (stated) was performed on a Kratos MS80 RFA Mass Spectrometer operated at 4 000 V in electron impact (EI) ionisation mode. Ionisation was performed at 70 eV.

The majority of the samples were analysed on a Micromass LCT mass spectrometer equipped with an electrospray ionisation (ESI) probe. Samples were analysed at a probe voltage of 3 200 V at 150°C with a nebuliser gas flow of 160 L/hr and desolvation gas flow of 520 L/hr with the source temperature at 80°C. The cone voltage was typically 20 V. The solvent flow from a syringe pump in direct injection ESIMS mode was 20 μL/min.

High Pressure Liquid Chromatography

The High Pressure Liquid Chromatography (HPLC) work described in this thesis was performed on one of two machines. A Shimadzu LC-4A instrument equipped with a Shimadzu UV Spectrotometric Detector SPD-2AS and Hewlett Packard 3390A integrator was used for preparative reverse phase work with the stated column, solvent mixture and flow rate. Solvents were degassed using a flow of helium.

Analytical and small scale preparative work was performed on a Shimadzu VP system. The complete setup involved a Shimadzu LC-10AC VP liquid chromatograph coupled to

a SIL-10A VP autoinjector, a CTO-10A VP column oven set to 40°C, and a SPD-M10A VP diode array detector. This system was controlled by Shimadzu CLASS-VP (Version 5.023) software. A Shimadzu degasser (DGU-14A) was utilised for the degassing of all solvents used in this machine.

Columns and flow rates used were a Phenomenex ODS(3) column (250 x 4.6 mm, 60 Å, 5 μm APD, 1 mL/min) for analytical work, a Phenomenex Luna C18(2) (250 x 10mm, 60 Å, 5 μm APD, 5 mL/min) for semi-preparative work and a Dynamax C18 (270 x 20 mm, 60 Å, 12 mL/min) for preparative work.

The solvents used were either mixtures of acetonitrile (BDH HiperSolv™ 'Far UV' grade) or methanol (BDH HiperSolv™ grade) with water (purified using a MilliQ deionising system). The aqueous phase was acidified with 0.05% trifluoroacetic acid (Scharlau, synthesis grade) where possible, as indicated by H_2O(A).

Standard gradients used are presented below:

Gradient I		Gradient II		Gradient III	
Time	B conc	Time	B conc	Time	B conc
0	10%	0	10%	0	37%
2	10%	2	10%	12	40%
14	75%	14	75%	32	80%
24	75%	19	75%	34	100%
26	100%	20	100%	36	100%
30	100%	22	100%	37	37%
32	10%	23	10%	40	37%
40	10%	26	10%		

Medium Pressure Liquid Chromatography

Medium Pressure Liquid Chromatography (MPLC) was performed using a Merck Lobar size B (310 x 25 mm) RP-18 Li Chroprep (40-63 μm) column connected to a Mill-Royal D pump with a flow rate of 10 mL/min. The system was equipped with a LKB Broma 2238 UVICORD SII detector and a LKB Broma 2210 recorder with detection at 254 nm.

Column Chromatography

All column chromatography was performed using glass columns of stated dimensions (height x diameter). Solvents were all of commercial grade, distilled once in glass distillation apparatus, except MeOH, which was distilled twice. 'Flash' columns were run under oxygen-free N_2 gas pressure (0.5 kPa).

Silica flash chromatography was performed on Merck silica gel 60 (230-400 mesh). Reverse phase C18 chromatography used Bakerbond spe™ Octadecyl (C_{18}) disposable solid phase extraction columns (40 mm APD, 60 Å) of a 500 mg / 3 mL size or if larger columns were required, they were prepared using Bakerbond C_{18} (40 μm preparative LC packing). Size-exclusion chromatography was carried out using Sephadex LH-20 (Pharmacia Biotech AB). Small scale ion-exchange chromatography was performed on either Bond Elut SCX solid phase extraction columns (40 μm APD, 60 Å, 500 mg, 3 mL) Analytichem International) or Bakerbond spe™ CBX (Carboxylic acid) disposable solid phase extraction columns (40 μm APD, 60 Å, 500 mg, 3 mL). Larger scale ion-exchange chromatography was performed on Trisacryl® M CM (carboxymethyl) preparative LC packing (40-80 μm swollen bead size, LKB).

Where UV detection is indicated, the system was equipped with a LKB Broma 2238 UVICORD SII detector and a LKB Broma 2210 recorder with detection at the stated wavelength.

Thin Layer Chromatography

All analytical thin layer chromatography (TLC) was performed on Merck silica gel 60 F_{254} aluminium backed sheets (0.2 mm thickness). The solvent(s) used for development are indicated in each case. Visualisation was performed first visually under normal light followed by short wavelength UV (254 nm). Staining was carried out using either iodine (I_2), potassium permanganate dip (3 g $KMnO_4$, 20 g K_2CO_3 and 5 mL 5% aqueous NaOH in 300 mL H_2O), phosphomolybdic acid spray (PMA, 10 % w/v phosphomolybdic acid in ethanol), vanillin dip (60 g vanillin and 10 mL c.H_2SO_4 in 1 L 95% EtOH) or ninhydrin spray (1.5 g ninhydrin and 5 mL glacial acetic acid in 500 mL 95% EtOH).

UV-Vis Spectroscopy

UV-Vis measurements were taken on a Hewlett Packard HP 8452A Diode Array Spectrometer. Samples were placed in 10 mm quartz glass cuvettes (Starna) with a solvent blank carried out prior to sample measurement.

Biological Assays

Compounds were assayed for cytotoxicity where applicable using the P388 MTT antitumour assay. The antitumour assay is the most sensitive assay for cytotoxicity. It consists of a 2-fold dilution series of the sample of interest followed by incubation for 72 hours with P388 (murine leukaemia) cells. The concentration of sample required to reduce the P388 cell growth by 50% (compared to control cells) is determined using the absorbance values obtained when the yellow MTT tetrazolium is reduced by healthy cells to produce the purple colour MTT formazan. The result is expressed as the IC_{50} (ng/mL).

IR Spectroscopy

IR measurements were taken on a Shimadzu FTIR-8201PC Spectrometer. Samples were measured using an ATR cell with a background measured first.

Kaiser Test

For SPPS of peptides the Kaiser test was used to determine the presence or absence of free amines. Several beads from the resin synthesis were removed and washed with EtOH (3 x 1 mL) in a small glass vial. The following three stock solutions were made and three drops from each were added to cover the beads.

2.5 g ninhydrin in 50 mL of EtOH
40 g phenol in 10 mL of EtOH
2 mL 0.001 M KCN (6.5 g in 100 mL water) and 98 mL of pyridine

The vial was capped and placed in an oven (120°C) for three minutes. A positive result was indicated by the beads turning blue while a negative result was shown by no change in colour (beads remained yellow).

Solvents

All technical grade solvents were distilled prior to use. MeOH was distilled twice. Dry solvents were obtained using the following standard methods. MeOH, toluene and pyridine were all refluxed over calcium hydride and distilled immediately before use. THF was refluxed over sodium metal and benzophenone before distillation directly prior to use. Both DMF and DMSO were dried by treating twice overnight with activated 4Å molecular sieves, followed by storage over 4Å sieves.

7.2 Work described in Chapter 2

7.2.2.1 Fmoc-Gly-Wang resin

A typical procedure is as follows: Wang resin (1 g, 0.83 mmol available benzyl alcohol positions) was stirred gently with Fmoc-glycine (284 mg, 0.95 mmol) in dry DMF (7 mL) for approximately fifteen minutes prior to the addition of pyridine (463 μL, 5.73 mmol) and 2,6-dichlorobenzoyl chloride (410 μL, 2.86 mmol). The reaction flask was then sealed with gentle stirring continuing overnight after which the resin was filtered under vacuum and washed thrice with DMF (5 mL each) and DCM (5 mL each). The resin was then dried thoroughly *in vacuo* prior to determination of the loading.

To ascertain the degree of resin loading, a small amount of resin (0.7 and 1.0 mg) was accurately weighed into two quartz cuvettes. Freshly made 20% piperidine/DMF (3 mL) was then dispensed into the cuvettes along with a third empty cuvette which was used as a solvent blank. The UV spectrum of each sample was taken after they had been mixed for approximately five minutes and allowed to settle and the exact absorbance at 290 nm was recorded (0.893 and 1.356 respectively). The loading of the resin was then calculated on the basis of a linear relationship between absorbance at 290 nm and the quantity of Fmoc-amino acid present, with one mmol of Fmoc-amino acid giving an absorbance of 1.650 to give loadings of 0.77 and 0.82 meq/g with an average of 0.8 meq/g. The remaining benzyl alcohol groups of the resin were capped by stirring the resin (1 g, 0.83 mmol total benzyl alcohol groups) with pyridine (404 μL, 5 mmol) and benzoyl chloride (406 μL, 3.5 mmol) in DCE (5 mL) for two hours followed by filtration and washing thrice with DCE (5 mL each) and DCM (5 mL each) before drying thoroughly.

7.2.2.2 Fmoc-Gly-Phe-Leu-Gly-Wang resin synthesis

The synthesis of Fmoc-Gly-Phe-Leu-Gly-Wang resin was carried out by standard solid phase technique in a glass reaction vessel equipped with a frit (porosity 3) to allow both filtration and agitation of the resin by application of vacuum or positive nitrogen pressure. The reaction sequence was carried out a number of times, with a typical synthesis proceeding as follows. Fmoc-glycine-Wang resin (1.2 g, 0.96 mmol) was allowed to swell in DMF (6 mL) for fifteen minutes, drained, and the Fmoc protecting group removed by reacting the resin with freshly made 20% piperidine/DMF (12 mL) for ten minutes. After draining and washing (3 x 15 mL DMF followed by 3 x 15 mL IPA) the Kaiser test was carried out (see Section **7.1**) with a blue colour change indicating the presence of free amines and hence the success of the deprotecting reaction. The resin was then washed again (3 x 15 mL DMF) before changing the collection flask to remove all traces of piperidine. A DMF solution (6 mL) of Fmoc-leucine (679 mg, 1.92 mmol) was activated for two minutes with HBTU (728 mg, 1.92 mmol) and DIPEA (669 μL, 3.84 mmol) prior to addition to the resin. The coupling reaction was gently agitated for one hour before draining, washing with DMF (3 x 15 mL) and carrying out the Kaiser test, resulting in no colour change thereby indicating an absence of free amines and thereby the success of the coupling reaction. This process of deprotection and coupling was repeated for Fmoc-phenylalanine (744 mg, 1.92 mmol) and Fmoc-glycine (571 mg, 1.92 mmol) with all other reagents used in the same quantities as described above. Following the final coupling reaction, the resin was washed with DMF (3 x 15 mL), MeOH (3 x 15 mL) and DCM (3 x 15 mL) before drying thoroughly.

7.2.2.3 Fmoc-Gly-Phe-Leu-Gly-OH (40)

The *N*-protected biolinker, **40**, was cleaved from the resin (3.0 g, 1.75 mmol) by agitation with a cleavage brew consisting of 95% TFA/2.5% H_2O/2.5% TES (15 mL) for 20 minutes followed by a wash with the cleavage brew (5 mL) then a second cleavage (10 mL, 20 minutes) and wash (5 mL). The combined acid solution was diluted with water (100 mL) and extracted with DCM (3 x 50 mL). The organic fractions were combined and taken to dryness before being dissolved in THF (25 mL) and filtered. Hexane (250 mL) was then added to the THF solution to give a white precipitate which was filtered off to give pure **40** (384 mg, 36%). HRESIMS 615.2807, $C_{34}H_{39}N_4O_7$ ($M + H^+$) requires 615.2819. ^{1}H NMR (d_6-DMSO) δ 8.22 (d, J_{HH} = 8.3 Hz, 1H, H12), δ 8.19 (t, J_{HH} = 5.9 Hz, 1H, H19), δ 8.10 (d, J_{HH} = 8.3 Hz, 1H, H4), δ 7.99 (d, J_{HH} = 7.5 Hz, 2H, H9'), δ 7.80 (d, J_{HH} = 7.6 Hz, 2H, H6'), δ 7.62 (t, J_{HH} = 6.1 Hz, 1H, H1), δ 7.51 (t, J_{HH} = 7.4 Hz, 2H, H8'), δ 7.42 (t, J_{HH} = 7.6 Hz, 2H, H7'), δ 7.31 (o, 2H, H8), δ 7.31 (o, 2H, H9), δ 7.26 (m, 1H, H10), δ 4.65 (m, 1H, H5), δ 4.44 (dt, J_{HH} = 7.3, 8.3 Hz, 1H, H13), δ 4.35 (o, 2H, H3'), δ 4.31 (o, 1H, H4'), δ 3.86 (dd, J_{HH} = 5.9, 17.5 Hz, 1H, H20a), δ 3.81 (dd, J_{HH} = 5.9, 17.5 Hz, 1H, H20b), δ 3.73 (dd, J_{HH} = 6.1, 16.8 Hz, 1H, H2a), δ 3.61 (dd, J_{HH} = 6.1, 16.8 Hz, 1H, H2b), δ 3.12 (dd, J_{HH} = 4.1, 13.7 Hz, 1H, H6a), δ 2.88 (d, J_{HH} = 9.3, 13.7 Hz, 1H, H6b), δ 1.70 (m, 1H, H15), δ 1.58 (t, J_{HH} = 7.3 Hz, 2H, H14), δ 0.97 (d, J_{HH} = 6.8 Hz, 3H, H16), δ 0.93 (d, J_{HH} = 6.5 Hz, 3H, H17), ^{13}C NMR (d_6-DMSO) δ 172.9 (C18), 172.0 (C21), 171.7 (C11), 169.6 (C3), 157.2 (C1'), 144.0 (C5'), 141.5 (C10'), 138.3 (C7), 129.8 (C8), 128.5 (C9), 128.3 (C8'), 127.7 (C7'), 126.8 (C10), 125.9 (C6'), 120.7 (C9'), 66.3 (C3'), 54.3 (C5), 51.4 (C13), 47.1 (C4'), 43.3 (C2), 41.5 (C14), 41.2 (C20), 37.6 (C6), 24.7 (C15), 23.5 (C16), 22.3 (C17).

7.2.3.1 Fmoc-Cys(Acm)-Wang resin

This preparation was carried out in exactly the same manner as described above for the synthesis of Fmoc-Gly-Wang resin (Section **7.2.1.1**) but using Fmoc-*S*-acetamidomethylcysteine (396 mg, 0.95 mmol) in place of Fmoc-glycine. All other procedures and reagents were identical. The loading level was determined to be approximately 0.74 meq/g from an average of two readings.

7.2.3.2 Fmoc-Cys(Acm)-Asn-Gly-Arg(Mtr)-Cys(Acm)-Wang resin

This synthesis proceeds as described above for the SPPS of Fmoc-Gly-Phe-Leu-Gly-Wang resin (Section **7.2.1.2**) but using Fmoc-Cys(Acm)-Wang resin (1.2 g, 0.89 mmol), Fmoc-N^G-4-methoxy-2,3,6-trimethylbenzenesulfonylarginine (1081 mg, 1.78 mmol), Fmoc-glycine (528 mg, 1.78 mmol), Fmoc-asparagine (629 mg, 1.78 mmol) and Fmoc-*S*-acetamidomethylcysteine (736 mg, 1.78 mmol). For the final two coupling reactions, NHS (205 mg, 1.78 mmol) was included.

7.2.3.3 Fmoc-Cys(Acm)-Asn-Gly-Arg(Mtr)-Cys(Acm)-OH (41)

In a typical reaction, the fully protected peptide **41** was liberated from the resin (600 mg) by agitation with 87% TFA/8% phenol/5% H_2O (6 mL, 20 minutes) followed by washing with the same solution (2 x 3 mL) then repetition of the cleaving/washing process. The combined TFA solutions were repetitively diluted with water and dried under vacuum to yield a yellow-brown oil (520 mg).

Purification was carried out using reverse phase MPLC run using an isocratic 50% ACN/H_2O(A) eluant. The peak eluting at 18-23 minutes was collected in three cuts – early, middle and late. The middle cut was pure except for the presence of a single contaminating *p*-substituted aromatic compound which co-eluted, even in analytical HPLC chromatography (C18, A: H_2O(A), B: ACN, gradient: 50% B (0 min), 50% B (4 min), 56% B (7 min), 100% B (8 min)).

In order to remove this lower molecular weight contaminant, size exclusion chromatography was carried out using LH20 (70 g, 420 x 18 mm) with UV detection at 254 nm and 50% ACN/H_2O as the eluant. The first peak, eluting at a volume of approximately 270 mL consisted of primarily the desired peptide **41** .

It was found that by an iterative cycle of MPLC and size exclusion chromatography the fully protected peptide **41** could be isolated in a pure state (135 mg, 6.6%). HRESIMS 1128.3947, $C_{49}H_{66}N_{11}O_{14}S_3$ ($M + H^+$) requires 1128.3953. ^{1}H NMR (CD_3CN/D_2O) δ 7.85 (t, J_{HH} = 7.6 Hz, 2H, H9'), δ 7.71 (t, J_{HH} = 7.6 Hz, 2H, H6'), δ 7.46 (d, J_{HH} = 7.6 Hz, 2H, H8'), δ 7.38 (t, J_{HH} = 7 Hz, 2H, H7'), δ 6.71 (s, 1H, H20'), δ 4.65 (t, J_{HH} = 5.9 Hz, 1H, H6), δ 4.57 (dd, J_{HH} = 4.9, 8.3 Hz, 1H, H25), δ 4.39 (o, 1H, H3'a), δ 4.38 (o, 1H, H2), δ 4.34 (o, 1H, H3'b), δ 4.34 (o, 1H, H11'a), δ 4.32 (o, 1H, H15), δ 4.27 (o, 1H, H4'), δ 4.27 (o, 2H, H26'), δ 4.20 (o, 1H, H11'b), δ 3.91 (o, 1H, H12a), δ 3.82 (s, 3H, H24'), δ 3.82 (m, 1H, H12b), δ 3.12 (m, 2H, H18), δ 3.08 (dd, J_{HH} = 4.8, 14.1 Hz, 1H, H26a), δ 3.03 (dd, J_{HH} = 4.9, 14.3 Hz, 1H, H3a), δ 2.93 (dd, J_{HH} = 8.3, 14.1 Hz, 1H, H26b), δ 2.82 (dd, J_{HH} = 8.8, 13.7 Hz, 1H, H3b), δ 2.78 (d, J_{HH} = 5.8 Hz, 2H, H7), δ 2.63 (s, 3H, H25'), δ 2.55 (s, 3H, H22'), δ 2.10 (s, 3H, H23'), δ 1.95 (s, 3H, H14'), δ 1.94 (s, 3H, H29'), δ 1.79 (m, 1H, H16a), δ 1.68 (m, 1H, H16b), δ 1.52 (m, 2H, H17), ^{13}C NMR (CD_3CN/D_2O) δ 173.3 (C8), 172.3 (C13'), 172.3 (C23), 172.1 (C28'), 172.0 (C27), 171.8 (C10), 171.5 (C4), 170.1 (C13), 158.2 (C19'), 156.7 (C1'), 143.4 (C5'), 140.6 (C10'), 138.1 (C17'), 132.9 (C16'), 131.4 (C21'), 127.4 (C8'), 126.9 (C7'), 124.9 (C6'), 124.3 (C18'), 119.6 (C9'), 111.7 (C20'), 66.5 (C3'), 55.0 (C24'), 54.2 (C2), 52.6 (C15), 52.2 (C25), 50.7 (C6), 46.3 (C4'), 42.9 (C12), 40.7 (26'), 40.6 (C26'), 40.0 (C11'), 40.0 (C18), 36.4 (C7), 31.8 (C3), 31.3 (C26), 27.9 (C16), 25.7 (C17), 22.8 (C25'), 21.6 (C14'), 21.6 (C29'), 17.3 (C22'), 10.8 (C23').

7.2.3.5 *cyclo*-Cys-Asn-Gly-Arg-Cys-OH (42)

The deprotection and cyclisation of the resin bound peptide **41** (700 mg, 0.45 mmol) was achieved by first cleaving the amino terminal Fmoc protecting group with 20% piperidine/DMF (7 mL, 10 minutes), washing the resin with DMF (3 x 10 mL), then deprotecting and cyclising the cysteine residues by agitation with $Tl(CF_3COO)_3$ (268 mg, 0.49 mmol) in DMF (5 mL) at 0°C for 80 minutes. Following this reaction, the resin was drained and washed thoroughly with DMF (3 x 10 mL), MeOH (3 x 10 mL) and DCM (3 x 10 mL) before being dried under vacuum. The peptide was removed from the resin with cleavage solution (10 mL) consisting of 95% TFA/5% H_2O and finally the resin was rinsed with the solution (2 x 5 mL). The progress of the arginine deprotection reaction was monitored by analytical HPLC (C18, A: H_2O(A), B: ACN, gradient I), and once determined to be complete, the reaction mixture was diluted with ACN and dried under vacuum repetitively to yield a thick yellow-brown oil (approximately 300 mg).

The oil was chromatographed on a small C18 column (3 g, 40 x 10 mm), with the peptide eluting in the initial aqueous fraction which was dried down to provide the crude peptide (49 mg), which was subjected to semi-preparative HPLC (Phenomenex Luna C18 column). The solvent system used was 100% H_2O(A) for eight minutes then a switch to 1% ACN/H_2O(A) for four minutes followed by a one minute rinse with 100% ACN before equilibrating back to 100% H_2O(A). The peak eluting at twelve minutes was collected and determined to be **42**. The yield of pure **42** was 19.3 mg (7.8%). HRESIMS 550.1862 $C_{18}H_{32}N_9O_7S_2$ ($M + H^+$) requires 550.1866. ^{1}H NMR (D_2O) δ 4.80 (dd, J_{HH} = 6.8, 7.8 Hz, 1H, H6), δ 4.56 (dd, J_{HH} = 3.4, 10.3 Hz, 1H, H25), δ 4.18 (t, J_{HH} = 7.3 Hz, 1H, H15), δ 4.07 (t, J_{HH} = 6.8 Hz, 1H, H2), δ 4.04 (d, J_{HH} = 15.6 Hz, 1H, H12a), δ 3.55 (d, J_{HH} = 15.6 Hz, 1H, H12b), δ 3.27 (dd, J_{HH} = 3.5, 14.6 Hz, 1H, H26a), δ 3.22 (dd, J_{HH} = 6.8, 14.6 Hz, 1H, H3a), δ 3.14 (dd, J_{HH} = 7.4, 14.6 Hz, 1H, H3b), δ 3.11 (t, J_{HH} = 6.9 Hz, 2H, H18), δ 3.01 (dd, J_{HH} = 10.3, 14.6 Hz, 1H, H26b), δ 2.73 (dd, J_{HH} = 6.7, 15.4 Hz, 1H, H7a), δ 2.61 (dd, J_{HH} = 7.9, 15.4 Hz, 1H, H7b), δ 1.74 (m, 1H, H16a), δ 1.67 (m, 1H, H16b), δ 1.57 (m, 2H, H17), ^{13}C NMR (D_2O) δ 174.1 (C8), 173.9 (C23), 173.2 (C27), 171.7 (C10), 170.8 (C13), 167.3 (C4), 156.8 (C20), 53.6

(C15), 52.9 (C2), 52.4 (C25), 50.2 (C6), 42.4 (C12), 41.2 (C3), 40.6 (C18), 40.2 (C26), 36.2 (C7), 27.3 (C16), 24.2 (C17).

7.2.4.1 Fmoc-*cyclo*-Cys-Asn-Gly-Arg-Cys-Gly-Phe-Leu-Gly-OH (43)

Fmoc-Gly-Phe-Leu-Gly-Wang resin (250 mg, 0.13 mmol) was deprotected by agitation with 20% piperidine/DMF (5 mL, 10 minutes) followed by washing with DMF (3 x 5 mL) and IPA (3 x 5 mL) at which point a Kaiser test was carried out. The test result was positive (blue colour change) so the resin was washed again with DMF (3 x 5 mL).

The protected peptide **41** (135 mg, 0.12 mmol) was dissolved in dry DMF (5 mL) and activated with HBTU (90.7 mg, 0.24 mmol) and DIPEA (83.4 μL, 0.48 mmol) in the presence of NHS (55.1 mg, 0.48 mmol) for two minutes before addition to the resin. The coupling reaction was allowed to proceed for one hour before draining and washing with DMF (5 mL). These combined washings were analysed by HPLC C18, A: H_2O(A), B: ACN, gradient: 50% B (0 min), 50% B (4 min), 56% B (7 min), 100% B (8 min)) which indicated the presence of unreacted **41**. The combined washings were dried and the fraction stored to allow recovery of the unused **41**.

The resin was acetylated with acetic anhydride (12.8 μL, 0.13 mmol) in DMF (3 mL) for 20 minutes, drained and washed with DMF (3 x 5 mL).

Cysteine deprotection and cyclisation was carried out by reacting the resin with $Tl(CF_3COO)_3$ (78 mg, 0.14 mmol) in DMF (2 mL) at 0°C for 80 minutes, after which the resin was drained, washed with DMF (3 x 5 mL), MeOH (3 x 5 mL) and DCM (3 x 5 mL) and dried thoroughly.

Cleavage of the peptide from the resin was carried out using 87% TFA/8% phenol/5% H_2O (10 mL, 20 minutes) followed by washing with the same solution (2 x 3 mL). The acid solutions were combined and the removal of the arginine side-chain protection was

monitored by HPLC (C18, A: H_2O(A), B: ACN, Gradient II). After 60 hours the reaction mixture was repetitively diluted with water and dried under vacuum to give the crude peptide mixture.

7.2.4.1.1 Purification of Fmoc-*cyclo*-CNGRCGFLG-OH (43)

The crude peptide material was dissolved, with sonication and heating, in 50% ACN/H_2O (5 mL) but remained cloudy so was filtered. The soluble material was subjected to size exclusion chromatography on LH20 (70 g, 420 x 18 mm) with UV detection at 254 nm using 50% ACN/H_2O as the eluant. Eight fractions were collected, which did not consist of specific peaks, but rather consisted of cuts across one very broad peak, with the desired material being found in fractions three (primarily) and four; however, these fractions were still heavily contaminated. The insoluble material was analysed by HPLC (C18, A: H_2O(A), B: ACN, Gradient II) and found to contain a low proportion of **43**.

Weak cation-exchange chromatography was attempted on a Trisacryl M CM column (30 g, 130 x 20 mm) which was equilibrated to 30% ACN/H_2O before application of the sample and elution with 30% ACN/H_2O (2 x 25 mL) followed by 30% ACN/H_2O + 0.1% TFA (3 x 25 mL) with the desired product eluting in the first two, un-acidified fractions which were combined and dried.

This material was then chromatographed on a silica column (10g, 180 x 12 mm) running 50% ACN/H_2O + 0.1% TFA with UV detection at 254 nm; however, no peaks were detected so all fractions were combined and taken to dryness.

Semi-preparative HPLC (Phenomenex Luna C18 column) was then carried out on the combined silica fractions as well as the insoluble material isolated prior to size exclusion chromatography, running an isocratic solvent system of 35% ACN/H_2O + 0.1% TFA for 12 minutes followed by a one minute wash with 100% ACN before re-equilibration.

Peaks eluting at 7:30, 8:00 and 12:00 minutes were collected and examined by NMR spectroscopy but were found to contain too little material to allow structural determination.

7.2.4.2 Resynthesis of Fmoc-*cyclo*-CNGRCGFLG-OH (43)

Fmoc-Gly-Phe-Leu-Gly-Wang resin (800 mg, 0.42 mmol) was used as the starting point for a synthesis that proceeded as described above for the SPPS of Fmoc-Cys(Acm)-Asn-Gly-Arg(Mtr)-Cys(Acm)-Wang resin (Section **7.2.2.2**) but using Fmoc-N^G-4-methoxy-2,3,6-trimethylbenzenesulfonylarginine (510 mg, 0.84 mmol), Fmoc-glycine (271 mg, 0.84 mmol), Fmoc-asparagine (297 mg, 0.84 mmol) and Fmoc-*S*-acetamidomethylcysteine (347 mg, 0.84 mmol) and including NHS (97 mg, 0.84 mmol) in the final two coupling reactions.

The cysteine residues of the peptide were deprotected and cyclised with $Tl(CF_3COO)_3$ (377 mg, 0.69 mmol) at 0°C for 80 minutes in DMF (4 mL) before being washed thoroughly with DMF (3 x 10 mL), MeOH (3 x 10 mL) and DCM (3 x 10 mL) and dried.

7.2.4.2.1 Cleavage of Fmoc-*cyclo*-CNGRCGFLG-OH (43)

Two subsamples of resin bound **43** (5 mg each, 2.7 μmol each) were cleaved using 95% TFA/H_2O and 87% TFA/8% phenol/5% H_2O and the reaction progress monitored by analytical HPLC (C18, A: H_2O(A), B: ACN, Gradient II).

The remaining resin bound **43** (820 mg, 0.42 mmol) was cleaved with 95% TFA/H_2O for 24 hours then the solvent was removed under vacuum to yield a dark yellow oil (220 mg).

7.2.4.2.2 Purification of Fmoc-*cyclo*-CNGRCGFLG-OH (43)

The crude peptide mixture was dissolved, with sonication, in 50% ACN/H_2O (15 mL) and ACN was added (100 mL). The precipitate that formed was filtered off and washed with ACN (20 mL) and MeOH (20 mL). The collected washings were analysed by analytical HPLC ((C18, A: H_2O(A), B: ACN, Gradient III) and found to contain negligible quantities of **43**. The solid was collected, analysed by HPLC and then purified collecting the peak eluting at 4.9 min on semi-preparative HPLC (C18, A: H_2O(A), B: ACN, gradient: 50% B (0 min), 50% B (4 min), 56% B (7 min), 100% B (8 min), 100% B (9 min, 50% B (10 min), 50% B (13 min)) to afford pure **43** (32.3 mg, 6.7%). HRESIMS 1146.4491, $C_{52}H_{68}N_{13}O_{13}S_2$ ($M + H^+$) requires 1146.4501. ^{1}H NMR (d_6-DMSO) δ 8.77 (d, J_{HH} = 7.6 Hz, 1H, H5), δ 8.34 (t, J_{HH} = 5.6 Hz, 1H, H28), δ 8.25 (d, J_{HH} = 8.4 Hz, 1H, H39), δ 8.20 (t, J_{HH} = 5.4 Hz, 1H, H46), δ 8.11 (o, 1H, H24), δ 8.09 (o, 1H, H31), δ 7.97 (d, J_{HH} = 7.4 Hz, 2H, H9'), δ 7.94 (br s, 1H, H11), δ 7.86 (d, J_{HH} = 8.0 Hz, 1H, H1), δ 7.80 (o, 2H, H6'), δ 7.79 (o, 1H, H14), δ 7.62 (t, J_{HH} = 5.5 Hz, 1H, H19), δ 7.51 (t, J_{HH} = 7.4 Hz, 2H, H8'), δ 7.42 (m, 2H, H7'), δ 7.33 (o, 2H, H36), δ 7.31 (o, 2H, H35), δ 7.26 (m, 1H, H37), δ 4.63 (o, 1H, H32), δ 4.62 (o, 1H, H6), δ 4.57 (m, 1H, H25), δ 4.46 (o, 2H, H3'), δ 4.43 (o, 1H, H15), δ 4.41 (o, 1H, H40), δ 4.32 (m, 1H, H4'), δ 4.28 (o, 1H, H12a), δ 4.27 (o, 1H, H2), δ 3.83 (o, 2H, H47), δ 3.75 (o, 2H, H29), δ 3.51 (o, 1H, H12b), δ 3.31 (o, 1H, H26a), δ 3.27 (o, 1H, H3a), δ 3.17 (o, 2H, H18), δ 3.13 (o, 1H, H33a), δ 3.05 (o, 1H, H26b), δ 3.01 (o, 1H, H3b), δ 2.84 (o, 1H, H33b), δ 2.81 (o, 1H, H7a), δ 2.40 (dd, J_{HH} = 15.1, 4.4 Hz, 1H, H7b), δ 2.00 (br s, 1H, H16a), δ 1.69 (m, 1H, H42), δ 1.63 (o, 2H, H16b), δ 1.58 (o, 2H, H41), δ 1.55 (o, 2H, H17), δ 0.97 (d, J_{HH} = 6.3 Hz, 3H, H43), δ 0.93 (d, J_{HH} = 6.3 Hz, 3H, H44), ^{13}C NMR (d_6-DMSO) δ 172.6 (C45), 172.0 (C8), 171.9 (C23), 171.3 (C48), 171.0 (C38), 171.0 (C4), 170.9 (C10), 170.2 (C27), 169.9 (C13), 168.5 (C30), 156.9 (C20), 156.4 (C1), 144.0 (C5'), 141.0 (C10'), 137.8 (C34), 129.5 (C35), 128.3 (C36), 128.0 (C8'), 127.4 (C7'), 126.5 (C37), 125.5 (C6'), 120.4 (C9'), 66.0 (C3'), 55.0 (C2), 54.0 (C32), 52.0 (C25), 52.0 (C15), 51.2 (C40), 49.8 (C6), 46.9 (C4'), 42.9 (C12), 42.1 (C29), 41.4 (C41), 41.3 (C3), 41.1 (C26), 40.9 (C47), 40.6 (C18), 37.8 (C33), 36.3 (C7), 28.5 (C16), 25.3 (C17), 24.3 (C42), 23.3 (C43), 21.9 (C44)

7.3 Work described in Chapter 3

7.3.2.1 Mycalamide A oxidative cleavage

To a vigorously stirred suspension of silica (50 mg) in DCM (300 μL) was added an aqueous solution of $NaIO_4$ (50 μL of 0.65 M, 32.5 μmol) followed 15 minutes later by mycalamide A **31** (10 mg, 19.9 μmol) in DCM (200 μL). After one hour, TLC (SiO_2, EtOAc, I_2) indicated the reaction was complete by the movement of the R_f 0.09 spot to R_f 0.59 so the reaction mixture was filtered and the solid washed with DCM. The organic fractions were combined and dried under vacuum to give pure **45** (9.3 mg, 19.8 μmol) in a 99.5% yield. HRESIMS 494.2373, $C_{23}H_{37}NO_9Na$ ($M + Na^+$) requires 494.2366. ^1H NMR ($CDCl_3$) δ 9.54 (t, J_{HH} = 2 Hz, 1H, H17), δ 7.48 (d, J_{HH} = 9.8 Hz, 1H, H9), δ 5.88 (t, J_{HH} = 9.5 Hz, 1H, H10), δ 5.13 (d, J_{HH} = 6.9 Hz, 1H, H10-OCH_2a), δ 4.87 (d, J_{HH} = 6.9 Hz, 1H, H10-OCH_2b), δ 4.84 (t, J_{HH} = 2 Hz, 1H, H4=CH_2a), δ 4.75 (t, J_{HH} = 2 Hz, 1H, H4=CH_2b), δ 4.27 (s, 1H, H7), δ 4.20 (dd, J_{HH} = 6.6, 10.0 Hz, 1H, H12), δ 4.09 (dd, J_{HH} = 4.4, 8.0 Hz, 1H, H15), δ 4.02 (dq, J_{HH} = 3.0, 6.6 Hz, 1H, H2), δ 3.76 (dd, J_{HH} = 6.6, 9.3 Hz, 1H, H11), δ 3.56 (s, 3H, H13-OCH_3), δ 3.51 (d, J_{HH} = 10.2 Hz, 1H, H13), δ 3.29 (s, 3H, H6-OCH_3), δ 2.37 (o, 2H, H16), δ 2.36 (o, 1H, H5a), δ 2.23 (dq, J_{HH} = 2.9, 7.0 Hz, 1H, H3), δ 2.08 (dt, J_{HH} = 2.0, 14.0 Hz, 1H, H5b), δ 1.17 (d, J_{HH} = 6.6 Hz, 3H, H2-CH_3), δ 1.02 (s, 3H, H14-CH_3a), δ 0.92 (d, J_{HH} = 7 Hz, 3H, H3-CH_3), δ 0.86 (s, 3H, H14-CH_3b) ^{13}C NMR ($CDCl_3$) δ 200.7 (C17), 171.9 (C8), 145.0 (C4), 111.0 (C4=CH_2), 100.0 (C6), 86.5 (C10-OCH_2), 79.1 (C13), 74.2 (C15), 74.1 (C12), 74.0 (C10), 71.2 (C7), 70.6 (C11), 69.5 (C2), 61.8 (C13-OCH_3), 48.5 (C6-OCH_3), 43.3 (C16), 41.2 (C14), 40.9 (C3), 33.2 (C5), 23.3 (C14-CH_3), 12.1 (C3-CH_3).

7.3.2.2 Reductive amination of aldehyde

Ammonium acetate (147 mg, 1.9 mmol) and **44** (9.0 mg, 19 μmol) were dried together under hi-vacuum before being dissolved in $(NH_4)_2CO_3$ saturated dry MeOH (900 μL) and stirred for 30 minutes prior to the addition of $NaCNBH_3$ (6.0 mg, 95 μmol) in $(NH_4)_2CO_3$ saturated dry MeOH (100 μL). A TLC (SiO_2, EtOAc, PMA) taken after twelve hours of reaction showed the disappearance of the aldehyde **45** (R_f 0.59) and the appearance of a baseline spot (R_f 0.01) that was positive to both ninhydrin and PMA. The reaction mixture was then dried down, redissolved in H_2O, applied to a C_{18} cartridge which had been equilibrated to H_2O, washed with H_2O (7 mL) and eluted with MeOH (3 mL) to give crude **45** which was acylated (Sections **4.4.1 and 5.5.1**) without further purification. HRESIMS 473.2876, $C_{23}H_{41}N_2O_8$ ($M + H^+$) requires 473.2863.

7.3.3.3 Mycalamide B azide (49)

Mycalamide B (**32**, 3.6 mg, 7.0 μmol) and PPh_3 (4.6 mg, 17.4 μmol) were dissolved in a suspension of $Zn(N_3)_2$.2Pyr (2.1 mg, 7.0 μmol) in dry toluene (200 μL). DEAD (2.7 μL, 17.4 μmol) was added. After four hours, HPLC (C18, A: H_2O, B: ACN, Gradient II) showed the reaction was still not complete so a solution of more PPh_3 (1.4 mg, 5.3 μmol) and DEAD (0.8 μL, 5.3 μmol) in toluene (30 μL) was added. A further HPLC (C18, A: H_2O, B: ACN, Gradient II) analysis after four more hours showed some starting material remaining so the reaction was refreshed with additional PPh_3 (0.9 mg, 3.5 μmol) and DEAD (0.5 μL, 3.5 μmol) in toluene (20 μL). After another two hours of reaction the starting material was seen to be completely consumed so the reaction was worked up by removal of the solvent under vacuum then passage through a C18 cartridge, washing with water, and 40% ACN/water before eluting the product with 80% ACN/water and 100% ACN. The combined product-containing fractions were dried down to provide the desired azide **49** (3.2 mg, 84%). HRESIMS 565.2847, $C_{25}H_{42}N_4O_9Na$ ($M + Na^+$) requires 565.2849. ^1H NMR ($CDCl_3$) δ 7.53 (d, J_{HH} = 9.8 Hz, H, H9), δ 5.78 (t, J_{HH} = 9.7 Hz, 1H, H10), δ 5.12 (d, J_{HH} = 7 Hz, 1H, H10-OCH_2a), δ

4.88 (t, J_{HH} = 2 Hz, 1H, H4=CH_2a), δ 4.87 (d, J_{HH} = 7 Hz, 1H, H10-OCH_2b), δ 4.76 (t, J_{HH} = 2 Hz, 1H, H4=CH_2b), δ 4.30 (s, 1H, H7), δ 4.21 (dd, J_{HH} = 6.5, 10.4 Hz, 1H, H12), δ 4.07 (dq, J_{HH} = 2.9, 6.8 Hz, 1H, H2), δ 3.78 (dd, J_{HH} = 6.6, 9.6 Hz, 1H, H11), δ 3.56 (s, 3H, H13-OCH_3), δ 3.44 (d, J_{HH} = 10.2 Hz, 1H, H13), δ 3.41 (dd, J_{HH} = 2.4, 13.1 Hz, 1H, H18a), δ 3.32 (s, 3H, H6-OCH_3), δ 3.31 (o, 1H, H15), δ 3.30 (o, 1H, H17), δ 3.25 (s, 3H, H17-OCH_3), δ 3.22 (o, 1H, H18b), δ 2.41 (d, J_{HH} = 14 Hz, 1H, H5a), δ 2.28 (dq, J_{HH} = 2.9, 7.1 Hz, 1H, H3), δ 2.23 (dt, J_{HH} = 1.9, 13.9 Hz, 1H, H5b), δ 1.60 (m, 2H, H16), δ 1.22 (d, J_{HH} = 6.8 Hz, 3H, H2-CH_3), δ 1.03 (d, J_{HH} = 7 Hz, 3H, H3-CH_3), δ 1.00 (s, 3H, H14-CH_3a), δ 0.87 (s, 3H, H14-CH_3b), ^{13}C NMR ($CDCl_3$) δ 171.7 (C8), 144.8 (C4), 111.4 (C4=CH_2), 100.0 (C6), 86.5 (C10-OCH_2), 79.1 (C13), 77.6 (C17), 75.5 (C15), 74.3 (C12), 74.0 (C10), 71.2 (C7), 70.9 (C11), 69.6 (C2), 61.8 (C13-OCH_3), 56.7 (C17-OCH_3), 52.2 (C18), 48.6 (C6-OCH_3), 41.6 (C14), 41.2 (C3), 33.6 (C5), 30.8 (C16), 23.3 (C14-CH_3(eq)), 18.0 (C2-CH_3), 13.6 (C14'-CH_3(ax)), 12.2 (C3-CH_3)

7.3.3.4 Mycalamide B amine (50)

Compound **49** (2.2 mg, 4.1 μmol) and PPh_3 (1.6 mg, 6.1 μmol) were dissolved in dry THF (160 μL) and allowed to react at 40°C. After three hours, TLC (SiO_2, 50:50:10:0.1 $CHCl_3$:Et2O:MeOH:cNH_4OH) showed the replacement of the starting material (Rf=0.83, PMA+) with a more polar compound (Rf=0.02, UV+ PMA+). Water (200μL) was added and the reaction was continued for a further three hours at 40°C at which point TLC (as above) indicated reaction was complete by the loss of UV response of the baseline spot. The reaction was dried down and the product **50** used without further purification.

7.3.4.1 Fumagillol oxidation

Chromium trioxide (106.3 mg, 1.06 mmol) was added to a stirred solution of pyridine (172 μL, 2.13 mmol) in DCM (1 mL) followed 15 minutes later by fumagillol **35** (20 mg, 0.071 mmol) in DCM (200 μL). TLC (SiO_2, 20% EtOAc/DCM, PMA) was used to follow the disappearance of the alcohol (R_f 0.40) and the appearance of the ketone at R_f 0.73 with the reaction reaching completion after 90 minutes. The reaction mixture was then applied directly to the top of a dry silica column (10 g, 80 x 18 mm) and eluted with DCM (20 mL) and EtOAc (15 mL). The organic fractions were combined and taken to dryness to yield pure **51** (18.5 mg, 0.066 mmol) in 97% yield. HREIMS 280.1673, $C_{15}H_{24}O_4$ (M^+) requires 280.1675. ^{1}H NMR ($CDCl_3$) δ 5.16 (m, 1H, H4'), δ 4.07 (dd, J_{HH} = 0.7, 10.7 Hz, 1H, H5), δ 3.48 (s, 3H, H8), δ 3.04 (dd, J_{HH} = 4.4 Hz, 1H, H7a), δ 2.71 (dd, J_{HH} = 4.4 Hz, 1H, H7b), δ 2.66 (dddd, J_{HH} = 0.7, 6.5, 6.7, 14.3 Hz, 1H, H1a), δ 2.58 (dd, J_{HH} = 5.8, 6.8 Hz, 1H, H2'), δ 2.48 (ddd, J_{HH} = 4.0, 5.3, 14.2 Hz, 1H, H1b), δ 2.37 (m, 1H, H3'a), δ 2.13 (m, 1H, H3'b), δ 2.04 (ddd, J_{HH} = 5.4, 6.8, 13.4 Hz, 1H, H2a), δ 1.86 (d, J_{HH} = 10.6 Hz, 1H, H4), δ 1.72 (s, 3H, H6'), δ 1.69 (ddd, J_{HH} = 4.0, 6.5, 13.8 Hz, 1H, H2b), δ 1.63 (s, 3H, H7'), δ 1.27 (s, 3H, H8'), ^{13}C NMR ($CDCl_3$) δ 207.1 (C6), 135.0 (C5'), 118.2 (C4'), 83.2 (C5), 60.4 (C2'), 58.6 (C1'), 58.5 (C8), 58.4 (C3), 53.6 (C4), 51.8 (C7), 36.8 (C1), 33.2 (C2), 27.3 (C3'), 25.7 (C6'), 18.0 (C7'), 13.8 (C8').

7.3.4.2 Fumagillone reductive amination

Compound **51** (7.0 mg, 0.025 mmol) was stirred with NH_4CH_3COO (192.6 mg, 2.5 mmol) in $(NH_4)_2CO_3$ saturated dry MeOH (400 μL) for 15 minutes prior to the addition of $NaCNBH_3$ (7.9 mg, 0.13 mmol). After two hours, TLC (SiO_2, 20% EtOAc/DCM, PMA) indicated the reaction was complete through disappearance of **51** (Rf 0.73) and appearance of a baseline spot (Rf 0.05), so the reaction solution were diluted with H_2O (8 mL) and passed through a C_{18} cartridge which was then washed with H_2O (10 mL)

and eluted with MeOH (2 mL). The methanol fraction was dried down to provide crude **52** which was acylated without further purification.

7.3.4.3 Fumagillol *S*-tosylate (53)

A solution of $ZnCl_2$ (4 g, 29.3 mmol) in H_2O was added slowly to a stirred solution of *p*-toluenesulphonic acid hydrate (11.2 g, 58.9 mmol) in H_2O (5 mL). The white precipitate of $Zn(OTos)_2$ that formed was filtered and dried thoroughly before use.

Fumagillol (**35**, 20 mg, 71 μmol) and PPh_3 (186 mg, 0.71 mmol) were dissolved in a stirred suspension of $Zn(OTos)_2$ (28.9 mg, 71 μmol) in dry toluene (500 μL). DEAD (111.6 μL, 0.71 mmol) was then added and the reaction was allowed to proceed at room temperature for ten hours. The crude reaction mixture was filtered through a silica column (0.6 g, 60 x 5 mm) eluting with Et_2O. The ether was removed under a stream of nitrogen and the material was chromatographed on a silica column (5 g, 90 x 12 mm) eluting with 20% PE/EtOAc. The product-containing fractions were combined and re-chromatographed on silica (5 g, 90 x 12 mm) using 10% Et_2O/DCM as the eluant. The only compound isolated was an undesired elimination product **53** (7.1 mg, 38%). HREIMS 264.1725, $C_{16}H_{24}O_3$ (M^+) requires 264.1730. ^{1}H NMR ($CDCl_3$) δ 5.97 (m, 1H, H6), δ 5.84 (m, 1H, H1), δ 5.21 (m, 1H, H4'), δ 4.22 (m, 1H, H5), δ 3.39 (s, 3H, H8), δ 2.84 (d, J_{HH} = 4.4 Hz, 1H, H7a), δ 2.72 (t, J_{HH} = 6.5 Hz, 1H, H2'), δ 2.6 (d, J_{HH} = 4.4 Hz, 1H, H7b), δ 2.38 (m, 1H, H2a), δ 2.37 (m, 1H, H3'a), δ 2.2 (m, 1H, H3'b), δ 2.05 (m, 1H, H2b), δ 1.74 (s, 3H, H6'), δ 1.66 (s, 3H, H7'), δ 1.6 (d, J_{HH} = 6.9 Hz, 1H, H4), δ 1.28 (s, 3H, H8'), ^{13}C NMR ($CDCl_3$) δ 134.7 (C5'), 127.8 (C6), 127.3 (C1), 118.6 (C4'), 76.0 (C5), 62.0 (C2'), 59.2 (C1'), 57.2 (C3), 55.4 (C8), 52.6 (C7), 50.5 (C4), 34.1 (C2), 27.4 (C3'), 25.8 (C6'), 18.0 (C7'), 14.4 (C8').

7.3.4.4 Fumagillol phthalimide (55)

To a stirred solution of fumagillol (**35**, 40 mg, 0.14 mmol) and phthalimide (31.3 mg, 0.21 mmol) in dry THF (1 mL) was added triphenylphosphine (78.1 mg, 0.3 mmol) and DEAD (37.7 μL, 0.28 mmol) in dry THF (200 μL). The reaction was allowed to stir overnight then TLC (SiO_2, 70% Et_2O/PE, PMA) showed the appearance of a non-polar compound (Rf 0.58) and disappearance of the starting material **35** (Rf 0.05) Reaction mixture was then dried and chromatographed on a silica column (20 g, 160 x 18 mm), eluting isocratically with 70% Et_2O/PE. Two large fractions (20 mL each) were taken followed by 16 smaller fractions (5 mL each), with the pure product **55** eluting in fractions nine and ten and co-eluting with 1,2-dicarbethoxyhydrazine in fractions eleven to 14. These contaminated fractions were combined and run on silica (10 g, 70 x 14 mm) eluting with 20% EtOAc/DCM, collecting twelve fractions (5 mL each) of which two (fractions 6 and 7) contained pure **55**. The pure material from both columns was combined to give an overall yield of 39.6 mg (68%). HRESIMS 450.1684, $C_{24}H_{29}NO_5K$ ($M + K^+$) requires 450.1683. ^1H NMR ($CDCl_3$) δ 7.83 (dd, J_{HH} = 3.4, 5.3 Hz, 2H, H3''), δ 7.71 (dd, J_{HH} = 3.4, 5.3 Hz, 2H, H4''), δ 5.2 (t, J_{HH} = 7.5 Hz, 1H, H4'), δ 4.68 (t, J_{HH} = 10.6 Hz, 1H, H5), δ 4.34 (m, 1H, H6), δ 3.3 (s, 3H, H8), δ 2.96 (d, J_{HH} = 4.4 Hz, 1H, H7a), δ 2.58 (m, 1H, H2'), δ 2.58 (m, 1H, H1a), δ 2.56 (m, 1H, H7b), δ 2.35 (m, 1H, H3'a), δ 2.15 (m, 1H, H3'b), δ 1.94 (m, 1H, H2a), δ 1.76 (m, 1H, H1b), δ 1.72 (s, 3H, H6'), δ 1.68 (d, J_{HH} = 11.2 Hz, 1H, H4), δ 1.64 (s, 3H, H7'), δ 1.29 (s, 3H, H8'), δ 1.26 (m, 1H, H2b) ^{13}C NMR ($CDCl_3$) δ 168.3 (C1''), 135 (C5'), 133.97 (C4''), 131.84 (C2''), 123.26 (C3''), 118.4 (C4'), 76.16 (C5), 61.36 (C2'), 59.09 (C1'), 58.78 (C3), 55.67 (C8), 52.9 (C6), 52.02 (C4), 50.12 (C7), 33.45 (C2), 27.38 (C3'), 25.7 (C6'), 25.45 (C1), 17.98 (C7'), 14.31 (C8').

7.3.4.6 Fumagillol *R*-tosylate (56)

Tosic acid hydrate (1 g, 5.26 mmol) and P_2O_5 (3 g, 21.1 mmol) were stirred overnight in dry DCM then more P_2O_5 was added (1 g, 7.05 mmol). After reacting for a total of 24 hours, the crude reaction mixture was passed through a dry silica column (30 g, 45 x 30 mm) and eluted with dry DCM. The combined organic solvent was removed under vacuum to yield tosic anhydride (520 mg, 61%) as a white crystalline solid (mp 112-124°C, lit 129.5-131.5°C).

Fumagillol (**35**, 10 mg, 35 μmol) and tosic anhydride (17.4 mg, 53 μmol) were dissolved in dry pyridine (200 μL) to give a solution which turned yellow immediately. After ten minutes the reaction was monitored by HPLC (C18, A: H_2O, B: ACN, Gradient II) and showed complete reaction. TLC (SiO_2, Et_2O, UV/PMA) showed a single UV and PMA positive spot at R_f=0.86. The reaction was worked up by dilution of the reaction solution with distilled water (2 mL) which was then applied to a C_{18} cartridge. The cartridge was then washed with distilled water (5 mL) and 20% ACN/H_2O before being eluted with ACN which was removed under nitrogen to yield pure tosylate **56** (14.7 mg, 95%). HREIMS 436.4925, $C_{23}H_{32}O_6S$ (M^+) requires 436.1920. ^{1}H NMR ($CDCl_3$) δ 7.84 (d, J_{HH} = 8.1 Hz, 2H, H3''), δ 7.30 (d, J_{HH} = 8.1 Hz, 2H, H4''), δ 5.16 (m, 1H, H4'), δ 5.04 (m, 1H, H6), δ 3.48 (dd, J_{HH} = 2.5, 10.8 Hz, 1H, H5), δ 3.01 (s, 3H, H8), δ 2.92 (d, J_{HH} = 4.4 Hz, 1H, H7a), δ 2.53 (t, J_{HH} = 6.3 Hz, 1H, H2'), δ 2.52 (d, J_{HH} = 4.4 Hz, 1H, H7b), δ 2.41 (s, 3H, H6''), δ 2.30 (m, 1H, H3'a), δ 2.23 (m, 1H, H1a), δ 2.13 (m, 1H, H3'b), δ 2.12 (m, 1H, H2a), δ 1.92 (d, J_{HH} = 10.8 Hz, 1H, H4), δ 1.78 (m, 1H, H1b), δ 1.72 (s, 3H, H6'), δ 1.62 (s, 3H, H7'), δ 1.13 (s, 3H, H8'), δ 1.12 (m, 1H, H2b), ^{13}C NMR ($CDCl_3$) δ 144.5 (C5''), 134.8 (C5'), 133.6 (C2''), 129.6 (C4''), 128.1 (C3''), 118.4 (C4'), 79.2 (C5), 75.5 (C6), 60.5 (C2'), 59.1 (C1'), 58.2 (C3), 56.4 (C8), 51.1 (C7), 47.7 (C4), 28.7 (C2), 27.2 (C3'), 26.4 (C1), 25.7 (C6'), 21.6 (C6''), 17.9 (C7'), 14.0 (C8')

7.3.4.8 Fumagillol azide (57)

Sodium azide (13 g, 0.2 mol) was added dropwise to a stirred aqueous solution of $Zn(NO_3)_2.6H_2O$ (29.75 g, 0.1 mol). The solution was heated to 50°C and pyridine (17 mL, 0.21 mmol) was added dropwise to form a dense white precipitate. The solution was allowed to cool to room temperature while stirring continued then the precipitate was filtered off and washed with cold H_2O. The product $Zn(N_3).2Pyr$ was used without further analysis or purification.

To a vigorously stirred suspension of $Zn(N_3).2Pyr$ (21.8 mg, 71 μmol), PPh_3 (46.5 mg, 177 μmol) and fumagillol (**35**, 20 mg, 71 μmol) in dry toluene (200 μL) was added DEAD (27.9 μL, 172 μmol). After stirring for 12 hours, HPLC (C18, A: H_2O, B: ACN, Gradient II) indicated that the reaction was approximately 50% complete, so a solution of PPh_3 (46.5 mg, 177 μmol) and DEAD (27.9 μL, 172 μmol) in dry toluene (50 μL) was added. After another 12 hours the reaction was worked up by passage through silica (5 g, 90 x 12 mm) eluting with 20% PE/Et2O. The desired product **57** was isolated in a relatively low yield (9.3 mg, 43%) HRESIMS 346.1527, $C_{16}H_{25}N_3O_3K$ ($M + K^+$) requires 346.1533. ^1H NMR ($CDCl_3$) δ 5.18 (m, 1H, H4'), δ 3.67 (s, 3H, H8), δ 3.58 (dd, J_{HH} = 9.2, 10.7 Hz, 1H, H5), δ 3.45 (m, 1H, H6), δ 2.92 (d, J_{HH} = 4.0 Hz, 1H, H7a), δ 2.53 (t, J_{HH} = 6.1 Hz, 1H, H2'), δ 2.53 (d, J_{HH} = 4.0 Hz, 1H, H7b), δ 2.36 (m, 1H, H3'a), δ 2.14 (m, 1H, H3'b), δ 1.96 (m, 1H, H1a), δ 1.84 (m, 1H, H2a), δ 1.73 (s, 3H, H6'), δ 1.68 (m, 1H, H1b), δ 1.64 (s, 3H, H7'), δ 1.54 (d, J_{HH} = 10.9 Hz, 1H, H4), δ 1.25 (s, 3H, H8'), δ 1.20 (m, 1H, H2b) ^{13}C NMR ($CDCl_3$) δ 135.1 (C5'), 118.3 (C4'), 82.3 (C5), 64.9 (C6), 61.2 (C2'), 58.9 (C8), 58.8 (C3), 58.3 (C1'), 52.3 (C4), 50.1 (C7), 32.5 (C2), 27.4 (C3'), 27.0 (C1), 25.7 (C6'), 18.0 (C7'), 14.3 (C8').

7.3.4.9 Fumagillol azide reduction

Fumagillol azide **57** (3.1 mg, 10 μmol) and PPh_3 (2.9 mg, 11 μmol) were dissolved in THF (100 μL). Water (1.5 μL, 83 μmol) was added immediately and the reaction was

stirred at room temperature for 18 hours. At this point, TLC (SiO_2, Et_2O) indicated the complete disappearance of the starting material (R_f=0.95, PMA) and appearance of a much more polar compound at R_f=0.08. The reaction mixture was dried down under a stream of nitrogen and chromatographed on a silica column (0.6 g, 60 x 5 mm) eluting with a solvent system consisting of 50:10:0.1 $CHCl_3$:MeOH:cNH_4OH to yield the desired amine **58** (1.5 mg, 53%). HRESIMS 282.2080, $C_{16}H_{28}NO_3$ ($M + H^+$) requires 282.2069. ^1H NMR ($CDCl_3$) δ 5.21 (m, 1H, H4'), δ 3.55 (s, 3H, H8), δ 3.47 (dd, J_{HH} = 9.3, 10.7 Hz, 1H, H5), δ 2.91 (d, J_{HH} = 4.4 Hz, 1H, H7a), δ 2.90 (m, 1H, H6), δ 2.55 (t , J_{HH} = 6.3 Hz, 1H, H2'), δ 2.51 (d, J_{HH} = 4.4 Hz, 1H, H7b), δ 2.36 (m, 1H, H3'a), δ 2.15 (m, 1H, H3'b), δ 1.88 (d, H, H1a), δ 1.85 (m, H, H2a), δ 1.74 (s, 3H, H6'), δ 1.65 (s, 3H, H7'), δ 1.57 (d, J_{HH} = 11.2 Hz, 1H, H4), δ 1.57 (m, 1H, H1b), δ 1.27 (s, 3H, H8'), δ 1.16 (m, 1H, H2b), ^{13}C NMR ($CDCl_3$) δ 135.3 (C5'), 118.6 (C4'), 84.2 (C5), 61.7 (C2'), 59.8 (C3), 58.9 (C1'), 56.5 (C8), 53.8 (C6), 51.1 (C4), 50.3 (C7), 33.2 (C2), 29.8 (C1), 27.6 (C3'), 25.9 (C6'), 18.0 (C7'), 14.7 (C8').

7.4 Work described in Chapter 4

7.4.2.1 Fmoc-*cyclo*-CNGRCGFLG-L-Tyrosinamide (59)

Fmoc-*cyclo*-Cys-Asn-Gly-Arg-Cys-Gly-Phe-Leu-Gly-OH (**43**, 3.2 mg, 2.8 μmol), L-tyrosinamide (**39**, 1.0 mg, 5.6 μmol), DCC (1.1 mg, 5.3 μmol) and NHS (0.6 mg, 5.6 μmol) were dissolved in DMF (320 μL). The reaction was allowed to proceed overnight at which point HPLC (C18, A: H_2O(A), B: ACN, Gradient III) and ESIMS showed no evidence of product formation. The reaction was recharged by the addition of extra DCC (3.1 mg, 15.0 μmol) and allowed to continue for a further 24 hours. At this point a small amount of product could be seen by HPLC (C18, A: H_2O(A), B: ACN, Gradient III). HBTU (2 mg, 5.3 μmol) was then added to recharge the reaction instead of DCC. An HPLC carried out one hour after the addition of the HBTU indicated the total consumption of the starting material so the reaction was quenched by the addition of water (50 μL) and refrigerated. Purification was carried out by semi-preparative HPLC (Phenomenex Luna C18 column) using an isocratic 40% ACN/H_2O(A) method on which the peak eluting at about 4.5 minutes was collected to provide the desired conjugate **59** (2.1 mg, 57%). HRESIMS 1308.5285, $C_{61}H_{78}N_{15}O_{14}S_2$ ($M + H^+$) requires 1308.5294.

7.4.2.2 H_2N-*cyclo*-CNGRCGFLG-L-Tyrosinamide (60)

Compound **59** (2.1 mg, 1.6 μmol) was dissolved in 20% piperidine/MeOH (500 μL) and allowed to stand at room temperature for 20 minutes before being dried under a stream of nitrogen. The residue was passed through a C18 cartridge, eluting with a stepped gradient from H_2O to MeOH followed by DMSO and finally 90% MeOH/H_2O + 0.1% TFA. The product was found to have eluted in the last fraction which was dried down to afford **60** (1.7 mg, 98%). HRESIMS 1086.4616, $C_{46}H_{68}N_{15}O_{12}S_2$ ($M + H^+$) requires 1086.4613.

7.4.3.1 Fmoc-*cyclo*-CNGRCGFLG-Doxorubicin

Doxorubicin (**19**, 2.6 mg, 4.8 μmol), **43** (5 mg, 4.4 μmol), HBTU (3.1 mg, 9.3 μmol) and NHS (1.0 mg, 9.7 μmol) were dissolved in dry DMF (350 μL) and allowed to react at room temperature overnight after which HPLC (C18, A: H_2O(A), B: ACN, Gradient III) indicated the reaction was complete. The reaction was quenched with water (50 μL) and refrigerated until purification by semi-preparative HPLC (Phenomenex Luna C18 column) eluting with isocratic 45% ACN/H_2O(A). The peak eluting at 4.8 minutes was collected to provide the desired conjugate **60** (2.1 mg, 29%). HRESIMS 1671.6136, $C_{79}H_{95}N_{14}O_{23}S_2$ ($M + H^+$) requires 1671.6136.

7.5 Work described in Chapter 5

7.5.2 Optimisation of Polymer Aminolysis

1-Amino-2-propanol (33.4 μL, 433 μmol) was stirred with polymer precursor **61** (39.6 mg, 216 μmol) in dry DMSO (400 μL) for four hours at 40°C. The reaction mixture was diluted with 60% MeOH/H_2O (12 mL) and placed in a CentriPrep ultrafiltration unit, MW cutoff 5 000 Da, and centrifuged at 1300 g for ten hours, removing the filtrate every two hours to leave approximately 500 μL of retentate. After removal of the solvent, the filtrate was found to contain nearly all of the mass, with the retentate containing less than 5% of the mass. The two fractions were combined and applied to the top of an LH20 column (40 g, 400 x 16 mm) and eluted with MeOH. The column had been previously calibrated by chromatography of a mixture of blue dextran (MW ~ 2 000 000, V_e ~ 20-30 mL), vitamin B12 (MW 1355, V_e ~ 50-80 mL) and fluorescein sodium (MW 370, V_e ~ 120-130 mL). Following passage through LH20 twice the polymer was isolated from low molecular weight contaminants (37.1 mg, 120%).

The polymer prepared above was reacted again with 1-amino-2-propanol (33.4 μL, 433 μmol) in stirred dry DMSO (200 μL) at 40°C for 16 hours before purification by LH20 chromatography (40 g, 400 x 16 mm). The low molecular weight, late eluting material was combined and chromatographed on silica (0.6 g, 60 x 5 mm) eluting with 20% MeOH/$CHCl_3$. The fractions containing ring-opened succinimide were combined and subjected to semi-preparative HPLC (C18, isocratic 2% ACN/H_2O(A)) to furnish the pure isomeric compounds **63** and **64**.

63: HRESIMS 175.1083, $C_7H_{15}N_2O_3$ ($M + H^+ - O$) requires 175.1082. ^1H NMR (D_2O) δ 3.80 (m, 1H, H9), δ 3.14 (dd, J_{HH} = 13.9, 4.5 Hz, 1H, H8a),δ 3.05 (dd, J_{HH} = 13.9, 7.0 Hz, 1H, H8b), δ 2.47 (t, J_{HH} = 7.1 Hz, 2H, H5), δ 2.35 (t, J_{HH} = 7.1 Hz, 2H, H4), δ 1.04 (d, J_{HH} = 6.4 Hz, 3H, H10), ^{13}C NMR (D_2O) δ 173.5 (C6), 172.3 (C3), 67.0 (C9), 46.9 (C8), 31.6 (C5), 28.8 (C4), 20.2 (C10). ^1H NMR (*d*6-DMSO) δ 10.39 (s, 1H, H2), δ 8.70 (br s, 1H, H1), δ 7.82 (t, J_{HH} = 5.5 Hz, 1H, H7), δ 4.65 (d, J_{HH} = 4.4 Hz, 1H, H11),

δ 3.62 (m, 1H, H9), δ 2.98 (m, 2H, H8), δ 2.33 (t, J_{HH} = 7.5 Hz, 2H, H5), δ 2.18 (t, J_{HH} = 7.5 Hz, 2H, H4), δ 1.01 (d, J_{HH} = 6.2 Hz, 3H, H10), ^{13}C NMR (*d*6-DMSO) δ 171.3 (C6), 168.6 (C3), 65.3 (C9), 46.5 (C8), 30.7 (C5), 28.0 (C4), 21.2 (C10).

64: HREIMS 191.1031, $C_7H_{15}N_2O_4$ ($M + H^+$) requires 191.1032. ^{1}H NMR (D_2O) δ 3.81 (m, 1H, H9), δ 3.16 (dd, J_{HH} = 13.9, 4.6 Hz, 1H, H8a),δ 3.07 (dd, J_{HH} = 13.9, 6.9 Hz, 1H, H8b), δ 2.46 (m, 4H, H4/H5), δ 1.06 (d, J_{HH} = 6.4 Hz, 3H, H10), ^{13}C NMR (D_2O) δ 178.6 (C3), 175.8 (C6), 67.0 (C9), 46.9 (C8), 31.7 (C4 or C5), 31.2 (C4 or C5), 20.1 (C10). ^{1}H NMR (*d*6-DMSO) δ 7.86 (t, J_{HH} = 5.6 Hz, 1H, H7), δ 7.37 (br s, 1H, H1), δ 6.82 (br s,1H, H2), δ 4.73 (br s, 1H, H11), δ 3.70 (m, 1H, H9), δ 3.06 (td, J_{HH} = 5.9, 2.0 Hz, 2H, H8), δ 2.38 (m, 4H, H4/H5), δ 1.09 (d, J_{HH} = 6.1 Hz, 3H, H10), ^{13}C NMR (*d*6-DMSO) δ 173.7 (C3), 171.7 (C6), 65.3 (C9), 46.5 (C8), 30.7 (C5, C4), 21.2 (C10).

1-Amino-2-propanol (38 μL, 492 μmol) was reacted with polymer precursor **61** (30 mg, 164 μmol) in stirred DMSO (300 μL) at 60°C with 50 μL samples being removed at 30 minute intervals. Each sample was passed once through LH20 (40 g, 400 x 16 mm) prior to examination by proton NMR spectroscopy.

1-Amino-2-propanol (38 μL, 492 μmol) was reacted with polymer precursor **61** (30 mg, 164 μmol) in stirred DMSO (300 μL) at 40°C. 50 μL samples were removed after 6, 8, 14, 24 and 48 hours of reaction. Each sample was passed once through LH20 (40 g, 400 x 16 mm) prior to examination by proton NMR spectroscopy.

7.5.3.1 Fmoc-Gly-Phe-Leu-Gly-L-Tyrosinamide (65)

L-Tyrosinamide (7 mg, 39 μmol), **40** (23.9 mg, 39 μmol), NHS (8.9 mg, 78 μmol) and DCC (15.2 mg, 74 μmol) were dissolved in dry THF (1 mL) and allowed to react overnight at 4°C after which HPLC (C18, A: H_2O(A), B: ACN, Gradient II) indicated the reaction was complete. The reaction solvent was removed under a stream of nitrogen and the crude reaction product was purified by preparative HPLC (Dynamax

C18 column) eluting isocratically with 90% MeOH/H_2O. The peak eluting at about 8.5 minutes was collected and dried down to furnish the desired conjugate **65** (13.6 mg, 45%). HRESIMS 777.3615, $C_{43}H_{49}N_6O_8$ ($M + H^+$) requires 777.3612. ^1H NMR (CD_3OD) δ 7.80 (d, J_{HH} = 7.5 Hz, 2H, H9''), δ 7.63 (t, J_{HH} = 8.3 Hz, 2H, H6''), δ 7.37 (t, J_{HH} = 7.5 Hz, 2H, H8''), δ 7.29 (m, 2H, H7''), δ 7.19 (o, 2H, H8), δ 7.19 (o, 2H, H9), δ 7.12 (o, 1H, H10), δ 7.05 (d, J_{HH} = 8.3 Hz, 2H, H5'), δ 6.68 (d, J_{HH} = 8.3 Hz, 2H, H6'), δ 4.59 (dd, J_{HH} = 5.9, 8.3 Hz, 1H, H5), δ 4.50 (dd, J_{HH} = 4.9, 9.0 Hz, 1H, H2'), δ 4.31 (dd, J_{HH} = 7.0, 10.3 Hz, 1H, H3''a), δ 4.25 (dd, J_{HH} = 7.0, 10.7 Hz, 1H, H3''b), δ 4.20 (o, 1H, H13), δ 4.19 (o, 1H, H4''), δ 3.81 (d, J_{HH} = 17.1 Hz, 1H, H20a), δ 3.74 (d, J_{HH} = 16.7 Hz, 1H, H2a), δ 3.69 (d, J_{HH} = 16.7 Hz, 1H, H2b), δ 3.62 (d, J_{HH} = 17.1 Hz, 1H, H20b), δ 3.14 (dd, J_{HH} = 5.5, 14.0 Hz, 1H, H6a), δ 3.07 (dd, J_{HH} = 5.1, 14.0 Hz, 1H, H3'a), δ 2.95 (dd, J_{HH} = 8.6, 14.0 Hz, 1H, H6b), δ 2.85 (dd, J_{HH} = 9.3, 14.0 Hz, 1H, H3'b), δ 1.60 (m, 2H, H14), δ 1.51 (m, 1H, H15), δ 0.86 (d, J_{HH} = 6.3 Hz, 3H, H16), δ 0.84 (d, J_{HH} = 6.3 Hz, 3H, H17), ^{13}C NMR (CD_3OD) δ 176.8 (C8'), 175.9 (C18), 174.4 (C11), 173.0 (C3), 171.9 (C21), 159.7 (C1''), 157.8 (C4'), 145.5 (C5''), 143.1 (C10''), 138.4 (C7), 131.3 (C5'), 130.3 (C8), 129.6 (C9), 129.6 (C7'), 128.9 (C8''), 128.1 (C7''), 127.9 (C10), 126.3 (C6''), 120.9 (C9''), 116.3 (C6'), 68.5 (C3''), 56.3 (C5), 56.2 (C2'), 54.1 (C13), 48.4 (C4''), 45.1 (C2), 43.7 (C20), 41.1 (C14), 38.2 (C6), 38.0 (C3'), 25.7 (C15), 23.7 (C16), 21.8 (C17).

7.5.3.2 H_2N-Gly-Phe-Leu-Gly-L-Tyrosinamide (66)

Piperidine (80 μL) was added to a solution of **65** (4.8 mg, 6.2 μmol) in MeOH (320 μL). The reaction was allowed to proceed for 20 minutes at room temperature after which it was dried down under a stream of nitrogen. The product was isolated by passage through a C_{18} cartridge, eluting with a stepped MeOH/H_2O gradient to afford **66** (1.9 mg, 55%). HRESIMS 555.2938, $C_{28}H_{39}N_6O_6$ ($M + H^+$) requires 555.2931.

7.5.3.3 Synthesis and purification of targeted polymer drug conjugate (67)

Compound **66** (1.9 mg, 3.5 μmol), **42** (1.9 mg, 3.5 μmol) and polymer precursor **61** (31.6 mg, 173 μmol of reactive sites) were dissolved together in dry DMSO (300μL) prior to addition of triethylamine (1.4 μL, 10.4 μmol). The reaction was stirred at 40°C for 16 hours. 1-amino-2-propanol (40 μL, 519 μmol) was added to the reaction and stirring was continued for a further 12 hours. The reaction solution was then applied to the top of an LH20 column (40 g, 400 x 16 mm) and eluted with MeOH. A second passage through LH20 afforded the polymer conjugate (**67**,16.1 mg, 57%).

7.5.4.1 Fmoc-Gly-Phe-Leu-Gly-Doxorubicin (68)

A solution of 1% cNH_4OH/H_2O (900 μL) was added to an aqueous solution of doxorubicin hydrochloride (3.5 mg, 5.8 μmol, 100 μL), causing an immediate colour change from deep red-orange to violet. The resulting solution was immediately passed down a C18 cartridge which was then rinsed with 1% cNH_4OH/H_2O (2 mL) and H_2O (2 mL) before eluting with acetone (10 mL). The organic fraction was dried down to afford desalted doxorubicin (**19**, 2.9 mg, 92%)

Doxorubicin (**19**, 2.9 mg, 5.2 μmol), **40** (3.5 mg, 5.7 μmol), NHS (1.2 mg, 10.4 μmol) and DCC (2.0 mg, 9.9 μmol) were dissolved in dry THF (1 mL) and allowed to react overnight at 4°C after which HPLC (C18, A: H_2O(A), B: ACN, Gradient II) indicated the reaction was complete. The reaction solvent was removed under a stream of nitrogen and the crude reaction product was purified by preparative HPLC (Dynamax C18 column) eluting isocratically with 90% $MeOH/H_2O$(A). The peak eluting at about 12.2 minutes was collected and dried down to furnish the desired conjugate **68** (3.1 mg, 52%). HRESIMS 1162.4281, $C_{61}H_{65}N_5O_{17}Na$ ($M + Na^+$) requires 1162.4273. ^1H NMR ($CDCl_3/CD_3OD$) δ 7.94 (d, J_{HH} = 7.8 Hz, 1H, H1'), δ 7.83 (m, 1H, H1), δ 7.69 (o, 1H, H12), δ 7.66 (o, 1H, H2'), δ 7.66 (o, 2H, H9'''), δ 7.52 (m, 2H, H6'''), δ 7.37 (o, 1H,

H4), δ 7.35 (o, 1H, H19), δ 7.32 (o, 1H, H3'), δ 7.30 (o, 2H, H8'''), δ 7.22 (t, J_{HH} = 7.3 Hz, 2H, H7'''), δ 7.15 (m, 2H, H9), δ 7.10 (o, 2H, H8), δ 7.09 (o, 1H, H10), δ 7.05 (o, 1H, 3''-NH), δ 5.42 (m, 1H, H1''), δ 5.16 (m, 1H, H7'), δ 4.69 (s, 2H, H14'), δ 4.47 (m, 1H, H5), δ 4.25 (m, 1H, H3'''a), δ 4.19 (m, 1H, H3'''b), δ 4.10 (o, 1H, H4'''), δ 4.08 (o, 1H, H5''), δ 4.05 (o, 1H, H13), δ 4.02 (o, 1H, H3''), δ 3.96 (s, 3H, H4'-OCH_3), δ 3.74 (o, 1H, H2), δ 3.72 (o, 1H, H20a), δ 3.64 (o, 1H, H2), δ 3.63 (o, 1H, H20b), δ 3.55 (m, 1H, H4''), δ 3.14 (m, 1H, H10'a), δ 2.99 (m, 2H, H6), δ 2.94 (m, 1H, H10'b), δ 2.26 (m, 1H, H8'a), δ 2.04 (m, 1H, H8'b), δ 1.82 (m, 1H, H2''a), δ 1.60 (m, 1H, H2''b), δ 1.49 (m, 2H, H14), δ 1.35 (m, 1H, H15), δ 1.22 (d, J_{HH} = 6.4 Hz, 3H, H5''-CH_3), δ 0.78 (o, 3H, H16), δ 0.77 (o, 3H, H17) ^{13}C NMR ($CDCl_3$/CD_3OD) δ 213.8 (C13'), 186.8 (C12'), 178.7 (C5'), 173.2 (C18), 172.7 (C11), 171.2 (C3), 169.2 (C21), 161.1 (C4'), 157.4 (C1'''), 143.5 (C5'''), 141.0 (C10'''), 135.8 (C7), 135.5 (C12a'), 134.5 (C6a'), 133.9 (C10a') 129.2 (C8), 128.9 (C9), 127.9 (C8'''), 127.3 (C10), 127.1 (C7'''), 125.1 (C6'''), 121.1 (C4a'), 121.0 (C2'), 120.1 (C9'''), 120.0 (C1'), 118.6 (C3'), 100.8 (C1''), 76.3 (C9'), 69.2 (C7'), 68.5 (C4''), 67.6 (C5''), 67.4 (C3'''), 65.3 (C14'), 56.7 (C4'-OCH_3), 54.7 (C5), 53.3 (C13), 47.0 (C4'''), 46.1 (C3''), 44.2 (C2), 43.0 (C20), 39.2 (C14), 37.1 (C6), 35.9 (C8'), 33.8 (C10'), 29.2 (C2''), 24.5 (C15), 22.7 (C16), 21.4 (C17), 16.8 (C5''-CH_3).

7.5.5.1 Fmoc-Gly-Phe-Leu-Gly-Mycalamide A (69)

Crude **45** (8.2 mg, 17 μmol), **40** (11.7 mg, 19 μmol), NHS (4.0 mg, 35 μmol) and DCC (6.8 mg, 33 μmol) were dissolved in dry THF (1 mL) and allowed to react overnight at 4°C after which HPLC (C18, A: H_2O, B: ACN, Gradient II) indicated the reaction was complete. The reaction solvent was removed under a stream of nitrogen and the crude reaction product was purified by preparative HPLC (Dynamax C18 column) eluting isocratically with 90% MeOH/H_2O at a flow rate of 10 mL/min. The peak eluting at about 10 minutes was collected and dried down to furnish the desired conjugate **69** (4.2 mg, 23% over two steps). HRESIMS 1091.5299, $C_{57}H_{76}N_6O_{14}Na$ ($M + Na^+$) requires 1091.5317. ^{1}H NMR ($CDCl_3$) δ 7.76 (d, J_{HH} = 7.4 Hz, 2H, H9''), δ 7.58 (d, J_{HH} = 6.6 Hz, 2H, H6''), δ 7.48 (o, 1H, NH9'), δ 7.47 (o, 1H, H12), δ 7.41 (t, J_{HH} = 7.4 Hz, 2H,

H8''), δ 7.32 (m, 2H, H7''), δ 7.24 (o, 2H, H8), δ 7.24 (o, 2H, H9), δ 7.22 (o, 1H, H10), δ 7.04 (t, J_{HH} = 5.5 Hz, 1H, 17'-NH), δ 6.87 (d, J_{HH} = 7.2 Hz, 1H, H4), δ 6.10 (m, 1H, H19), δ 5.77 (t, J_{HH} = 9.7 Hz, 1H, H10'), δ 5.65 (t, J_{HH} = 5.3 Hz, 1H, H1), δ 5.14 (d, J_{HH} = 6.9 Hz, 1H, H10'-OCH_2a), δ 4.87 (m, 1H, H4'=CH_2a), δ 4.83 (d, J_{HH} = 6.9 Hz, 1H, H10'-OCH_2b), δ 4.80 (o, 1H, H5), δ 4.77 (o, 1H, H4'=CH_2b), δ 4.54 (m, 1H, H13), δ 4.37 (o, 1H, H7'), δ 4.34 (o, 2H, H3''), δ 4.20 (o, 1H, H12'), δ 4.18 (o, 1H, H4''), δ 4.02 (m, 1H, H2'), δ 3.96 (m, 1H, H20a), δ 3.82 (o, 2H, H2), δ 3.80 (o, 1H, H11'), δ 3.55 (s, 3H, H13'-OCH_3), δ 3.48 (o, 1H, H20b), δ 3.47 (o, 1H, H13'), δ 3.38 (o, 1H, H17'a), δ 3.34 (o, 1H, H15'), δ 3.30 (s, 3H, H6'-OCH_3), δ 3.09 (d, J_{HH} = 7.1 Hz, 2H, H6), δ 2.79 (m, 1H, H17'b), δ 2.43 (d, J_{HH} = 14.2 Hz, 1H, H5'a), δ 2.26 (o, 1H, H3'), δ 2.23 (d, J_{HH} = 14.2 Hz, 1H, H5'b), δ 1.84 (o, 1H, H14a), δ 1.82 (o, 1H, H16'a), δ 1.43 (o, 1H, H15), δ 1.39 (o, 1H, H14b), δ 1.23 (o, 1H, H16'b), δ 1.21 (d, J_{HH} = 6.3 Hz, 3H, H2'-CH_3), δ 1.01 (d, J_{HH} = 6.8 Hz, 3H, H3'-CH_3), δ 0.93 (s, 3H, H14'-CH_3(eq)), δ 0.87 (d, J_{HH} = 6.4 Hz, 3H, H16), δ 0.84 (d, J_{HH} = 6.4 Hz, 3H, H17), δ 0.80 (s, 3H, H14'-CH_3(ax)) ^{13}C NMR ($CDCl_3$) δ 172.3 (C18), 172.1 (C8'), 170.9 (C11), 170.3 (C3), 169.1 (C21), 157.1 (C1''), 145.2 (C4'), 143.7 (C5''), 141.6 (C10''), 136.1 (C7), 129.7 (C9), 129.4 (C8), 128.0 (C8''), 127.7 (C10), 127.3 (C7''), 125.1 (C6''), 120.3 (C9''), 111.2 (C4'=CH_2), 100.1 (C6'), 86.4 (C10'-OCH_2), 79.2 (C13'), 75.9 (C15'), 74.8 (C12'), 73.8 (C10'), 71.8 (C7'), 71.5 (C11'), 70.2 (C2'), 67.9 (C3''), 62.0 (C13'-OCH_3), 55.0 (C5), 51.4 (C13), 48.5 (C6'-OCH_3), 46.9 (C4''), 44.9 (C2), 43.4 (C20), 41.5 (C3), 41.2 (C14'), 40.2 (C14), 37.7 (C6), 36.2 (C17'), 33.3 (C5'), 27.8 (C16'), 24.7 (C15), 23.3 (C16), 23.0 (C14'-CH_3(eq)), 21.5 (C17), 18.0 (C2'-CH_3), 13.3 (C14'-CH_3(ax)), 12.1 (C3'-CH_3).

7.5.5.2 H_2N-Gly-Phe-Leu-Gly-Mycalamide A (70)

Piperidine (160 μL) was added to a solution of **69** (4.2 mg, 3.9 μmol) in MeOH (640 μL). The reaction was allowed to proceed for 20 minutes at room temperature after which it was dried down under a stream of nitrogen. The product was isolated by

passage through a C_{18} cartridge, eluting with a stepped MeOH/H_2O gradient to afford **70** (3.3 mg, 100%). HRESIMS 847.4825, $C_{42}H_{66}N_6O_{12}$ ($M + H^+$) requires 847.4817.

7.5.5.3 Synthesis and purification of targeted polymer drug conjugate

Compounds **70** (3.3 mg, 3.9 μmol) and **42** (2.1 mg, 3.9 μmol) and polymer precursor **61** (35.7 mg, 195 μmol of reactive sites) were dissolved together in dry DMSO (300μL) prior to addition of triethylamine (1.6 μL, 11.7 μmol). The reaction was stirred at 40°C for 16 hours. 1-amino-2-propanol (45.2 μL, 585 μmol) was added to the reaction and stirring was continued for a further 12 hours. The reaction solution was then applied to the top of an LH20 column (40 g, 400 x 16 mm) and eluted with MeOH. A second passage through LH20 afforded the pure polymer conjugate (17.6 mg, 53%).

7.5.6.1 Fmoc-Gly-Phe-Leu-Gly-Mycalamide B (71)

Crude **50** (1.4 mg, 2.6 μmol), **40** (1.8 mg, 2.9 μmol), NHS (0.6 mg, 5.2 μmol) and DCC (1.0 mg, 4.9 μmol) were dissolved in dry THF (300 μL) and allowed to react overnight at 4°C. The reaction solvent was removed under a stream of nitrogen and the crude reaction product was purified by preparative HPLC (Dynamax C18 column) eluting isocratically with 80% ACN/H_2O at a flow rate of 10 mL/min. The peak eluting at about 6 minutes was collected and dried down to furnish the desired conjugate **71** (2.3 mg, 79% over two steps). HRESIMS 1135.5576, $C_{59}H_{80}N_6O_{15}Na$ ($M + Na^+$) requires 1135.5579. ^1H NMR ($CDCl_3$) δ 7.78 (d, J_{HH} = 7.6 Hz, 2H, H9''), δ 7.63 (d, J_{HH} = 9.3 Hz, 1H, NH9'), δ 7.58 (m, 2H, H6''), δ 7.42 (t, J_{HH} = 7.6 Hz, 2H, H8''), δ 7.32 (m, 2H, H7''), δ 7.23 (o, 2H, H9), δ 7.20 (o, 2H, H8) , δ 7.19 (o, 1H, H10), δ 6.99 (br d, 1H, H12), δ 6.85 (o, 1H, H4), δ 6.85 (o, 1H, H19), δ 6.73 (br t, 1H, H18'-NH), δ 5.93 (br t, 1H, H1), δ 5.79 (t, J_{HH} = 9.6 Hz, 1H, H10'), δ 5.15 (d, J_{HH} = 6.8 Hz, 1H, H10'-OCH_2a), δ 4.85 (s, 1H, H4'=CH_2a), δ 4.80 (d, J_{HH} = 6.8 Hz, 1H, H10'-OCH_2b), δ 4.71 (s, 1H, H4'=CH_2b), δ 4.59 (q, J_{HH} = 6.7 Hz, 1H, H5), δ 4.40 (br m, 1H, H13), δ 4.37 (dd, J_{HH} =

7.0, 10.2 Hz, 1H, H3"a), δ 4.28 (o, 1H, H7'), δ 4.27 (o, 1H, H3"b), δ 4.18 (o, 1H, H12'), δ 4.18 (o, 1H, H4"), δ 4.01 (dq, J_{HH} = 6.6, 2.5 Hz, 1H, H2'), δ 3.93 (dd, J_{HH} = 6.0, 16.0 Hz, 1H, H20a), δ 3.87 (dd, J_{HH} = 9.7, 7.0 Hz, 1H, H11'), δ 3.79 (d, J_{HH} = 5.2 Hz, 2H, H2), δ 3.74 (dd, J_{HH} = 5.4, 17.2 Hz, 1H, H20b), δ 3.53 (s, 3H, H13'-OCH_3), δ 3.50 (m, 1H, H13'), δ 3.42 (d, J_{HH} = 9.7 Hz, 1H, H15'), δ 3.31 (m, 2H, H18'), δ 3.28 (s, 3H, H6'-OCH_3), δ 3.22 (m, 1H, H17'), δ 3.17 (s, 3H, H17'-OCH_3), δ 3.12 (t, J_{HH} = 6.6 Hz, 2H, H6), δ 2.37 (d, J_{HH} = 14.3 Hz, 1H, H5'a), δ 2.25 (o, 1H, H3'), δ 2.25 (o, 1H, H5'b), δ 1.74 (o, 1H, H14a), δ 1.54 (m, 1H, H16'a), δ 1.48 (m, 1H, H16'b), δ 1.44 (m, 1H, H14b), δ 1.40 (m, 1H, H15), δ 1.20 (d, J_{HH} = 6.4 Hz, 3H, H2'-CH_3), δ 1.01 (d, J_{HH} = 6.8 Hz, 3H, H3'-CH_3), δ 0.92 (s, 3H, H14'-CH_3(eq)), δ 0.87 (d, J_{HH} = 6.6 Hz, 3H, H16), δ 0.84 (d, J_{HH} = 6.6 Hz, 3H, H17), δ 0.82 (s, 3H, H14'-CH_3(ax)) ^{13}C NMR ($CDCl_3$) δ 172.3 (C8'), 171.3 (C11), 170.6 (C3), 157.4 (C1"), 145.4 (C4'), 143.7 (C5"), 141.4 (C10"), 136.0 (C7), 129.4 (C8), 129.1 (C9), 128.2 (C8"), 127.6 (C10), 127.3 (C7"), 125.3 (C6"), 120.3 (C9"), 111.2 (C4'=CH_2), 100.2 (C6'), 86.5 (C10'-OCH_2), 79.1 (C13'), 76.7 (C17'), 75.3 (C15'), 74.5 (C12'), 74.1 (C10'), 71.8 (C7'), 71.1 (C11'), 69.8 (C2'), 67.7 (C3"), 62.0 (C13'-OCH_3), 56.5 (C17'-OCH_3), 55.6 (C5), 52.1 (C13), 48.6 (C6'-OCH_3), 47.0 (C4"), 45.0 (C2), 43.5 (C20), 41.7 (C18'), 41.5 (C14'), 41.4 (C3'), 39.8 (C14), 37.3 (C6), 33.6 (C5'), 30.9 (C16'), 24.7 (C15), 23.3 (C17), 23.0 (C14'-CH_3(eq)), 21.4 (C16), 18.0 (C2'-CH_3), 13.3 (C14'-CH_3(ax)), 12.3 (C3'-CH_3).

7.5.6.2 H_2N-Gly-Phe-Leu-Gly-Mycalamide B (72)

Piperidine (160 μL) was added to a solution of **71** (2.3 mg, 2.0 μmol) in MeOH (640 μL). The reaction was allowed to proceed for 20 minutes at room temperature after which it was dried down under a stream of nitrogen. The product was isolated by passage through a C_{18} cartridge, eluting with a stepped MeOH/H_2O gradient to afford **72** (1.6 mg, 96%). HRESIMS 891.5119, $C_{44}H_{70}N_6O_{13}$ ($M + H^+$) requires 891.5079.

7.5.6.3 Synthesis and purification of targeted polymer drug conjugate

Compounds **72** (1.6 mg, 1.8 μmol) and **42** (1.0 mg, 1.8 μmol) and polymer precursor **61** (16.4 mg, 89.8 μmol of reactive sites) were dissolved together in dry DMSO (300μL) prior to addition of triethylamine (0.75 μL, 5.4 μmol). The reaction was stirred at 40°C for 16 hours. 1-amino-2-propanol (21.4 μL, 270 μmol) was added to the reaction and stirring was continued for a further 12 hours. The reaction solution was then applied to the top of an LH20 column (40 g, 400 x 16 mm) and eluted with MeOH. A second passage through LH20 afforded the pure polymer conjugate (10.1 mg, 66%).

7.5.7.1 Fmoc-Gly-Phe-Leu-Gly-*R*-Fumagillol (73)

Crude **52** (7.0 mg, 25 μmol), **40** (16.9 mg, 27.5 μmol), NHS (5.8 mg, 50 μmol) and DCC (9.8 mg, 48 μmol) were dissolved in dry THF (1 mL) and allowed to react overnight at 4°C. The reaction solvent was removed under a stream of nitrogen and the crude reaction product was purified by repeated analytical HPLC injections (C18, A: H_2O, B: ACN, gradient: 68% B (0 min), 68% B (2 min), 71% B (14 min)). The peak eluting at 11.8 minutes was collected and dried down to furnish the desired conjugate **73** (2.8 mg, 13% over two steps). HRESIMS 878.4709, $C_{50}H_{64}N_5O_9$ ($M + H^+$) requires 878.4704. ^1H NMR ($CDCl_3$) δ 7.77 (d, J_{HH} = 7.3 Hz, 2H, H9'''), δ 7.56 (d, J_{HH} = 7.1 Hz, 2H, H6'''), δ 7.40 (t, J_{HH} = 7.4 Hz, 2H, H8'''), δ 7.39 (m, 1H, H4), δ 7.30 (t, J_{HH} = 7.4 Hz, 2H, H7'''), δ 7.25 (o, 1H, H19), δ 7.25 (o, 2H, H8), δ 7.18 (o, 1H, H10), δ 7.17 (o, 2H, H9), δ 6.66 (o, 1H, H12), δ 6.65 (o, 1H, H6'-NH), δ 6.05 (br s, 1H, H1), δ 5.15 (t, J_{HH} = 7.4 Hz, 1H, H4''), δ 4.84 (m, 1H, H6'), δ 4.39 (o, 1H, H5), δ 4.36 (o, 1H, H3'''a), δ 4.25 (o, 1H, H20a), δ 4.21 (o, 1H, H3'''b), δ 4.17 (o, 1H, H13), δ 4.13 (o, 1H, H4'''), δ 3.88 (dd, J_{HH} = 4.9, 17.0 Hz, 1H, H2a), δ 3.68 (dd, J_{HH} = 4.4, 10.7 Hz, 1H, H5'), δ 3.65 (o, 1H, H2b), δ 3.51 (dd, J_{HH} = 4.4, 17.1 Hz, 1H, H20b), δ 3.29 (s, 3H, H8'), δ 3.25 (o, 1H, H6a), δ 3.14 (dd, J_{HH} = 6.8, 14.0 Hz, 1H, H6b), δ 2.92 (d, J_{HH} = 3.9

Hz, 1H, H7'a), δ 2.78 (t, J_{HH} = 6.1 Hz, 1H, H2''), δ 2.55 (d, J_{HH} = 3.9 Hz, 1H, H7'b), δ 2.36 (d, J_{HH} = 11.2 Hz, 1H, H4'), δ 2.25 (o, 1H, H3''a), δ 2.20 (o, 1H, H3''b), δ 2.01 (m, 1H, H2'a), δ 1.88 (m, 1H, H1'a), δ 1.80 (m, 1H, H1'b), δ 1.65 (s, 3H, H6''), δ 1.61 (o, 1H, H14a), δ 1.58 (s, 3H, H7''), δ 1.49 (m, 1H, H14b), δ 1.31 (m, 1H, H15), δ 1.17 (s, 3H, H8''), δ 1.08 (m, 1H, H2'b), δ 0.83 (d, J_{HH} = 6.2 Hz, 3H, H16), δ 0.82 (d, J_{HH} = 6.0 Hz, 3H, H17), ^{13}C NMR ($CDCl_3$) δ 172.5 (C18), 172.2 (C11), 171.9 (C3), 169.7 (C21), 157.2 (C1'''), 143.9 (C5'''), 141.6 (C10'''), 135.9 (C7), 135.6 (C5''), 129.2 (C8), 129.1 (C9), 128.0 (C8'''), 127.6 (C10), 127.3 (C7'''), 125.1 (C6'''), 120.3 (C9'''), 118.6 (C4''), 79.0 (C5'), 67.3 (C3'''), 61.7 (C2''), 60.3 (C1''), 60.2 (C3'), 56.4 (C8'), 55.8 (C5), 53.9 (C13), 51.7 (C7'), 47.1 (C4'''), 45.0 (C2), 44.5 (C6'), 43.3 (C20), 39.8 (C14), 36.2 (C6), 29.4 (C2'), 27.4 (C3''), 26.4 (C1'), 25.8 (C6''), 24.7 (C15), 23.3 (C16), 21.2 (C17), 18.0 (C7''), 13.9 (C8'').

7.5.7.2 H_2N-Gly-Phe-Leu-Gly-*R*-Fumagillol (74)

Piperidine (160 μL) was added to a solution of **73** (2.8 mg, 3.2 μmol) in MeOH (640 μL). The reaction was allowed to proceed for 20 minutes at room temperature after which it was dried down under a stream of nitrogen. The product was isolated by passage through a C_{18} cartridge, eluting with a stepped MeOH/H_2O gradient to afford **74** (1.7 mg, 81%). HRESIMS 656.4004, $C_{35}H_{53}N_5O_7$ ($M + H^+$) requires 656.4023.

7.5.7.3 Synthesis and purification of targeted polymer drug conjugate

Compounds **74** (1.7 mg, 2.6 μmol) and **42** (1.4 mg, 2.6 μmol) and polymer precursor **61** (23.7 mg, 130 μmol of reactive sites) were dissolved together in dry DMSO (300μL) prior to addition of triethylamine (1.1 μL, 7.3 μmol). The reaction was stirred at 40°C for 16 hours. 1-amino-2-propanol (31.2 μL, 390 μmol) was added to the reaction and

stirring was continued for a further 12 hours. The reaction solution was then applied to the top of an LH20 column (40 g, 400 x 16 mm) and eluted with MeOH. A second passage through LH20 afforded the pure polymer conjugate (11.5 mg, 53%).

7.5.8.1 Fmoc-Gly-Phe-Leu-Gly-*S*-Fumagillol (75)

Compounds **58** (2.9 mg, 10 μmol) and **40** (7.0 mg, 11 μmol), NHS (2.4 mg, 21 μmol) and DCC (4.0 mg, 20 μmol) were dissolved in dry THF (500 μL) and allowed to react overnight at 4°C. The reaction solvent was removed under a stream of nitrogen and the crude reaction product was purified by preparative HPLC (Dynamax C18 column) eluting isocratically with 69% ACN/H_2O at a flow rate of 10 mL/min. The peak eluting at about 10 minutes was collected and dried down to furnish the desired conjugate **75** (4.9 mg, 56%). HRESIMS 878.4709, $C_{50}H_{64}N_5O_9$ ($M + H^+$) requires 878.4704. ^{1}H NMR (d_6-DMSO) δ 8.25 (d, J_{HH} = 7.4 Hz, 1H, H12), δ 8.19 (t, J_{HH} = 5.9 Hz, 1H, H19), δ 8.09 (d, J_{HH} = 7.9 Hz, 1H, H4), δ 7.99 (d, J_{HH} = 7.6 Hz, 2H, H9'''), δ 7.92 (d, J_{HH} = 9.2 Hz, 1H, H6'-NH), δ 7.80 (d, J_{HH} = 7.6 Hz, 2H, H6'''), δ 7.63 (t, J_{HH} = 5.9 Hz, 1H, H1), δ 7.51 (t, J_{HH} = 7.6 Hz, 2H, H8'''), δ 7.42 (t, J_{HH} = 7.6 Hz, 2H, H7'''), δ 7.32 (o, 2H, H8), δ 7.32 (o, 2H, H9), δ 7.26 (m, 1H, H10), δ 5.29 (t, J_{HH} = 7.4 Hz, 1H, H4''), δ 4.65 (m, 1H, H5), δ 4.35 (o, 1H, H13), δ 4.34 (o, 2H, H3'''), δ 4.30 (o, 1H, H4'''), δ 4.06 (dt, J_{HH} = 4.1, 10.4 Hz, 1H, H6'), δ 3.79 (o, 1H, H5'), δ 3.76 (o, 2H, H20), δ 3.71 (o, 1H, H2a), δ 3.61 (dd, J_{HH} = 5.5, 16.5 Hz, 1H, H2b), δ 3.31 (s, 3H, H8'), δ 3.15 (dd, J_{HH} = 4.4, 14.1 Hz, 1H, H6a), δ 2.92 (d, J_{HH} = 4.4 Hz, 1H, H7'a), δ 2.89 (dd, J_{HH} = 9.3, 13.9 Hz, 1H, H6b), δ 2.68 (d, J_{HH} = 4.4 Hz, 1H, H7'b), δ 2.63 (t, J_{HH} = 6.4 Hz, 1H, H2''), δ 2.27 (t, J_{HH} = 6.8 Hz, 2H, H3''), δ 1.99 (dt, J_{HH} = 4.5, 13.7 Hz, 1H, H2'a), δ 1.88 (d, J_{HH} = 11.5 Hz, 1H, H4'), δ 1.80 (s, 3H, H6''), δ 1.79 (o, 1H, H1'a), δ 1.70 (s, 3H, H7''), δ 1.69 (m, 1H, H15), δ 1.59 (t, J_{HH} = 7.3 Hz, 2H, H14), δ 1.54 (m, 1H, H1'b), δ 1.20 (s, 3H, H8''), δ 1.09 (m, 1H, H2'b), δ 0.97 (d, J_{HH} = 6.5 Hz, 3H, H17), δ 0.93 (d, J_{HH} = 6.5 Hz, 3H, H16), ^{13}C NMR (d_6-DMSO) δ 172.8 (C18), 171.7 (C11), 169.8 (C3), 168.7 (C21), 157.1 (C1'''), 144.4 (C5'''), 141.4 (C10'''), 138.3 (C7), 134.4 (C5''), 129.8 (C8), 128.8 (C9), 128.3 (C8'''), 127.7 (C7'''), 126.8 (C10), 125.9 (C6'''), 120.7 (C9'''), 120.0

(C4''), 78.8 (C5'), 66.4 (C3'''), 60.6 (C2''), 60.5 (C3'), 58.8 (C1''), 54.2 (C5), 53.6 (C8'), 52.0 (C13), 51.1 (C7'), 49.8 (C6'), 49.5 (C4'), 47.1 (C4'''), 43.9 (C2), 42.7 (C20), 41.1 (C14), 37.9 (C6), 32.6 (C2'), 28.8 (C1'), 27.4 (C3''), 26.1 (C6''), 24.7 (C15), 23.5 (C16), 22.3 (C17), 18.3 (C7''), 14.4 (C8'').

7.5.8.2 H_2N-Gly-Phe-Leu-Gly-*S*-Fumagillol (76)

Piperidine (160 μL) was added to a solution of **75** (4.9 mg, 5.6 μmol) in MeOH (640 μL). The reaction was allowed to proceed for 20 minutes at room temperature after which it was dried down under a stream of nitrogen. The product was isolated by passage through a C_{18} cartridge, eluting with a stepped MeOH/H_2O gradient to afford **76** (0.9 mg, 25%). HRESIMS 656.4036, $C_{35}H_{53}N_5O_7$ ($M + H^+$) requires 656.4023.

7.5.8.3 Synthesis and purification of targeted polymer drug conjugate

Compounds **76** (0.9 mg, 1.4 μmol) and **42** (0.75 mg, 1.4 μmol) and polymer precursor **61** (12.6 mg, 68.7 μmol of reactive sites) were dissolved together in dry DMSO (300μL) prior to addition of triethylamine (0.6 μL, 4.1 μmol). The reaction was stirred at 40°C for 16 hours. 1-amino-2-propanol (14.2 μL, 210 μmol) was added to the reaction and stirring was continued for a further 12 hours. The reaction solution was then applied to the top of an LH20 column (40 g, 400 x 16 mm) and eluted with MeOH. A second passage through LH20 afforded the pure polymer conjugate (8.0 mg, 70%).

References

(1) Stewart, B. W.; Kleihues, P. World Cancer Report; IARC*Press*: Lyon, 2003.

(2) Sikora, K. Developing a global strategy for cancer. *European Journal of Cancer* **1999**, *35*, 1870-1877.

(3) Hodgen, E.; Tobias, M.; Cheung, J. Cancer in New Zealand: Trends and Projections; Public Health Intelligence, Ministry of Health: Wellington, 2002.

(4) Alberts, B.; Johnson, A.; Lewis, J.; Raff, M.; Roberts, K.; Walter, P. Cancer. *Molecular Biology of the Cell*; 4th ed.; Garland Science: New York, 2002; pp 1313-1362.

(5) Karp, G. *Cell and molecular biology: concepts and experiments*; 3rd ed.; John Wiley & Sons, Inc.: New York, 2002.

(6) Ruoslahti, E. How Cancer Spreads. *Scientific American* **1996**, *275*, 42-47.

(7) Weinberg, R. A. How Cancer Arises. *Scientific American* **1996**, *275*, 32-40.

(8) Evan, G. I.; Vousden, K. H. Proliferation, cell cycle and apoptosis in cancer. *Nature* **2001**, *411*, 342-348.

(9) Hellman, S.; Vokes, E. E. Advancing Current Treatments for Cancer. *Scientific American* **1996**, *275*, 84-89.

(10) Sikora, K.; Advani, S.; Koroltchouk, V.; Magrath, I.; Levy, L.; Pinedo, H.; Schwartsmann, G.; Tattersall, M.; Yan, S. Essential drugs for cancer therapy: A World Health Organization consultation. *Annals of Oncology* **1999**, *10*, 385-390.

(11) Gupta, S. P. Quantitative Structure-Activity Relationship Studies on Anticancer Drugs. *Chemical Reviews* **1994**, *94*, 1507-1551.

(12) Longley, D. B.; Harkin, D. P.; Johnston, P. G. 5-Fluorouracil: Mechanisms of action and clinical strategies. *Nature Reviews* **2003**, *3*, 330-338.

(13) Elgemeie, G. H. Thioguanine, Mercaptopurine: Their Analogs and Nucleosides as Antimetabolites. *Current Pharmaceutical Design* **2003**, *9*, 2627-2642.

(14) Galmarini, C. M.; Jordheim, L.; Dumontet, C. Pyrimidine nucleoside analogs in cancer treatment. *Expert Reviews of Anticancer Therapy* **2003**, *3*, 717-728.

(15) Genestier, L.; Paillot, R.; Quemeneur, L.; Izeradjene, K.; Revillard, J.-P. Mechanisms of action of methotrexate. *Immunopharmacology* **2000**, *47*, 247-257.

(16) Nieto, Y.; Jones, R. B. DNA-binding agents. *Cancer Chemotherapy and Biological Response Modifiers*, 2002.

(17) Connors, T. A. Alkylating Agents. *Topics in Current Chemistry* **1974**, *52*, 141-171.

(18) McLean, A.; Newell, D.; Baker, G.; Connors, T. The Metabolism of Chlorambucil. *Biochemical Pharmacology* **1980**, *29*, 2039-2047.

(19) Brock, N. The History of the Oxazaphosphorine Cytostatics. *Cancer* **1996**, *78*, 542-547.

(20) Jordan, P.; Carmo-Fonseca, M. Molecular mechanisms involved in cisplatin cytotoxicity. *Cellular and Molecular Life Sciences* **2000**, *57*, 1229-1235.

(21) Reedijk, J. New clues for platinum antitumor chemistry: Kinetically controlled metal binding to DNA. *Proceedings of the National Academy of Sciences of the United States of America* **2003**, *100*, 3611-3616.

(22) Reed, D. J. Procarbazine. *Handbook of Experimental Pharmacology*; Springer Verlag: New York, 1975; pp 747-765.

(23) Tweedie, D. J.; Erikson, J. M.; Prough, R. A. Metabolism of Hydrazine Anti-cancer Agents. *Pharmacology and Therapeutics* **1987**, *34*, 111-127.

(24) Erikson, J. M.; Tweedie, D. J.; Ducore, J. M.; Prough, R. A. Cytotoxicity and DNA Damage Caused by the Azoxy Metabolites of Procarbazine in L1210 Tumor Cells. *Cancer Research* **1989**, *49*, 127-133.

(25) Roca, J. The mechanisms of DNA topoisomerases. *Trends in Biological Sciences* **1995**, *20*, 156-160.

(26) Watson, J. D.; Hopkins, N. H.; Roberts, J., W.; Steitz, J. A.; Weiner, A. M. The Structures of DNA. *Molecular Biology of the Cell*; 4th ed.; The Benjamin/Cummings Publishing Company, Inc.: Menlo Park, California, 1987; pp 240-281.

(27) Liu, L. F. DNA topoisomerase poisons as antitumor drugs. *Annual Review of Biochemistry* **1989**, *58*, 351-375.

(28) Gewirtz, D. A. A Critical Evaluation of the Mechanisms of Action Proposed for the Antitumor Effects of the Anthracycline Antibiotics Adriamycin and Daunorubicin. *Biochemical Pharmacology* **1999**, *57*, 727-741.

(29) Schimmel, K. J. M.; Richel, D. J.; van den Brink, R. B. A.; Guchelaar, H.-J. Cardiotoxicity of cytotoxic drugs. *Cancer Treatment Reviews* **2004**, *30*, 181-191.

(30) Gordaliza, M.; Castro, M. A.; Miguel del Corral, J. M.; San Feliciano, A. Antitumor Properties of Podophyllotoxin and Related Compounds. *Current Pharmaceutical Design* **2000**, *6*, 1811-1839.

(31) Hande, K. R. Clinical applications of anticancer drugs targeted to topoisomerase II. *Biochimica et Biophysica Acta* **1998**, *1400*, 173-184.

(32) Jordan, A.; Hadfield, J. A.; Lawrence, N. J.; McGown, A. T. Tubulin as a Target for Anticancer Drugs: Agents Which Interact with the Mitotic Spindle. *Medical Research Reviews* **1998**, *18*, 259-296.

(33) Hecht, S. M. Bleomycin: New Perspectives on the Mechanism of Action. *Journal of Natural Products* **2000**, *63*, 158-168.

(34) Goldberg, I. H. Actinomycin D. *Handbuch der Experimentellen Pharmakologie*; Springer Verlag: New York, 1975; pp 582-592.

(35) Nelson, R. P., Jr; Ballow, M. 26. Immunomodulation and immunotherapy: Drugs, cytokines, cytokine receptors and antibodies. *Journal of Allergy and Clinical Immunology* **2003**, *111*, S720-732.

(36) Bentrem, D. J.; Jordan, V. C. Antiestrogens: the Past and the Future. *Zentralblatt fur Gynakologie* **2002**, *124*, 551-558.

(37) Clemons, M.; Danson, S.; Howell, A. Tamoxifen ('Nolvadex'): a review. *Cancer Treatment Reviews* **2002**, *28*, 165-180.

(38) Wang, T.-H.; Wang, H.-S. p53, Apoptosis and Human Cancers. *Journal of the Formosan Medical Association* **1996**, *95*, 509-522.

(39) Osanto, S. Gene Therapy of Cancer. *Drug Delivery Systems in Cancer Therapy*; Humana Press Inc.: Totawa, N.J., 2004.

(40) McNeish, I. A.; Bell, S. J.; Lemoine, N. R. Gene Therapy Progress and Prospects: cancer gene therapy using tumour suppressor genes. *Gene Therapy* **2004**, *11*, 497-503.

(41) Pearson, G. R. In Vitro and in Vivo Investigations on Antibody-Dependent Cellular Cytotoxicity. *Current Topics in Microbiology and Immunology* **1978**, *80*, 65-96.

(42) Old, L. J. Immunotherapy for Cancer. *Scientific American* **1996**, *275*, 102-109.

(43) King, H. D.; Yurgaitis, D.; Willner, D.; Firestone, R. A.; Yang, M. B.; Lasch, S. J.; Hellstroem, K. E.; Trail, P. A. Monoclonal Antibody Conjugates of Doxorubicin Prepared with Branched Linkers: A Novel Method for Increasing the Potency of Doxorubicin Immunoconjugates. *Bioconjugate Chemistry* **1999**, *10*, 279-288.

(44) Maison, W.; Farangioni, J. V. Improved Chemical Strategies for the Targeted Therapy of Cancer. *Angewandte Chemie, International Edition in English* **2003**, *42*, 4726-4728.

(45) Garnett, M. C. Targeted drug conjugates: principles and progress. *Advanced Drug Delivery Reviews* **2001**, *53*, 171-216.

(46) Coley, W. B. The treatment of malignant tumors by repeated inoculations of erysipelas. With a report of 10 original cases. 1893. *Clinical Orthopaedics and Related Research* **1991**, *262*, 3-11.

(47) Risau, W. Mechanisms of angiogenesis. *Nature (London)* **1997**, *386*, 671-674.

(48) Hanahan, D.; Folkman, J. Patterns and emerging mechanisms of the angiogenic switch during tumorigenesis. *Cell (Cambridge, Mass.)* **1996**, *86*, 353-364.

(49) Folkman, J. Tumor angiogenesis: therapeutic implications. *The New England Journal of Medicine* **1971**, *285*, 1182-1186.

(50) Weidner, N. Tumor vascularity: what does it tell us about the growth and spread of cancer? *Basic and Clinical Oncology* **2001**, *24*, 465-486.

(51) Cristofanilli, M.; Charnsangavej, C.; Hortobagyi, G. N. Angiogenesis modulation in cancer research: novel clinical approaches. *Nature Reviews Drug Discovery* **2002**, *1*, 415-426.

(52) Zogakis, T. G.; Libutti, S. K. General aspects of anti-angiogenesis and cancer therapy. *Expert Opinion on Biological Therapy* **2001**, *1*, 253-275.

(53) Shimizu, K.; Oku, N. Cancer Anti-angiogenic Therapy. *Biological and Pharmaceutical Bulletin* **2004**, *27*, 599-605.

(54) Scappaticci, F. A. Mechanisms and Future Directions for Angiogenesis-Based Cancer Therapies. *Journal of Clinical Oncology* **2002**, *20*, 3906-3927.

(55) Brahimi Horn, C.; Berra, E.; Pouyssegur, J. Hypoxia: the tumor's gateway to progression along the angiogenic pathway. *Trends in Cell Biology* **2001**, *11*, S32-S36.

(56) Teo, N. B.; Shoker, B. S.; Martin, L.; Sloane, J. P.; Holcombe, C. Angiogenesis in pre-invasive cancers. *Anticancer Research* **2002**, *22*, 2061-2072.

(57) Griffioen, A. W.; Barendsz-Janson, A. F.; Mayo, K. H.; Hillen, H. F. P. Angiogenesis, a target for tumor therapy. *Jounal of Laboratory and Clinical Medicine* **1998**, *132*, 363-368.

(58) Eichhorn, M. E.; Strieth, S.; Dellian, M. Anti-vascular tumor therapy: recent advances, pitfalls and clinical perspectives. *Drug Resistance Updates* **2004**, *7*, 125-138.

(59) Bocci, G.; Nicolaou, K. C.; Kerbel, R. S. Protracted low-dose effects on human endothelial cell proliferation and survival in vitro reveal a selective antiangiogenic window for various chemotherapeutic drugs. *Cancer Research* **2002**, *62*, 6938-6943.

(60) Folkman, J.; Browder, T.; Palmblad, J. Angiogenesis research: guidelines for translation to clinical application. *Thrombosis and Haemostasis* **2001**, *86*, 23-33.

(61) Kerbel, R. S.; Kamen, B. A. The Anti-angiogenic Basis of Metronomic Chemotherapy. *Nature Reviews Cancer* **2004**, *4*, 423-436.

(62) Masiero, L.; Figg, W. D.; Kohn, E. C. New anti-angiogenesis agents: review of the clinical experience with carboxyamido-triazole (CAI), thalidomide, TNP-470, and interleukin-12. *Angiogenesis* **1997**, *1*, 23-35.

(63) Li, W. W.; Li, V. W.; Brainerd, N.; Fagen, S. J. Global development of angiogenesis inhibitors for cancer: principles, progress and new paradigms. *Gan to Kagaku Ryoho* **2002**, *29*, 50-58.

(64) Arap, W.; Pasqualini, R.; Ruoslllahti, E. Cancer treatment by targeted drug delivery to tumor vasculature in a mouse model. *Science (Washington, D. C.)* **1998**, *279*, 377-380.

(65) Koivunen, E.; Arap, W.; Rajotte, D.; Lahdenranta, J.; Pasqualini, R. Identification of receptor ligands with phage display peptide libraries. *Journal of Nuclear Medicine* **1999**, *40*, 883-888.

(66) Pasqualini, R.; Ruoslahti, E. Organ targeting in vivo using phage display peptide libraries. *Nature (London)* **1996**, *380*, 364-366.

(67) Koivunen, E.; Wang, B.; Ruoslahti, E. Phage libraries displaying cyclic peptides with different ring sizes: ligand specificities of the RGD-directed integrins. *Bio/Technology* **1995**, *13*, 265-270.

(68) Healy, J. M.; Murayama, O.; Maeda, T.; Yoshino, K.; Sekiguchi, K.; Kikuchi, M. Peptide Ligands for Integrin $\alpha_v\beta_3$ Selected from Random Phage Display Libraries. *Biochemistry* **1995**, *34*, 3948-3955.

(69) Assa-Munt, N.; Jia, X.; Laakkonen, P.; Ruoslahti, E. Solution Structures and Integrin Binding Activities of an RGD Peptide with Two Isomers. *Biochemistry* **2001**, *40*, 2373-2378.

(70) Koivunen, E.; Wang, B.; Ruoslahti, E. Isolation of a highly specific ligand for the $\alpha_5\beta_1$ integrin from a phage display library. *Journal of Cell Biology* **1994**, *124*, 373-380.

(71) Pasqualini, R.; Koivunen, E.; Kain, R.; Lahdenranta, J.; Sakamoto, M; Stryhn, A.; Ashmun, R. A.; Shapiro, L. H.; Arap, W.; Ruoslahti, E. Aminopeptidase N is a receptor for tumor-homing peptides and a target for inhibiting angiogenesis. *Cancer Research* **2000**, *60*, 722-727.

(72) Olsen, J.; Kehlen, A. Molecular biology of aminopeptidase N - structural predictions and tissue-specific transcriptional regulation. *International Congress Series* **2001**, *1218*, 317-327.

(73) Noren, O.; Sjostrom, H.; Olsen, J. Aminopeptidase N. *Cell Surface Peptidases*, 1997; pp 175-191.

(74) Olsen, J.; Kokholm, K.; Noren, O.; Sjostrom, H. Structure and expression of aminopeptidase N. *Advances in Experimental Medicine and Biology*, 1997; pp 47-57.

(75) van Hensbergen, Y.; Broxterman, H. J.; Elderkamp, Y. W.; Lankelma, J.; Beers, J. C. C.; Heijn, M.; Boven, E.; Hoekman, K.; Pinedo, H. M. A. A doxorubicin-CNGRC-peptide conjugate with prodrug properties. *Biochemical Pharmacology* **2002**, *63*, 897-908.

(76) Curnis, F.; Sacchi, A.; Corti, A. Improving chemotherapeutic drug penetration in tumors by vascular targeting and barrier alteration. *Journal of Clinical Investigation* **2002**, *110*, 475-482.

(77) Williams, D. H.; Stone, M. J.; Hauck, P. R.; Rahman, S. K. Why are Secondary Metabolites (Natural Products) Biosynthesized? *Journal of Natural Products* **1989**, *52*, 1189-1208.

(78) Da Rocha, A. B.; Lopes, R. M.; Schwartsmann, G. Natural products in anticancer therapy. *Current Opinion in Pharmacology* **2001**, *1*, 364-369.

(79) Faulkner, D. J.; He, H.-Y.; Unson, M. D.; Bewley, C. A.; Garson, M. J. New Metabolites from Marine Sponges: are Symbionts Important? *Gazzetta Chimica Italiana* **1993**, *123*, 301-307.

(80) Garson, M. J. The biosynthesis of sponge secondary metabolites: Why it is important. *Sponges in Time and Space*; Balkema: Rotterdam, 1994; pp 427-440.

(81) Munro, M. H. G. Personal Communication: Christchurch, 1999.

(82) Litaudon, M.; Hart, J. B.; Blunt, J. W.; Lake, R. J.; Munro, M. H. G. Isohomohalichondrin B, a new antitumor polyether macrolide from the New Zealand deep-water sponge *Lissodendoryx sp. Tetrahedron Letters* **1994**, *35*, 9435-9438.

(83) Perry, N. B.; Ettouati, L.; Litaudon, M.; Blunt, J. W.; Munro, M. H. G.; Parkin, S.; Hope, H. Alkaloids from the antarctic sponge Kirkpatrickia varialosa. Part 1: Variolin B, a new antitumor and antiviral compound. *Tetrahedron* **1994**, *50*, 3987-3992.

(84) Northcote, P. T.; Blunt, J. W.; Munro, M. H. G. Pateamine: a potent cytotoxin from the New Zealand marine sponge, *Mycale sp. Tetrahedron Letters* **1991**, *32*, 6411-6414.

(85) Dumdei, E. J.; Blunt, J. W.; Munro, M. H. G.; Pannell, L. K. Isolation of Calyculins, Calyculinamides, and Swinholide H from the New Zealand Deep-Water Marine Sponge *Lamellomorpha strongylata. Jounal of Organic Chemistry* **1997**, *62*, 2636-2639.

(86) Perry, N. B.; Blunt, J. W.; McCombs, J. D.; Munro, M. H. G. Discorhabdin C, a Highly Cytotoxic Pigment from a Sponge of the Genus *Latrunculia. Journal of Organic Chemistry* **1986**, *51*, 5476-5478.

(87) Urban, S.; Blunt, J. W.; Munro, M. H. G. Coproverdine, a novel, cytotoxic marine alkaloid from a New Zealand ascidian. *Journal of Natural Products* **2002**, *65*, 1371-1373.

(88) Cassidy, J. Conference Address, *4th International Symposium on Polymer Therapeutics*: London, 2000.

(89) Perry, N. B.; Blunt, J. W.; Munro, M. H. G.; Pannell, L. K. Mycalamide A, an antiviral compound from a New Zealand sponge of the genus *Mycale*. *Journal of the American Chemical Society* **1988**, *110*, 4850-4851.

(90) Perry, N. B.; Blunt, J. W.; Munro, M. H. G.; Thompson, A. M. Antiviral and antitumor agents from a New Zealand sponge, Mycale sp. 2. Structures and solution conformations of mycalamides A and B. *Journal of Organic Chemistry* **1990**, *55*, 223-227.

(91) Burres, N. S.; Clement, J. J. Antitumor activity and mechanism of action of the novel marine natural products mycalamide-A and -B and onnamide. *Cancer Research* **1989**, *49*, 2935-2940.

(92) Hong, C. Y.; Kishi, Y. Total synthesis of mycalamides A and B. *Journal of Organic Chemistry* **1990**, *55*, 4242-4245.

(93) Kocienski, P.; Narquizian, R.; Raubo, P.; Smith, C.; Farrugia, L. J. ; Muir, K.; Boyle, F. T. Synthetic studies on the pederin family of antitumor agents. Syntheses of mycalamide B, theopederin D and pederin. *Journal of the Chemical Society. Perkin Transactions 1* **2000**, 2357-2384.

(94) Roush, W. R.; Pfeifer, L. A. Total Synthesis of Mycalamide A and 7-epi-Mycalamide A. *Organic Letters* **2000**, *2*, 859-862.

(95) Hanson, F. R.; Eble, T. E. An Antiphage Agent Isolated From *Aspergillus Sp.* *Journal of Bacteriology* **1949**, *58*, 527-529.

(96) Tarbell, D. S.; Carman, R. M.; Chapman, D. D.; Huffman, K. R.; McCorkindale, N. J. The Structure of Fumagillin. *Journal of the American Chemical Society* **1960**, *82*, 1005-1007.

(97) Turner, J. R.; Tarbell, D. S. The Stereochemistry of Fumagillin. *Proceedings of the National Academy of Sciences of the United States of America* **1962**, *48*, 733-735.

(98) Ingber, D.; Fujita, T.; Kishimoto, S.; Sudo, K.; Kanamaru, T.; Brem, H.; Folkman, J. Synthetic analogs of fumagillin that inhibit angiogenesis and suppress tumor growth. *Nature (London, United Kingdom)* **1990**, *348*, 555-557.

(99) Marui, S.; Itoh, F.; Kozai, Y.; Sudo, K.; Kishimoto, S. Chemical modification of fumagillin. I. 6-O-acyl, 6-O-sulfonyl, 6-O-alkyl, and 6-O-(N-substituted-carbamoyl)fumagillols. *Chemical & Pharmaceutical Bulletin* **1992**, *40*, 96-101.

(100) Marui, S.; Kishimoto, S. Chemical modification of fumagillin. II. 6-Amino-6-deoxyfumagillol and its derivatives. *Chemical & Pharmaceutical Bulletin* **1992**, *40*, 575-579.

(101) Kusaka, M.; Sudo, K.; Fujita, T.; Marui, S.; Itoh, F.; Ingber, D.; Folkman, J. Potent antiangiogenic action of AGM-1470: comparison with the fumagillin parent. *Biochemical and Biophysical Research Communications* **1991**, *174*, 1070-1076.

(102) Yamamoto, T.; Sudo, K.; Fujita, T. Significant inhibition of endothelial cell growth in tumor vasculature by an angiogenesis inhibitor, TNP-470 (AGM-1470). *Anticancer Research* **1994**, *14*, 1-3.

(103) Griffith, E. C.; Su, Z.; Turk, B. E.; Chen, S.; Chang, Y.-H.; Wu, Z.; Biemann, K.; Liu, J. O. Methionine aminopeptidase (type 2) is the common target for

angiogenesis inhibitors AGM-1470 and ovalicin. *Chemistry & Biology* **1997**, *4*, 461-471.

(104) Griffith, E. C.; Su, Z.; Niwayama, S.; Ramsay, C. A.; Chang, Y.-H.; Liu, J. O. Molecular recognition of angiogenesis inhibitors fumagillin and ovalicin by methionine aminopeptidase 2. *Proceedings of the National Academy of Sciences of the United States of America* **1998**, *95*, 15183-15188.

(105) Liu, S.; Widom, J.; Kemp, C. W.; Crews, C. M.; Clardy, J. Structure of human methionine aminopeptidase-2 complexed with fumagillin. *Science (Washington, D. C.)* **1998**, *282*, 1324-1327.

(106) Taber, D. F.; Christos, T. E.; Rheingold, A. L.; Guzei, I. A. Synthesis of (-)-Fumagillin. *Journal of the American Chemical Society* **1999**, *121*, 5589-5590.

(107) Ringsdorf, H. Structure and Properties of Pharmacologically Active Polymers. *Journal of Polymer Science* **1975**, *51*, 135-153.

(108) Torchilin, V. P. Drug targeting. *European Journal of Pharmaceutical Sciences* **2000**, *11*, S81-S91.

(109) Maeda, H.; Matsumura, Y. Tumoritropic and Lymphotropic Principles of Macromolecular Drugs. *Critical Reviews in Therapeutic Drug Carrier Systems* **1989**, *6*, 193-210.

(110) Matsumura, Y.; Maeda, H. A New Concept for Macromolecular Therapeutics in Cancer Chemotherapy: Mechanism of Tumoritropic Accumulation of Proteins and the Antitumor Agent Smancs. *Cancer Research* **1986**, *46*, 6387-6392.

(111) Duncan, R. Polymer Conjugates for Tumour Targeting and Intracytoplasmic Delivery. The EPR Effect as a Common gateway? *PSTT* **1999**, *2*, 441-449.

(112) Steyger, P. S.; Baban, D. F.; Brereton, M.; Ulbrich, K.; Seymour, L. W. Intratumoral distribution as a determinant of tumor responsiveness to therapy using polymer-based macromolecular prodrugs. *Journal of Controlled Release* **1996**, *39*, 35-46.

(113) Minko, T.; Kopeckova, P.; Pozharov, V.; Jensen, K. D.; Kopecek, J. The influence of cytotoxicity of macromolecules and of VEGF gene modulated vascular permeability on the enhanced permeability and retention effect in resistant solid tumors. *Pharmaceutical Research* **2000**, *17*, 505-514.

(114) Duncan, R. Drug-Polymer Conjugates: Potential for Improved Chemotherapy. *Anti-Cancer Drugs* **1992**, *3*, 175-210.

(115) Banker, G. S. Pharmaceutical applications of controlled release: an overview of the past, present, and future. *Medical applications of controlled release*; CRC Press: Boca Raton, 1984; pp 1-34.

(116) Shiah, J. G.; Dvorak, M.; Kopeckova, P.; Sun, Y.; Peterson, C. M.; Kopecek, J. Biodistribution and antitumor efficacy of long-circulating N-(2-hydroxypropyl)methacrylamide copolymer-doxorubicin conjugates in nude mice. *European Journal of Cancer* **2001**, *37*, 131-139.

(117) Kopecek, J.; Kopeckova, P.; Minko, T.; Lu, Z. R. HPMA copolymer-anticancer drug conjugates: design, activity, and mechanism of action. *European Journal of Pharmaceutics and Biopharmaceutics* **2000**, *50*, 61-81.

(118) Brocchini, S.; Duncan, R. Pendent Drugs, Release from Polymers. *Encyclopedia of Controlled Drug Delivery*; John Wiley & Sons, Inc.: New York, 1999.

(119) Seymour, L. W.; Duncan, R.; Kopeckova, P.; Kopecek, J. Daunomycin- and adriamycin-N-(2-hydroxypropyl)methacrylamide copolymer conjugates; toxicity

reduction by improved drug-delivery. *Cancer Treatment Reviews* **1987**, *14*, 319-327.

(120) Choi, W.-M.; Kopeckova, P.; Minko, T.; Kopecek, J. Synthesis of HPMA copolymer containing adriamycin bound via an acid-labile spacer and its activity toward human ovarian carcinoma cells. *Journal of Bioactive and Compatible Polymers* **1999**, *14*, 447-456.

(121) Kratz, F.; Beyer, U.; Schutte, M. T. Drug-polymer conjugates containing acid-cleavable bonds. *Critical Reviews in Therapeutic Drug Carrier Systems* **1999**, *16*, 245-288.

(122) Mueller, B. M.; Wrasidlo, W. A.; Reisfeld, R. A. Antibody conjugates with morpholinodoxorubicin and acid cleavable linkers. *Bioconjugate Chemistry* **1990**, *1*, 325-330.

(123) Putnam, D. A.; Shiah, J.-G.; Kopecek, J. Intracellularly biorecognizable derivatives of 5-fluorouracil. Implications for site-specific delivery in the human condition. *Biochemical Pharmacology* **1996**, *52*, 957-962.

(124) Dubowchik, G. M.; Firestone, R. A.; Padilla, L.; Willner, D.; Hofstead, S. J.; Mosure, K.; Knipe, J. O.; Lasch, S. J.; Trail, P. A. Cathepsin B-Labile Dipeptide Linkers for Lysosomal Release of Doxorubicin from Internalizing Immunoconjugates: Model Studies of Enzymatic Drug Release and Antigen-Specific In Vitro Anticancer Activity. *Bioconjugate Chemistry* **2002**, *13*, 855-869.

(125) Subr, V.; Strohalm, J.; Ulbrich, K.; Duncan, R.; Hume, I. C. Polymers containing enzymically degradable bonds, XII. Effect of spacer structure on the rate of release of daunomycin and adriamycin from poly[N-(2-hydroxypropyl)methacrylamide] copolymer drug carriers in vitro and antitumor activity measured in vivo. *Journal of Controlled Release* **1992**, *18*, 123-132.

(126) Duncan, R.; Dimitrijevic, S.; Evagorou, E. G. The Role of Polymer Conjugates in the Diagnosis and Treatment of Cancer. *S.T.P. Pharma Sciences* **1996**, *6*, 237-263.

(127) Šprincl, L.; Exner, J.; Šterba, O.; Kopecek, J. New Types of Synthetic Infusion Solutions. III. Elimination and Retention of Poly-[*N*-(2-hydroxypropyl)Methacrylamide] in a Test Organism. *Journal of Biomedical Materials Research* **1976**, *10*, 953-963.

(128) Duncan, R.; Seymour, L. W.; O'Hare, K. B.; Flanagan, P. A.; Wedge, S.; Hume, I. C.; Ulbrich, K.; Strohalm, J.; Subr, V.; Spreafico, F.; Grandi, M.; Ripamonti, M.; Farao, M.; Suarato, A. Preclinical evaluation of polymer-bound doxorubicin. *Journal of Controlled Release* **1992**, *19*, 331-346.

(129) Minko, T.; Kopeckova, P.; Kopecek, J. Mechanisms of anticancer action of HPMA copolymer-bound doxorubicin. *Macromolecular Symposia* **2001**, *172*, 35-47.

(130) Seymour, L. W.; Ulbrich, K.; Steyger, P. S.; Brereton, M.; Subr, V.; Strohalm, J.; Duncan, R. Tumour Tropism and Anti-Cancer Efficacy of Polymer-Based Doxorubicin Prodrugs in the Treatment of Subcutaneous Murine B16F10 Melanoma. *British Journal of Cancer* **1994**, *70*, 636-641.

(131) Seymour, L. W.; Ulbrich, K.; Strohalm, J.; Kopecek, J.; Duncan, R. The pharmacokinetics of polymer-bound adriamycin. *Biochemical Pharmacology* **1990**, *39*, 1125-1131.

(132) Yeung, T. K.; Hopewell, J. W.; Simmonds, R. H.; Seymour, L. W.; Duncan, R.; Bellini, O.; Grandi, M.; Spreafico, F.; Strohalm, J.; Ulbrich, K. Reduced cardiotoxicity of doxorubicin given in the form of N-(2-

hydroxypropyl)methacrylamide conjugates: an experimental study in the rat. *Cancer Chemotherapy and Pharmacology* **1991**, *29*, 105-111.

(133) Duncan, R. Polymer Therapeutics for Tumour Specific Delivery. In *Chemistry & Industry*, 1997; pp 262-264.

(134) Hopewell, J. W.; Duncan, R.; Wilding, D.; Chakrabarti, K. Preclinical evaluation of the cardiotoxicity of PK2: A novel HPMA copolymer-doxorubicin-galactosamine conjugate antitumour agent. *Human & Experimental Toxicology* **2001**, *20*, 461-470.

(135) Seymour, L. W.; Ulbrich, K.; Wedge, S. R.; Hume, I. C.; Strohalm, J.; Duncan, R. N-(2-hydroxypropyl)methacrylamide copolymers targeted to the hepatocyte galactose-receptor: pharmacokinetics in DBA2 mice. *British Journal of Cancer* **1991**, *63*, 859-866.

(136) Seymour, L. W.; Ferry, D. R.; Anderson, D.; Hesslewood, S.; Julyan, P. J.; Poyner, R.; Doran, J.; Young, A. M.; Burtles, S.; Kerr, D. J. Hepatic drug targeting: phase I evaluation of polymer-bound doxorubicin. *Journal of Clinical Oncology* **2002**, *20*, 1668-1676.

(137) Trail, P. A.; Willner, D.; Hellström, K. E. Site-Directed Delivery of Anthracyclines for Treatment of Cancer. *Drug Development Research* **1995**, *34*, 196-209.

(138) Pimm, M. V.; Perkins, A. C.; Strohalm, J.; Ulbrich, K.; Duncan, R. Gamma scintigraphy of the biodistribution of ^{123}I-labeled N-(2-hydroxypropyl)methacrylamide copolymer-doxorubicin conjugates in mice with transplanted melanoma and mammary carcinoma. *Journal of Drug Targeting* **1996**, *3*, 375-383.

(139) Merrifield, R. B. Solid Phase Peptide Synthesis. I. The Synthesis of a Tetrapeptide. *Journal of the American Chemical Society* **1963**, *85*, 2149-2154.

(140) Han, S.-Y.; Kim, Y.-A. Recent development of peptide coupling reagents in organic synthesis. *Tetrahedron* **2004**, *60*, 2447-2467.

(141) Fields, G. B.; Noble, R. L. Solid-phase peptide synthesis utilizing 9-fluorenylmethoxycarbonyl amino acids. *International Journal of Peptide and Protein Research* **1990**, *35*, 161-214.

(142) Carpino, L. A.; Han, G. Y. 9-Fluorenylmethoxycarbonyl amino-protecting group. *Journal of Organic Chemistry* **1972**, *37*, 3404-3409.

(143) Wang, S.-S. p-Alkoxybenzyl alcohol resin and p-alkoxybenzyloxycarbonylhydrazide resin for solid phase synthesis of protected peptide fragments. *Journal of the American Chemical Society* **1973**, *95*, 1328-1333.

(144) Sieber, P. An improved method for anchoring of 9-fluorenylmethoxycarbonyl amino acids to 4-alkoxybenzyl alcohol resins. *Tetrahedron Letters* **1987**, *28*, 6147-6150.

(145) Fujii, N.; Otaka, A.; Funakoshi, S.; Bessho, K.; Yajima, H. New procedure for the synthesis of cystine peptides by oxidation of S-substituted cysteine peptides with thallium(III) trifluoroacetate. *Journal of the Chemical Society, Chemical Communications* **1987**, 163-164.

(146) Maruyama, T.; Terasawa, I. Studies on side reactions of asparagine. *Peptide Chemistry 1992, Proceedings of the Japan Symposium, 2nd* **1993**, 87-90.

(147) Katritzky, A. R.; Pilarski, B.; Urogdi, L. Efficient conversion of nitriles to amides with basic hydrogen peroxide in dimethyl sulfoxide. *Synthesis* **1989**, 949-950.

(148) Liu, K. T.; Shih, M. H.; Huang, H. W.; Hu, C. J. Catalytic hydration of nitriles to amides with manganese dioxide on silica gel. *Synthesis* **1988**, 715-717.

(149) Kaminskaia, N. V.; Kostic, N. M. Nitrile hydration catalyzed by palladium(II) complexes. *Journal of the Chemical Society, Dalton Transactions: Inorganic Chemistry* **1996**, 3677-3686.

(150) Thompson, A. M.; Blunt, J. W.; Munro, M. H. G.; Perry, N. B.; Pannell, L. K. Chemistry of the mycalamides, antiviral and antitumor compounds from a marine sponge. Part 3. Acyl, alkyl and silyl derivatives. *Journal of the Chemical Society, Perkin Transactions 1: Organic and Bio-Organic Chemistry (1972-1999)* **1992**, 1335-1342.

(151) Thompson, A. M.; Blunt, J. W.; Munro, M. H. G.; Clark, B. M. Chemistry of the mycalamides, antiviral and antitumor compounds from a marine sponge. Part 4. Reactions of mycalamide A and alkyl derivatives with basic nucleophiles. *Journal of the Chemical Society, Perkin Transactions 1: Organic and Bio-Organic Chemistry (1972-1999)* **1994**, 1025-1031.

(152) Thompson, A. M.; Blunt, J. W.; Munro, M. H. G.; Perry, N. B. Chemistry of the mycalamides, antiviral and antitumor compounds from a marine sponge. Part 5. Acid-catalyzed hydrolysis and acetal exchange, double bond additions and oxidation reactions. *Journal of the Chemical Society, Perkin Transactions 1: Organic and Bio-Organic Chemistry* **1995**, 1233-1242.

(153) Lill, R. E. Studies on New Zealand Marine Natural Products. PhD Thesis, *Chemistry Department*; University of Canterbury: Christchurch, 1999.

(154) Squire, M. A. personal communication, 1999.

(155) Daumas, M.; Yen Vo, Q.; Vo Quang, L.; Le Goffic, F. A new and efficient heterogeneous system for the oxidative cleavage of 1,2-diols and the oxidation of hydroquinones. *Synthesis* **1989**, 64-65.

(156) Borch, R. F.; Bernstein, M. D.; Durst, H. D. Cyanohydridoborate anion as a selective reducing agent. *Journal of the American Chemical Society* **1971**, *93*, 2897-2904.

(157) Ishihara, K.; Kurihara, H.; Yamamoto, H. An extremely simple, convenient, and selective method for acetylating primary alcohols in the presence of secondary alcohols. *Journal of Organic Chemistry* **1993**, *58*, 3791-3793.

(158) Mitsunobu, O. The use of diethyl azodicarboxylate and triphenylphosphine in synthesis and transformation of natural products. *Synthesis* **1981**, 1-28.

(159) Viaud, M. C.; Rollin, P. Zinc azide mediated Mitsunobu substitution. An expedient method for the one-pot azidation of alcohols. *Synthesis* **1990**, 130-132.

(160) Staudinger, H.; Hauser, E. New organic phosphorus compounds. IV. Phosphinimines. *Helvetica Chimica Acta* **1921**, *4*, 861-886.

(161) Knouzi, N.; Vaultier, M.; Carrie, R. Reduction of azides by triphenylphosphine in the presence of water: a general and chemoselective access to primary amines. *Bulletin de la Societe Chimique de France* **1985**, 815-819.

(162) Galynker, I.; Still, W. C. A simple method for tosylation with inversion. *Tetrahedron Letters* **1982**, *23*, 4461-4464.

(163) Jackman, L. M.; Sternhell, S. Vicinal Interproton Coupling. *Applications of Nuclear Magnetic Resonance Spectroscopy in Organic Chemistry*; 2nd ed.; Pergamon Press: Braunschweig, Germany, 1969; pp 280-304.

(164) Bera, S.; Nair, V. Isonucleosides with exocyclic methylene groups. *Helvetica Chimica Acta* **2000**, *83*, 1398-1407.

(165) Busacca, C. A.; Grossbach, D.; Spinelli, E. A convenient synthesis of (1*S*)-tert-butyl-1,2-ethylenediamine. *Tetrahedron: Asymmetry* **2000**, *11*, 1907-1910.

(166) Ojima, I.; Lin, S.; Chakravarty, S.; Fenoglio, I.; Park, Y. H.; Sun, C.-M.; Appendino, G.; Pera, P.; Veith, J. M.; Bernacki, R. J. Syntheses and Structure-Activity Relationships of Novel Nor-seco Taxoids. *Journal of Organic Chemistry* **1998**, *63*, 1637-1645.

(167) Han, C. K.; Ahn, S. K.; Choi, N. S.; Hong, R. K.; Moon, S. K.; Chun, H. S.; Lee, S. J.; Kim, J. W.; Hong, C. I.; Kim, D.; Yoon, J. H.; No, K. T. Design and synthesis of highly potent fumagillin analogues from homology modeling for a human MetAP-2. *Bioorganic & Medicinal Chemistry Letters* **2000**, *10*, 39-43.

(168) Godwin, A.; Hartenstein, M.; Muller, A. H. E.; Brocchini, S. Synthesis of a polymeric precursor by ATRP for conversion to polymer-drug conjugates. *Book of Abstracts, 219th ACS National Meeting, San Francisco, CA, March 26-30, 2000* **2000**, OLY-519.

(169) Godwin, A.; Hartenstein, M.; Muller, A. H. E.; Brocchini, S. Narrow molecular weight distribution precursors for polymer-drug conjugates. *Angewandte Chemie, International Edition in English* **2001**, *40*, 594-597.

(170) Matyjaszewski, K.; Xia, J. Atom Transfer Radical Polymerization. *Chemical Reviews* **2001**, *101*, 2921-2990.

(171) Chang, H.-I. Polymer Therapetics. Masters Thesis, *Chemistry Department*; University of Canterbury: Christchurch, 2002.

(172) Pace, C. N.; Shirley, B. A.; McNutt, M.; Gajiwala, K. Forces contributing to the conformational stability of proteins. *FASEB Journal* **1996**, *10*, 75-83.

(173) Paquet, A.; Bergeron, M. Formation of unusual side-products from succinimidyl esters of fatty acids during the acylation of amino acids. *Canadian Journal of Chemistry* **1982**, *60*, 1806-1808.

(174) Šavrda, J. An Unusual Side Reaction of 1-Succinimidyl Esters during Peptide Synthesis. *Journal of Organic Chemistry* **1977**, *42*, 3199-3200.

(175) Degrand, C.; Limoges, B. Synthesis of Nitroxides for Use as Procationic Labels and Their Incorporation into Nafion Films. *Journal of Organic Chemistry* **1993**, *58*, 2573-2577.

(176) Akers, H. A.; Atkin, C. L.; Neilands, J. B. Mass Spectroscopy of Hydroxamic Acids: Fragmentation by the Loss of the Hydroxylamino Oxygen. *Organic Mass Spectrometry* **1975**, *10*, 259-262.

(177) Allman, T.; Lenkinski, R. E. A conformational analysis of adriamycin based upon its ^{1}H nuclear magnetic resonance spectrum in various solvents. *Canadian Journal of Chemistry* **1987**, *65*, 2405-2410.

(178) Pinciroli, V.; Rizzo, V.; Angelucci, F.; Tato, M.; Vigevani, A. ^{1}H NMR Characterisation of Methacrylamide Polymer Conjugates with the Anti-Cancer Drug Doxorubicin. *Magnetic Resonance in Chemistry* **1997**, *35*, 2-8.

(179) Bekers, O.; Beijnen, J. H.; Storm, G.; Bult, A.; Underberg, W. J. M. Chemical stability of N-trifluoroacetyldoxorubicin-14-valerate (AD-32) in aqueous media

and after liposome encapsulation. *International Journal of Pharmaceutics* **1989**, *56*, 103-109.

(180) Beijnen, J. H.; van der Houwen, O. A. G. J.; Underberg, W. J. M. Aspects of the degradation kinetics of doxorubicin in aqueous solution. *International Journal of Pharmaceutics* **1986**, *32*, 123-131.

(181) Wassermann, K.; Bundgard, H. Kinetics of the acid-catalyzed hydrolysis of doxorubicin. *International Journal of Pharmaceutics* **1983**, *14*, 73-78.

(182) Cameron, D. W.; Feutrill, G. I.; Griffiths, P. G. 5-Deoxy, 12-Deoxy, 5,12-Bisdeoxy, and 4,5,12-Trisdeoxy Anthracyclines: Synthesis of New Analogues of Daunorubicin and Doxorubicin by Controlled Deoxygenation of the C-Ring. *Australian Journal of Chemistry* **2000**, *53*, 25-40